The Late Cenomanian Anoxic Event; implications for foraminiferal evolution.

by

Paul Niell Leary BSc.,DMS.

Thesis submitted in partial fulfillment for the Degree of Doctor of Philosophy to the Council for National Academic Awards.

Doctor of Philosophy

to

The Council for National Academic Awards

Research conducted at Plymouth Polytechnic.

September 1987.

The Late Cenomanian Anoxic Event; implications for foraminiferal evolution.

P.N. Leary

Abstract:

This study investigates the effect of the late Cenomanian Oceanic Anoxic Event (OAE) on the planktonic and benthonic foraminifera.

On the former, the OAE was the cause of major extinctions within the population, the return to pre-OAE oxygen levels permitting recolonization of the vacated niches. On the latter, the OAE caused extinctions but resulted in a low oxygen tolerant fauna which slowly evolved into the vacated niches on the post-OAE recovery of oxygen levels.

The changes in the foraminiferal populations have been integrated with changes in other marine organisms through the late Cenomanian.

Declaration:

This is to certify that the work submitted for the Degree of Doctor of Philosophy under the title "The Late Cenomanian Anoxic Event; implications for foraminiferal evolution" is the result of original work.

All authors and works consulted are fully acknowledged. No part of this work has been accepted in substance for any other degrees and is not being concurrently submitted in candidature for any other degree.

Candidate 

P.N. LEARY

Research supervisor

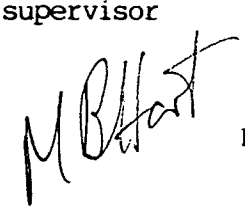

Prof. M.B. HART

Thoughts for the day:

"Caw", said the Crow.

"Balls", said Milligan.

Spike Milligan, Puckoon.

"I am not French, I am Belgian."

Hercule Poirot, Agatha Christie.

"If a little knowledge is a dangerous thing, just think what a lot could do."

Senior tutor. In Porterhouse Blue, Tom Sharpe.

Art is bullshit,

Science is Art with numbers.

Anon.

Contents:

Acknowledgements:

This research was funded by the Natural Environment Research Council and I would like to express my eternal gratitude for the opportunity this gave me. In addition, their support for attending conferences, particularly abroad, was most appreciated.

Similarly, I am much indebted to Professor Malcolm Hart for encouraging and guiding me through the three years. His tolerance and steadying influence will be long remembered.

The attention and interest of Dr. Bruce Tocher and Dr. Ian Jarvis was most welcome especially during discussions of the topic. Also the latters' help in the lithostratigraphy of the onshore sections proved invaluable.

I would like to express my thanks for the technical support provided, especially Spike Emmet with thin sections, Teresa Emmet with rock processing and Graham Mott with optical photomicroscopy. In addition, the efforts of the staff of Media Services cannot be ignored.

Many researchers around the world have kindly provided preprints and reprints. I cannot mention them all but the following are offered particular thanks:

Prof. O.R. Anderson, Prof. M. Arthur, Dr. M. Caron, Dr. Ch. Hemleben and Dr. H. Jenkyns.

I am also indebted to Dave Howard who kindly translated some Russian texts and to Dr. J. Harvey who provided the English framework of a few German papers.

The kindness and interest of some of my research colleagues will be long remembered.

Dr. P. Copestake (BritOil) kindly provided material from three wells in the southern and northern North Sea, as did B.P. (Dyce) from the Southern Irish Sea.

The willing help, with typing letters and manuscripts, of Marilyn was most appreciated.

Finally, I would like to make mention of "Pigdog" who battled with a word processor to prepare this manuscript and "The Boy", whose company was most enjoyable and I wish them every success in their chosen careers.

I offer my apologies to anyone I have omitted and beg their forgiveness.

List of figures.

Figure 8.6 Abundances from Dover.

List of Text-figures.

List of Text Plates

List of enclosures.

Enclosure 1 Locality map.

Chapter 1: Introduction and History of Previous Research.

1.1 Overview of planktonic foraminiferal evolution.

Modelling of the evolution of planktonic foraminifera has advanced over the past decade in the light of developments in palaeoceanography coupled with a greater understanding of the ontogeny of extant species.

The three iterative radiations have variously been attributed to temperature (Cifelli,1969; Frerichs,1971), or the recolonization of deeper water niches (Hart,1980a; Caron,1983a), brought about by changes in palaeoceanographic conditions. Alternatively, they may be induced by extra-terrestrial influences (Smit,1982), possibly on a regular basis (Raup,1987).

1.2 The late Cenomanian Anoxic Event.

The late Cenomanian Anoxic Event saw world-wide water column stagnation (Jenkyns,1980; Arthur et al.,1987; Schlanger et al. 1987) with a major change in the foraminiferal composition (Hart,1985; Hilbrecht and Hoefs,1986; Hart and Ball,1987). The world-wide off-shore recovery of the Cenomanian - Turonian interval is poor (Figure 1.1), with only 14 of the 36 DSDP Legs encountering pre-Cenomanian sediments and yielding Cenomanian - Turonian rocks. Furthermore,only 4 of these contained well-preserved planktonic faunas. Leg 80, DSDP, forms one of the latter, with several metres of organic-rich laminated clays being recorded (Waples,1985) and a rich planktonic assemblage (Graciansky et al.,1985).

The on-shore Cenomanian - Turonian succession is laterally

Figure 1.1 Plot of DSDP Legs against designated categories

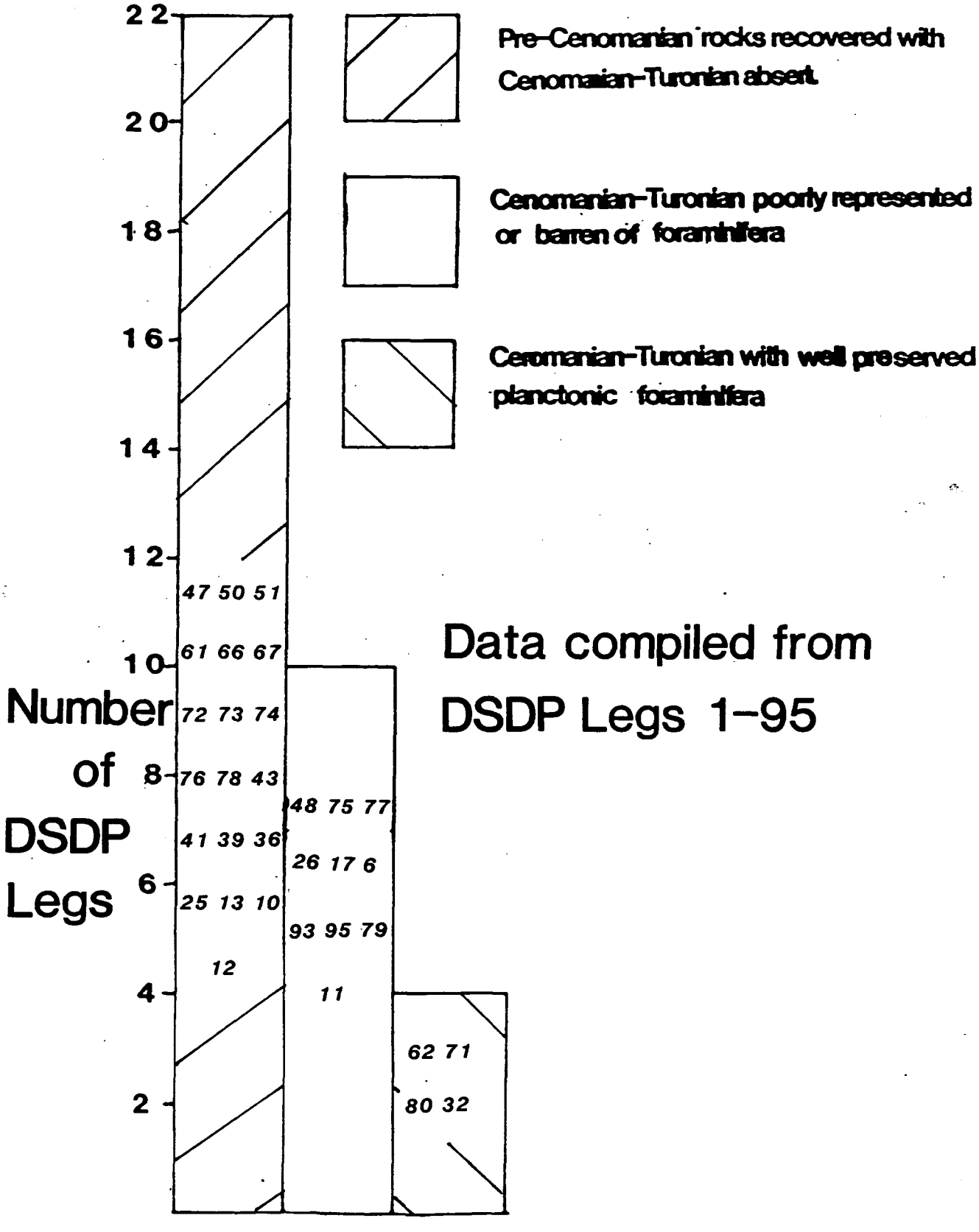

persistant but with many facies overprints on the background carbonate deposition (Jarvis and Woodroof,1984; Robinson,1986), and as a result varies in its completeness and suitability for the study of the evolution of foraminifera (see Chapter 6). In the off-shore North Sea Basin, Cenomanian rocks are poorly represented in the Southern North Sea Basin whereas in the Northern North Sea Basin rocks of Cenomanian and Turonian age are well developed. Conversely, in the Northern Viking Graben there is little evidence of Cenomanian strata (Copestake,pers.comm.).

1.3 Foraminiferal studies.

Previous foraminiferal studies of the Plenus Marls (Jeffries,1962),the Albian - Cenomanian (Hart,1970; Carter and Hart,1977) and Turonian (Owen,1970; Hart and Weaver,1977; Hart,1982b) successions have been undertaken. Only the biostratigraphically important foraminifera from B.P. Well 93\2-1 have been documented (Williamson,1979).

A study of nine sections across the Boreal Cenomanian - Turonian interval has been undertaken to look in detail at the late Cenomanian foraminiferal turnover.

Chapter 2: Methods.

2.1 Sampling.

At each locality the surface of the rock face was cleaned thoroughly to remove the surface weathered material, primarily to avoid the effects of decalcification on the tests. The size of each sample was between 0.5 and 1.0 kilogrammes. Each sample was placed in a plastic bag which was labelled inside and out, with the location of each recorded against a detailed lithological log. At all times the sampling equipment (hammer and trowel) were kept clean to avoid contamination from undesirable material.

The sample spacing is variable being carried out on a bed by bed basis. When bed thickness was greater than 1 metre a sample from both lower and upper portions was taken. Above and below the target area samples were collected at a 1 metre spacing.

The material provided by the Deep Sea Drilling Project was already in Plymouth Polytechnic; material from B.P and Britoil was requested by the author who had no control over its collection.

2.2 Sample Processing.

In keeping with other foraminiferal studies of chalk (Hart,1970; Bailey,1978), the processing technique depended on

the type of lithology:

(A) For rocks with a high clay content (marls).

The samples were broken with the fingers or, failing that, lightly with a hammer, into approximately 1 - 2 centimetre pieces, taking care not to crush the sediment. The pieces were dried for at least 24 hours in a ventilated oven at 60°C.

On removal from the oven, the hot dry samples were placed in a fume cupboard and soaked in white spirit for 2 - 4 hours. The white spirit was filtered off for re-use and the samples were immersed in distilled water, again for 2 - 4 hours. The disaggregated sample was filtered through a 63 μm mesh sieve, great care being taken to thoroughly remove the <63 um fraction. The residue was re-dried in an oven at 60°C and placed in a suitably labelled container.

Samples treated in the above manner were designated with the symbol O .

(B) For those rocks with a lower clay content the approach of Todd, Low and Mello (1965) was adopted.

The samples were broken as in (A), but then they were placed in a metal bowl containing a simmering solution of washing soda (2 heaped tablespoons of $Na_2CO_3 10 H_2O$ per 250 millilitres of distilled water), for 1 - 3 hours.

The solution was washed out through a 63 ⁄um sieve along with the <63 ⁄um fraction. As before the residue was dried and placed in a suitably labelled jar.

Samples so treated were designated □.

(C) Rarely, some samples were so heavily cemented that they defied disaggregation by methods (A) and (B). These were thin sectioned. At least six randomly orientated thin sections were obtained for each sample.

Samples thus treated were designated ☆.

For some samples all three techniques were used. The different techniques may be ranked in terms of the quality of results and thus preferentially

○>□>☆.

2.3 Residue Examination.

The dried residues were sieved through a nest of sieves containing 500um, 250um, 125um meshes and a collecting tray.

The total faunal picks of the planktonic foraminifera were made from the 500um and 250um fractions. This included broken specimens where they formed more than half of an individual. This approach ensured no picking bias, as opposed

to the more common practice of selecting 300 specimens for biostratigraphical study. The latter is only free of bias when the sample is randomly picked.

In some cases total faunal picks resulted in over a thousand specimens from one sample. Despite the time-consuming nature of the work it was worthwhile in terms of the confidence levels that could be placed on subsequent interpretations.

From the >125um fraction and collecting tray only representative faunal assemblages were taken, especially the gerontic forms of those not present in the top two fractions.

For the 500um and 250um fractions, the species present were sorted and the numbers of each were recorded. The relative percentage of the planktonic foraminifera were graphed at the generic level, with some subdivision into species for those of particular interest. (Figure 2.1).

Due to their very nature, thin sections were approached differently. For each, ten 10x power views were checked and the number of each planktonic species recorded. Thus, for each sample, the number of planktonic foraminifera from some sixty views was amassed. Thin section identification of planktonic foraminifera is poorly covered in the literature. In this study comparisons were made with Glaessner (1937), Pessagno (1967), Postuma (1971) and Fleurry (1980).

Figure 2.1 Relative frequencies of selected Planktonic genera

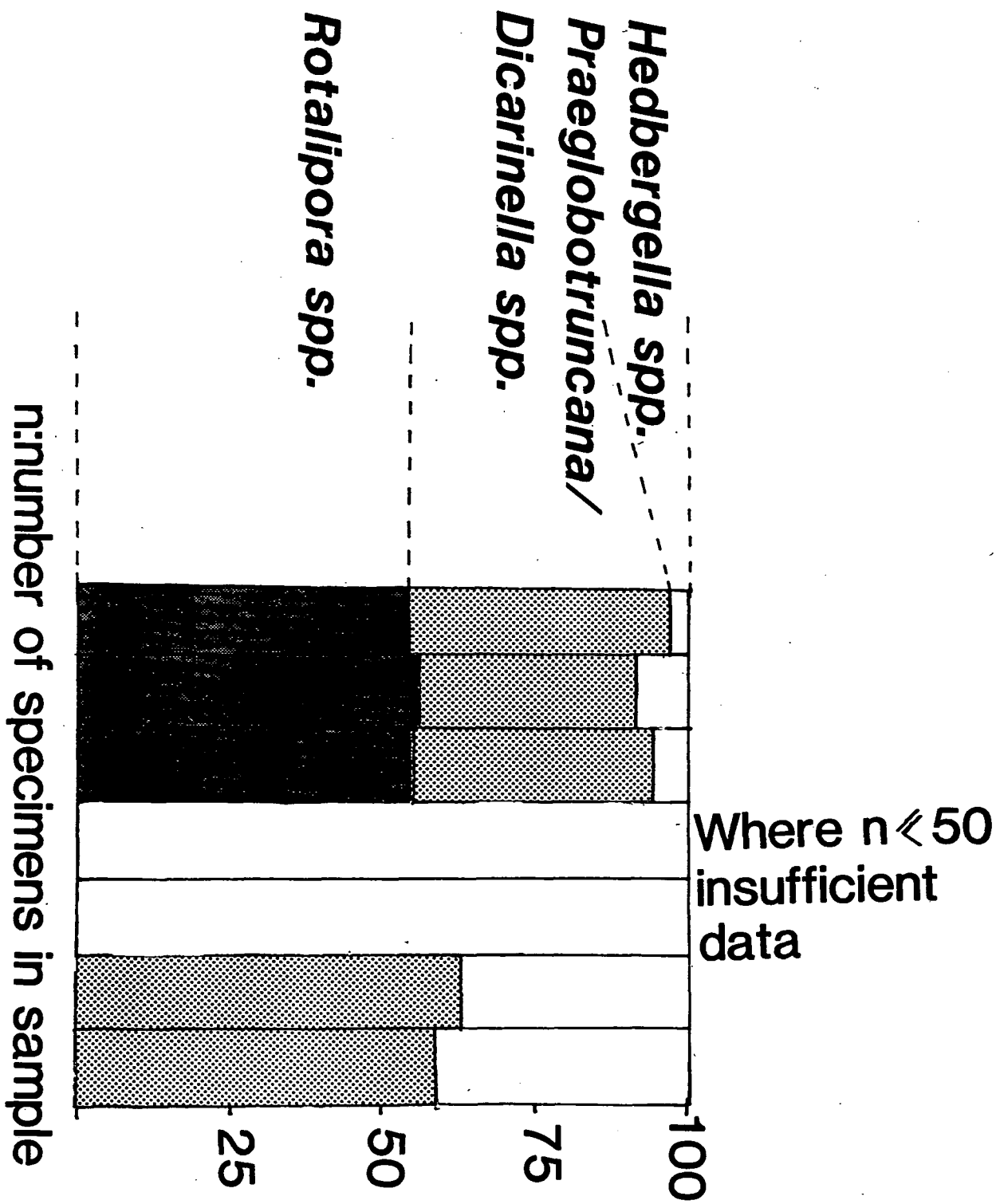

2.4 Optical Photomicroscopy.

Plane polarized photomicroscopy was performed using an Olympus Vanox Microscope and overhead mounted Olympus C-35 AD camera with Kodacolour CP135-36 film. For cross polarized photomicroscopy an Olympus Vanox polarising microscope was used with same film and camera attachment.

This arrangement provided the oppurtunity of maintaining a pictorial record of the faunal content. Each photograph was coded and a record kept.

2.5 Scanning Electron Microscopy.

The selected specimens were affixed to the stub with double sided tape. This was coated with approximately 10Å of Au. All pictures were taken using a Joel JSM\T-20 electron microscope. A record was kept of each photograph and a note made of the stub number, magnification, the identity of the specimen and its orientation.

2.6 X-Ray Photomicroscopy.

To facilitate the rapid and efficient biometric analysis of many planktonic specimens, they were X-rayed first and then analysed with an optical microscope. The technique was amended from Hedley (1951), Arnold (1982) and Be et al. (1969) as the Kodak films they advocated are not available in the U.K..

The specimens were photographed using a scanray Torrex 150 D X-ray machine with Mx5 high resolution film (9x12cm) and an exposure of 3.4 mA minutes (20kV) at a distance of 30cms. Specimens were lightly glued and orientated using a paint brush on a cell (Text Figure 2.1) and the source of the specimens recorded.

Text-figure 2.1
Xray cell

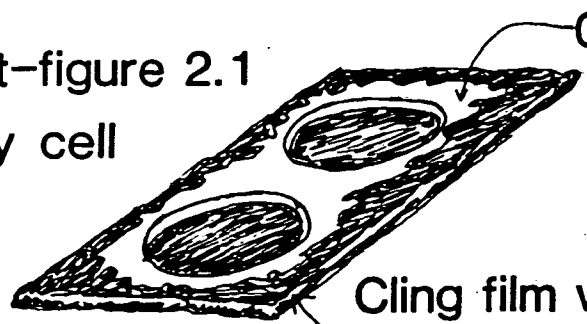

Three cells were photographed at once with metal alphabet labels to avoid confusion. The processed cells were cut to a relevant size and positioned between two labelled glass slides. Optical microscopy was then performed using the same equipment as previously described in 2.4.

Chapter 3: Description of localities.

3.1 Introduction.

The spatial distribution of localities examined during the present study (Enclosure 1) shows that they form a transect from the eastern passive margin of the North Atlantic Ocean (Goban Spur , B.P 93\2-1) through to the clastic dominated and attenuated facies of South East Devon (Beer Stone Adit, Shapwick Grange Quarry), and onto the more marly facies of the Anglo-Paris Basin (White Nothe, Compton Bay, Eastbourne, Dover, BritOil 48\22-1).

As a result of both the marked facies variations and the contrast between studies of off-shore and on-shore material, three different lithostratigraphic schemes exist, (though the Plenus Marls is common to two). No standard lithostratigraphic framework is used for the material recovered by the Deep Sea Drilling Project.

3.2 The eastern Atlantic passive margin.

Structurally, the region is dominated by Mesozoic en-echelon listric normal faults associated with a period of extension (Graciansky et al., 1985), the South Celtic Sea Basin being separated by an extension of the Cornish Palaeozoic basement (Weighall, 1979).

Figure 3.1 shows the location of B.P borehole 93\2-1 (lat.50°57'19.8"N; long.06°46'56.5"W), which was drilled to a

Figure3.1 Location of DSDP Leg80,Site551 and BP Borehole 93/2-1

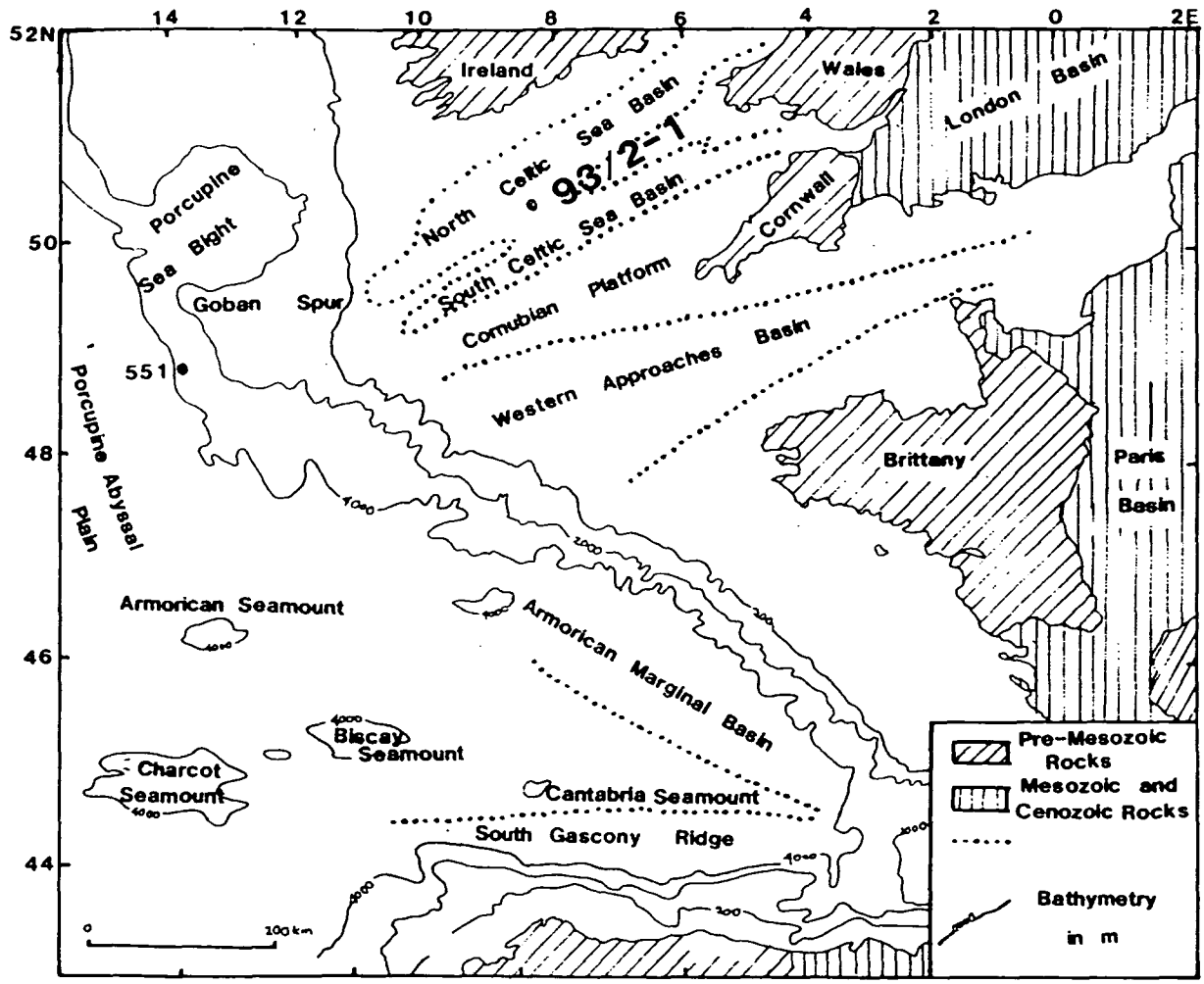

Depths are in metres below sea level. Regional ages refer to age of surficial rocks. After de Graciansky, Poag and Foss (1985). Base map after Montadert. Roberts, de Charpel, et al. (1979).

depth of 2,127m. The Cretaceous deposits commence at 266m and comprise a thick sequence of chalk (814m), which ranges from soft white micritic limestones to well-indurated micrites. At 1,110m the lithology shows a marked change to calcareous silty mudstones (35m) which are underlain by interbedded calcareous siltstones and mudstones and, at 1,150m by Wealden deposits (Williamson, 1979). Albian, Cenomanian and Turonian sediments are all represented. Above these is a hiatus which is overlain by Campanian and Maastrichtian deposits. The Cenomanian - Turonian boundary is placed at the top of the calcareous silty mudstones (op cit.). Side-wall core and ditch cutting samples were analysed from the Upper Cenomanian and Turonian.

Site 551, Leg 80 is located at lat.48°54.64'N; long.13°30.09'W (Figure 3.1), and was drilled to a depth of 3,887m. The lowest sediments were 4.1m of Late Cenomanian nannofossil chalk which rested unconformably on basaltic basement. These were overlain by 4.1m of black, organic rich, finely laminated shale which grades into pale green nannofossil chalk (2.1m) of early Turonian age. The overlying 31.6m of light grey nannofossil chalk was dated as Late Campanian and Maastrichtian in age, indicating that Upper Turonian - Upper Campanian sediments are absent (Graciansky et al, 1985; Ball, 1985)(see Figure 5.1.).

The syn-rift sedimentary sequences of the Goban Spur are considerably less complete than the more expansive deposits of the South Celtic Sea Basin (B.P 93\2-1). This may to some

extent be related to the positioning of the Goban Spur DSDP sites on the thinnest Mesozoic drape away from the fault escarpments.

3.3 South-east Devon.

The Cretaceous outliers of south-east Devon contain sediments of Albian-Cenomanian age (Hart, 1982a; Jarvis and Tocher, 1987). The Cenomanian sequence is highly attenuated and comprises a sequence of limestones punctuated by numerous hardgrounds (Jarvis and Woodruff, 1984; Jarvis and Tocher, 1983). As a consequence, a revised lithostratigraphic scheme has been erected which provides much more detail than the standard stratigraphy of the central Anglo-Paris Basin (Hamblin and Wood, 1976; Jarvis and Woodruff, 1984); see 3.4.

The thickest, most complete section is at Hooken Cliffs (Figure 5.3), where the Beer Head Limestone (Cenomanian) attains a thickness of 12.4m. Its uppermost unit, the Pinnacles Member, is a quartzose and glauconitic biomicrite with weakly developed nodular horizons, the top being the heavily indurated Haven Cliff Hardground. The overlying Connett's Hole Member of the Seaton Chalk (Turonian) is a nodular chalk containing abundant inoceramid debris with many incipient hardgrounds at its base (Figure 5.3). Access to Hooken Cliffs was limited because of dense undergrowth, but with the aid of a rope samples could be collected 2m into the Connett's Hole Member.

To the east, a working concern, Shapwick Grange Quarry

Figure3.2 Location of Hooken Cliffs,Beer

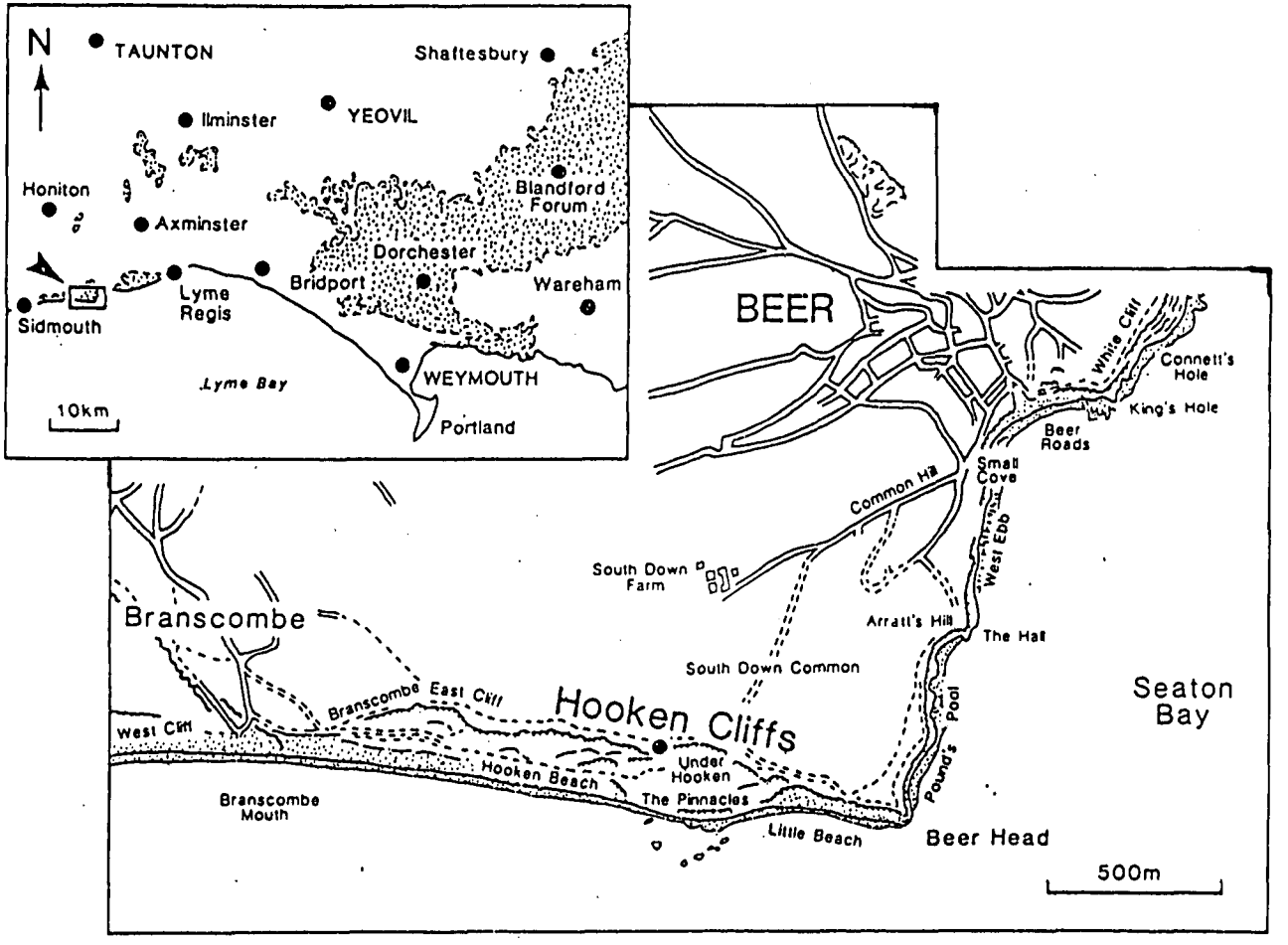

(Figures 3.3, 5.6), exposes Upper Greensand, Beer Head Limestone (Cenomanian) and Seaton Chalk (Turonian), (Hart et al., 1979; Jarvis et al. in press). The Upper Greensand comprises yellow to light grey, occasionally trough cross-bedded, medium-coarse calcarenites which locally contain proportions of coarse quartz and glauconite sand. The top of the Upper Greensand is marked by the heavily mineralized Humble Point Hardground.

The Beer Head Limestone (70cm) is much reduced, compared to Hooken Cliffs, and the Humble Point Hardground is overlain by 35cm of strongly indurated yellow nodular micrite with scattered quartz sand and glauconite. This represents the Haven Cliff Hardground portion of the Pinnacles Member. The top surface of the Haven Cliff Hardground marks the base of the Seaton Chalk.

The Seaton Chalk (19m) consists of 0.5-1m thick weakly developed rhythms of alternating nodular and marly chalks. At its base, a 5cm thick moderately indurated nodular hardground is present above the Haven Cliff Hardground (op.cit.), Figure 5.6.

The high clastic component and laterally persistant and accreting hardgrounds are characteristic of the Cenomanian and lower Turonian of south-east Devon. This probably reflects the influence on sedimentation of the high Cornubian Massif to the north-east.

Figure3.3 Location of Shapwick Grange Quarry

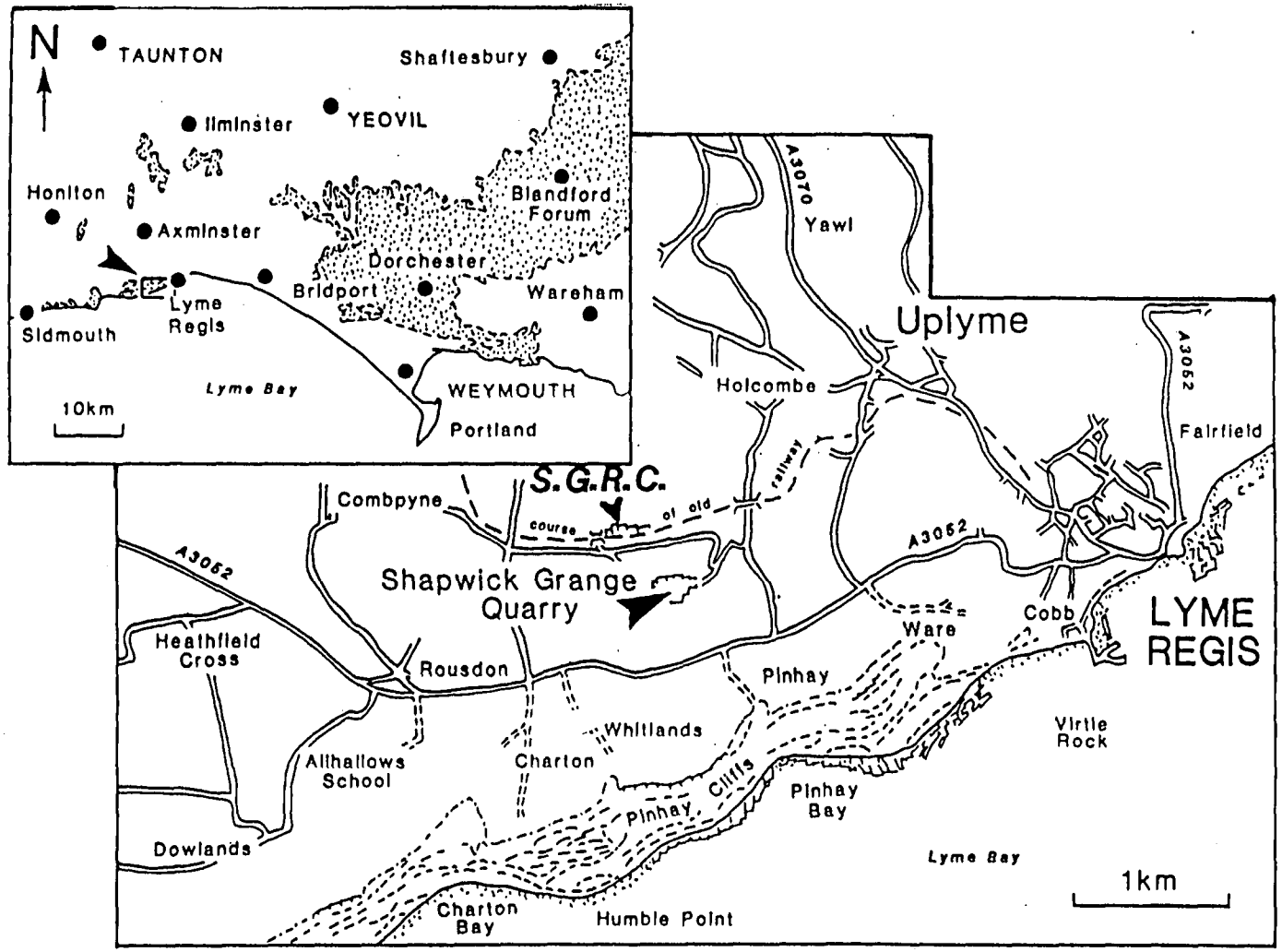

3.4 Southern England onshore Anglo-Paris Basin.

The Cenomanian (65+m) and Turonian (70+m) sequences of S.E England are considerably thicker (Jukes-Browne and Hill, 1903) than those further west and consist of soft white chalks with varying amounts of marl. The early tripartite subdivision of the Chalk Group has recently been revised (Mortimore, 1986; Robinson, 1986) and the relevant lithostratigraphic units, in ascending order, comprise the Abbots Cliff, Plenus Marl and Dover Formations. Four localities (Dover, Figure 3.4; Eastbourne, Figure 3.5; Isle of Wight, Figure 3.6; White Nothe, Figure 3.7) across the interval were sampled.

Only the top few metres of the Abbots Cliff Formation were sampled at all localities. These consist typically of rhythmically bedded chalks and marls (Text Plate 1), often displaying intense bioturbation.

The base of the Plenus Marls is marked by the sub-Plenus erosion surface which can be recognized throughout the Anglo-Paris Basin (Jeffries, 1962, 1963) (Text Plates 2 and 4). In most of the Basin the Plenus Marls consist of 8 distinct units which vary in thickness locally (Text Plates 3 and 4).

The Shakespeare Cliff Formation at Dover consists of finely bedded (0.2-0.3m) nodular chalks containing coarse bioclastic material at its base, expanding into more marly chalks (Text Plate 3). In contrast, the Shakespeare Cliff Formation to the West is more marly (Text Plate 5) throughout.

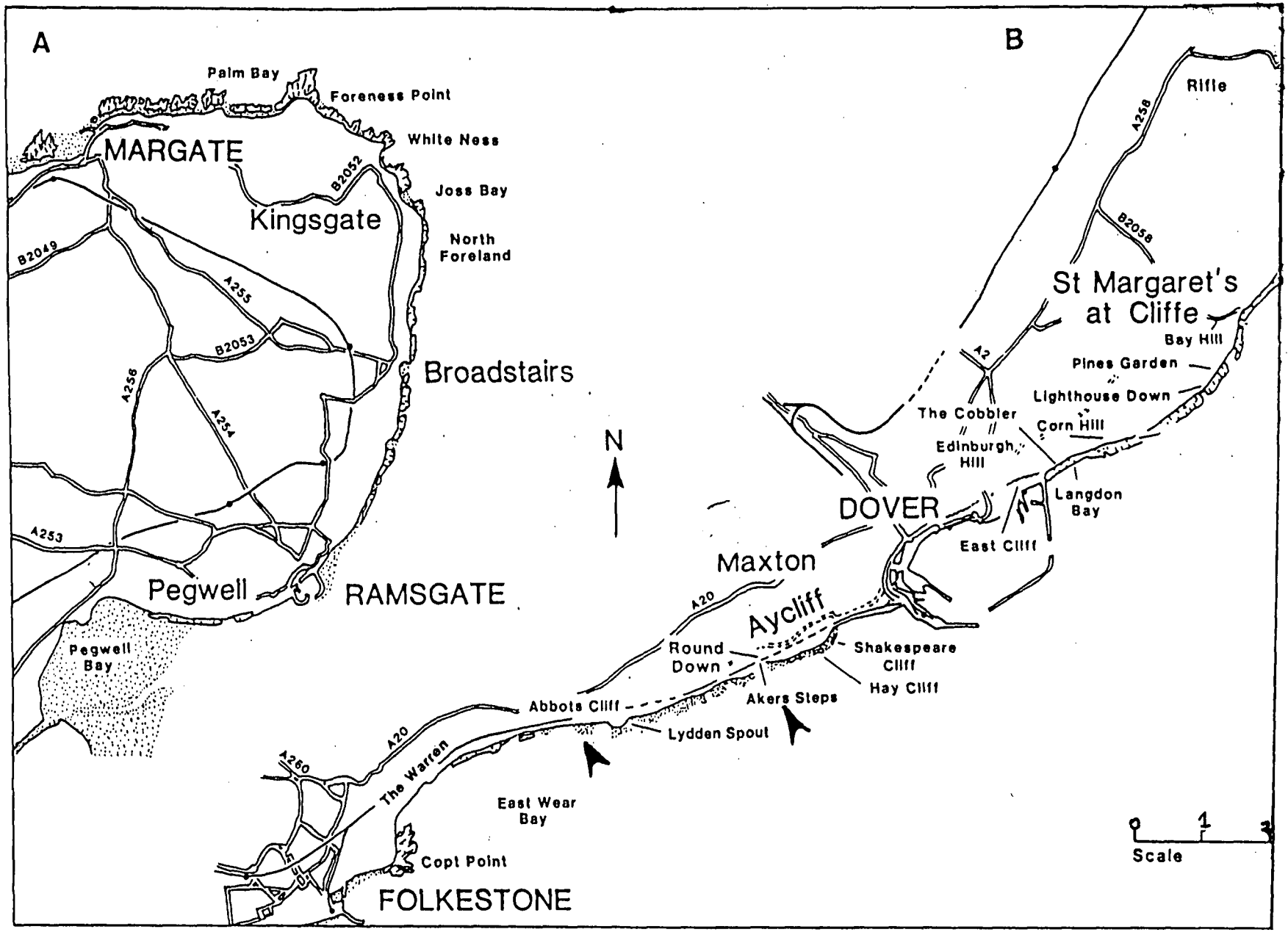

Figure3.4 Location of Dover

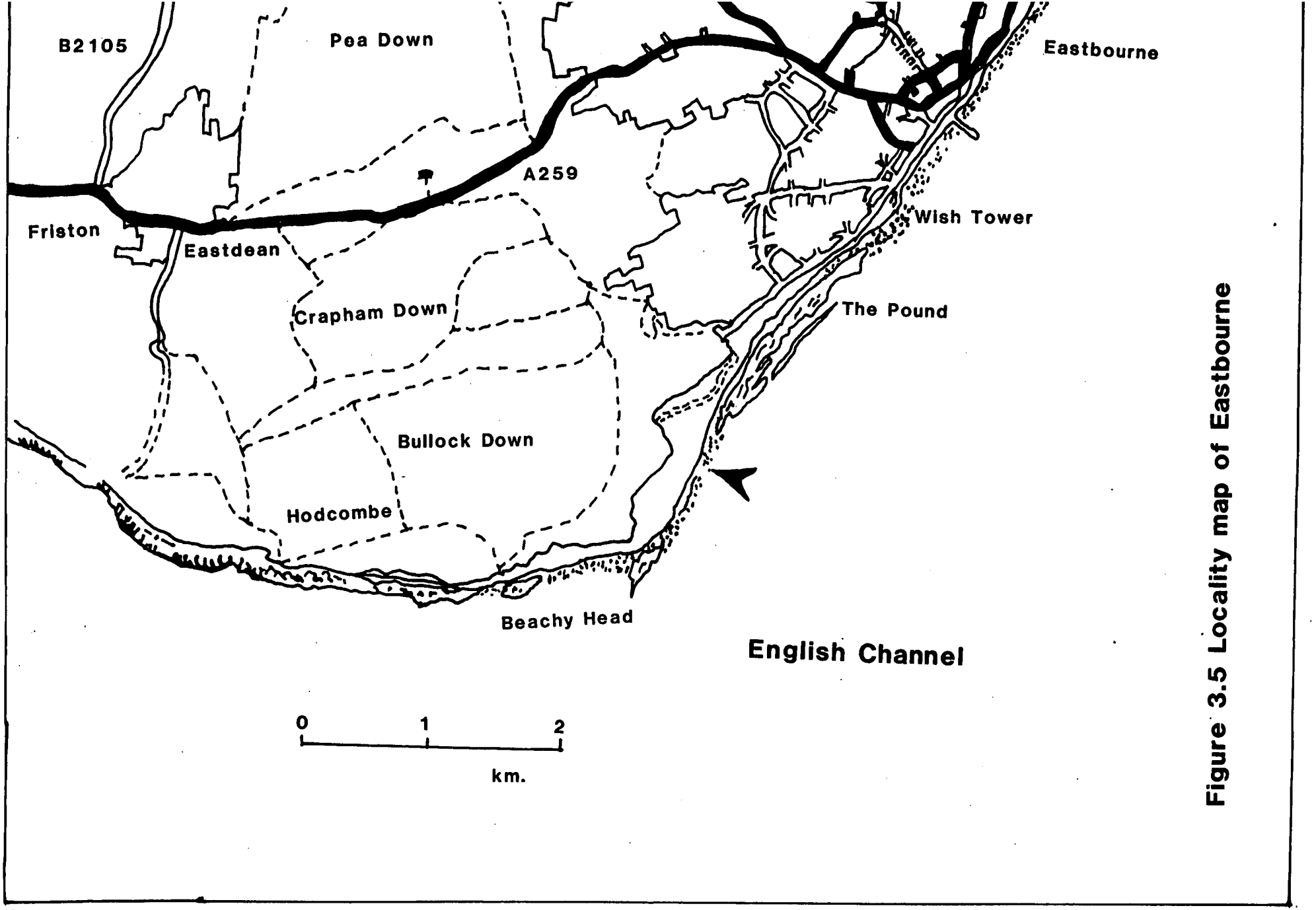

Figure 3.5 Locality map of Eastbourne

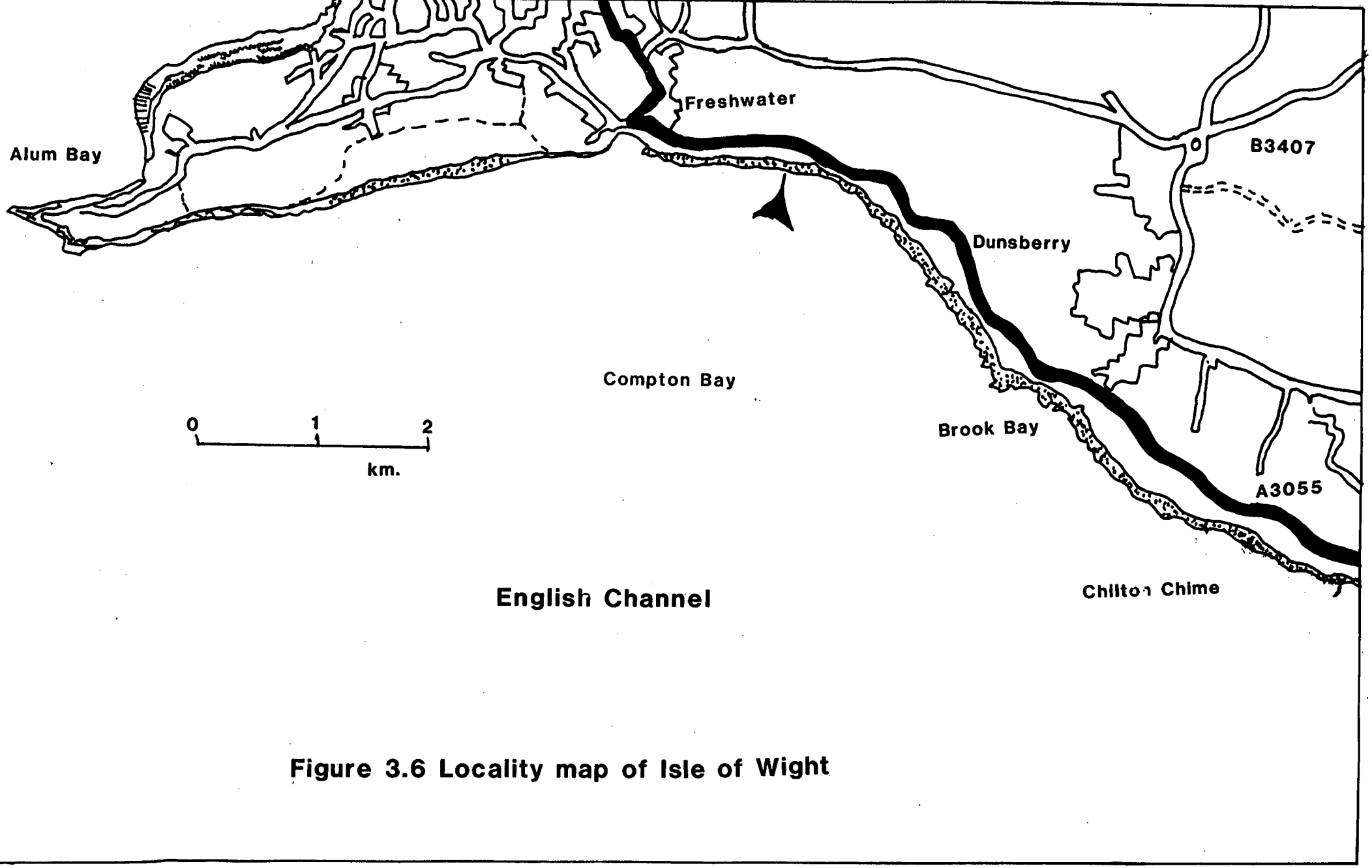

Figure 3.6 Locality map of Isle of Wight

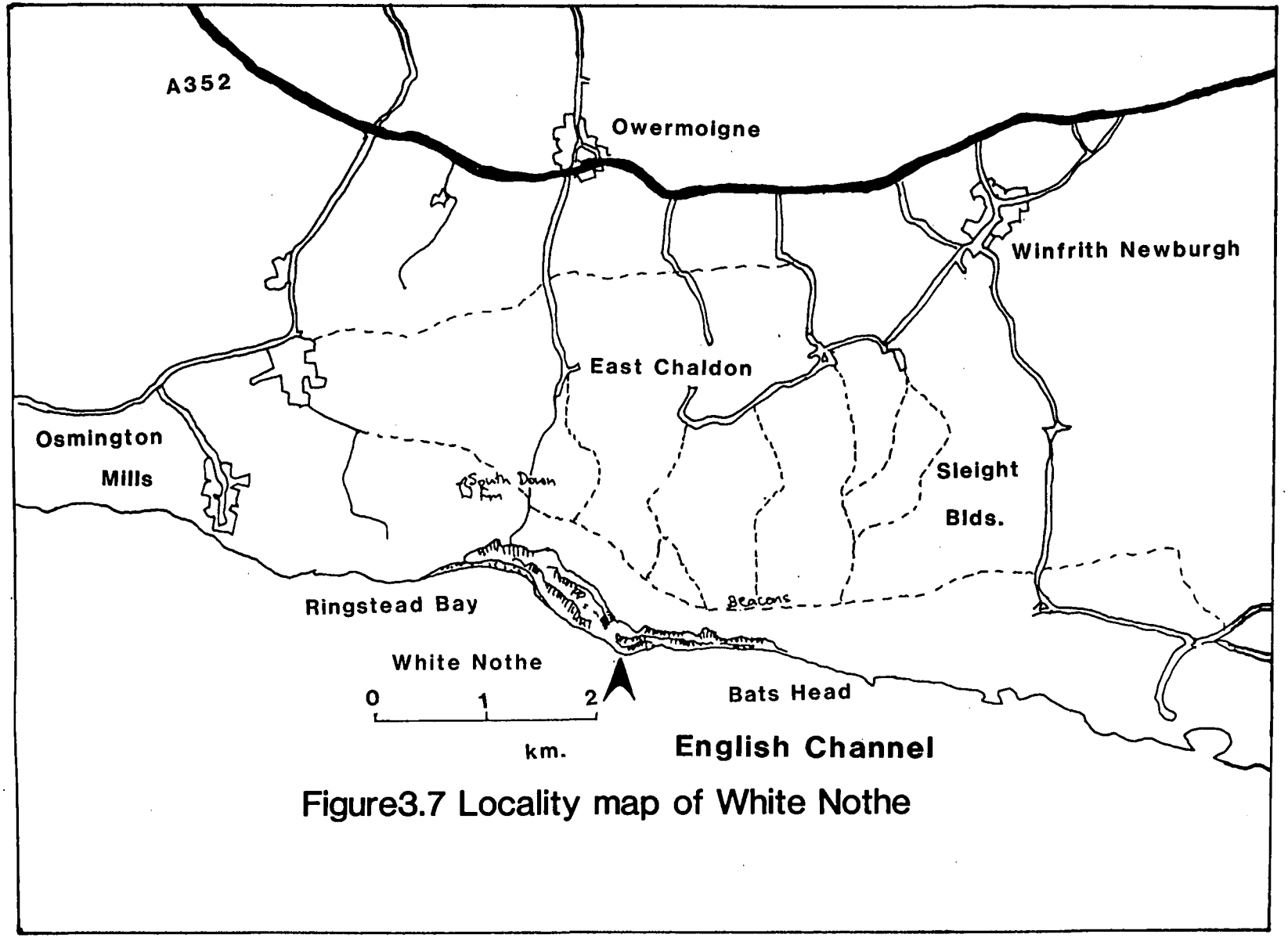

Figure3.7 Locality map of White Nothe

The Dover section is made up of a composite from Abbots and Shakespeare Cliffs.

3.5 The North Sea.

The high degree of lithostratigraphic resolution possible with on-shore sequences is not possible with off-shore material. A standard lithostratigraphic scheme operates in the North Sea (Deegan and Scull, 1977).

The relevant units comprise the Hidra Formation (Cenomanian), Plenus Marl Formation (Late Cenomanian) and Hod Formation (Turonian to Campanian). The Hidra - Plenus Marl formational boundary is marked by a distinctive higher gamma ray response, and the Plenus Marl - Hod formational boundary by a return to the lower gamma ray signature. The latter boundary may be more transitional than the lower one (Deegan and Scull, 1977).

The Sole Pit Basin contains over 1,000m of Upper Cretaceous chalk sedimentation (Hancock, 1983, 1984). BritOil well 48\22-1 is situated at lat.53°15'15"N; long.01°23'08"E (Enclosure 1), and yielded 86m of Upper Cretaceous carbonates. The weak gamma ray response shows that the Plenus Marl Formation is poorly developed at 121m (Figure 5.16). Washed and dried ditch cuttings were analysed from 50m either side of the Plenus Marl Formation.

Text Plate 1.

Top of Abbots Cliff Formation, Gun Gardens (Eastbourne), showing rhythmic sedimentation. The slight colour contrast in the marl highlighting the intense bioturbation.

The Estwing hammer is approximately Ø.3m long.

Text Plate 2.

Abbots Cliff, Plenus Marl and Dover Formations, Compton Bay, Isle of Wight. The figure is pointing to the the sub-Plenus erosion surface.

View looking east.

Text Plate 3.

Plenus Marls and base of Shakespeare Cliff Member (Dover Formation), Abbots Cliff, Dover. The more nodular chalks of the Shakespeare Cliff Member standing proud above the softer Plenus Marls.

The hammer is approximately 0.3m long.

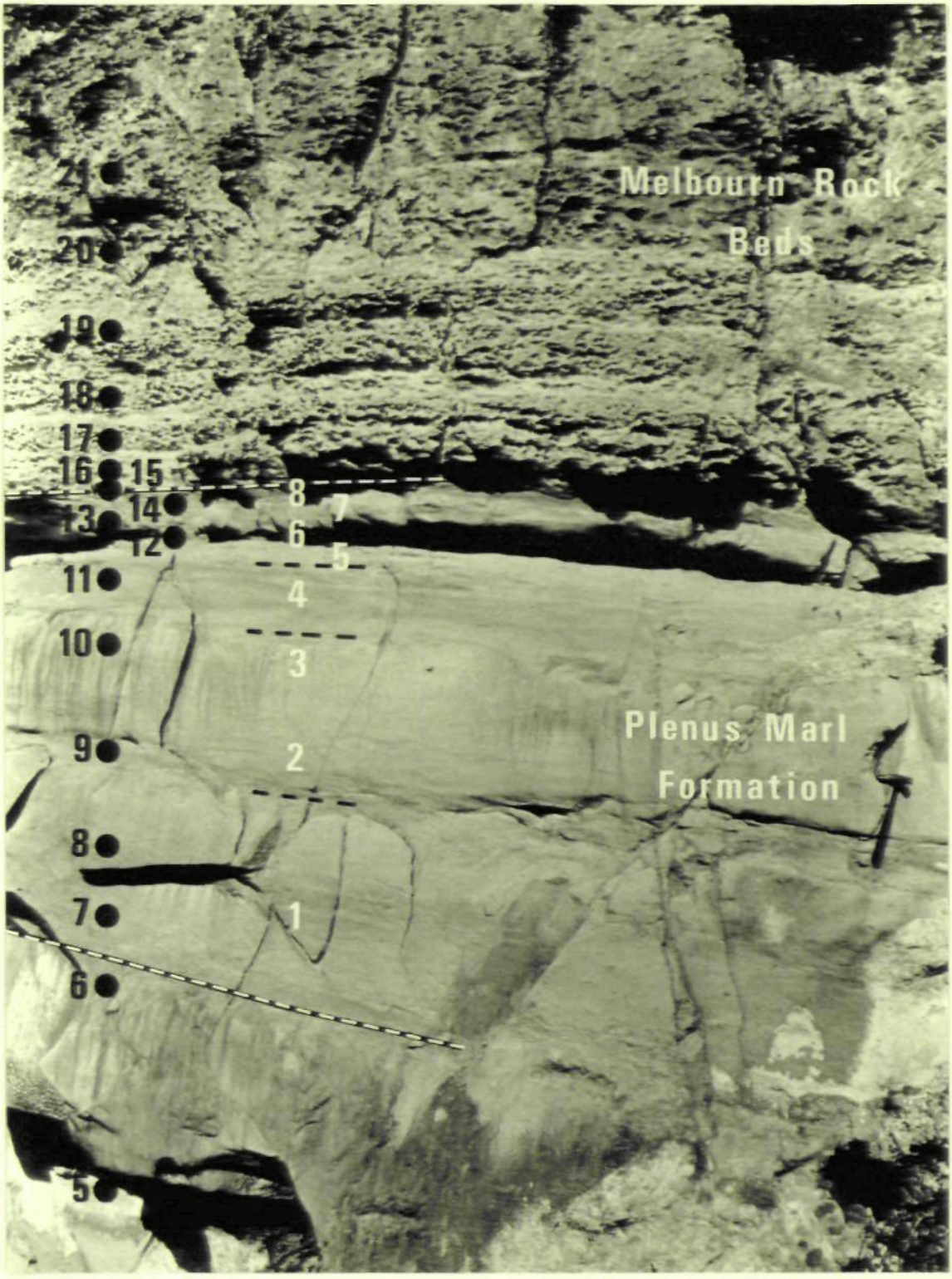
Melbourn Rock Beds
Plenus Marl Formation
21
20
19
18
17
16
15
14
13
12
11
10
9
8
7
6
5
8
7
6
5
4
3
2
1

PhD Thesis by _____

We have given the above thesis the Document Supply Centre identification number:

D 80811

In your notification to Aslib please show this number, so that it can be included in their published Index to Theses with Abstracts.

Theses Office

Text Plate 4.

Plenus Marls and Shakespeare Cliff Formations, Gun Gardens, Eastbourne. The figures' head marks the level of the sub-Plenus erosion surface. The basal beds of the Shakespeare Cliff Formation are of a more marly facies than at Dover (Text Plate 3).

Text Plate 5.

Basal beds of Shakespeare Cliff Formation and top of Plenus Marl Formation, Gun Gardens, Eastbourne. Note the more marly former as opposed to Dover.

Figures' head marks base of Shakespeare Cliff Formation.

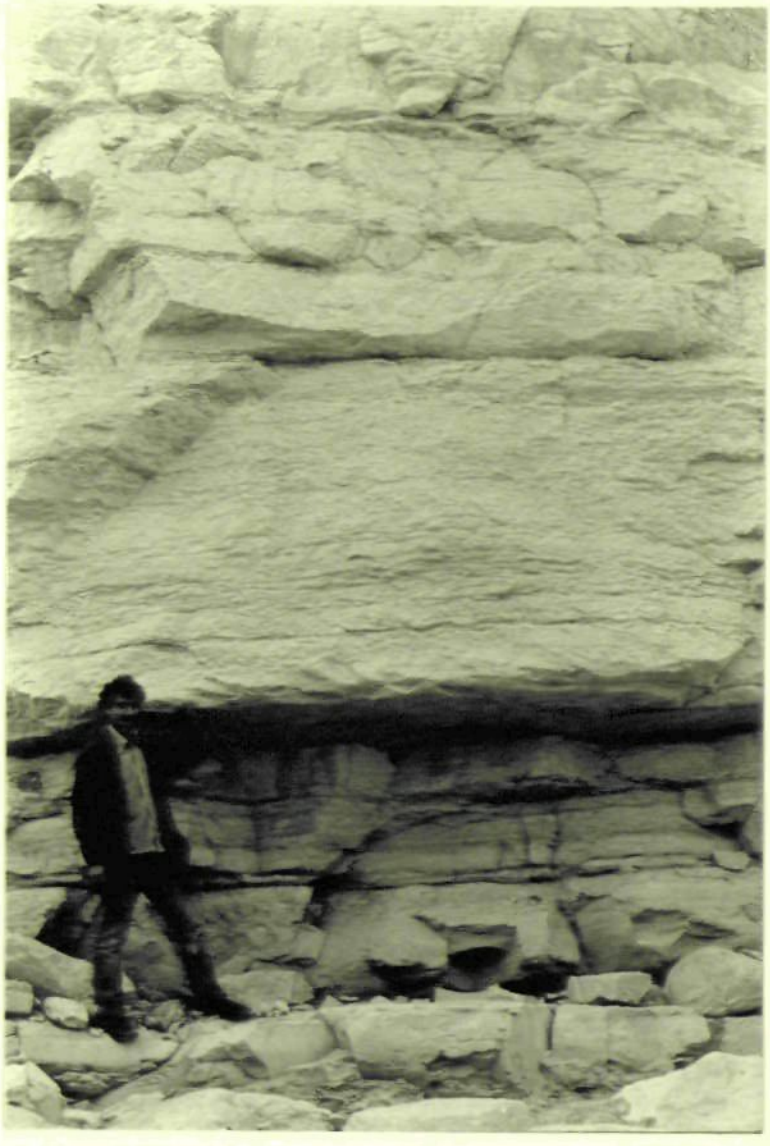

Chapter 4: Systematic micropalaeontology.

For the purposes of this study the basic classification framework of Loeblich and Tappan (1964) has been followed. Minor generic and specific alterations are recommended and are highlighted at the appropriate points in the text.

All groups have been viewed as moving populations and thus many previously established species are viewed as ecophenotypic variations. Where possible, this has been acknowledged but the high degree of subgeneric subdivision in the literature, especially for the Nodosariidae, has meant the adoption of a "local" taxonomy.

The occurrence of each species is listed as a set of the appropriate samples, the exact position of which may be determined by consulting the relevant sedimentary log.

Unlike the previous foraminiferal studies (Hart, 1970; Owen, 1970) with their emphasis on taxonomic relationships, in this study lists of references are kept to a minimum. If a previous published list of references is thought relevant, it is cited.

The taxonomic revision proposed by the European Working Group on planktonic foraminifera (Robaszynski and Caron, 1979) has largely been adopted. Any evolutionary relationships are covered in Chapters 6 and 7.

Order FORAMINIFERIDA Eichwald, 1830

Suborder Textulariina Delage and Herouard, 1896

Superfamily Ammodiscacea Reuss, 1862

Family Ammodiscidae Reuss, 1862

Subfamily Ammodiscinae Reuss, 1862

Genus Ammodiscus Reuss, 1862

Genotype Ammodiscus infimus Bornemann, 1874

Ammodiscus cretaceous (Reuss), 1845

Pl. 1, Figs 1-7.

1845 Operculina cretacea Reuss,p.35,pl.8,figs.64,65.

1860 Cornuspira cretacea (Reuss);Reuss,p.177,pl.1, fig.1a,b.

1934 Ammodiscus cretacea (Reuss);Cushman,p.45.

1946 Ammodiscus cretaceus (Reuss);Cushman,p.17,pl.1,fig.35.

Occurrence: B.P. 93/2-1,6,9; SGQ 7,18; WND 1,2,13,14,19,20,22; CBI 1,4-6,8,17,26,32,35,36; EGG 1,11-15,18,20,25,26,31,32; ABC 4, 9,11,13,19; AKS 8,12,13; BritOil 48/22-1 3-16,18.

Remarks: A. cretaceus shows some small variation in outline from circular to ovoid. The number of whorls may be between 6 to 11 but usually number 8.

Superfamily Lituolacea de Blainville, 1825

Family Lituolidae de Blainville, 1825

Subfamily Lituolinae de Blainville, 1825

Genus Ammobaculites Cushman, 1910

Genotype Spirolina agglutinans D'Orbigny, 1846

Ammobaculites sp.a

Pl. 1, Fig. 8.

Description: The chambers increase moderately in size around the initial planispiral portion of the test but only slightly in the latter uniserial portion. The sutures are markedly depressed. The rounded terminal aperture is large.

Occurrence: WND 10,11; CBI 1,2.

Remarks: The chambers in the uniserial portion of the test may be moderately inflated.

Genus Haplophragmium Maync, 1952

Genotype Haplophragmium aequale Reuss, 1860

Haplophragmium aequale Reuss

Pl. 1, Figs. 9-12

1866 Haplophragmium aequale Reuss,p.218,pl.11,fig.2a.

1946 Haplophragmium aequale Reuss,ten Dam,p.570,pl.87,figs.3-4.

Occurrence: B.P. 93/2-1 1,4,7; WND 1; CBI 5.

Remarks: A very rare species which shows much variation. The later

uniserial portion may be moderately to markedly compressed.

Subfamily Placopsilininae Rhumbler, 1913

Genus Subbdelloidina Frentzen, 1944

Genotype Subbdelloidina haeusleri Frentzen

cf. Subbdelloidina sp.a

Pl.1, Fig. 13

Description: Test finely agglutinated, well rounded chambers with depressed sutures. The chamber size varies slightly.

Occurrence: CBI 4.

Remarks: Only one specimen was found the aperture of which was indistinct.

Family Textulariidae Ehrenburg, 1838

Subfamily Textulariinae Ehrenburg, 1838

Genus Textularia Defrance in de Blainville, 1824

Genotype Textularia saggittula Ehrenburg, 1839

Textularia chapmani Lalicker

Pl. 1, Figs 14,15

Pl. 2, Figs 1-14

Pl. 3, Figs 1-8

1935 Textularia chapmani Lalicker,p.13,pl.2,figs.8,9.

1962 Textularia chapmani Lalicker;Jefferies,pl.78,fig.23.

Occurrence: B.P. 93/2-1 2,7; WND 11,19; CBI 2,12-18; EGG 9-14, 16,17; ABC 8-14; BritOil 48/22-1 8,9.

Remarks: The sutures may be markedly to moderately depressed. The number of chambers varies from 10-15. The aperture may be deep or narrow but is predominantly the former. T. chapmani has been recorded from the rocks of Albian - Cenomanian and Lower Turonian age (Jefferies,1962; Hart,1970; Owen,1970) in southern England. Occasionally, a smaller form, T. minuta Berthelin, has been associated with T. chapmani, in the Plenus Marls (Jefferies, 1962), in the Gault Clay (Hart, 1970). The distinguishing feature of T. minuta being its small size.

A study of the textularid population from Dover, measuring the height and width, (Text Figure 4.1),

Text-figure4.1 Measured characteristcs of ***Textularia chapmani*** Lalicker

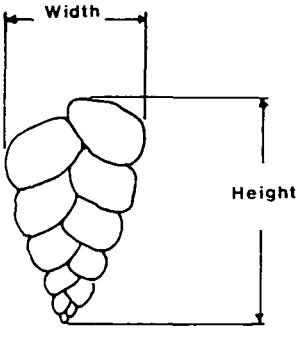

and counting the chambers, shows that there is no simple relationship. The populations from ABC 9-11 show a systematic

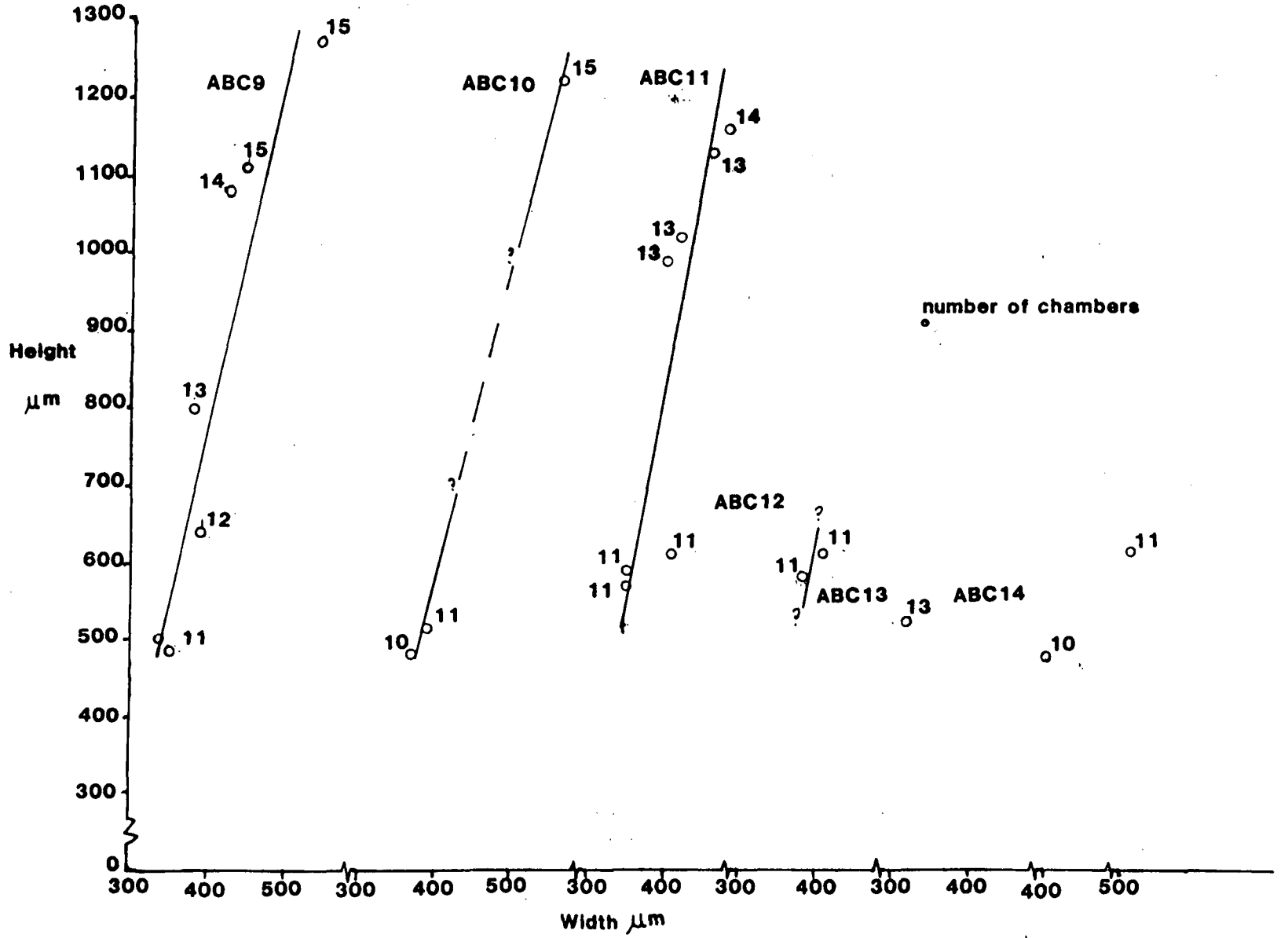

Figure 4.1 Height against width and number of chambers of *Textularia chapmani* Lalicker population from Dover

linear trend with an increase in size with chamber addition. The populations from ABC 12-14 are too small to show any trend but all the forms are the corresponding size for their respective number of chambers as the specimens from ABC 9-11. Except for one specimen from ABC 13 which exhibits the size equivalent to eleven chambers but possesses thirteen.

Thus the smaller forms, referred to as T. minuta are probably immature forms, though there is some evidence of dwarfism in ABC 13. A further study of larger populations and from other localities would be required to completely elucidate any relationships.

Importantly, the moving population does exhibit a reduction in size and a lowering in population numbers.

Subfamily Pseudobolivininae Wiesner, 1931

Genus Pseudobolivina Wiesner, 1931

Genotype Pseudobolivina antarctica

Pseudobolivina sp.a

Pl. 3, Figs 9-10.

Description: Test is coarsely agglutinated, with only the last two chambers tending towards the uniserial form. The test is moderately twisted. The chambers increase moderately in size along the test and the sutures are slightly depressed. The aperture is subrounded, slightly raised and terminally positioned.

Occurrence: Goban Spur 5/2 13-17

Remarks: P. sp.a only appears in one sample and in very small numbers.

Family Trochamminidae Schwager, 1877

Subfamily Trochammininae Schwager, 1877

Genus Trochammina Parker and Jones, 1859

Genotype Nautilus inflatus Montagu, 1801

Trochammina depressa Lozo, 1944

Pl. 3, Fig. 11.

1944 Trochammina depressa Lozo,p.552,pl.2,figs 4-5.

1970 Trochammina depressa Lozo;Owen,p.45,46,pl.3,figs 14-16.

Occurrence: B.P. 93/2-1 2; WND 11; CBI 2,4.

Remarks: T. depressa was only found in small numbers.

Family Ataxophragmiidae Schwager, 1877

Subfamily Verneuilininae Cushman, 1911

Genus Pseudospiroplectinata Gorbenko, 1957

Genotype Pseudospiroplectinata plana Gorbenko

Pseudospiroplectinata plana Gorbenko

Pl. 3, Figs 12-17.

1957 Pseudospiroplectinata plana Gorbenko,p.879,text fig.1,a-c.

1970 Pseudospiroplectinata plana Gorbenko;Owen,p.87-88,pl.9, fig.1-2.

Occurrence: WND 2-6,8,9; CBI 1,10,15; EGG 2-7; ABC 7,8.

Remarks: The initial chambers may be in the same plane as the rest of the test or offset at an angle of 40°. The test is not always totally planar but may be slightly twisted. The number of chambers in the later uniserial portion of the test varies greatly. The aperture may be ovate to subrounded.

Genus Tritaxia Reuss, 1860

Genotype Textularia tricarinata Reuss, 1844

Tritaxia macfadyeni Cushman

Pl. 4, Figs 1-13.

1936 Tritaxia macfadyeni Cushman,p.3,pl.1,fig.6a-b.

1948 Tritaxia macfadyeni Cushman;Williams-Mitchell,p.48,pl.8, fig.2.

1953 Tritaxia macfadyeni Cushman;Barnard and Banner,p.195,pl.7, fig.2a-b.

Occurrence: Goban Spur 6/2 70-72, 26-29; 6/1 30-33; 5/2 13-17; 5/1 101-106; BSA 1; WND 1,2,4,6,10; CBI 1,4,5,8-10; EGG 1,2,4,7-9; ABC 1,2,4,5,7,8.

Remarks: T. macfadyeni varies in the number of chambers present in the late stage, uniserial portion, of the test, though most specimens have 3-4 chambers. In addition, these chambers may not be added along the same axis, forming a twisted test.

Tritaxia pyramidata Reuss

Pl. 4, Fig. 3.

1862 Tritaxia pyramidata Reuss,p.32,88,fig.9a-c.

1928 Tritaxia pyramidata Reuss;Franke,p.138,pl.7,fig.18a-c.

1948 Tritaxia pyramidata Reuss;Williams-Mitchell,p.98,pl.8, fig.5a-c.

1950 Tritaxia pyramidata Reuss;ten Dam,p.12-13.

1953 Tritaxia pyramidata Reuss;Barnard and Banner,p.195,pl.7, fig.1a-b.

Occurrence: B.P. 93/2-1 1; BSA 4; WND 1-11; CBI 1-11; EGG 1-10; ABC 1-6; BritOil 48/22-1 8.

Remarks: T. pyramidata is very distinctive and forms the dominant proportion of the Tritaxia population until its extinction when T. tricarinata takes over.

Tritaxia tricarinata (Reuss) Reuss, 1860

Pl. 5, Figs. 1-7.

1844 Textularia tricarinata Reuss,p.215.

1845 Textularia tricarinata Reuss;Reuss,p.39,pl.8,fig.60.

1860 Tritaxia tricarinata (Reuss);Reuss,p.228,pl.7,figs 1,2.

1937 Tritaxia dubia (Reuss);Cushman,p.26,pl.4,figs 1-4.

1953 Tritaxia tricarinata (Reuss);Barnard and Banner,p.193, pl.8,fig.1a-e,text fig.3a-j.

1966 Tritaxia tricarinata (Reuss);Butt,p.171,pl.1,fig.1.

Occurrence: Goban Spur 5/2 13-17; BSA 6; SGQ 8,9,12-17,19,20,23; WND 14; CBI 11,17,26,28; EGG 11-17; ABC 5-9,19; AKS 1.

Remarks: Through the Plenus Marls the overall test form of T. tricarinata varies (Pl.5, Figs.1-7), with a decrease in the concavity of the test sides and a general rounding of the overall test. Banner and Desai (1985) postulate the phylogenic relationship of T. pyramidata - T. tricarinata but the populations over this interval indicate that they are distinct, although it is possible that this is manifested in specimens from older rocks.

Tritaxia tricarinata var. jongmansi

Pl. 5, Figs. 8-15.

1946 Tritaxia compressa Schijfsma,(non Egger 1899-1900),p.33, pl.1,fig.5a-b.

1950 Tritaxia jongmansi Schijfsma (nom.nov. for T.compressa Schijfsma (1946)),p.43.

1953 Tritaxia jongmansi Schijfsma;Barnard and Banner,p.195-196, pl.8,fig.2a-b,text fig.3k-l.

Occurrence: BSA 10,11; WND 19,21-29; CBI 29,31,34,35; EGG 25,

30-34; AKS 10-12; BritOil 48/22-1 19.

Remarks: T. tricarinata var jongmansi differs from T. tricarinata by the abrupt termination of the test giving it a wider test approximately three-quarters of the way down.

Subfamily Globotextulariinae Cushman, 1927

Genus Arenobulimina Cushman, 1927

The arenobuliminid group has recieved much attention. The European Albian lineages were established as A. chapmani Cushman giving rise to A. frankei Cushman, A. truncana (Reuss), A. obliqua (d'Orbigny) and A. advena (Cushman) in a late Albian radiation. This scenario was confirmed, with minor extinctions and no evolutionary radiations through the Cenomanian, except for the development of A. preslii (Reuss) from A. advena just below the Plenus Marls (Carter and Hart, 1977).

The differentiation of simple interiored forms (under Arenobulimina s.s) and those with partitions (under A. (Voloshinoides))(Barnard and Banner, 1980), has not been adopted as partitions are difficult to differentiate and their development appears highly variable.

Genotype Bulimina preslii Reuss, 1846

Arenobulimina advena Cushman, 1936

Pl. 6, Figs 5-8.

1936 Hagenowella advena Cushman,p.43,pl.6,fig.21a-b.

1969 Arenobulimina advena (Cushman);Gawor-Biedowa,p.86-90.

1977 Arenobulimina advena (Cushman);Carter and Hart,p.14,pl.2, fig.4.

Occurrence: Goban Spur 6/2 26-29; B.P. 93/2-1 1-4,6,8; BSA 5; WND 1-5,7-10; CBI 1,2,5,6,9,10; EGG 1,3,5,6; ABC 1,2,4,6,7; BritOil 48/22-1 1,2,10,11,13.

Arenobulimina bulletta (Barnard and Banner)

Pl. 6, Figs 1-4.

1980 Arenobulimina (Voloshinoides) bulletta (Barnard and Banner), p.408-410,pl.3,figs 1-6;pl.6,figs 14-20.

Occurrence: ABC 1.

Remarks: A. bulletta is highly distinctive because of its large size and bullet-like test shape. Its appearance is spasmodic and its relationship to the A. advena - A. preslii plexus is unclear.

Arenobulimina preslii (Reuss)

Pl. 6, Figs 9-10.

1845 Bulimina preslii Reuss,p.38,pl.13,fig.72.

1934 Arenobulimina preslii (Reuss);Cushman and Parker,p.29,Pl.5, figs 12-13.

Occurrence: B.P. 93/2-1 10-12; CBI 32,34-36; EGG 22,30-34; AKS 2; BritOil 48/22-1 19.

Remarks: This morphotype with a flattened apertural face and inflated chambers is characteristic of the early Turonian (Owen, 1970).

Arenobulimina sp.a

Pl. 6, Figs 11-12.

Description: Test is small and coarsely agglutinated, the chambers increase rapidly in size giving the test an inflated subtriangular appearance. The aperture is small and depressed.

Occurrence: BSA 3-5; WND 3-5,8; CBI 5-10; EGG 2-4,13;ABC 4.

Remarks: A. sp.a occurs as a minor portion of the A. advena population but is very small in comparison. It may well be a variant of that population or the megalosperic form of A. advena (Carter and Hart, 1977).

Genus Dorothia Plummer, 1931

Genotype Gaudyrina bulleata Carsey, 1926

Dorothia gradata (Berthelin)

Pl. 6, Figs 13-14.

1880 Gaudrina gradata Berthelin,p.24,pl.1,fig 6a-b.

1937 Dorothia gradata (Berthelin);Cushman,p.74,pl.8,fig 5a-b.

1950 Dorothia gradata (Berthelin);ten Dam,p.16.

1970 Dorothia gradata (Berthelin);Hart,p.110-111,pl.5,figs 1-2.

Occurrence: WND 1-11; CBI 1-6,8-10; EGG 1-7; ABC 1.

Remarks: It is only present in very small numbers and forms a minor portion of the benthonic population.

Genus Marssonella Cushman

Genotype Gaudyrina oxycona Reuss, 1860.

Marssonella sp.a

Pl. 7, Figs 1-8.

Description: The initial portion of the test is sub-triangular passing into a sub-ovate form in cross-section. The sutures are depressed.

Occurrence: WND 11-19; CBI 11-18;EGG 9-17; ABC 8-14.

Remarks: M. sp.a forms a major portion of the marssonellid population within beds 2-8 of the Plenus Marl Formation.

Marssonella trochus (d'Orbigny) 1840

Pl. 7, Figs 9-16.

Pl. 8, Figs 1-2.

1840 Textularia trochus d'Orbigny,p.45,pl.4,fig 25-26.

1937 Marssonella oxycona (Reuss);Cushman,p.58,pl.6,fig 6-7,16.

Occurrence: Goban Spur 6/2 70-72; B.P. 93/2-1 7,8; BSA 7-8; WND 2,12,14,16,23,24; CBI 2-4,6,11,14,16-18,22,24; EGG 2,10,14,16,19, 22,26,27,29; ABC 2,3,5,8,9; AKS 6,10,11,13; BritOil 48/22-1 4,14, 19.

Remarks: The distinction of M. trochus, M. turris and M. oxycona is largely based on the apical angle: M. oxycona with an angle>45° and M. turris with an angle<45°, (Owen, 1970). This is a function of the rate of increase in chamber height with respect to width as they are added around the test, M. trochus being distinguished by the development of slight concavity when viewed in side view. The closeness between these forms has been noted (Barnard and Banner, 1953; Hart, 1970), with their synonomy under M. trochus.

A scanning electron microscopy study was made of the marssonellid population from Dover. For each specimen the maximum apical angle was measured, as not all specimens were circular in cross-section and plotted against the outcrop (Figure 4.2), and an apical angle frequency was constructed (Figure 4.3). Figure 4.3 shows that the subdivision of the marssonellid population on the basis of the apical angle is artificial and that the apical angle of the population varies consistantly through the section. The "early" forms in each population possess a narrow apical angle, with the development of the population the apical angle increases and decreases as the population wanes. It indicates that there may be several periods of recolonization of the niche after vacation (Figure 4.2).

M. trochus has precedent over M. turris and M. oxycona

Figure 4.2 Apical angle of Marssonellid population from Dover

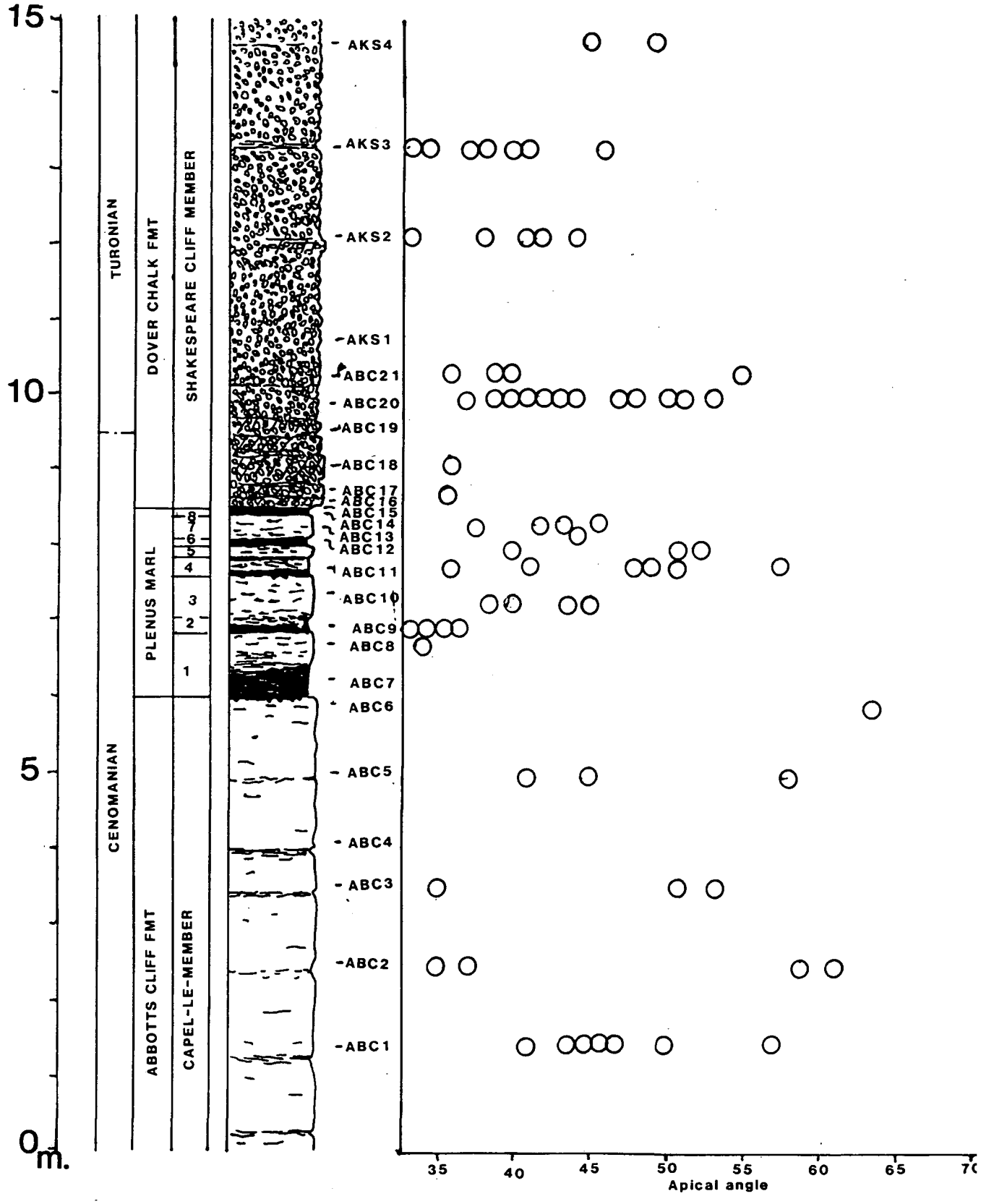

Figure 4.2 Apical angle of Marssonellid population from Dover(cont.)

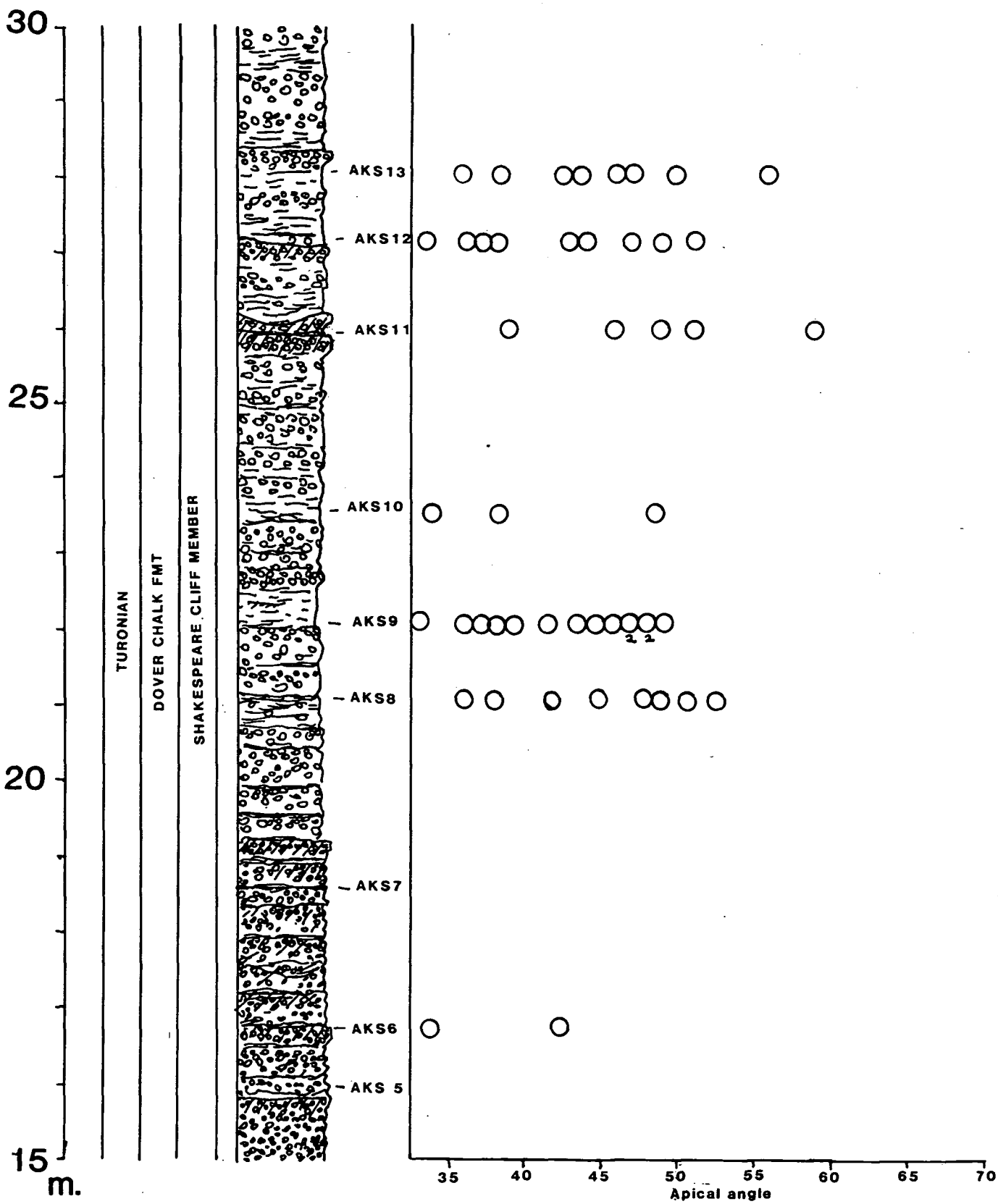

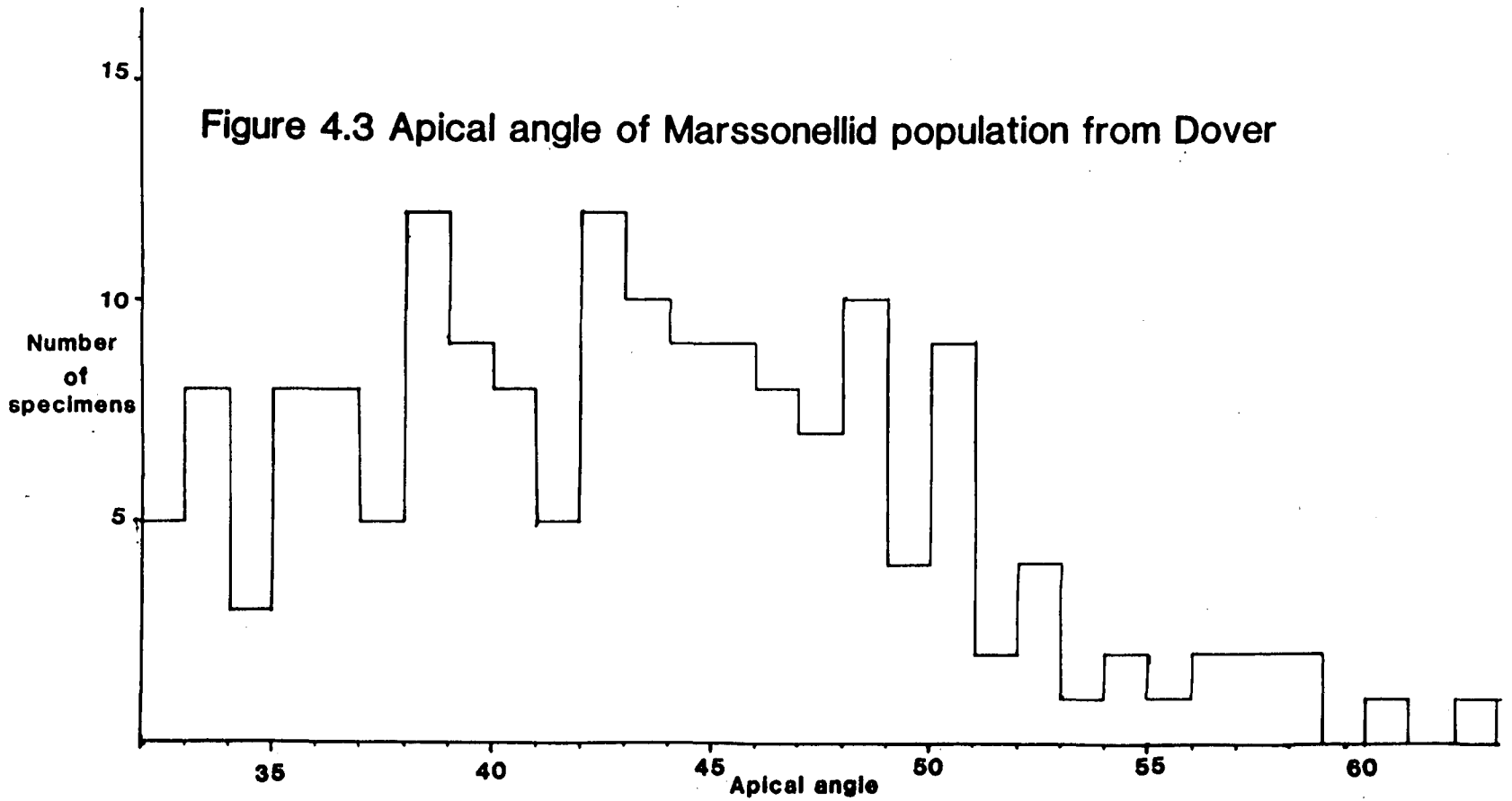

Figure 4.3 Apical angle of Marssonellid population from Dover

but to note the relevant dominance of each morphotype it is proposed to place M. turris and M. oxycona as varieties of M. trochus.

Marssonella. trochus var. oxycona

Pl. 8, Figs 7-9.

Pl. 9, Figs 11-16.

1860 Gudryina oxycona Reuss,p.229,pl.12,fig.3.

1937 Marssonella oxycona (Reuss);Cushman,p.56,pl.6,figs 6-7.

Occurrence: Goban Spur 6/2 70-72; 5/2 13-17; B.P. 93/2-1 2-4,6,7, 9,11-15; BSA 10-13; SGQ 8,9,12-17; WND 1-3,5,6,8,22,23,25,26,28; CBI 4,10,14,16,18,19; EGG 2,3,14,15,19,22,26,27,30,33,34; ABC 1-3, 5,6,11,12,21; AKS 1,5,6,9-11; BritOil 48/22-1 12.

Marssonella. trochus var. turris

Pl. 8, Figs 3-6.

Pl. 9, Figs 1-10.

1840 Textularia turris d'Orbigny,p.46,pl.4,figs 22,28.

Occurrence: Goban Spur 5/2 13-17; B.P. 93/2-1 1-3,5,6,11-14; BSA 3-8,10,11; SGQ 7,8; WND 1-10,13,15-29; CBI 2-6,8,10-14,18-23, 24; EGG 1-5,11-15,17,19-26,28,29,31-34; ABC 1-3,5,8-14,19,21; AKS 1,3-5,7,9-13; BritOil 48/22-1 1,2,5,7,9,11,13,14,16.

Genus Eggerellina Marie, 1941

Genotype Bulimina brevis d'Orbigny, 1840

The specific subdivision of Eggerellina in the mid-Cretaceous has proved problematic, with consistant morphotypes through the Albian - Cenomanian and Turonian but with a proliferation of forms in the Plenus Marls (Carter and Hart, 1977). Carter and Hart (1977) placed emphasis on this short term proliferation and interpreted all the forms as ecophenotypic variations of E. mariae ten Dam. As this study is primarily concerned with the late Cenomanian the approach of Owen (1970) has been adopted.

Eggerellina brevis (d'Orbigny) var. conica Marie

Pl. 10, Figs 1-6.

1941 Eggerellina brevis (d'Orbigny) var. conica Marie,p.34, pl.7,fig.70.

1970 Eggerellina brevis (d'Orbigny) var. conica Marie;Owen, p.63-64,pl.5,figs 6-9.

Occurrence: Goban Spur 6/2 70-72; B.P. 93/2-1 8; WND 3,5-8,14-16; CBI 2-6,10-13,15-18; EGG 9,10,12,14; ABC 1-3,5,7-12.

Remarks: E. brevis (d'Orbigny) var. conica Marie occurs in very large numbers in some samples from the Plenus marls. The variability in the size and shape of the aperture noted by Owen (1970), has been bourne out in this study.

Eggerellina mariae ten Dam, 1950

Pl. 10, Figs 7-9.

1950 Eggerellina mariae ten Dam,p.15-16,pl.1,fig.17.

Occurrence: B.P. 93/2-1 1,4-8; WND 3,6,8,11,13-17; CBI 1-2,6, 11-14,16-20;EGG 4,5,10-14,16; ABC 1-3,5-7,9-12; BritOil 48/22-1 7,9.

Eggerellina murchisoniana (d'Orbigny), 1840

Pl. 10, Figs 10-11.

1840 Bulimina murchisoniana d'Orbigny,p.41,pl.4,fig.15.

1953 Eggerellina intermedia (Reuss);Barnard, in Barnard and Banner,p.203.

1970 Eggerellina murchisoniana (d'Orbigny);Owen,p.64-65,pl.6, figs 1-4.

Occurrence: ABC 10,11.

Remarks: E. murchisoniana only occurs in small numbers when present.

Subfamily Valvulininae Berthelin, 1880

Genus Plectina Marsson, 1878

Genotype Gaudyrina ruthenica Reuss, 1851

Plectina mariae (Franke)

Pl. 11, Figs 1-2.

1928 Gaudyrina ruthenica Reuss var. mariae Franke,p.146,pl.13, fig.15a-b.

1937 Plectina ruthenica (Reuss) var. mariae (Franke);Cushman, p.106,pl.11,fig.15.

1970 Plectina mariae (Franke);Owen,p.84-86,pl.9,figs 4-7,text fig.32.

Occurrence: B.P. 93/2-1 6-8; BSA 3; WND 3-10; CBI 1-6,9,10; EGG 2,4-9; ABC 1-3; BritOil 48/22-1 15,16,17.

Remarks: The variability in the size, shape and position of the aperture as noted by Owen (1970), has been bourne out in this study.

Plectina cenomana (Carter and Hart)

Pl. 11, Figs 13-14.

1970 "Plectina" sp.21, sp.nov. Hart,p.114,pl.5,fig.12.

1977 Plectina cenomana Carter and Hart,p.12-13,pl.2,fig.9.

Occurrence: WND 3,6,7,10,12; CBI 2-7; EGG 1,5-10; ABC 5,7,8.

Remarks: P. cenomana occurs after the disappearance of P. mariae. It may be an ecophenotypic variation of the latter, but has been noted from lower in the Cenomanian (zones 11-13 of Carter and Hart, 1977).

Subfamily Ataxophragmiinae Schwager, 1877

Genus Ataxophragmium Reuss, 1860

Genotype Bulimina variabilis d'Orbigny, 1840

Ataxophragmium depressum (Perner) 1892

Pl. 12, Figs 1-11.

1892 Bulimina depressa Perner,p.55,pl.3,fig.3a-b.

1964 Ataxophragmium depressum (Perner);Loeblich and Tappan, p.C283,fig.191.3,4.

Occurrence: B.P. 93/2-1 4; BSA 4,6; WND 1; CBI 1,4,9,10; EGG 8; ABC 3,5-8.

Remarks: A. depressum first appears in the very top of the Abbots Cliff Formation with small and rare specimens, increasing rapidly both in the size of the specimens and abundance in bed 1 of the Plenus Marls to disappear at the top of bed 1.

Family Pavonitinidae Loeblich and Tappan, 1961

Subfamily Pfenderininae Smout and Sugden, 1962

Genus Pseudotextulariella Barnard, in Barnard and Banner.

Genotype Textulariella cretosa Cushman, 1932

Pseudotextulariella cretosa (Cushman), 1932

Pl. 13, Figs 1-3.

1926 Textulariella cretosa Cushman,p.97,pl.11,figs 17-19.

1953 Pseudotextulariella cretosa (Cushman);Barnard (in Barnard and Banner),p.198,fig.6b-c.

1977 Pseudotextulariella cretosa (Cushman);Carter and Hart,p.23, pl.2,fig12.

Occurrence: B.P. 93/2-1 2; BSA 1,3,5,6; BritOil 48/22-1 6-8,10, 11,13.

Remarks: P. cretosa is particularly common in the lower levels of the Cenomanian (Hart, 1970; Carter and Hart, 1977). It only occurs in very small numbers in the Upper Cenomanian and the specimens were much smaller than those described (op cit.).

Suborder Miliolina Delage and Herouard, 1896

Superfamily Miliolacea Ehrenburg, 1839

Family Nubeculariidae Jones, 1875

Subfamily Quinqueloculininae Cushman, 1917

Genus Quinqueloculina d'Orbigny, 1826

Genotype Serpula seminulum Linne, 1758

Quinqueloculina antiqua Franke

Pl. 13, Figs 4-5.

1891 Miliolina venusta Karrer;Chapman,p.9,pl.9,figs 5-6.

1928 Miliolina (Quinqueloculina) antiqua Franke,p.126,pl.11, fig.26.

Occurence: B.P. 93/2-1 6; WND 4; CBI 17,19,20,22,24,32; EGG 5; BritOil 48/22-1 15,16.

Remarks: Q. antiqua occurs in very small numbers when it is present.

Suborder Rotaliina Delage and Herouard, 1896

Superfamily Nodosariacea Ehrenburg, 1838

Family Nodosariidae Ehrenburg, 1838

Subfamily Nodosariinae Ehrenburg, 1838

Genus Nodosaria Lamarck, 1812

Genotype Nautilus radicula Linne, 1758

Nodosaria sp.a

Pl. 13, Figs 6-15.

Description: The chambers may be rounded, or flush, with depressed or indistinct sutures. The chambers may increase slightly in size in both width and length on addition. The aperture may be radiate and well-developed, but many forms possess indistinct apertures or with subordinate rays.

Occurrence: Goban Spur 6/2 70-72; 6/2 26-29; B.P. 93/2-1 2,9; WND 1,2,5,6,8; CBI 1,2,5,6,10,12,14,16,17; EGG 3-7,11,14; ABC 3-5, 8,10; BritOil 48/22-1 2.

Remarks: The variability in test size, chamber addition, sutures, chamber shape and the development of the aperture affords little systematic subdivision of N. sp.a.

Genus Astacolus De Montfort, 1808

Genotype Astacolus crepidulatus De Montfort, 1808

Astacolus sp.a

Pl. 14, Figs 1-2.

Description: The test is slightly compressed with a sub-triangular terminal chamber. The sutures are moderately depressed and subtended at around 40° to the test. The aperture is well-developed with equal rays.

Occurrence: CBI 13; EGG 10,13; ABC 4,8.

Genus Dentalina Risso, 1826

Genotype Nodosaria (Dentaline) cuvieri d'Orbigny, 1826

Dentalina sp.a

Pl. 14, Figs 3-6.

Description: The chambers increase moderately in size on addition, dominantly lengthways as opposed to width. The sutures are strongly depressed and at 90° to the test.

Occurrence: CBI 7,8; EGG 6; ABC 4.

Remarks: D. sp.a is markedly smaller than D. sp.b and D. sp.c.

Dentalina sp.b

Pl. 14, Figs 7-15.

Description: The chambers are slightly longer than wide giving the test an elongate appearance. The chambers vary in their relative increase in size on addition. The sutures are moderate to well-depressed. The apertural region may be rounded to sub-angular with an equi-ray aperture.

Occurrence: WND 3; CBI 1,3,5,6,8,10,12,14; EGG 3,5,7,11-14; ABC 5, 7-10.

Remarks: D. sp.b is more common than D. sp.a and D. sp.c and formed the dominant morphotype in the Dentalina population.

Dentalina sp.c

Pl. 14, Figs 16-18.

Description: The chambers increase moderately in size on addition, with well-rounded form on the more arcuate side of the test. The sutures are subtended at a low angle (15°- 20°) to the test and are moderately depressed. The aperture is well pronounced radiate.

Occurrence: WND 2; CBI 1,2,6,8,10,12,18; EGG 5,13-15; ABC 8.

Genus Frondicularia Defrance in d'Orbigny, 1826

Genotype Renulina complanata Defrance, 1824

Frondicularia cordai Reuss, 1844

Pl. 15, Fig. 1.

1844 Frondicularia cordai Reuss,p.302.

1970 Frondicularia cordai Reuss;Hart,p.136,pl.9,fig.12.

Occurrence: EGG 2,11; ABC 5.

Remarks: F. cordai is extremely rare in the sections studied but is more common in the early Cretaceous (Hart, pers. comm.).

Frondicularia gaultina Reuss, 1860

Pl. 15, Fig. 2.

1860 Frondicularia gaultina Reuss,p.194,pl.5,fig.5.

1970 Frondicularia gaultina Reuss;Hart,p.136-137,pl.9,fig.13.

Occurrence: WND 13,24; CBI 2,9,11,14; EGG 10,13; ABC 3,21; AKS 3, 8,9,13.

Remarks: F. gaultina was recorded only in the Middle to Upper Albian clays by Hart (1970) and is very rare in the late Cenomanian.

Frondicularia sp.a

Pl. 15, Figs 3-4.

Description: The test is gradually tapering with the new chambers widening along their length. The sutures may be very prominent.

Occurrence: WND 5,10,13,14; CBI 36; EGG 5,6,8; AKS 11.

Remarks: In keeping with the other representatives of the genus, F. sp.a is very rare.

Genus Lagena Walker and Jacob in Kanmacher,1798

Genotype Serpula (Lagena) sulcata Walker and Jacob,1798

Lagena sp.a

Pl. 15, Figs 5-6.

Description: The test is nearly spherical and highly perforate. The aperture is placed on a thick, gradually tapering neck.

Occurrence: Goban Spur 6/2 70-72

Genus Lenticulina Lamarck, 1804

Genotype Lenticulites rotulata Lamarck, 1804

Lenticulina ovalis (Reuss) 1845

Pl. 15, Figs 7-9.

1845 Cristellaria ovalis Reuss,p.34,pl.12,fig.19,Pl.13,fig.62.

1941 Lenticulina ovalis (Reuss);Marie,p.99,pl.9,fig.103.

Occurrence: AKS 6.

Remarks: L. ovalis is most distinctive because of its large proloculus leading to uninflated chambers giving it a pyramidal

form. It may well be an extreme form of the L. rotulata var. b population.

Lenticulina rotulata var. a

Pl. 15, Figs 10-11.

Pl. 16, Figs 1-6.

Description: The swept back sutures are slightly thickened and raised forming slightly concave chambers. This produces a slight squaring of the chambers in peripheral view.

Occurrence: BSA 3,4; WND 1-3,6,10,12,25; CBI 1,2,4,9,10,12,14-16; EGG 1,2,4,7; ABC 1,3-10; AKS 5,11-13; BritOil 48/22-1 6.

Remarks: The raised ribs and squaring of the chambers distinguishes L. rotulata var. a. from L. rotulata var. b. In addition, the latter is predominantly thinner when viewing the apertural face.

Lenticulina rotulata var. b

Pl. 16, Figs 7-12.

Pl. 17, Figs 1-12.

Description: The test surface is smooth with a smooth periphery. The degree of enrollment of the test varies considerably as does the height to width ratio. The angle of the test at the periphery is predominantly narrow forming a slight keel.

Occurrence: Goban Spur 6/2 70-72; 26-29; 6/1 30-33; 5/2 13-17; B.P. 93/2-1 1,4,8-10; BSA 5,6,8,10,12; SGQ 8,12-17,19-21,23; WND 1-25; CBI 1-22,24-26,28,30-32,34-36; EGG 1,2,4-11,13,14,16-19,22,

28,31-34; ABC 1 - AKS 13; BritOil 48/22-1 1,2,4,5,11,12,15,16,18.

Remarks: The variability of L. rotulata var. b would allow the erection of many "species" but such a subdivision would confuse the characters contained within the population.

Lenticulina rotulata var. c

Pl. 17, Figs 13-14.

Description: The test is smooth, with a smooth periphery. The test is slightly unrolled.

Occurrence: B.P. 93/2-1 1,5,8,9,12; BSA 8; WND 9,10; CBI 10,12, 13; EGG 8; AKS 13.

Remarks: L. rotulata var. c contains all the features of L. rotulata var. b but is so unrolled as to warrant separation from the latter.

Lenticulina sp.a

Pl. 18, Figs 1-3.

Description: The test is small with a poorly developed keel. The chambers are markedly depressed giving the test a corrugated appearance.

Occurrence: Goban Spur 5/2 13-17; 5/1 101-106; 76-78.

Remarks: Lenticulina sp.a is very distinctive and the specimens present are all of the same size.

Genus Marginulina d'Orbigny, 1826

Genotype Marginulina raphanus d'Orbigny, 1826

Marginulina sp.a

Pl. 18, Figs 4-5.

Description: The sutures are strongly depressed and are subtended to the test at an angle of 40°. The chambers are moderately inflated.

Occurrence: SGQ 14.

Remarks: M. sp.a is very rare in the sections studied.

Genus Marginulinopsis Silvestri

Genotype Marginulinopsis densicostata Thalmann, 1937

Marginulinopsis acuticostata Reuss

Pl. 18, Figs 6-8.

1845 Cristellaria acuticostata Reuss,p.36.

1985 Lenticulina (Marginulinopsis) acuticostata (Reuss); Ball, p.241,pl.5,fig.8.

Occurrence: BritOil 48/22-1 7,8.

Genus Neoflabellina Bartenstein

Genotype Flabellina rugosa d'Orbigny, 1840

Neoflabellina sp.a

Pl. 19, Fig. 9.

Description: Chambers increase moderately in size on addition with less pronounced sutures in last portion of test.

Occurrence: WND 14; ABC 10

Remarks: N. sp.a is very rare and only occurs in the upper levels of the Plenus Marls.

Neoflabellina sp.b

Pl. 18, Figs 10-12.

Description: Chambers increase gradually in size and are moderately inflated. Test is markedly compressed.

Occurrence: 93/2-1 14,15; ABC 10.

Remarks: The specimens recovered were poorly preserved.

Genus Pandaglandulina Loeblich and Tappan

Pandaglandulina sp.a

Pl. 18, Figs 13-16.

Description: Chambers are narrow with slight inflation towards their bases, this gives the test a "bullet-like" appearance.

Occurrence: EGG 11; ABC 5.

Remarks: P. sp.a is very rare and forms a very low proportion of the the nodosariid population when it is present.

Genus Planularia Defrance in Blainville, 1824

Genotype Peneroplis auris Defrance in Blainville, 1824

Planularia? sp.a

Pl. 19, Fig. 1.

Description: The chambers are indistinct but appear to be of consistant size on addition.

Occurrence: WND 15; CBI 11; ABC 10.

Remarks: P? sp.a is very rare.

Genus Vaginulina d'Orbigny

Genotype Nautilus legumen Linne, 1758

Vaginulina costulata var.a

Pl. 19, Figs 2-4.

1842 Vaginulina costulata Roemer,p.273,pl.7B,fig.3.

1966 Vaginulina costulata Roemer;Butt,p.173,pl.1,fig.11.

1970 Vaginulina costulata Roemer;Owen,pp.129-131,pl.15,fig.5.

Description: The test is broad with curved sides and thin raised sutures which are subtended at an angle of 40°-50° from the periphery.

Occurrence: WND 1,8-11,13,14; CBI 2,5,6,10-14; EGG 2,4,5,7-12,16; ABC 5,7.

Remarks: Some slight variation in the degree of broadness of the test is present.

Vaginulina costulata var.b

Pl. 19, Figs 5-7.

1970 Vaginulina costulata Roemer;Owen,pp.129-131,pl.15,figs 1-3.

Description: The test is very elongate, the chambers may not be completely in contact with all of the previous one giving the test a "stepped" appearance.

Occurrence: WND 7,12; CBI 3,5,10,11,13; EGG 2,4,8,10,11; ABC 8; BritOil 48/22-1 7,11,13.

Vaginulina costulata var.c

Pl. 19, Figs 8-10.

Description: The test is broad with strongly raised sutures. The peripheries are straight and the aperture is raised on a circular neck.

Occurrence: WND 6,10,13; CBI 9-11; EGG 1,2,5,8,11,16; ABC 9,10.

Vaginulina costulata var.d

Pl. 19, Fig. 11.

1970 Vaginulina costulata Roemer;Owen,pl.15,figs 6-7.

Description: The sutures are predominantly raised and aligned at an angle of 50 to the periphery. The chambers have, to a varying degree, short aligned striations.

Occurrence: WND 2; EGG 6; ABC 9.

Family Polymorphinidae d'Orbigny, 1839

Subfamily Polymorphininae d'Orbigny, 1839

Genus Eoguttulina Cushman and Ozawa, 1930

Genotype Eoguttulina anglica Cushman and Ozawa, 1930

Eoguttulina? sp.a

Pl. 19, Fig. 12.

Description: The chambers show rapid expansion on addition.

Occurrence: WND 5,7; CBI 1,2,4; EGG 4.

Remarks: E? sp.a is extremely rare and the preservation of the

specimens is poor, thus little comment is possible.

Subfamily Ramulininae Brady, 1884

Genus Ramulina Jones and Wright, 1875

Genotype Ramulina laevis Jones and Wright, 1875

Ramulina aculeata (d'Orbigny), 1840

1840 Nodosaria (Dentalina) aculeata d'Orbigny,p.13,pl.1,figs 2-3.

The morphotypes figured under R. aculeata vary considerably (Cushman, 1936) with little apparent intergrading. Thus the morphotypes encountered in this study have been placed within the framework of R. aculeata but each separate one has been described.

Ramulina aculeata form a

Pl. 19, Figs 14-16.

1950 Ramulina fusiformis Khan,p.272,Pl.2,figs.1-2.

1970 Ramulina fusiformis Khan;Owen,pp.140-141,pl.16,figs 10-12.

Description: The test is elongate with broad stolons. The test surface is variously ornamented with randomly positioned pustules.

Ramulina aculeata form b

Pl. 19, Figs 17-18.

1970 Ramulina aculeata (d'Orbigny);Owen,pp.139-140,pl.15,fig.9.

Description: Bulbous tests with randomly positioned pustules, the stolon opens out to form a wide neck.

Ramulina aculeata form c

Pl. 20, Fig. 1.

Description: Bulbous test with rapidly tapering stolons and coarse pustular ornament.

Ramulina aculeata form d

Pl. 20, Figs 2-3.

Description: Bulbous test with thin circular stolons which may be added obliquely to the line of the test.

Ramulina aculeata form e

Pl. 20, Fig. 4.

Description: Thin test with stolons formed by slight narrowing of the test. The ornament is poorly developed.

Ramulina aculeata form f

Pl. 20, Figs 5-6.

Description: The test is bulbous which gently tapers to wide stolons. The ornament is very coarse and randomly positioned.

Occurrence of R. aculeata: BSA 7; CBI 2,3,5,9-11; EGG 4-6; ABC 1-3,5; BritOil 48/22-1 10,15.

Family Glandulinidae Reuss, 1860

Subfamily Glandulininae Reuss, 1860

Genus Tristix Macfadyen

Genotype Rhabdogonium liasinum Berthelin, 1879

Tristix excavatum (Reuss)

Pl. 20, Figs 7-8.

1862 Rhabdogonium excavatum Reuss,p.91,pl.12,fig.8a-c.

1970 Tristix excavatum (Reuss);Hart,pp.167-168,pl.14,fig.11.

Description: The test is elongate with a slight tapering, the faces are flush or slightly concave.

Occurrence: CBI 4; EGG 3,10,13.

Subfamily Oolininae Loeblich and Tappan, 1981

Genus Oolina d'Orbigny, 1839

Genotype Oolina laevigata Galloway and Wissler, 1927

Oolina sp.a

Pl. 20, Figs 9-12.

Description: Test ovate to sub-ovate with the aperture on a large pronounced neck.

Occurrence: B.P. 93/2-1 4,5,7; BSA 7; ABC 3.

Remarks: The shape of the test varies slightly and there may be a micro-ornament on the test surface.

Superfamily Buliminacea Jones, 1875

Family Turrilinidae Cushman, 1927

Subfamily Turrilininae Cushman, 1927

Genus Praebulimina Hofker, 1953

Genotype Bulimina ovulum Reuss, 1844

Praebulimina sp.a

Pl. 20, Figs 13-16.

Description: The chambers are elongate and moderately bulbous with depressed sutures. The aperture is very small.

Occurrence: B.P. 93/2-1 5,8,9; SGQ 8,13.

Remarks: All the specimens of P. sp.a were small.

Superfamily Globigerinacea Carpenter, Parker and Jones, 1862

Family Heterohelicidae Cushman, 1927

Subfamily Guembelitriinae Montanaro Gallitelli, 1957

Genus Guembelitria Cushman

Genotype Guembelitria cretacea Cushman, 1933

Guembelitria cenomana (Keller)

Pl. 21, Figs 1-10.

1935 Guembelina cenomana Keller,p.547-8,table 3,figs.13,14.

1940 Guembelitria harrisi Tappan,p.115,pl.19,fig.2a-b.

Occurrence: Goban Spur 6/2 70-72; 6/1 30-33; 5CCA; B.P. 93/2-1 4,6,8; BSA 7,8; SGQ 2,9,12,13,17,23; WND 2-5,7-15; CBI 2-5,7-11, 13,14,17; EGG 2,3,6-8,11-13; ABC 1,2,4,6.

Remarks: There is some variation in the development of the apertural lip with some forms exhibiting thicker more robust lips. The extent of pustule ornament is highly variable but in most forms it is absent on the last formed chamber. Keller incorrectly illustrates G. cenomanica on table 3, figures 13,14 as Reussia spinulosa.

Genus Guembelitriella Tappan

Genotype Guembelitriella graysonensis Tappan

Guembelitriella sp.a

Pl. 21, Fig. 11.

Description: The latter stage of randomly positioned chambers is

comprised of moderately inflating chambers. The ornamentation is the same as for G. cenomana and the early triserial stage is identical to the equivalent portion of test development of G. cenomana. G. sp. a occurs in a population of G. cenomana and thus may well be an aberrant or ecophenotypic variant of the latter.

Occurrence: SGQ 14; ABC 1.

Subfamily Heterohelicinae Cushman, 1927

Genus Heterohelix Ehrenburg, 1843

Genotype Spiroplecta americana Ehrenburg, 1844

Heterohelix globulosa (Ehrenburg)

Pl. 22, Figs 14-16.

1840 Textularia globulosa Ehrenburg,p.135,pl.4,figs 2b,4b,5b,7b,8b.

1967 Heterohelix globulosa (Ehrenburg);Pessagno,p.260,pl.87,figs 5-9,11-13.

Occurrence: Goban Spur 5/1 76-78; B.P. 93/2-1 11; SGQ 8; CBI 21, 22,24,26,32-36; EGG 33,34; ABC 21; AKS 1,12.

Remarks: H. globulosa is very close to H. moremani (Cushman) in that transitional forms exist within the heterohelixid population. These comprise forms with moderately inflated chambers and less pronounced depressed sutures.

Heterohelix moremani (Cushman)

Pl. 22, Figs 1-13.

1938 Guembelina moremani Cushman,p.10,pl.2,figs 1-3.

1967 Heterohelix moremani Cushman;Pessagno,pp.260-1,pl.89,figs 1-2.

Occurrence: Goban Spur 6/2 70-72, 26-29; 6/1 30-33;5/1 76-78, 7-10. B.P. 93/2-1 4,11; BSA 3-7; SGQ 2,3,7-9,10-21,23; WND 2-6,11-13,15, 16,21; CBI 1-5,7-14,16,17; EGG 2,3,5,7; ABC 1,3,4,6-12,14,21; AKS 1-4,6.

Remarks: H. moremani forms the bulk of the late Cenomanian heterohelixid population. The ornamentation varies considerably though much of the "heaviest" ornament may be due to post-depositional syntaxial overgrowth of calcite.

The heterohelixid population exhibits a progressive change in ornamentation (Pl.22), the pre-OAE population shows random pustules that may be concentrated on single chambers or the earlier portion of the test. The post-OAE population yields morphotypes of H. moremani and H. globulosa but with varying degrees of costae. These consist of orientated lines of pustules to well-developed costae running the length of the test.

Family Planomalinidae Bolli, Loeblich and Tappan, 1957

Genus Globigerinelloides Cushman and ten Dam, 1948

Genotype Globigerinelloides algeriana Cushman and ten Dam, 1948.

Globigerinelloides bentonensis (Morrow)

Pl. 23, Figs 1-5.

1934 Anomalina bentonensis Morrow,p.201,pl.30,fig.4a-b.

1977 Globigerinelloides bentonensis (Morrow);Carter and Hart, pp.27-8, pl.1,fig.11;pl.2,figs 19-20.

Occurrence: Goban Spur 6/2 70-72, 26-29; 5CCA; B.P. 93/2-1 5; BSA 7; SGQ 17(?); WND 3,6,18,21-28; CBI 7; EGG 4,8-10,14.

Remarks: The size of G. bentonensis varies, with the extremes illustrated (Pl.22,Figs 1-5), this has been noted many times (reviewed Carter and Hart, 1977). The low numbers found means that little comment can be made on the relative merits of G. caseyi and G. bentonensis.

Family Rotaliporidae Sigal, 1958

Subfamily Hedbergellinae Loeblich and Tappan, 1961

Genus Favusella Michael, 1973

Genotype Globigerina washitensis Carsey

Favusella washitensis (Carsey)

Pl. 25, Fig. 2.

1926 Globigerina washitensis Carsey,p.44,pl.7,fig.10.

1985 Favusella washitensis (Carsey);Caron,p.45,fig.25,no.25,26a-b.

Occurrence: SGQ 6,7.

Remarks: F. washitensis was only recorded from Shapwick Grange Quarry and identified in thin section.

Genus Hedbergella Bronniman and Brown

Genotype Anomalina lorneiana d'Orbigny var.trocoidea Gandolfi

The genus Whiteinella Pessagno has not been adopted in this study as many of the forms are of a transitional nature (H. delrioensis - H. aprica - "H". archaeocretacea) and many of the generic characters are not completely developed. In particular, the

wide umbilicus and portici. Thus these forms have been designated under "Hedbergella".

"Hedbergella" aprica (Loeblich and Tappan)

Pl. 23, Figs 6-8.

1961 Ticinella aprica Loeblich and Tappan,p.292,pl.4,figs 14-16.

1979 Whiteinella aprica (Loeblich and Tappan);Robaszynski and Caron, pp.157-160,pl.32,figs 1a-c,2a-c.

Occurrence: Goban Spur 5/2 13-17; 5/1 101-106, 76-78, 7-10; B.P. 93/2-1 12,14; BSA 9-13; SGQ 7-11,15-23; WND 2,4-12,22; CBI 3-5,7,9,10,19,20,22,24,32,33; EGG 5,8,9,11-17,19,20,28-31,34; ABC 2,3,5-14,16,21; AKS 1,2,3,4,6,7,10,12; BritOil 48/22-1 16-19.

Remarks: "H". aprica is represented in the pre-OAE hedbergellid population but the specimens are smaller than H. aprica sensu stricto with a slightly higher trochospire. Post-OAE H. aprica sensu stricto is prevalent with a large umbilicus and low trochospire. "H". aprica is probably the precursor to "H". archaeocretacea (Pessagno).

"Hedbergella" archaeocretacea (Pessagno)

Pl. 23, Figs 9-12.

1967 Whiteinella archaeocretacea Pessagno,p.298,pl.51,figs 2-4; pl.54,figs 19-25;pl.100,fig.8.

1979 Whiteinella archaeocretacea Pessagno;Robaszynski and Caron, pp.161-168,pl.33,figs 1a-c,2a-c,3a-c;pl.34,figs 1a-c,2a-c.

Occurrence: Goban Spur 5/2 13-17; 5/1 101-106, 76-78, 7-10; BSA 9-11; SGQ 15-17,19,20; WND 22; CBI 24,25,28,30,32-35; EGG 27,32-33; ABC 21; AKS 1-4,6,7,10,12; BritOil 48/22-1 19.

Remarks: The development of "H". archaeocretacea from "H". aprica stock is rapid. The delicate portici are poorly preserved (if present in the first place). The ornament is comprised of randomly positioned pustules, though to some extent they are concentrated along the periphery.

Hedbergella delrioensis (Carsey)

Pl. 24, Figs 1-11.

1926 Globigerina cretacea d'Orbigny var. delrioensis Carsey,p.43.

1937 Globigerina infracretacea Glaessner,p.28.

1977 Hedbergella delrioensis (Carsey);Carter and Hart,p.35,pl.4, figs 1-3.

Occurrence: Goban Spur 6/2 70-72, 26-29; 6/1 30-33; 5CCA; B.P. 93/2-1 1,6-15; BSA 1,2-8,10,11; SGQ 1,3,6-9,1-13,15-22; WND 1-12, 14,16; CBI 1-19; EGG 1-6,8-11,13,14,20,26; ABC 1-14,19,21; AKS 1,2,4,6; BritOil 48/22-1 1,4,5-7,11-13,15,16,19.

Remarks: H. delrioensis exhibits variability in chamber size, their rate of increase and ornament. In some individuals the ornament is concentrated on the umbilical surface of the first formed chambers of the last whorl. The pustules may be coalesced into thin stringers

which are very broadly aligned parallel to the periphery. The density and distribution of pores varies but no systematic analysis has been undertaken. H. delrioensis forms the "middle" morphotype in the variability of the hedbergellid population (in terms of height of trochospire, test size and chamber shape).

"Hedbergella" brittonensis Loeblich and Tappan

Pl. 23, Figs 13-14.

1934 Globigerina cretacea d'Orbigny;Morrow,p.198,pl.30,figs 7,8, 10a-b.

1977 Hedbergella brittonensis Loeblich and Tappan;Carter and Hart, pp.31-2,pl.4,figs 13-15.

Occurrence: Goban Spur 6/2 70-72, 26-29; 6/1 30-33; 5/1 7-10; B.P. 93/2-1 4,5,8; BSA 3-7; SGQ 8,11,15-17,19,20,23; WND 3,4,10; CBI 9-11,13,14,16; EGG 19,20,22,25,27,30; ABC 3-5,7,9,21; AKS 2,4,13; BritOil 48/22-1 5,10,12,13,16.

Remarks: H. brittonensis forms a minor part of the hedbergellid population when present. It exhibits considerable variation in size, but each sample population is consistant.

Hedbergella planispira (Tappan)

Pl. 24, Figs 12-14.

1940 Globigerina planispira Tappan,p.12,pl.19,fig.12.

1977 Hedbergella planispira (Tappan);Carter and Hart,pp.36-37, pl.4,figs 4-6.

Occurrence: B.P. 93/2-1 2,4,5,9; SGQ 17,18; CBI 4,14; ABC 8,11,12; BritOil 48/22-1 2-10,12,13.

Remarks: H. planispira is not a constant part of the hedbergellid population but when it is present it forms a major part. This implies that H. planispira is an ecophenotypic variant of the standing hedbergellid stock possibly related to H. delrioensis.

Hedbergella simplex (Morrow)

Pl. 25, Fig. 1.

1934 Hastigerinella simplex Morrow,pp.198-199,pl.30,fig.6a-b.

1977 Hedbergella amabilis Loeblich and Tappan;Carter and Hart, pp.29-30,pl.3,figs 22-23.

1979 Hedbergella simplex (Morrow);Robaszynski and Caron, pp.145-150,pl.29,figs 1a-c,2a-c,3a-c;pl.30,figs 1a-c,2a-c.

Occurrence: B.P. 93/2-1 3,4,5,7; BSA 6; WND 15,17,18,22; CBI 9-11,13,14,16; ABC 8.

Remarks: In a similar manner to H. planispira, H. simplex does not form a consistant component of the hedbergellid population and thus it may also be an ecophenotypic variant.

Genus Helvetoglobotruncana Reiss, 1957

Genotype Globotruncana helvetica Bolli

Helvetoglobotruncana helvetica (Bolli)

Pl. 25, Figs 11-14.

1945 Globotruncana helvetica Bolli,p.226,pl.9,figs 6-8,text-fig.1 (9-12).

1977 Praeglobotruncana helvetica (Bolli);Carter and Hart,pp.39-40, pl.3,figs 16-17.

1979 Praeglobotruncana helvetica (Bolli);Robaszynski and Caron, pp.39-42,pl.46,figs 1a-c,2a-c.

1985 Helvetoglobotruncana helvetica (Bolli);Caron,p.60,fig.30, nos.7.8a-c.

Occurrence: Goban Spur 5/1 76-78, 7-10; B.P. 93/2-1 15; SGQ 15, 16,19,23; CBI 36.

Remarks: The N.W. European H. helvetica is not as well developed in terms of size of test and flattening of the spiral surface as forms described from lower latitudes. This may be the result of it being towards the limit of its distribution.

Helvetoglobotruncana praehelvetica (Trujillo)

Pl. 25, Figs 3-10.

1960 Rugoglobigerina praehelvetica Trujillo,pp.340-341,pl.49,figs 6a-c.

1979 Praeglobotruncana praehelvetica (Trujillo);Robaszynski and Caron,pp.43-46,pl.47,figs 1d,2c.

1985 Helvetoglobotruncana praehelvetica (Trujillo);Caron,p.60,fig. 30,nos.9a-c,10a-c.

Occurrence: Goban Spur 5/2 13-17; 5/1 101-106,76-78,7-10; BSA 9, 11-13; SGQ 17,18; WND 19,21-26; CBI 23,24,27-32,35,36; EGG 23-26, 28-30,33; AKS 7-10,12.

Remarks: H. praehelvetica is thought to be the ancestor of H. helvetica (Bolli) (Hart and Bailey, 1979) with which the author agrees.Thus the differentiation between the two species is equivocal.

Genus Praeglobotruncana Bermudez

Genotype Globorotalia delrioensis Plummer

Praeglobotruncana delrioensis (Plummer)

Pl. 26, Fig. 1.

1931 Globorotalia delrioensis Plummer,p.199,pl.13,fig.2a-c.

1977 Praeglobotruncana delrioensis (Plummer);Carter and Hart, pp.38-39,pl.4,figs 22-24.

1979 Praeglobotruncana delrioensis (Plummer);Robaszynski and Caron, pp.29-32,pl.43,figs 1a-c,2a-c.

Occurrence: B.P. 93/2-1 1; SGQ 6.

Remarks: The differentiation of the species within Praeglobotruncana

based on the height of the trochospire (progressively increasing through P. delrioensis - P. stephani (Gandolfi) - P. gibba (Klaus)) has been shown to be fallacious Klaus,(1960), as intermediate forms are found between all three morphotypes. Unfortunately, Klaus did not illustrate the position of the forms against time, as such a treatment would have shown that the increase in the height of the spire (and size) was a developing feature within the moving population.

Praeglobotruncana gibba Klaus

Pl. 26, Figs 2-3.

1960 Praeglobotruncana stephani var. gibba Klaus,p.306,text-fig.1.

1979 Praeglobotruncana gibba Klaus;Robaszynski and Caron,pp.33-38, Pl.44,figs.1a-c,2a-c;Pl.45,figs.1a-c.2a-c.

Occurrence: Goban Spur 6/2 70-72, 26-29; 6/1 30-33; SGQ 7.

Remarks: P. gibba forms the end member of the P. delrioensis - P. stephani - P. gibba plexus. P. gibba has a restricted development across the Anglo-Paris Basin (see Chapter 7) and thus forms the least significant portion of the population.

Praeglobotruncana stephani (Gandolfi)

Pl. 26, Figs 4-10.

1942 Globotruncana stephani Gandolfi,p.130,pl.3,figs 4-5;pl.4,figs

36-37.

1977 Praeglobotruncana stephani (Gandolfi);Carter and Hart pp.40-41, pl.4,figs 16-21.

1979 Praeglobotruncana stephani (Gandolfi);Robaszynski and Caron, pp.47-50,pl.48,figs 1a-c,2a-b,3a-b.

Occurrence: Goban Spur 6/2 70-72, 26-29; 6/1 30-33; B.P. 93/2-1 1,7,8,11; BSA 5-7; SGQ 7,8,12,15,16,19; WND 1-5,7,9-12,14,16-19; CBI 1-18; EGG 1-6,8-12,19; ABC 1,2,4-9,11,12; BritOil 48/22-1 9-16.

Remarks: P. stephani forms the middle morphotype in the P. delrioensis - P. stephani - P. gibba plexus. It is ubiquitous across the sections studied (Chapter 5) and thus forms the bulk of the praeglobotruncanid population.

Genus Dicarinella Porthault

Genotype Globotruncana indica Jacob and Sastry, 1950

Dicarinella algeriana (Caron)

Pl. 27, Figs 1-3.

1966 Praeglobotruncana algeriana (Reuz);Caron,pl.2,fig.5a-c.

1979 Dicarinella algeriana (Caron);Robaszynski and Caron, pp.57-60,pl.50,figs 1a-d,2a-d.

Occurrence: Goban Spur 6/2 70-72, 26-29; 6/1 30-33; 5CCA; 5/2 13-17;

5/1 101-106, 76-78, 7-10; B.P. 93/2-1 12; BSA 5-7; SGQ 8,14-16,19,20,23; WND 9,11,14-18,22,23,25,28; CBI 4,5,14-18,20,21, 25,26,32; EGG 5,9-14,19,20,30,31,33; ABC 3-8,10,11,21; AKS 1-5,8; BritOil 48/22-1 18.

Remarks: The differentiation of the early forms of D. algeriana from P. stephani is problematical as the development of the keels is very variable with many forms showing only two poorly differentiated keels.

Dicarinella hagni (Scheibnerova)

Pl. 27, Figs 4-10.

1962 Globotruncana hagni Scheibnerova,pp.219-221,text-fig.6a-c.

1979 Dicarinella hagni (Scheibnerova);Robaszynski and Caron, pp.79-86,pl.56,figs 1a-c,2a-c;pl.57,figs 1a-c,2a-d.

Occurrence: Goban Spur 6/2 70-72,26-29;6/1 30-33;5CCA; 5/2 13-17; 5/1 101-106, 76-78, 7-10; B.P. 93/2-1 5,7,8,10,12; BSA 7,12; SGQ 8, 14-16,19-21,23; WND 9,11,13-19,22,23; CBI 7-27; EGG 6,9,21,24,25, 28,31-33; ABC 3,6,7,9-14,21; AKS 2-12; BritOil 48/22-1 18,19.

Remarks: D. hagni exhibits variability in the shape of the chambers and the degree of spacing between the keels. The early forms have indistinct closely spaced keels.

Dicarinella imbricata (Mornod)

Pl. 27, Figs 11-12.

1950 Globotruncana imbricata Mornod,p.589,text-fig.5,3a-d.

1979 Dicarinella imbricata (Mornod);Robaszynski and Caron, pp.87-92,pl.58,figs 1a-c,2a-d;pl.59,figs 1a-c,2a-c.

Occurrence: Goban Spur 6/2 70-72, 26-29; 6/1 30-33; 5CCA; 5/2 13-17; 5/1 101-106, 76-78, 7-10; SGQ 8,9,14-16,19-21; WND 9,11,13-19; CBI 7-10,13-17,25-27,36; EGG 6,12-15,27; ABC 10-12,14; AKS 2-5,8-10,12; BritOil 48/22-1 18,19.

Remarks: D. imbricata is derived from D. hagni by the development of offset keels.

Genus Marginotruncana Hofker, 1956

Genotype Rosalina marginata Reuss, 1845

Marginotruncana marginata (Reuss)

Pl. 28, Figs 1-4.

1845 Rosalina marginata Reuss,p.36,pl.8,figs 54a-b,74a-b.

1979 Marginotruncana marginata (Reuss);Robaszynski and Caron, pp.107-114,pl.63,figs 1a-c,2a-d;pl.64,figs 1a-c,2a-d.

Occurrence: AKS 9,10,12.

Remarks: M. marginata is very rare in this study and the umbilical thickenings are poorly developed. The designation of M. marginata used is the one established by Robaszynski and Caron, 1979, though

there may well be some confusion in the neotype they adopted from Jirova (1956) between M. marginata and M. canaliculata (Reuss) (Bailey, 1978).

Marginotruncana sp. cf. M. sigali (Reichel)

Pl. 28, figs. 5-8.

1950 Globotruncana (Globotruncana) sigali Reichel,pp.610-612, text-figs 5-6,pl.16,fig.7.

1979 Marginotruncana sigali (Reichel);Robaszynski and Caron, pp.141-146,pl.72,fig.1a-c,2a-b;pl.73,fig.a-f.

Occurrence: SGQ 20; CBI 36.

Remarks: M. sp. cf. sigali is extremely rare in this study and the specimens small and poorly preserved which makes its identification problematical.

Subfamily Rotaliporinae Sigal, 1958

Genus Rotalipora Brotzen, 1942

Genotype Rotalipora turonica = Globorotalia cushmani Morrow, 1934

The rotaliporid population shows variation in its relative percentage of the planktonic population across the sections studied. In addition, the relative dominance of the component species within the rotaliporid population and the size of specimens varies. This is

detailed and discussed in Chapter 5.

Rotalipora appenninica (Renz)

Pl. 28, Fig. 9.

1936 Globotruncana appenninica Renz,p.13,text-fig.2.

1979 Rotalipora appenninica (Renz);Robaszynski and Caron,pp.59-64, pl.4,figs 1a-c,2a-c,3a-c;pl.5,figs 1a-c,2a-c,3a-c.

Occurrence: SGQ 7; BritOil 48/22-1 8.

Remarks: R. appenninica is rare and is only present from Shapwick Grange Quarry. The specimens were identified in thin section. The forms present show very poor keel development.

Rotalipora cushmani (Morrow)

Pl. 28, Figs 10-14.

Pl. 29, Figs 1-3.

1934 Globorotalia cushmani Morrow,p.199,pl.31,figs 2a-b,4a-b.

1977 Rotalipora cushmani (Morrow);Carter and Hart,pp.41-44,pl.2, fig.18;pl.4.figs 7-9.

1979 Rotalipora cushmani (Morrow);Robaszynski and Caron,pp.69-74, pl.7,fig.1a-c;pl.8,figs 1a-c,2a-c.

Occurrence: Goban Spur 6/2 70-72, 26-29; 6/1 30-33; B.P. 93/2-1 1,6; BSA 1,4-7; SGQ 8; WND 1-13; CBI 1-13; EGG 1-5,8-12; ABC 1-10;

BritOil 48/22-1 11,13-16.

Remarks: R. cushmani forms the dominant part of the rotaliporid population and increasingly so into the Anglo-Paris Basin (see 5.14).

Rotalipora deecki (Franke)

Pl. 29, Figs 4-6.

1925 Rotalipora deecki Franke,pp.90-91,text-fig.7a-c.

1979 Rotalipora deecki (Franke);Robaszynski and Caron,pp.75-80, pl.9,figs 1a-c,2a-c;pl.10,figs 1a-c,2a-c.

Occurrence: Goban Spur 6/2 70-72, 26-29; 6/1 30-33.

Remarks: R. deecki forms the minor portion of the rotaliporid population and significantly only from Goban Spur.

Rotalipora greenhornensis (Morrow)

Pl. 29, Figs 7-9.

1934 Globorotalia greenhornensis Morrow,p.199,pl.39,fig.1.

1977 Rotalipora greenhornensis (Morrow);Carter and Hart,pp.44-45, pl.4,figs 10-12.

1979 Rotalipora greenhornensis (Morrow);Robaszynski and Caron, pp.85-90,pl.12,figs 1a-c,2a-c;pl.13,figs 1a-c,2a-c.

Occurrence: Goban Spur 6/2 70-72,26-29; 6/1 30-33; B.P. 93/2-1

7,8; BSA 5; WND 1-3,5,10-12; CBI 2,3,10; EGG 9; ABC 1,3,7,8; BritOil 48/22-1 15.

Remarks: R. greenhornensis decreases in influence as part of the rotaliporid population into the Anglo-Paris Basin (see 5.14).

Rotalipora sp. cf. R. reicheli Mornod

Pl. 29, Fig. 10.

1950 Globotruncana (Rotalipora) reicheli Mornod,p.583,fig.5 (1Va-c),fig.6(1-6),pl.15,figs 2a-p,3-8.

1979 Rotalipora reicheli Mornod;Robaszynski and Caron,pp.99-106, pl.16,fig.1a-c;pl.17,fig.1a-c;pl.18,figs 1a-c,2a-c.

Occurrence: Shapwick Grange Quarry 5.

Remarks: R. sp. cf. R. reicheli is only present in thin section. The specimens are very low trochospired, with angular chambers and are poorly preserved thus their identification is problematical.

Superfamily Cassidulinacea d'Orbigny, 1839

Family Pleurostomellidae Reuss,1860

Subfamily Pleurostomellinae Reuss, 1860

Genus Pleurostomella Reuss, 1860

Genotype Dentalina subnodosa Reuss, 1851

Pleurostomella subnodosa (Reuss)

Pl. 29, Figs 11-14.

1851 Dentalina subnodosa Reuss,p.24.

1964 Pleurostomella subnodosa (Reuss);Loeblich and Tappan,C275-276, pl.594,fig.la-b.

Occurrence: Goban Spur 5/1 101-106.

Remarks: The degree of inflation of the chambers on addition varies slightly, but the population from Goban Spur is of a consistant size.

Family Alabaminidae Hofker,1951

Genus Gyroidina d'Orbigny

Genotype Gyroidina orbicularis Cushman, 1927

Gyroidina sp.a

Pl. 29, Figs 15-16.

Description: The test increases moderately in size on chamber addition. The periphery is well-rounded in cross-section but in umbilical view there is a slight angle between chambers.

Occurrence: Goban Spur 6/2 70-72.

Remarks: G. sp.a is only found from Goban Spur and forms a very small part of the benthonic assemblage.

Family Osangulariidae Loeblich and Tappan, 1964

Genus Gyroidinoides Brotzen, 1942

Genotype Rotalina nitida Reuss, 1844

Gyroidinoides parva (Khan)

Pl. 30, Fig. 1.

1898 Rotalina soldanii d'Orbigny var. nitida Reuss;Chapman,pp.9-10, pl.2,fig.2a-c.

1970 Gyroidinoides parva (Khan);Hart,pp.208-209,pl.22,figs 5-7.

Occurrence: WND 4; CBI 7; ABC 2,5; BritOil 48/22-1 13,16.

Remarks: G. parva only forms a very small part of the benthonic population when present.

Family Anomalinidae Cushman, 1927

Subfamily Anomalininae Cushman, 1927

Genus Gavelinella Brotzen, 1942

Type species Discorbina pertusa Marsson, 1878

Gavelinella baltica Brotzen

Pl. 30, Figs 2-7.

1942 Gavelinella baltica Brotzen,p.50,pl.1,fig.7.

1977 Gavelinella baltica Brotzen;Carter and Hart,p.46,pl.1, figs 36-38.

Occurrence: B.P. 93/2-1 5; SGQ 3,6; WND 2,3,5,8,9,11; CBI 2,4-6, 9; EGG 1,2,4,6,8; ABC 1-3,5-8; BritOil 48/22-1 4.

Remarks: G. baltica is very distinctive and is usually noticeably larger than G. cenomanica (Brotzen) and G. intermedia (Berthelin) with which it occurs. It is derived in the early Cenomanian from G. intermedia (Carter and Hart, 1977).

Gavelinella berthelini (Keller)

Pl. 30, Figs 8-11.

1935 Anomalina berthelini Keller,pp.552-553,pl.3,figs 25-27.

1967 Gavelinella berthelini (Keller);Fuchs,p.336,pl.18,fig.8a-c.

Occurrence: B.P. 93/2-1 1-3,5-8,10-12,14,15; BSA 4,6,7,8,10-12; SGQ 8-18; WND 11,12,14,16-21; CBI 11-24,26-28,34-36; EGG 10-22, 24-26,28-34; ABC 2-4,6,7,9,11-21; AKS 1-9; BritOil 48/22-1 11,14-16,18-19.

Remarks: G. berthelini has a much larger boss than G. reussi (Khan) from which it is derived. These species form a more significant part of the gavelinellid population than alluded to by others (e.g. Hart and Swiecicki, 1987). G. tourainensis Butt is thought to be an ecophenotypic form of G. berthelini.

Gavelinella cenomanica (Brotzen)

Pl. 30, Figs 12-15.

1942 Cibicioloides (Cibicides) cenomanica Brotzen,p.54,pl.2, fig.2a-c.

1977 Gavelinella cenomanica (Brotzen);Carter and Hart,pp.46-47, pl.1,figs 27-28.

Occurrence: B.P. 93/2-1 1-3,5-9; BSA 3; WND 1-10; CBI 1-6,8-9; EGG 1,2,4-9; ABC 2-6,8; BritOil 48/22-1 1-3,5-8,11,13,14,16.

Remarks: The degree of development of the umbilical rim is variable.

Gavelinella intermedia (Berthelin)

Pl. 31, Figs 1-3.

1880 Anomalina intermedia Berthelin,p.67,pl.4,fig.14a-b.

1977 Gavelinella intermedia Berthelin;Carter and Hart,p.48, pl.1,figs 33-35.

Occurrence: Goban Spur 6/2 70-72; B.P. 93/2-1 1-8; BSA 3,4,6; SGQ 8; WND 1-11; CBI 1-6,8-10; EGG 1,2,4-9; ABC 1-11; BritOil 48/22-1 1,2,4-8,11-17.

Remarks: G. intermedia forms the major part of the pre-OAE gavelinellid population.

Gavelinella reussi (Khan)

Pl. 31, Figs 4-5.

1863 Rosalina complanata Reuss var. Reuss,p.86,pl.11,fig.3a-c.

1970 Gavelinella reussi (Khan);Hart,pp.213-214,pl.23,figs 7-9.

Occurrence: Goban Spur 6/2 70-72; B.P. 93/2-1 1-2; BSA 3,4; WND 1,3-13; CBI 1-12; EGG 1,2,4-11; ABC 1,3,4,6,10-14; BritOil 48/22-1 1-3,5,8,9,11-13,17.

Remarks: G. reussi is the ancestor of G. berthelini.

Genus Lingulogavelinella Malapris, 1965

Genotype Lingulogavelinella albiensis Malapris, 1965

Lingulogavelinella globosa (Brotzen)

Pl. 31, Figs 7-9.

1942 Anomalinoides globosa Brotzen,p.58,pl.2,fig.6a-c.

1977 Lingulogavelinella globosa (Brotzen);Carter and Hart,p.49, pl.1,figs 12-14.

Occurrence: B.P. 93/2-1 4,8,9,11,12,14; BSA 5-8,10-12; SGQ 8,9, 12-15,18; WND 1-7,10-16; CBI 1-3,5,7-19; EGG 6-20,28,31-34; ABC 3,6-9,11-AKS 4,8,9; BritOil 48/22-1 12,14.

Remarks: L. globosa shows a rapid increase in size and numbers after the extinction of G. baltica, G. intermedia and G. cenomanica.

Lingulogavelinella aumalensis (Sigal)

Pl. 31, Figs 10-11.

1952 Anomalina aumalensis Sigal,p.27,text-fig.26.

1970 Lingulogavelinella aumalensis (Sigal);Owen,pp.200-201,pl.30, figs 10-12.

Occurrence: B.P. 93/2-1 10-12; WND 23-29; CBI 18,20,24,26,29,32,

35,36; EGG 23-25,32,34; AKS 12,13.

Incerti ordinis

Family Calicispherulidae Bonet, 1956

Genus Pithonella Lorenz, 1902

Pithonella ovalis (Kaufmann)

Pl. 31, Figs 12-13.

1865 Lagena ovalis Kaufmann,p.196-197,text-fig.107a-b.

1902 Pithonella ovalis (Kaufmann);Lorenz,pp.13-14,pl.9,fig.2.

1976 Pithonella ovalis (Kaufmann);Bein and Reiss,p.85,pl.1, figs 3-8;pl.2,figs 1-6.

Remarks: P. ovalis is sporadically present but occurs in great numbers when present.

Description: Calcareous(?) spheres with chipped (striated) surface.

Pl. 31, Figs 14,15.

Occurrence: 93/2-1 1090'.

Remarks: The exact compostition has not been established. The

randomly oriented striae may well be post-depositional damage.

Incertae cedis

Description: Calcareous subconical protruberance formed by the cementation of small calcareous(?) grains.

Pl. 31, Fig. 16.

Occurrence: Abbots Cliff 9.

Remarks: It only appears in ABC9 but in large numbers (>30).

Chapter 5: Biostratigraphical implications, methods of basinal correlation and pre-Oceanic Anoxic Event palaeoenvironmental analysis .

5.1. Previous work.

Previous biostratigraphical studies of the Cenomanian and Turonian of southern England (Hart, 1970, 1982b; Owen, 1970; Carter and Hart, 1977), have integrated the planktonic and benthonic foraminifera. In addition, the European Working Group on Foraminifera has established a series of Cretaceous planktonic foraminiferal zones (Robaszynski and Caron, 1979). Comparison with the above has been made in this study.

5.2. The existance world-wide of organic-rich shales of late Cenomanian age is well documented (see Schlanger et. al., 1987, for a recent review). This Cenomanian - Turonian Oceanic Anoxic Event is marked by a positive excursion in the $\delta^{13}C$ curve due to the preferential extraction of 12C by marine plankton whose organic components were not recycled because of enhanced organic carbon burial (Arthur et al., 1987).

5.3. Goban Spur (Figures 3.1 and 5.1).

5.3(1). Lithostratigraphy.

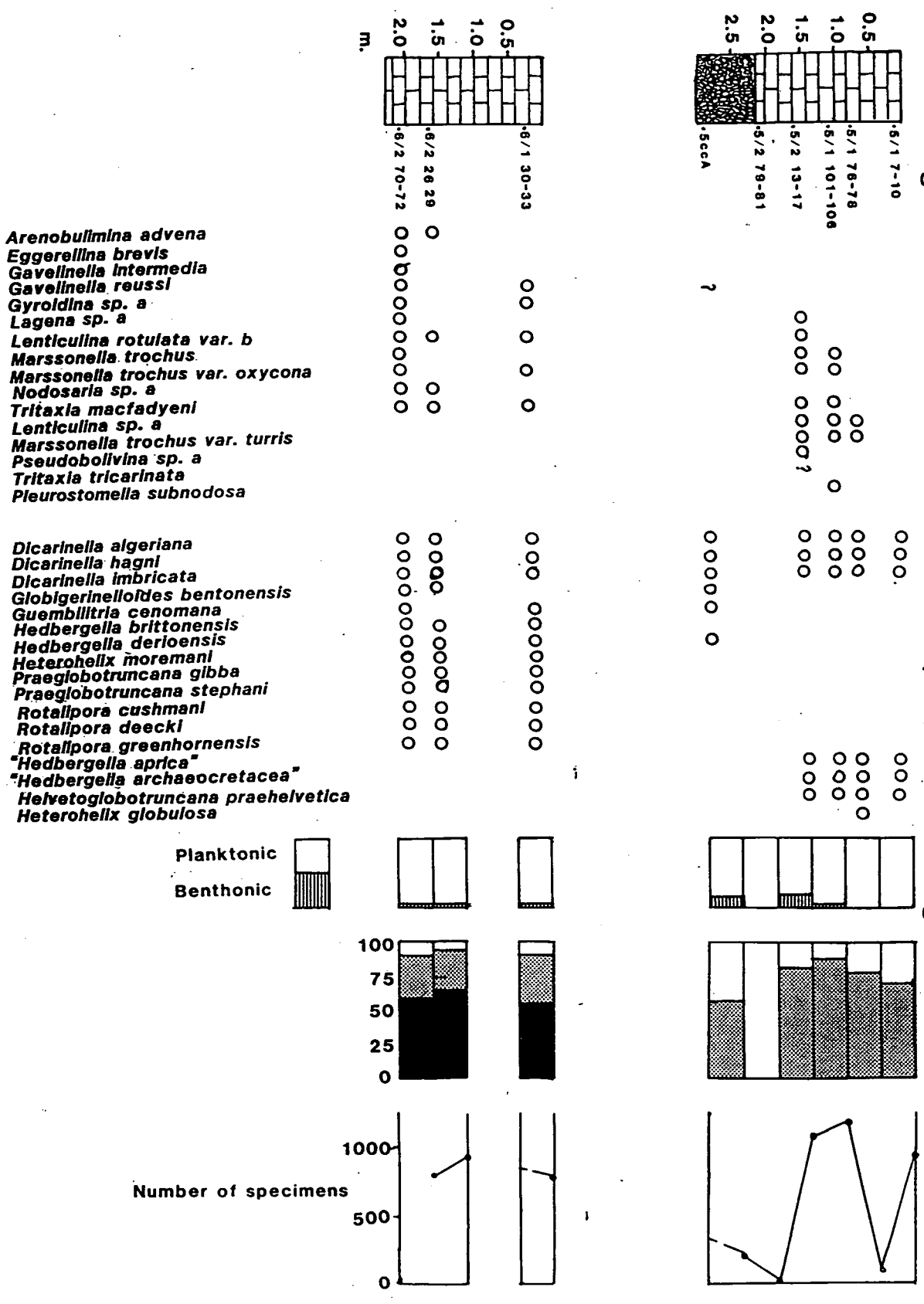

Figure 5.1 Foraminifera from Goban Spur , Site 551 Leg 80

The basal sedimentary sequence recovered from the Goban Spur (DSDP Leg 80), has been described by Graciansky et al. (1985). It comprises 4.1m of nannofossil chalk (Core 6; Figure 5.1), which underlies an unknown thickness of poorly recovered, partially laminated black shale, This, in turn, is overlain by a further 4.1m of nannofossil chalk (Core 5; Figure 5.1).

5.3(ii). δ13C isotope curve.

The total org.C curve from the Goban Spur shows a marked deflection (Arthur et al., 1987), but it is not shown against a lithological log, thus its exact position cannot be illustrated.

5.3(iii). Macropalaeontological biostratigraphy.

No fragments of any macropalaeontological fauna were recorded (Graciansky et al., 1985).

5.3(iv). Foraminiferal biostratigraphy.

The presence of R. cushmani and R. greenhornensis in Core 6 (figure 5.1), is taken to confirm a late Cenomanian age for this part of the succession, while the occurrence of H. praehelvetica and H. archaeocretacea in Core 5 (Figure 5.1), indicates an early Turonian age (Graciansky et al., 1985; Hart, 1985, 1987b).

5.3(v). Foraminiferal assemblage.

The planktonic foraminiferal assemblage is dominated by rotaliporids (R. cushmani 45%; R. greenhornensis 15%; R. deecki 3%), with praeglobotruncanids/dicarinellids (29%) and hedbergellids (8%) comprising the remainder. The differentiation of the praeglobotruncanid and dicarinellid population is problematical as many of the forms are transitional. The planktonic assemblage shows little change in the relative proportion of these three populations prior to the OAE. During this interval the benthonic population forms a very small part (<2%) of the gross foraminiferal population. It is comprised of a limited assemblage which show a marked size consistancy within their respective populations (Figure 5.1).

The post-OAE population shows less consistancy in its overall composition. The lower samples (5CCA and 5\2 79-81, Figure 5.1) yield low population numbers (<200 specimens). The specimens are pitted, indicating the effects of carbonate dissolution. Although the overlying population is constant (praeglobotruncanid/dicarinellid, 65-70% and hedbergellid 30-15%), the number of specimens contained in each sample varies considerably (>1,200 to <75). This implies that even though the number of specimens is small, it can still provide an accurate picture of the relative proportions of the

population. As in the pre-OAE population, the post-OAE benthonic foraminifera form a small percentage of the total (3-10%).

5.4. B.P 93\2-1 (Figure 5.2).

5.4(i). Lithostratigraphy.

The succession studied consists of 35m of chalk limestone overlain by 80m of hard chalk limestone, for which no detailed lithological logs or downhole logs were available. The seventeen samples comprised both sidewall core and ditch cuttings.

5.4(ii). δ13C isotope curve.

There is no δ 13C isotope curve available from B.P 93\2-1 (Copestake, pers. comm.).

5.4(iii). Macropalaeontological biostratigraphy.

No macropalaeontological fauna was recorded from the interval under discussion (Williamson, 1979; Copestake, pers. comm.).

5.4(iv). Foraminiferal biostratigraphy.

The presence of R. cushmani and R. greenhornensis places samples 2-8 (Figure 5.2) within the top of R. cushmani

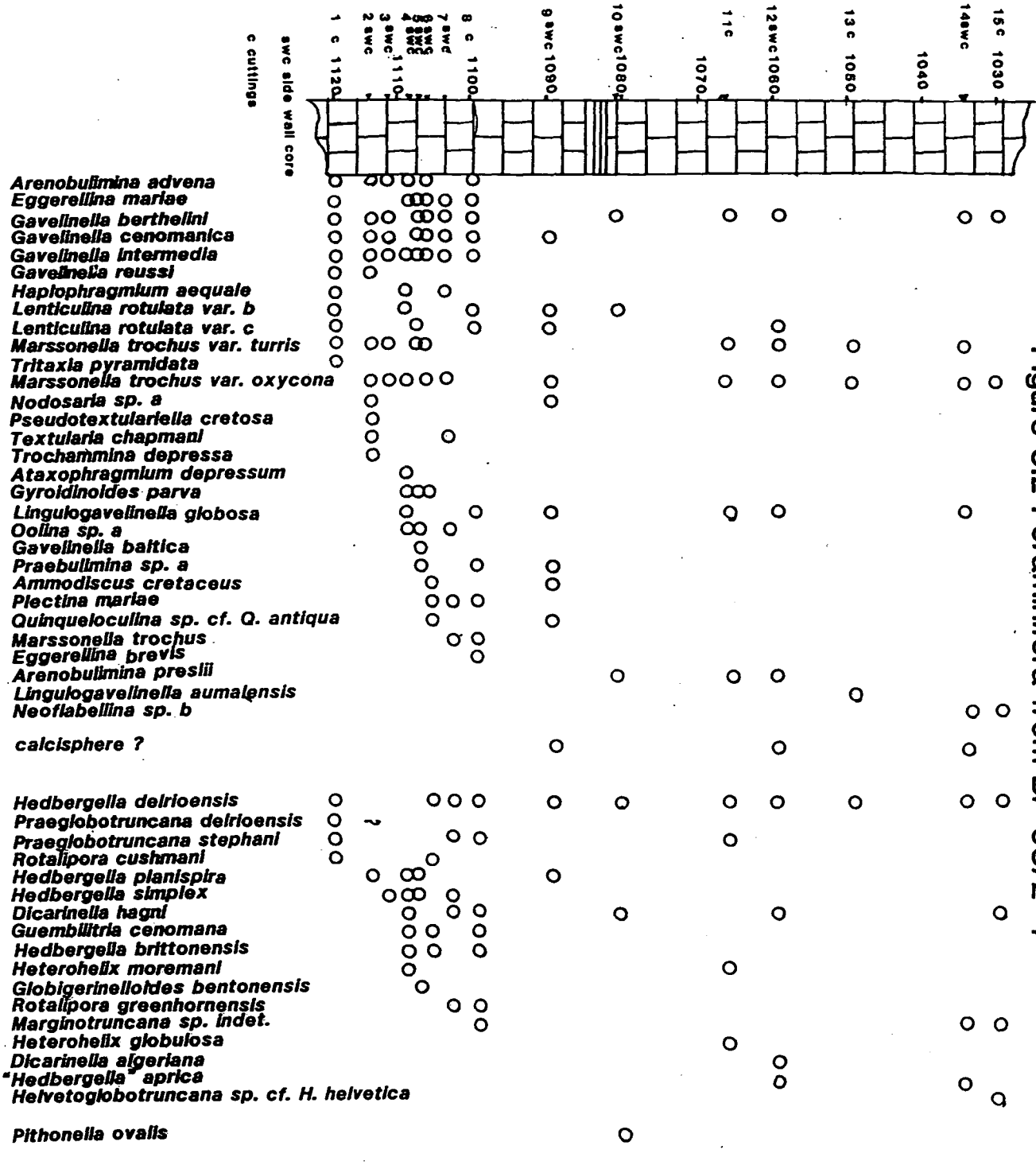

Figure 5.2 Foraminifera from BP 93/2-1

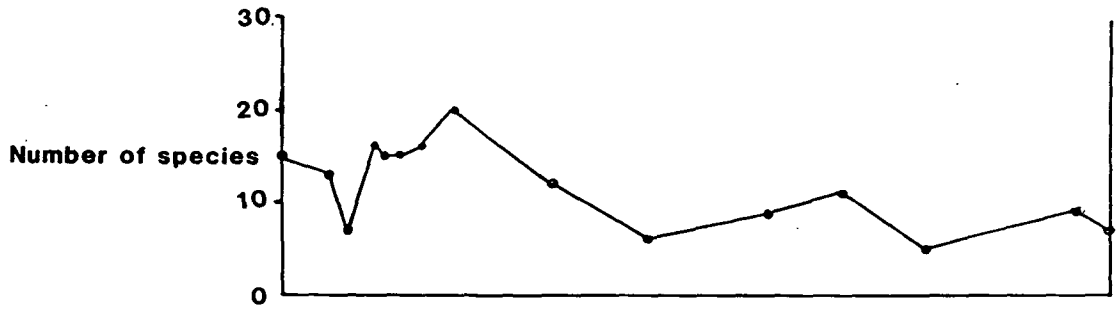

i.z. and this is in agreement with Williamson (1979). Furthermore, the occurrence of benthonic species such as G. cenomanica, G. intermedia and G. baltica with forms of the G. reussi - G. berthelini plexus is consistant with this (Carter and Hart, 1977; also see 5.7-10). The Marginotruncana sp. indet. in sample 9 is probably caved. "H". archaeocretacea was not recorded but the presence of H. sp. cf. helvetica in sample 15 places that sample, at least, within the H. helvetica i.z..

5.4(v). Foraminiferal assemblage.

The marked diversity change between samples 8-10 is consistant with the changes recorded onshore (see 5.5 -11), notably with the loss of G. cenomanica, G. intermedia, G. baltica, the Eggerellina population, P. mariae and the increased dominance of L. globosa and G. berthelini and the appearance of A. preslii. This interval contains the thin "calcareous mudstone" which is probably equivalent to the Plenus Marls which cover much of the Anglo-Paris Basin to the east (see 5.7-10). The gamma ray log was not available to investigate any possible deflection as exemplified by the offshore Plenus Marl Formation (Deegan and Scull, 1977).

5.5. Hooken Cliffs, Beer (Figures 3.2, 5.3-5).

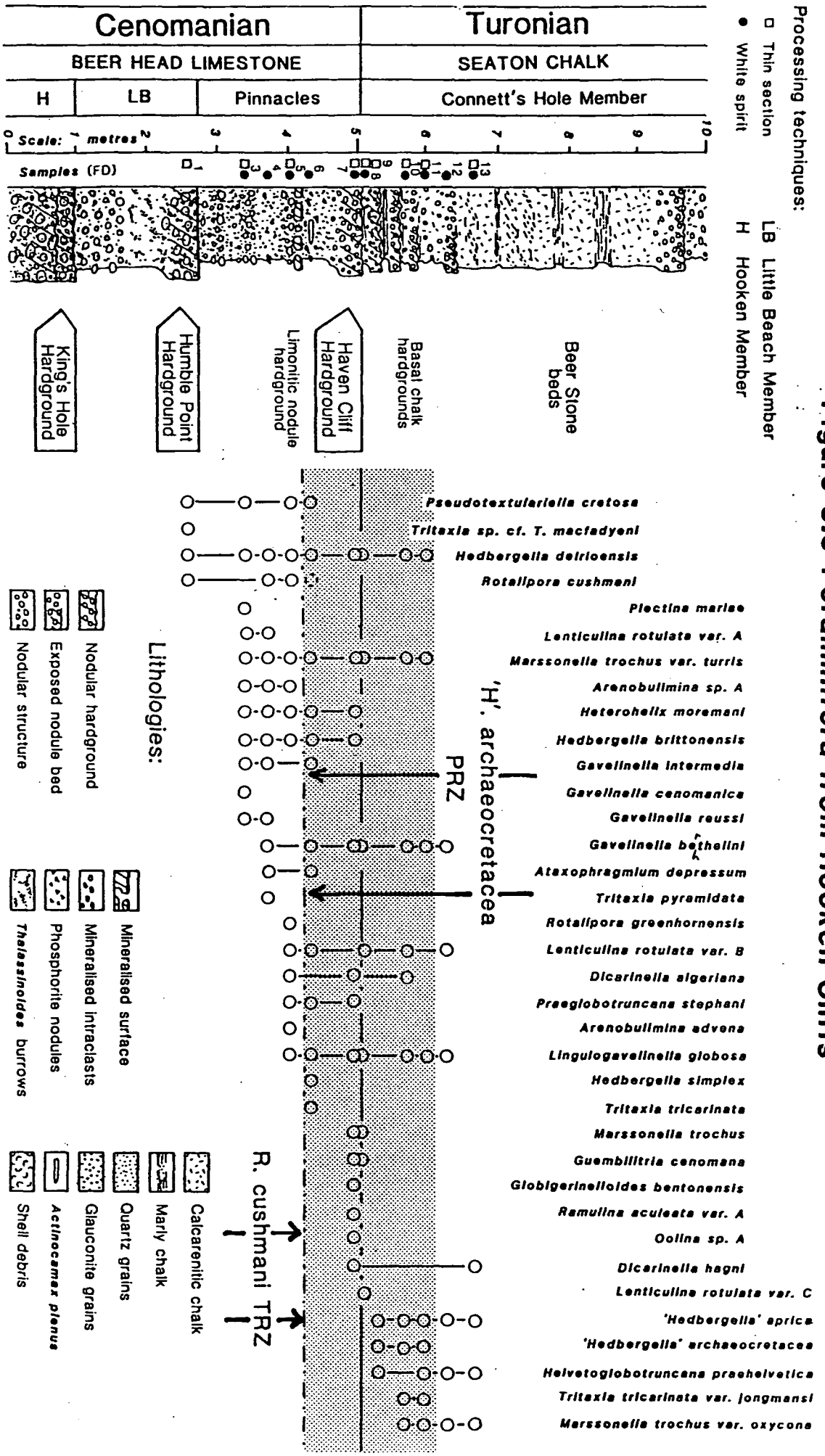

Figure 5.3 Foraminifera from Hooken Cliffs

5.5(i). Lithostratigraphy.

The sequence examined comprises the upper 2.5m of the Beer Head Formation and the lower 2m of the Seaton Chalk Formation (Jarvis and Woodroof, 1984), and is locally the thickest representation. The Beer Head Limestone Formation consists of a number of well-indurated hardgrounds superimposed on detritus-rich limestones, the most prominent of which are used to delimit a number of members. The Humble Point Hardground, a massively indurated intraclastic hardground with a strongly phosphatized and glauconitized surface, marks the summit of the Little Beach Member. This is overlain by the Pinnacles Member: 2.3m of poorly indurated yellowish-grey glauconitic limestones with a weakly developed limonitic nodular hardground (Haven Cliff Hardground), at its summit, (op cit. Jarvis et al., in press).

The overlying Connett's Hole Member (the basal member of the Seaton Chalk Formation), has weakly indurated limestones at its base passing up into chalks containing little detritus. In all, thirteen samples were examined from this succession (Figure 5.3).

5.5(ii). δ 13C isotope curve.

The δ 13C isotope (and oxygen isotope) curve (Figure 5.5) exhibits a marked excursion at the limonitic nodular hardground within the Pinnacles Member which is comparable

Figure 5.4 Details of foraminifera from Hooken Cliffs

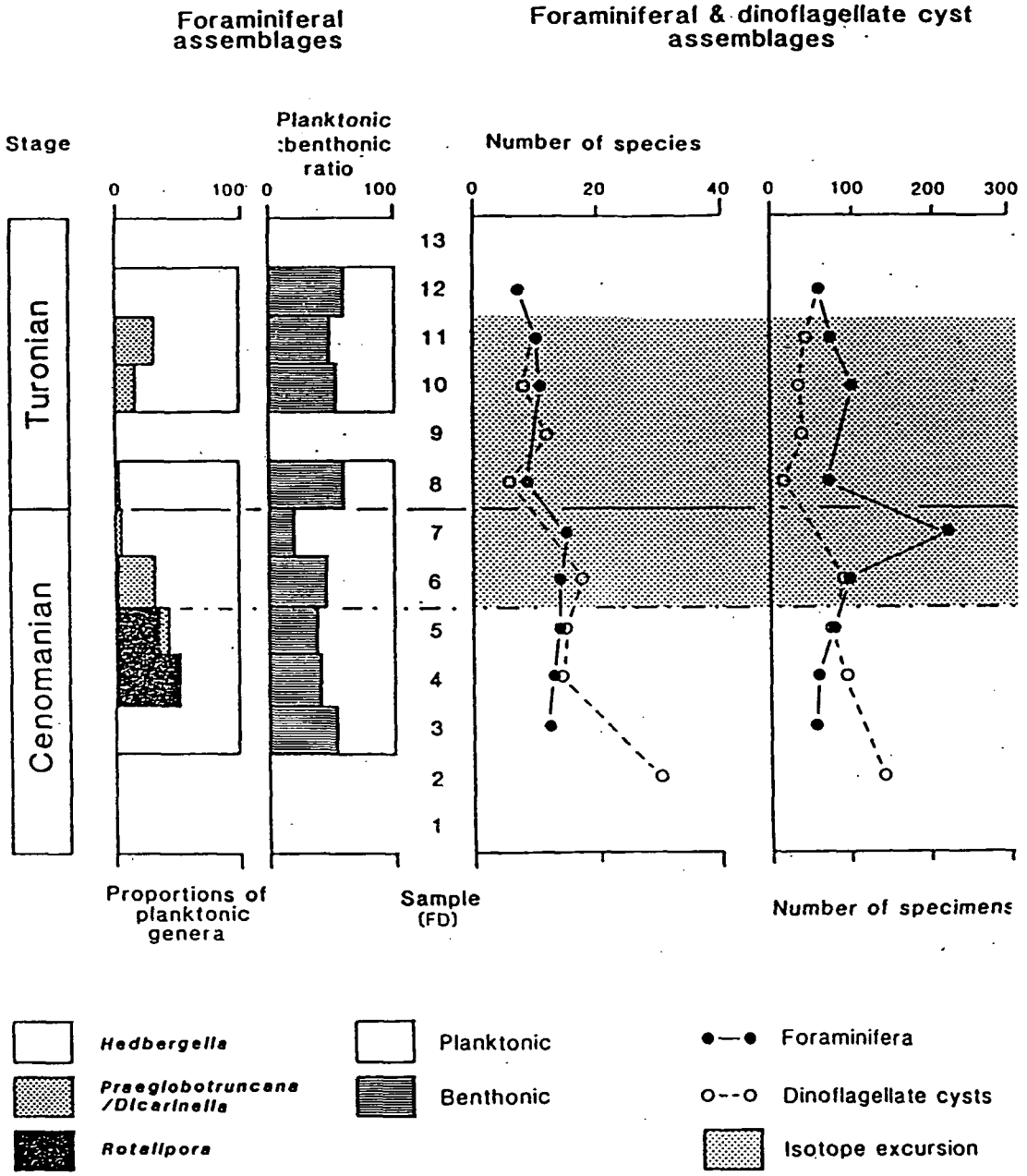

with other late Cenomanian records (Arthur et al., 1987), (see Figure 5.13 for detailed basin correlation).

5.5(iii). Macropalaeontological biostratigraphy.

The base of the Turonian in N.W. Europe is defined on ammonites and inoceramid bivalves, Watinoceras spp. and Mytiloides sp. cf. M. opalensis (sensu Kaufman non Bose), (Birkelund et al., 1984). These have been recorded from immediately above the Haven Cliff Hardground (Wright and Kennedy, 1981), and thus it marks the base of the Turonian in S.E. Devon (Wright and Kennedy, 1981; Jarvis and Tocher, 1983; Jarvis and Woodroof, 1984; Jarvis et al., in press). In addition, the assemblage also contains reworked ammonites of the Neocardioceras juddii zone (latest Cenomanian).

5.5(iv). Foraminiferal biostratigraphy.

The presence of R. cushmani (samples 1,4 and 5) and R. greenhornensis (sample 5), places these within the top of the R cushmani i.z., this in agreement with Hart (1970) and Carter and Hart (1977). The presence of "H". archaeocretacea (samples 9, 10, 11), places these within the H. archaeocretacea i.z. of Robaszynski and Caron (1979) which is in agreement with Hart and Weaver (1977), though they did not record any planktonics from the lowermost Connett's Hole Member.

Figure 5.5 Isotope curves from Hooken Cliffs

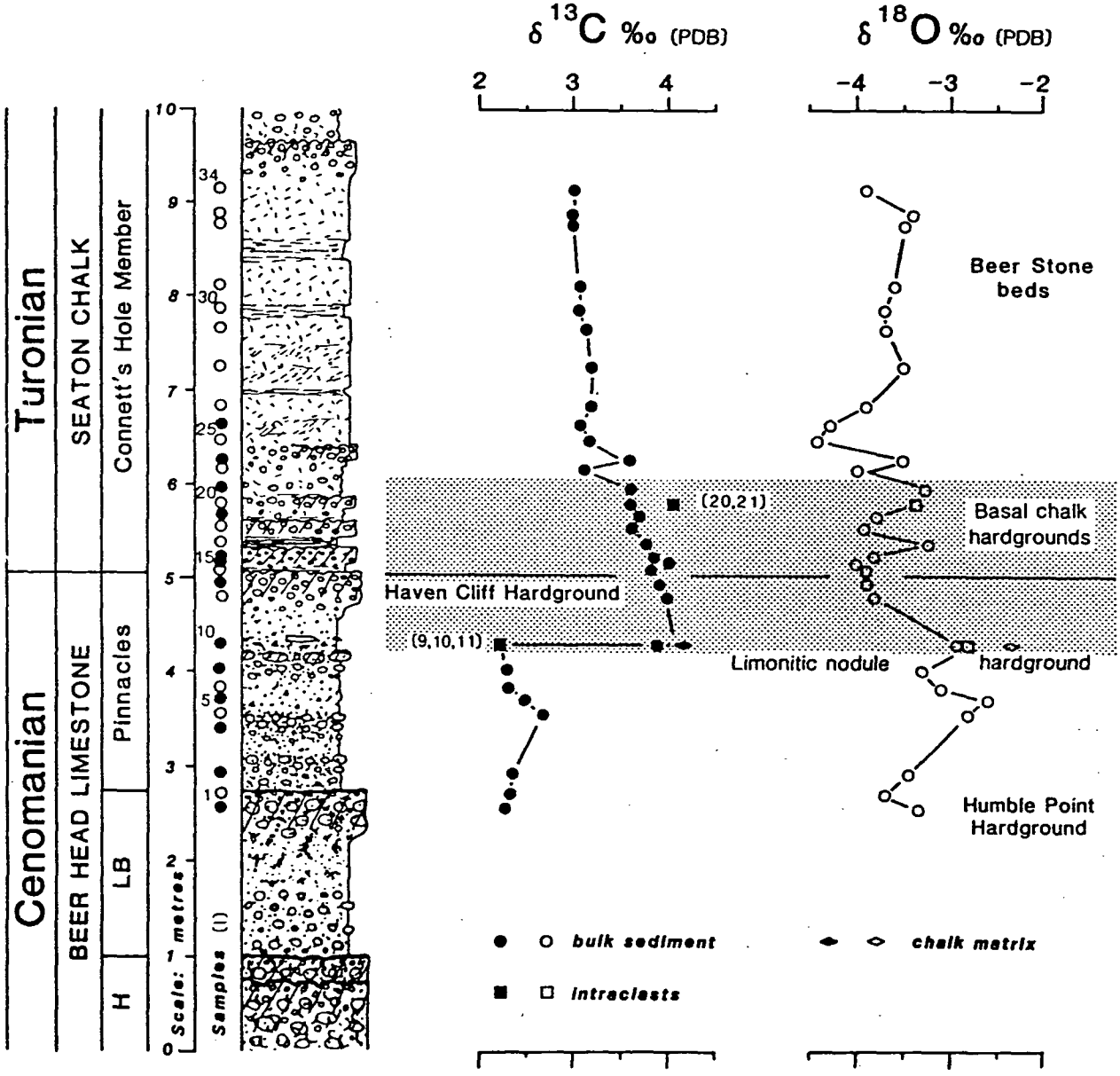

5.5(v). Foraminiferal assemblage.

The foraminiferal assemblage (Figure 5.3) is impoverished compared to the basinal facies to the east (see 5.7-10), and the preservation of the specimens very variable, with many broken and exhibiting intense dissolution (particularly samples 3,6 and 8). The intense induration of some of the samples, especially those associated with hardgrounds, only permitted analysis of the foraminifera using thin sections. Thus no measurement of the relative proportions of each species was possible.

The foraminiferal assemblage is comparable to that recorded from a laterally equivalent sequence in a large isolated stack (the Pinnacles), by Carter and Hart (1977).

The foraminiferal assemblage shows a slight drop in diversity up the sequence (Figure 5.4), and a low specimen count for each sample except for one (sample 7), and this is due to an increase in the numbers of H. delrioensis with the appropriate change in the planktonic : benthonic ratio (Figure 5.4).

5.6. Shapwick Grange Quarry (Figures 3.3, 5.6).

5.6(i). Lithostratigraphy.

Shapwick Grange Quarry exposes the Upper Greensand, the Beer Head Limestone and the lower part of the Seaton Chalk

(Jarvis et al., in press). The Upper Greensand comprises 7m of yellow-light grey calcarenites which locally contain high proportions of quartz and glauconite sand. The sequence also contains prominent chalcedonic cherts at the base and in the middle of the sequence (Figure 5.6).

Two nodular hardgrounds with glauconitized surfaces occur in the succession. The lower one is found between the chert levels and the other forms the top of the Upper Greensand. The latter has been called the Small Cove Hardground in the comparable succession in the Beer area (Jarvis and Woodroof, 1984).

The Beer Head Limestone is strongly attenuated (60cm.), and two beds may be recognized. The lower one (25cm.) is comprised of intensely indurated light grey, quartz-rich micritic limestone. The structure of the bed is very complex, exhibiting many phases of sedimentation, bioturbation, cementation, reworking, mineralization, encrustation and boring (Jarvis et al., in press). These characteristics are diagnostic of the Humble Point Hardground (top of the Little Beach Member) in severely attenuated successions (Jarvis and Woodroof, 1984; Jarvis et al.,in press).

The Humble Point Hardground is overlain by 35cm. of strongly indurated nodular micrites containing occasional quartz sand. Its surface is uneven and has pebble intraclasts plastered upon it. This is representative of the Haven Cliff

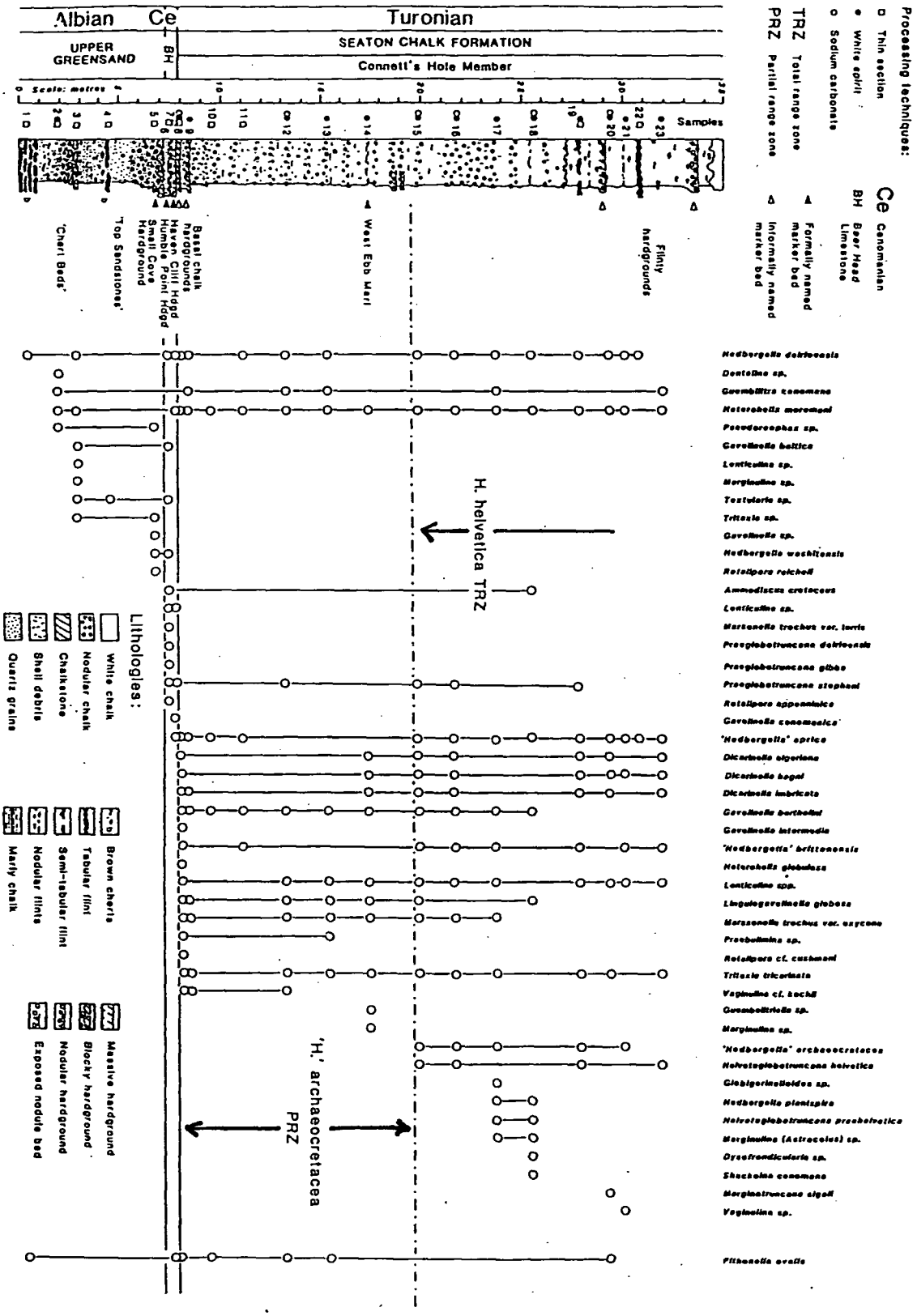

Figure 5.6 Foraminifera from Shapwick Grange Quarry

Hardground which is the top of the Pinnacles Member (Jarvis and Woodroof, 1984; Jarvis et al., in press). The surface of the Haven Cliff Hardground marks the base of the Seaton Chalk.

The Seaton Chalk Formation (20m) consists of two moderately indurated hardgrounds at its base overlain by ~1m thick weakly developed rhythms of alternating poorly nodular and marly chalks. Nodular flints are associated with an omission suface developed 20m above the base of the Seaton Chalk Formation. The uppermost 6m of section consists of marly chalks including a second prominant semitabular flint and two weakly developed nodular hardgrounds. The sequence is comparable to the Connett's Hole Member (Jarvis and Woodroof, 1984; Jarvis et al., in press).

5.6(ii). δ 13C isotope curve.

There are no isotope curves available for this section.

5.6(iii). Macropalaeontological biostratigraphy.

Shapwick has yielded many diverse and biostratigraphically important ammonite assemblages (Hamblin and Wood, 1976; Wright and Kennedy, 1981; Kennedy et al., 1982; Wright and Kennedy, 1984), that are usually associated with hardground surfaces.

An assemblage of Stoliczkaia dispar (d'Orbigny) and

species of Callihoplites and Discohoplites were recorded from the "Upper Greensand" (Hamblin and Wood, 1976), providing a definite late Albian S. dispar zone age for the top of the Upper Greensand, though the exact position of this fauna was not made against a lithological log. They were later positioned (Wood, in Hart et al., 1979), 1.5m above the tabular cherts, placing them within the Small Cove Hardground. These ammonites are now thought to have come from 1m above the tabular cherts from a fine sand unit just below the Small Cove Hardground (Wood, pers. comm.).

From immediately above the Humble Point Hardground (base of the Pinnacles Member), Euomphaloceras euomphalum (Sharpe) and Calyoceras naviculare (Mantell) have been recorded belonging to the early late Cenomanian Calyoceras guerangeri zone (Wright and Kennedy, 1981).

Ammonites of the latest Cenomanian Neocardioceras judii zone have been recorded as some of the intraclasts welded to the surface of the Haven Cliff Hardground (Wright and Kennedy, 1981; Kennedy et al., 1982).

An assemblage of earliest Turonian Watinoceras spp. occurs in the nodular hardground at the bottom of the Seaton Chalk.

5.6(iv). Foraminiferal biostratigraphy.

A foraminiferal study of the greensand yielded a very

poor fauna of Patellina trochiformis (Shacko), Arenobulimina sp. cf. A. obliqua (d'Orbigny), Arenobulimina sp. cf. A. depressa (Perner) and Marssonella oxycona (Reuss) from just below the chert beds (Hart et al., 1979). The assemblage did not permit a finer biostratigraphical resolution than an Albian - Cenomanian age (op cit.).

The Small Cove Hardground has yielded R. reicheli and Favusella washitensis (Figure 5.6). The presence of the former indicates that part of the sediment within the hardground is of an early Cenomanian age (Robaszynski and Caron, 1979). In addition, its association with F. washitensis is comparable to other local clastic dominated sequences of early Cenomanian age, e.g. Wilmington (Hart, 1970; Carter and Hart, 1977; Hart, 1983). Thus it implies the Small Cove Hardground contains sediment of Pounds Pool Member equivalent even though it is not present as a unit at Shapwick.

The presence of R. appenninica within the Humble Point Hardground infers an early to middle Cenomanian age (Robaszynski and Caron, 1979) for part of that unit. The nodular hardground at the base of the Seaton Chalk yielded T. tricarinata, G. berthelini and L. globosa, a characteristic early Turonian benthonic assemblage (Owen, 1970; Carter and Hart, 1977; see 5.7-10). Also present are a small number of G. intermedia and Rotalipora sp. cf. R. cushmani which are characteristic of the Cenomanian. These specimens are very

poorly preserved and heavily pitted. The rotaliporids are neanic and this, coupled with their poor preservation, makes their identification problematical. These specimens are probably reworked.

These features of downworking through burrowing and reworking on top of the hardground surfaces causes intermixing of the fauna and thus negates against biostratigraphical resolution.

The presence of H. helvetica 12m from the base of the Connett's Hole Member, infers an early - middle Turonian age (Robaszynski and Caron, 1979). "H". archaeocretacea is not recorded from below the sample containing H. helvetica which may be the result of the poor recovery of such delicate planktonic species from highly nodular chalks such as those found at the base of the Connett's Hole Member.

5.6(v). Foraminiferal assemblage.

The foraminiferal assemblage, in keeping with Hooken Cliffs (5.5(v)), is very poor when compared to the diversity of the most basinal sections (5.8-11).

5.7. Introduction to the lithostratigraphy and biostratigraphy of the mid-Cretaceous Chalk facies of southern England.

The mid-Cretaceous lithostratigraphy of the Chalk

facies of the Anglo-Paris Basin in southern England has recieved much attention (Phillips, 1818, 1821; Jukes-Browne and Hill, 1903,1904; Jefferies, 1962; Hancock, 1976; Mortimore, 1986; Robinson, 1986). All workers recognized the Plenus Marl (Robinson, 1986), and for the purpose of this study, which only covers this short interval, one lithostratigraphic scheme has been adopted (see 3.4).

The studied interval covers the Abbots Cliff Chalk Formation (part), Plenus Marl Formation and the Dover Chalk Formation (part). Only the top of the former, the Chapel-le-Ferne Member is covered in this study and consists of bioturbated chalks with occasional marl seams. The base of the Plenus Marl Formation is marked by an erosion surface (Jefferies, 1962), the sub-Plenus erosion surface, and the overlying Plenus Marl Formation consists of eight distinct beds numbered 1-8, the relative thicknesses of which may vary. The Dover Chalk Formation consists of a variety of lithologies: white chalk, calcarenitic chalk, nodular chalk and intraclastic chalk with occasional flints. Well-developed marl seams occur throughout the Formation (Robinson, 1986). It consists of three members: the Shakespeare Cliff, Aycliff and Akers Steps Members. The Shakespeare Cliff Member may consist of very nodular chalks with incipient hardgrounds at its base (Melbourn Rock facies) (Robinson, 1986).

The Cenomanian - Turonian boundary is proposed on

ammonites as the base of the Pseudaspidoceras flexuosum zone (Birkelund et al., 1984), although this is a tethyan form. In Europe, the appearance of a Watinoceras coloradoense zone ammonite assemblage is used (Wright and Kennedy, 1981; Kennedy et al., 1982; Kennedy, 1984), although the subspecies W. coloradoense coloradoense (Henderson) is absent in Europe.

The associated inoceramid fauna is useful. The base of the P. flexuosum zone is marked by the appearance of Mytiloides opalensis sensu Kauffman non Bose in America and a widespread appearance of early Mytiloides throughout the Tethyan and Boreal realms (Kauffman et al., 1977; Birkelund, 1984; Hancock, 1984). Thus, because of the poor ammonite records in the onshore basinal sections, the inoceramid faunal change is a good Turonian indicator (Jefferies, 1963; Kennedy and Wright, 1981; Woodroof, 1981).

The foraminiferal zones previously proposed (Williams-Mitchell, 1948; Carter and Hart, 1977), use an integrated benthonic and planktonic scheme. The latter is particularly well-suited to correlation of the more basinal facies of the Anglo-Paris Basin. This study covers the upper level of zone 13 and all of zone 14, sensu Carter and Hart, 1977. Zone 14 coinciding with the Plenus Marl Formation (op cit.). Carter and Hart (1977) did not consider the whole of the succession above the Plenus Marl Formation. Owen (1970), established a series of local planktonic assemblage zones

through the Turonian based upon relative abundances and occurrence. These have been coupled with the international zones proposed by Robaszynski and Caron (1979), and combined with locally significant benthonic species (Hart, 1982b).

5.8 White Nothe (Figures 3.7, 5.7, 5.8).

5.8(i). Lithostratigraphy.

The sequence at White Nothe comprises 10m of the top of the Abbots Cliff Formation, 3.6m of the Plenus Marl Formation and 15m of the Dover Chalk Formation of which the first 1.5m is not exposed (Figure 5.7).

The Abbots Cliff Formation consists of 1m-0.5m marl-marly chalk rhythms with their frequency increasing up the succession. There are occasional flints towards the base.

All eight beds (sensu Jefferies, 1963) of the Plenus Marl Formation are present, with beds 1-4 being well represented, comprising 2.5m of the 3.6m unit.

The base of the Dover Chalk Formation is not exposed. The overlying sequence is composed of thinly bedded nodular chalks with incipient hardgrounds passing into nodular chalk-marl rhythms the thickness of which varies from 0.75m-1.75m. Nodular chalks become dominant towards the top of the sequence.

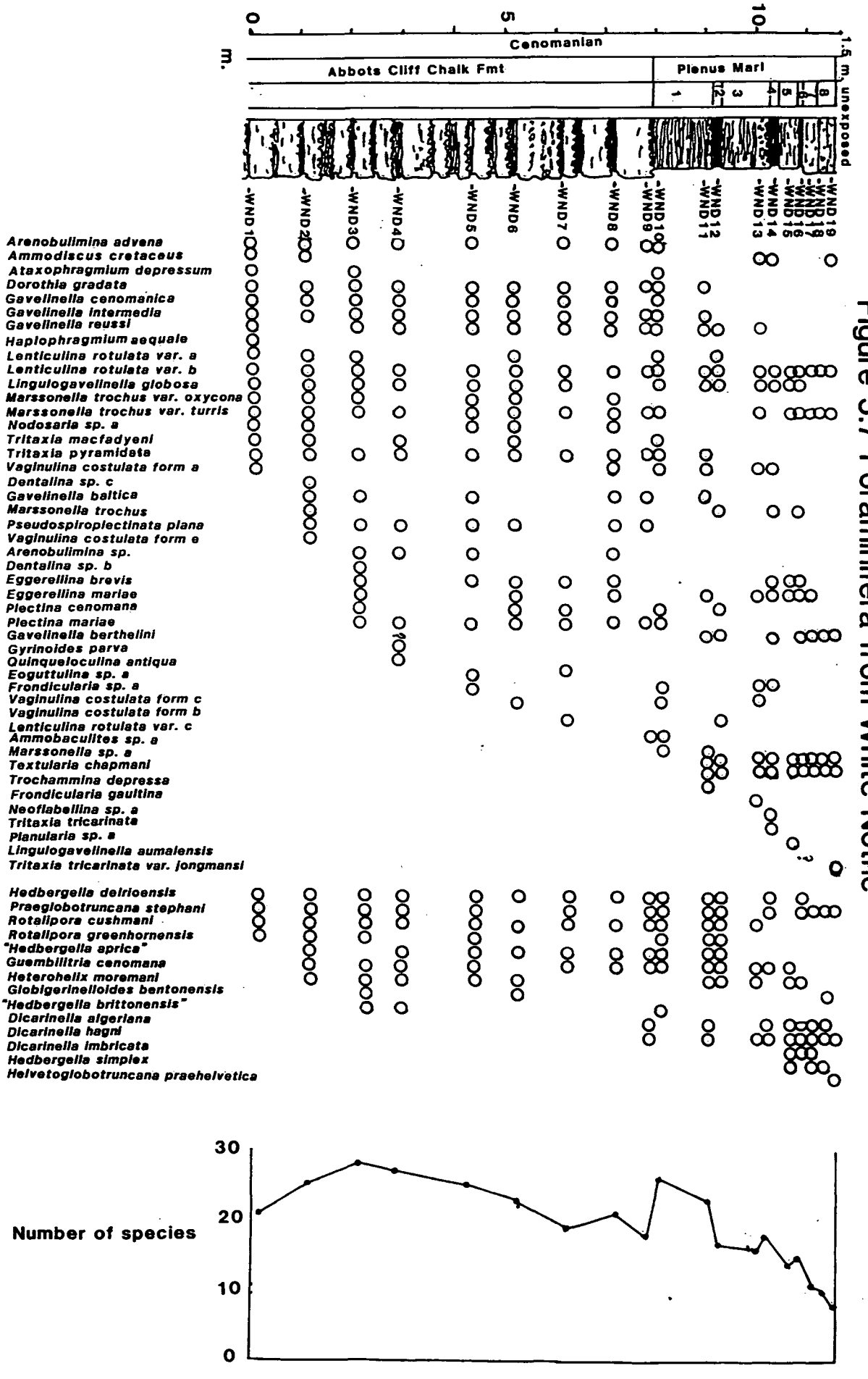

Figure 5.7 Foraminifera from White Nothe

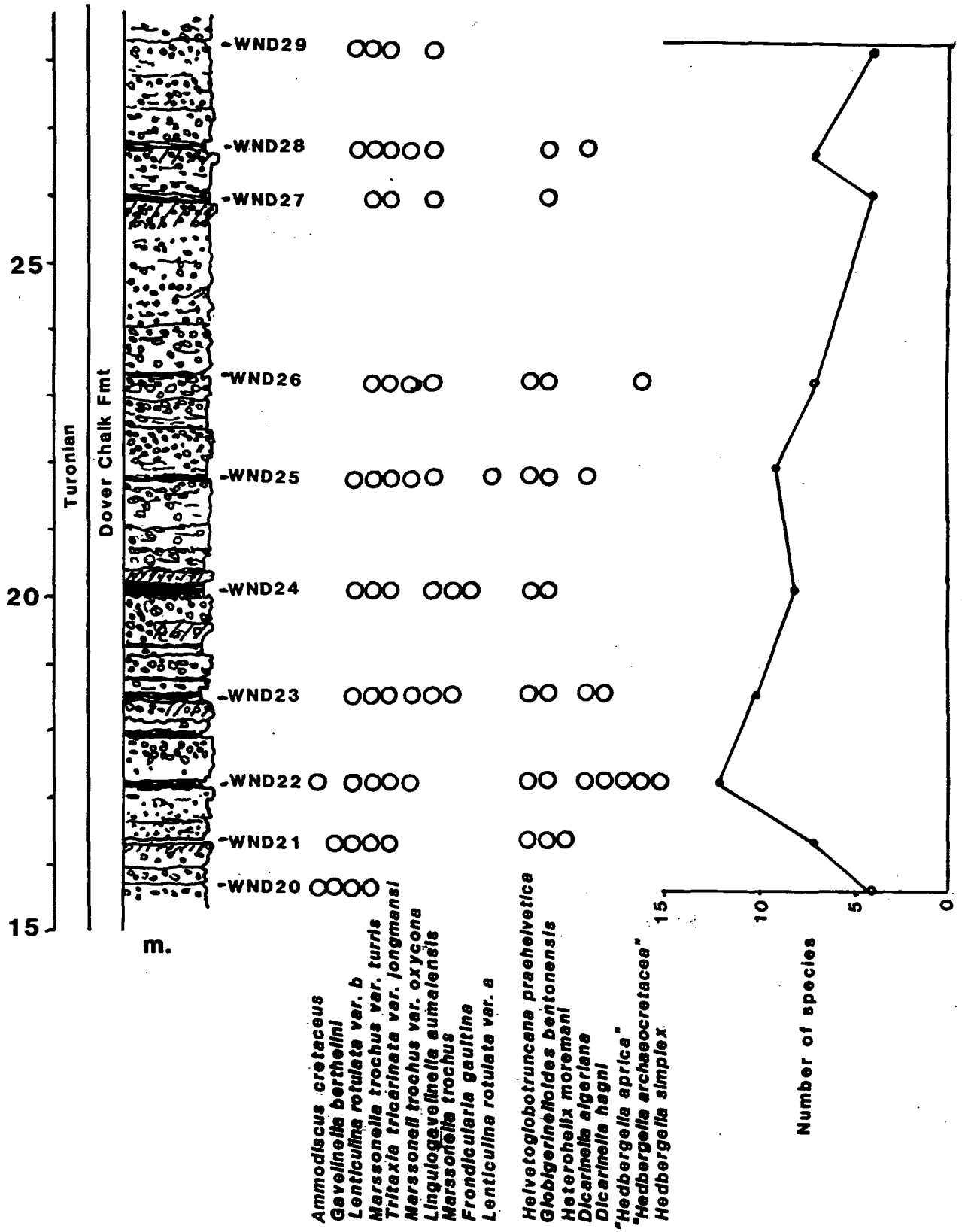

Figure 5.7 Foraminifera from White Nothe (cont.)

5.8(ii). δ13C isotope curve.

There is no δ13C isotope curve available for White Nothe.

5.8(iii). Macropalaeontological biostratigraphy.

The base of the M. sp. cf. M. opalensis zone appears to be 2.8m above bed 8 of the Plenus Marls (Woodroof, 1981).

5.8(iv). Foraminiferal biostratigraphy.

The presence of R. cushmani (samples 1-13), and R. greenhornensis (samples 1-3, 5, 10-12), places the lower part of the sequence, up to the top of bed 3 (Plenus Marls), within the top of the R. cushmani i.z.. "H". archaeocretacea is rare (samples 22, 26), and definitely places the early portion of the Dover Chalk Formation within the "H". archaeocretacea i.z.. Early forms of the H. praehelvetica - H. helvetica plexus also occur (samples 19, 21-26) in this interval.

5.8(v). Foraminiferal assemblage.

The numbers of the foraminiferal population recovered varies considerably across the interval (Figure 5.8) which is a result of the interaction of benthonic diversity, planktonic diversity and preservation.

Within the Abbots Cliff Chalk Formation (samples 1-9), the population varies around 150 specimens (minimum), and 340

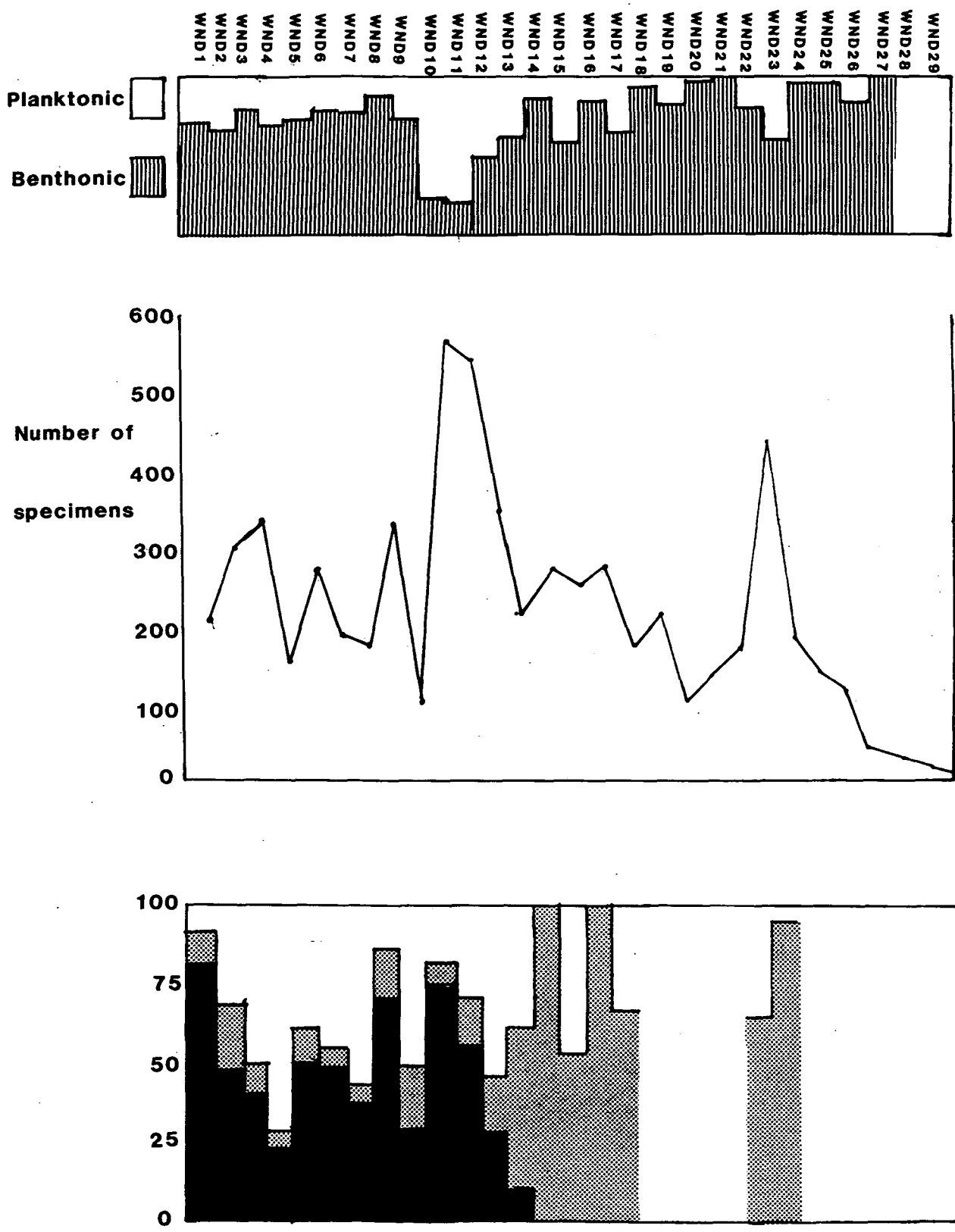

Figure 5.8 Foraminiferal details from White Nothe

specimens (maximum) per sample, but shows a marked drop at the summit of the unit (sample 9) to 105 specimens. The planktonic diversity remains constant but the benthonic diversity largely mirrors the population numbers. The planktonic : benthonic ratio shows a gradual decrease (through samples 1-8) but a slight increase at the top (sample 9). Within the planktonic population the rotaliporid component shows a steady decline (samples 1-4) with a small recovery (samples 5-7) and a complex change (samples 8 and 9). The praeglobotruncanid/dicarinellid population remains constant and no planktonic or benthonic species becomes extinct throughout.

The Plenus Marl Formation, in contrast, shows major changes in diversity, population numbers and the relative numbers of planktonic and benthonic specimens. Bed 1 shows a significant increase in numbers (550 specimens) with an increase in benthonic diversity, though there is a slight decline at the top of bed 1. The planktonic diversity remains the same as from the Abbots Cliff Chalk Formation but the planktonic : benthonic ratio is very high, with the planktonic population forming 80% of the total. Within the planktonic population the rotaliporid component is high (75%) but declines slightly through the bed. At the top of bed 1 A. advena, D. gradata, G. cenomanica, G. intermedia, G. baltica, T. macfadyeni, A. depressum and P. plana disappear.

Through beds 2-8 the benthonic diversity declines as does the number of specimens recovered, from 340-120. The planktonic : benthonic ratio decreases up these beds with the planktonic population forming as little as 10% of the total population. Within the planktonic population, the decline in the rotaliporid component (started in bed 1) continues with R. cushmani disappearing at the top of bed 3. Unlike the Abbots Cliff Chalk Formation the praeglobotruncanid/dicarinellid component becomes the dominant component of the total population. The benthonic population becomes dominated by an assemblage of L. rotulata var.b , G. berthelini, L. globosa and T. chapmani, the latter disappearing in bed 7. The specimens from beds 4 to 8 show pitted tests indicative of dissolution, the intensity of which is most marked in the tests of the planktonic species.

The decline in the total number of specimens continues into the Dover Chalk Formation except for one sample (no. 22). At the base of the Formation, the population is totally dominated by benthonic specimens. There is a slight increase in the planktonic influence (samples 22 and 23), mainly dicarinellids, which accounts for the increased number specimens from these samples. There are not sufficient number of planktonic specimens to warrant a detailed breakdown of the population.

5.9. Compton Bay, Isle of Wight (Figures 3.6, 5.9, 5.10).

5.9(i). Lithostratigraphy.

The sequence comprises 9.75m of the Abbots Cliff Formation, the Plenus Marl Formation (4.2m) and 24.2m of the Dover Chalk Formation (Figure 5.9). The sequence dips steeply to the N.W. and is complicated by faulting in the Dover Chalk Formation (Text Plate 2).

The Abbots Cliff Formation consists of bedded chalk marl - marl rhythms of variable thickness, 0.5 - 2.0m, though mostly they are >1m. Intense bioturbation is discernable where there is sufficient lithological contrast.

The Plenus Marl Formation (Text Plate 2), is well-developed with all eight beds present. The sub-Plenus erosion surface is poorly developed compared to Eastbourne (5.10(i)) and Dover (5.11(i)).

The base of the Dover Chalk Formation is marked by 2m of pebbly hardgrounds with a minor detrital component of shell debris. Above this is a sequence of chalk marls with the occasional well-developed marl. At 6.5m above bed 8 there is a prominent discontinuous sponge-rich hardground. The sequence is incomplete (11.5m above bed 8) because of strong local faulting. Apart from the thin nodular hardgrounds at the base

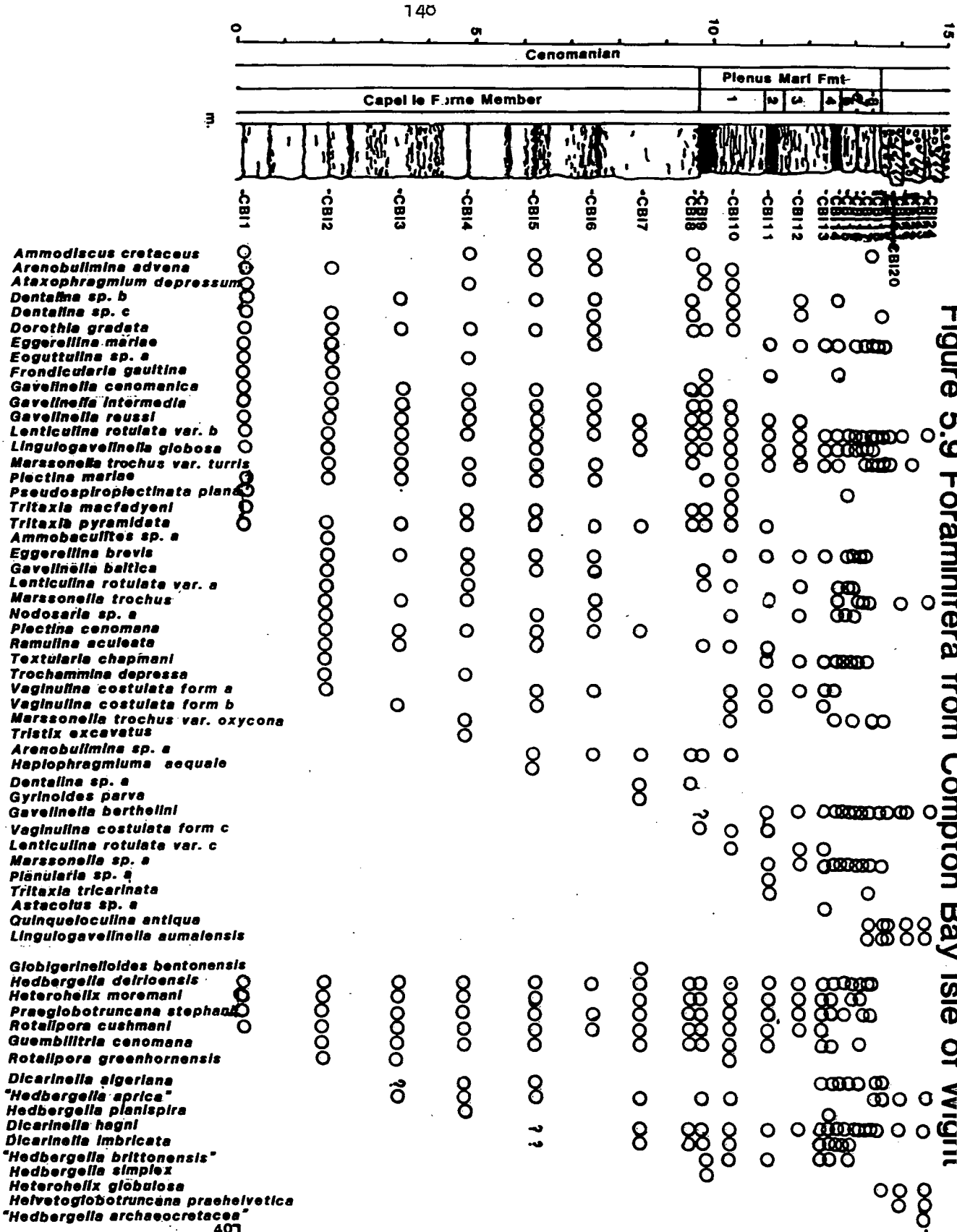

Figure 5.9 Foraminifera from Compton Bay, Isle of Wight

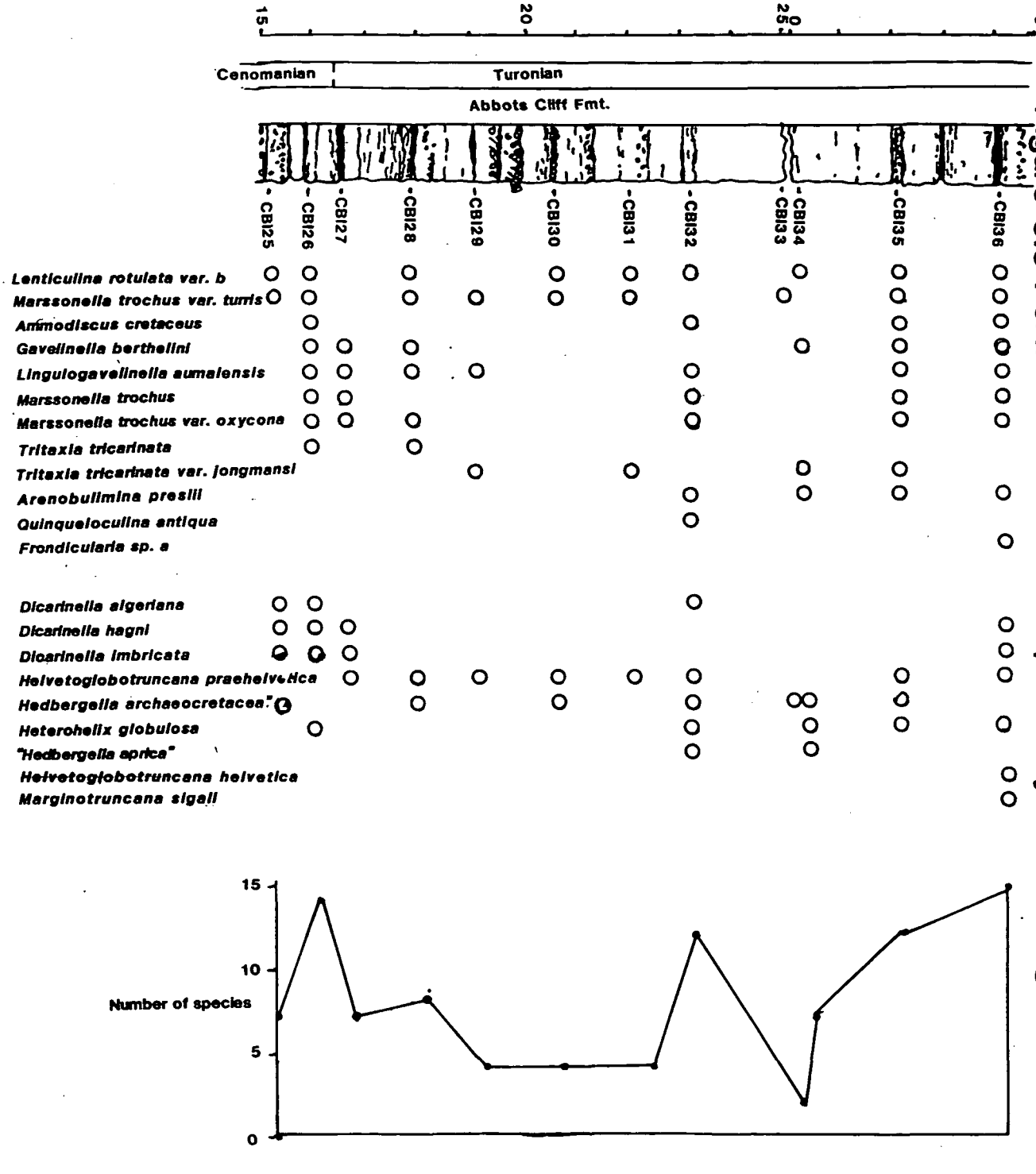

Figure 5.9 Foraminifera from Compton Bay Isle of Wight (cont.)

of the Dover Chalk Formation, it is considerably less nodular and pebbly than the sequences to the east, particularly Dover.

5.9(ii). δ13C curve.

There is no δ 13C isotope curve available for this section.

5.9(iii). Macropalaeontological biostratigraphy.

The base of the M. sp. cf. M. opalensis zone is 3.1m above the base of the Dover Chalk Formation (Woodroof, 1981).

5.9(iv). Foraminiferal biostratigraphy.

The presence of R. cushmani (samples 1-13), and R. greenhornensis (samples 2, 3 and 10), places the lower part of the sequence up to the top of bed 3 (Plenus Marls), within the top of the R. cushmani i.z.. "H". archaeocretacea appears in the basal beds of the Dover Chalk Formation (samples 21, 22, 24-26, 28, 30-32, 34-36), and places up to sample 36 within the "H". archaeocretacea i.z.. The presence of H. helvetica (samples 36, 37), places these within the H. helvetica i.z..

5.9(v). Foraminiferal assemblage.

The number of the foraminiferal population recovered varies considerably across the interval (Figure 5.10) which is a result of the interaction of benthonic diversity, planktonic

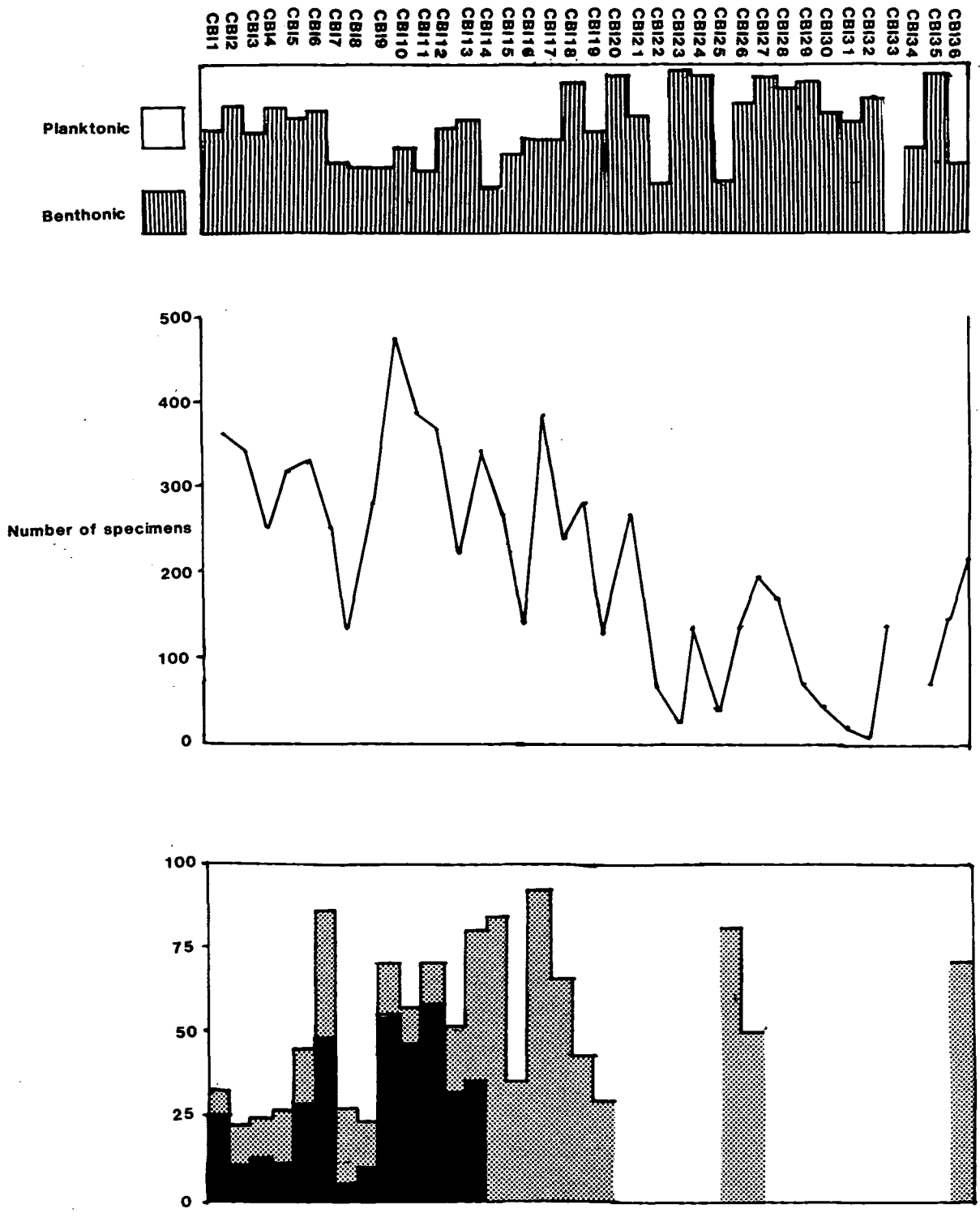

Figure 5.10 Foraminiferal details from Compton Bay Isle of Wight

diversity and preservation.

Within the Abbots Cliff Chalk Formation (samples 1-8), the population varies around 140 specimens (minimum) and 360 (maximum) per sample, but the population shows an increase at the top of the unit. The planktonic diversity remains constant but the benthonic diversity mirrors the population numbers. The planktonic : benthonic ratio shows a gradual decrease up the sequence (samples 1-7) with a sudden increase at the summit (sample 8). Within the planktonic population, the rotaliporid component forms much less than 50% of the total population. It decreases at the base of the section (samples 1-4), shows a small recovery (samples 5, 6) and then a decrease at the summit (samples 7, 8). The praeglobotruncanid/dicarinellid population forms around 5-35% of the total population. Major changes occur in the hedbergellid population.

The Plenus Marl Formation, in contrast, shows major changes in diversity, population numbers and the relative numbers of planktonic and benthonic specimens. Bed 1 shows a significant increase in the numbers of specimens (~460), although it is declining towards the middle of the bed. The benthonic diversity, in contrast, increases through the bed. The planktonic diversity remains the same as for the Abbots Cliff Chalk Formation and the planktonic : benthonic ratio remains as high as for the top of the Abbots Cliff Chalk

Formation, with around 55% planktonics.

5.10. Eastbourne, Gun Gardens (Figures 3.5, 5.11, 5.12).

5.10(i) Lithostratigraphy.

The succession at Eastbourne is expanded compared to Dover (5.11(i)), White Nothe (5.8(i)) and the Isle of Wight (5.9(i)) (Jefferies, 1962; Carter and Hart, 1977; Woodroof, 1981). It comprises 10.5m of the top of the Abbots Cliff Chalk Formation, the Plenus Marl Formation (8.3m) and 37m of the Dover Chalk Formation. Although towards the top of the sequence part of the Dover Chalk Formation is inaccessible (Figure 5.11).

The Abbots Cliff Formation comprises <0.5-1.0m chalk marl- marl rhythms which exhibit a high degree of bioturbation (Text Plate 1).

The Plenus Marl Formation is significantly thicker, at 8.3m, than to the east (Dover) and west (Compton Bay, White Nothe), with a prominent sub-Plenus omission surface.

The Dover Chalk Formation comprises 5-6m of slightly nodular chalks and marl seams at its base passing into marl chalks with prominent marl seams. Towards the top of the

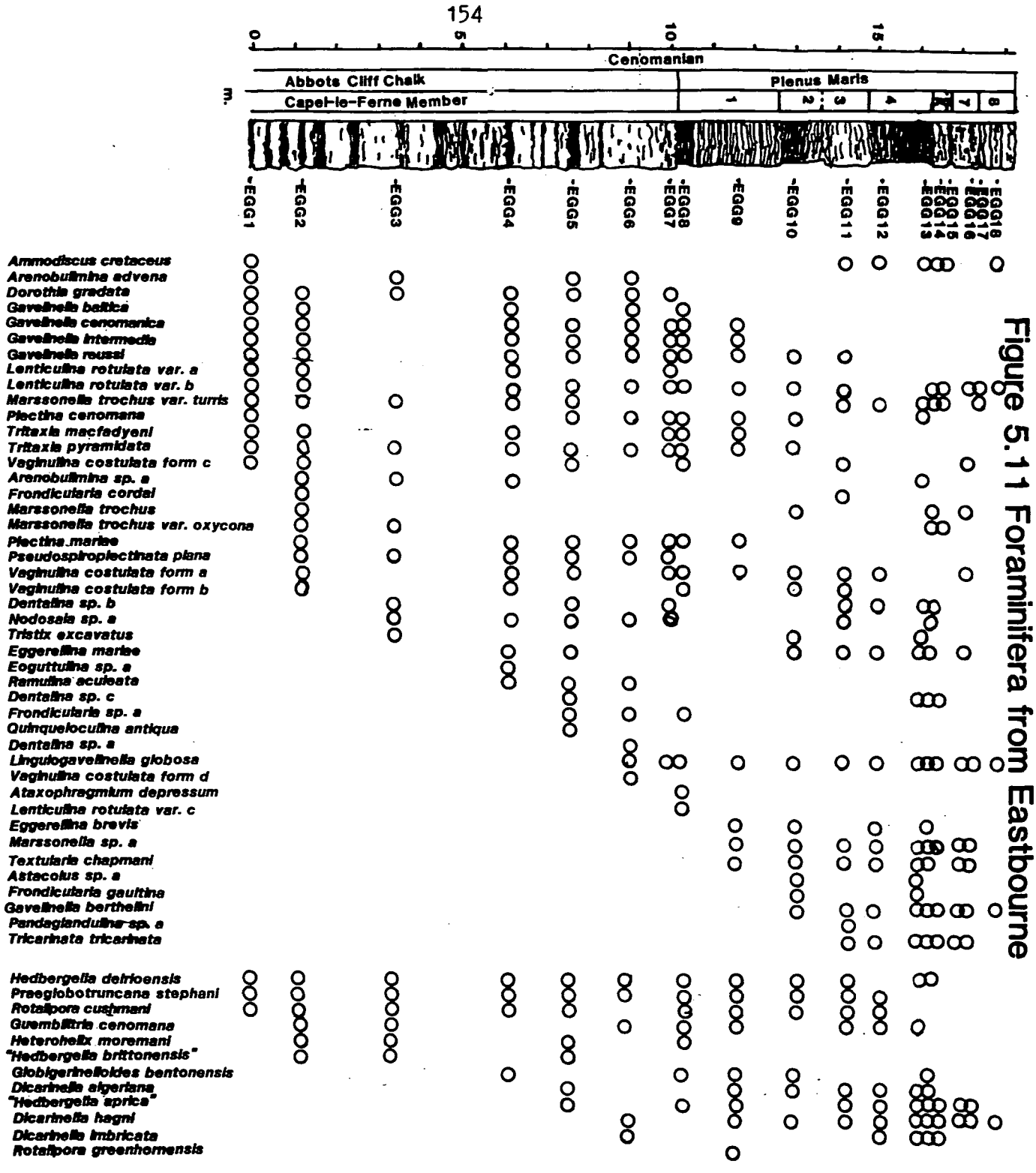

Figure 5.11 Foraminifera from Eastbourne

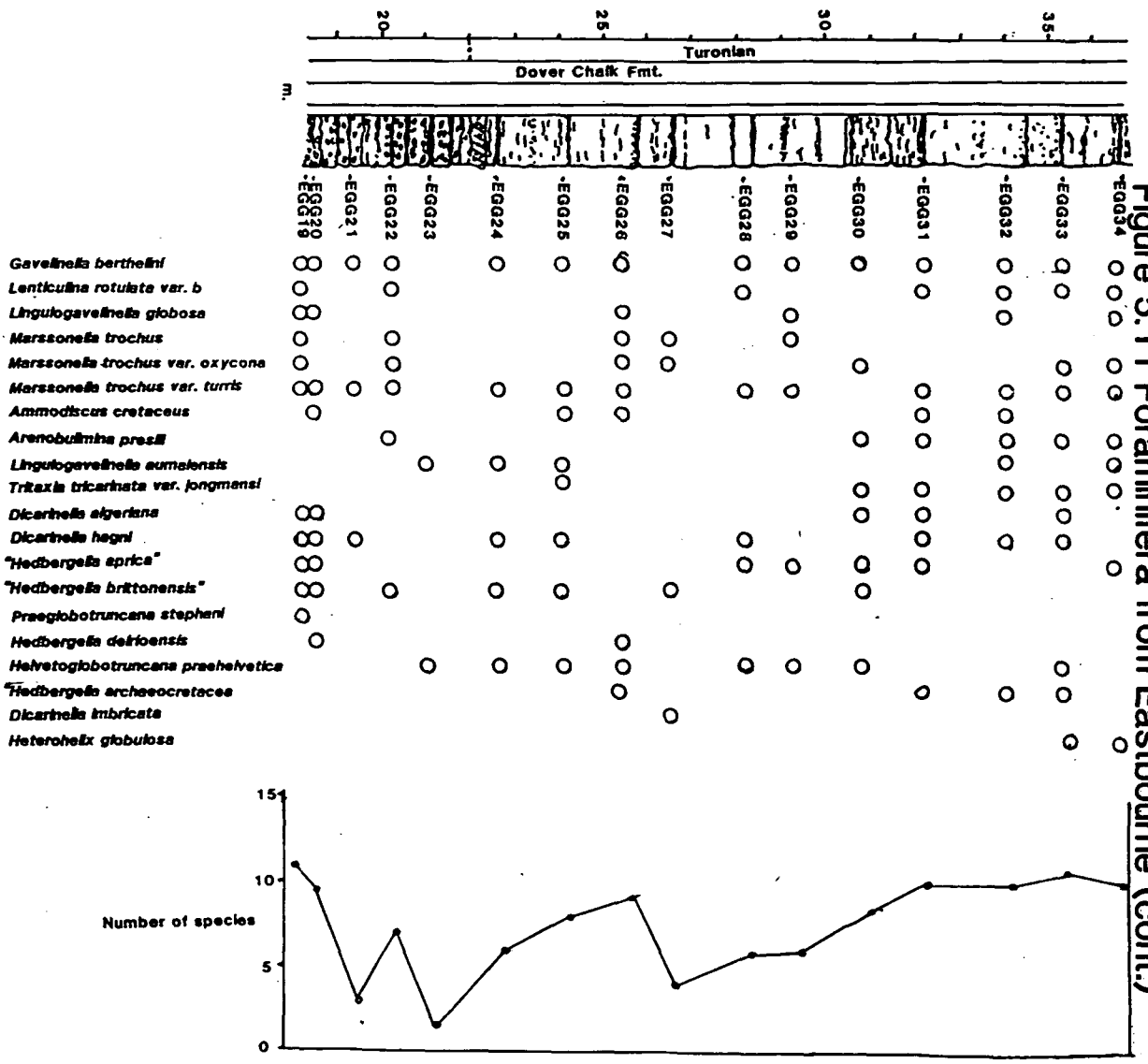

Figure 5.11 Foraminifera from Eastbourne (cont.)

sequence there are very occasional locally developed incipient hardgrounds. These chalks are much more marly than the nodular, pebbly chalks of the Melbourn Rock facies at Dover (5.11(ii).

5.10(ii). δ 13C isotope curve.

There is no δ 13C isotope curve available for Eastbourne.

5.10(iii). Macropalaeontological biostratigraphy.

The M. sp. cf. M. opalensis zone appears 4m from the base of the Dover Chalk Formation (Woodroof, 1981). The expansion in the sequence is displayed by the inoceramid zones,here the M. sp. cf. M. opalensis zone is 18m thick whereas to the west it is 3m thick (Compton Bay) and to the east 4.8m thick (Dover op cit.). A detailed study of this fauna is in progress (by Gale and Wood, Gale pers. comm.).

5.10(iv). Foraminiferal biostratigraphy

The presence of R. cushmani (samples 1-5, 7-11) and R. greenhornensis (sample 8), places the lower part of the sequence up to the top of bed 3 (Plenus Marls) within the uppermost part of the R. cushmani i.z.. "H". archaeocretacea first appears in the basal levels of the Dover Chalk Formation (samples 20, 24, 30-32 and 34) and places up to sample 33

within the "H". archaeocretacea i.z.. H. helvetica appears in sample 33 and places the very top of the sequence within the H. helvetica i.z..

5.10(V). Foraminiferal assemblage.

The number of the foraminiferal population recovered varies considerably across the interval (Figure 5.12), which is a result of the interaction of benthonic diversity, planktonic diversity and preservation.

Within the Abbots Cliff Chalk Formation (samples 1-7), the population varies between 280 specimens (maximum) and 105 specimens (minimum) per sample. The planktonic diversity remains constant but the benthonic diversity mirrors the population numbers. The planktonic : benthonic ratio decreases in the base of the sequence (samples 1-3), increases slightly again (samples 4-6) only to decrease sharply at the top of the unit (sample 7). Within the planktonic population the rotaliporid component forms much less than 50% of the total population. It decreases at the base of the section (samples 1-3), shows a small recovery (sample 4), then a decline (sample 5) to zero (sample 6) to recover at the summit of the unit, (sample 7). The praeglobotruncanid/dicarinellid population forms around 5-25% of the total population. Major changes occur in the hedbergellid population.

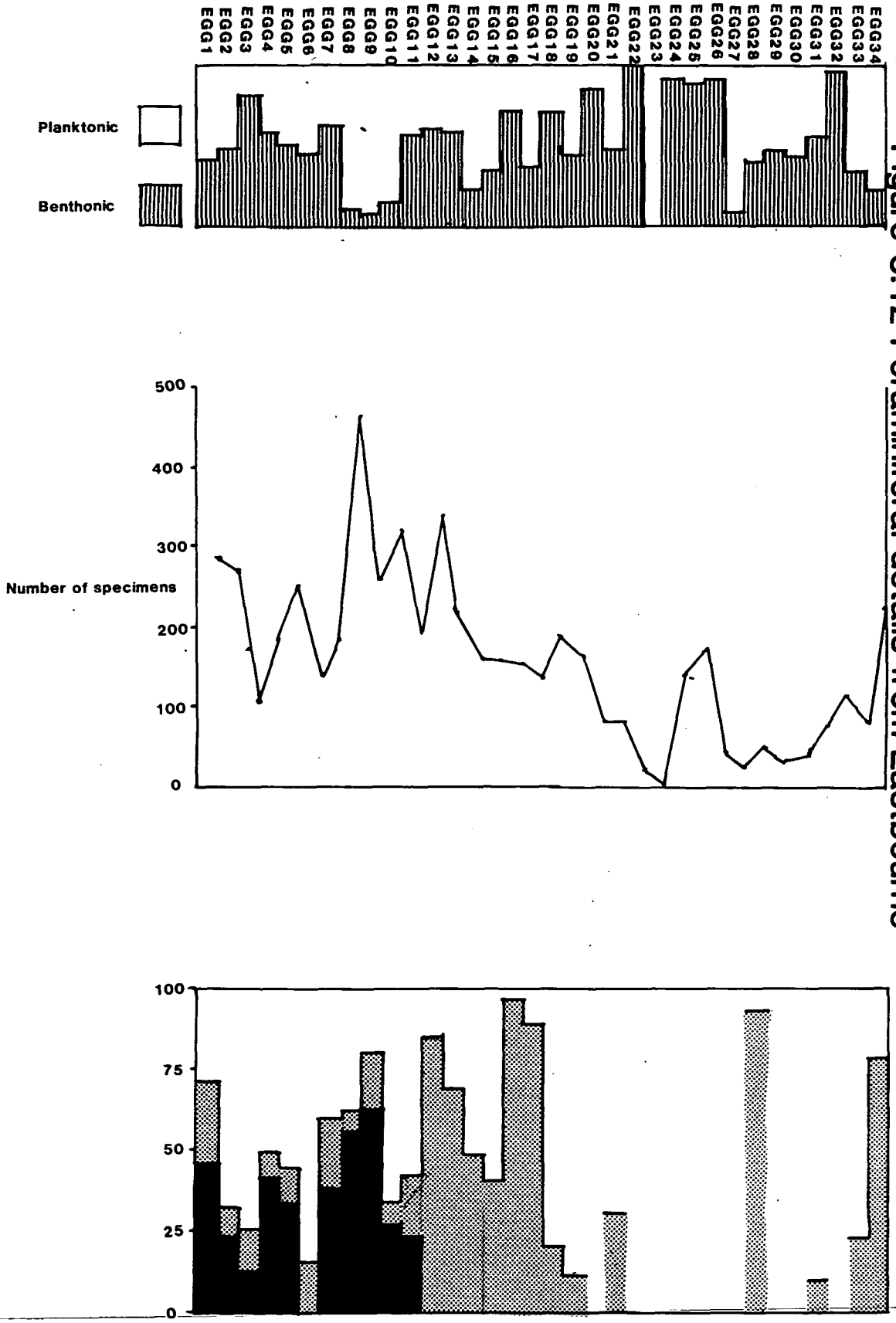

Figure 5.12 Foraminiferal details from Eastbourne

The Plenus Marl Formation, in contrast, shows major changes in diversity, population numbers and the relative numbers of planktonic and benthonic specimens. Bed 1 shows a significant increase in the number of specimens (~440), although it declines towards the middle of the bed. Benthonic diversity decreases through the bed. The planktonic diversity continues level as from the Abbots Cliff Chalk Formation. The planktonic : benthonic ratio increases dramatically with over 80% planktonic specimens. Within the planktonic population, the rotaliporid component continues the increase started in the top of the Abbots Cliff Chalk Formation, rising to 60% of the total. At the top of bed 1 G. baltica, D. gradata, T. macfadyeni, G. intermedia, P. mariae, A. depressum, G. cenomanica all disappear.

Through beds 2-8 the benthonic diversity shows a steady decline, with major fluctuations, as does the total number of specimens from 320 to under 200. The planktonic : benthonic ratio decreases up the succession with the occasional anomalous increase: bed 6 (sample 14) and the bottom of bed 8 (sample 16). Within the planktonic population the rotaliporid component declines, with R. cushmani disappearing in the middle of bed 3 (sample 11). Unlike the Abbots Cliff Chalk Formation, the praeglobotruncanid/ dicarinellid component becomes the dominant proportion of the planktonic population. The benthonic population becomes

dominated by an assemblage of L. rotulata var.b, G. berthelini, L. globosa and T. chapmani. The specimens from bed 8 (samples 16,17) exhibit pitted tests indicative of dissolution.

The decline in the total number of specimens continues into the Dover Chalk Formation though the benthonic diversity shows a moderate recovery. The assemblage is dominated by benthonics with a low planktonic : benthonic ratio. The number of planktonic specimens recovered was generally very low and in many cases there were not sufficient specimens to warrant a detailed breakdown of the planktonic population. All the specimens exhibit pitted tests indicative of dissolution.

5.11. Dover (Figures 3.4, 5.13, 5.14, 5.15).

5.11.(i) Lithostratigraphy.

The succession comprises the top of the Abbots Cliff Chalk Formation, the Plenus Marl Formation (2.5m), and 22m of the Dover Chalk Formation (Figure 5.13).

The Abbots Cliff Chalk Formation consists of weakly rhythmic marly chalks of decimetere scale alternations of friable marl and indurated chalk (Jukes-Browne and Hill, 1903; Kennedy, 1969; Carter and Hart, 1977), though at the top the rhythms are very poorly developed and the spacing increased.

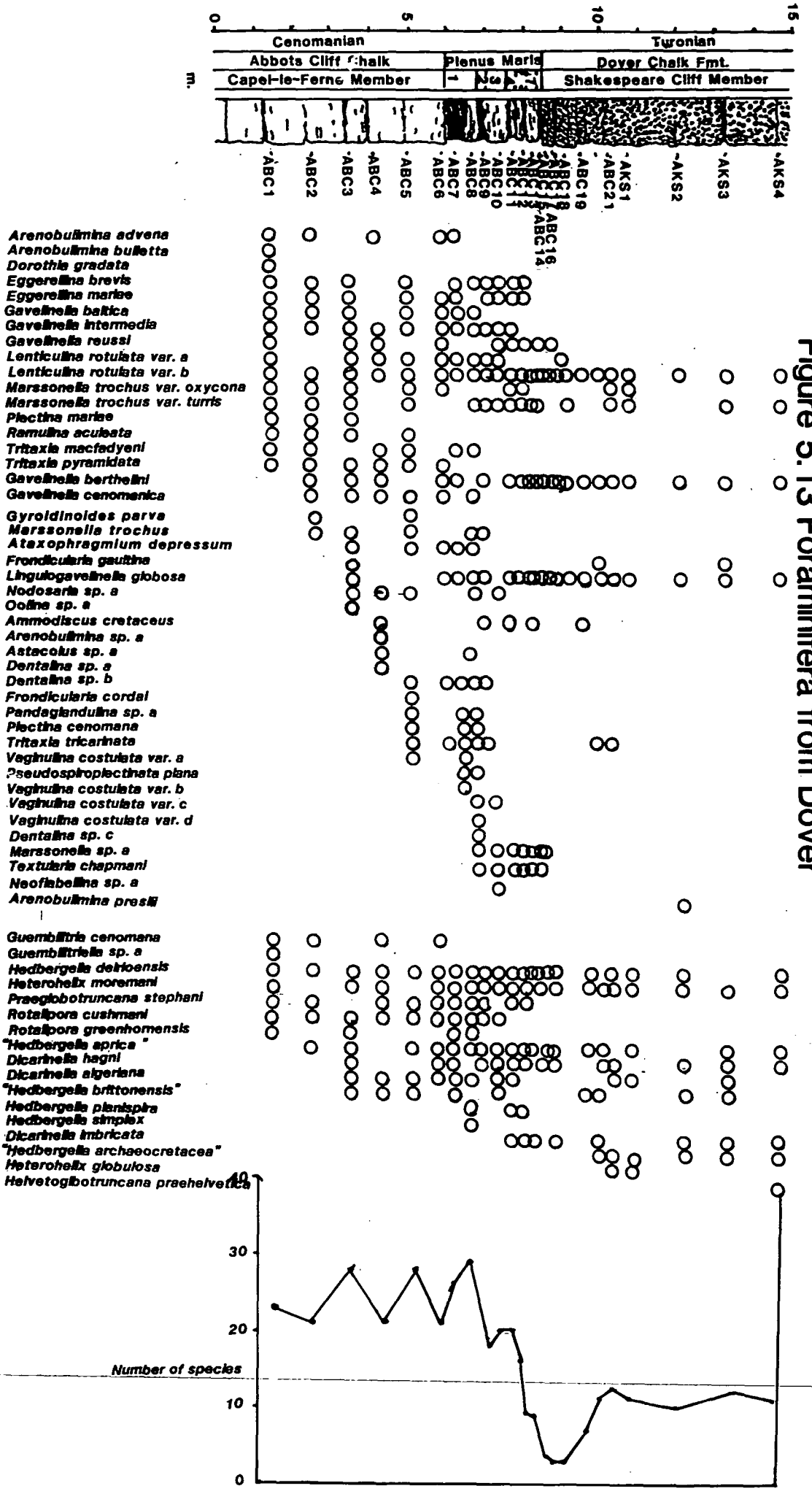

Figure 5.13 Foraminifera from Dover

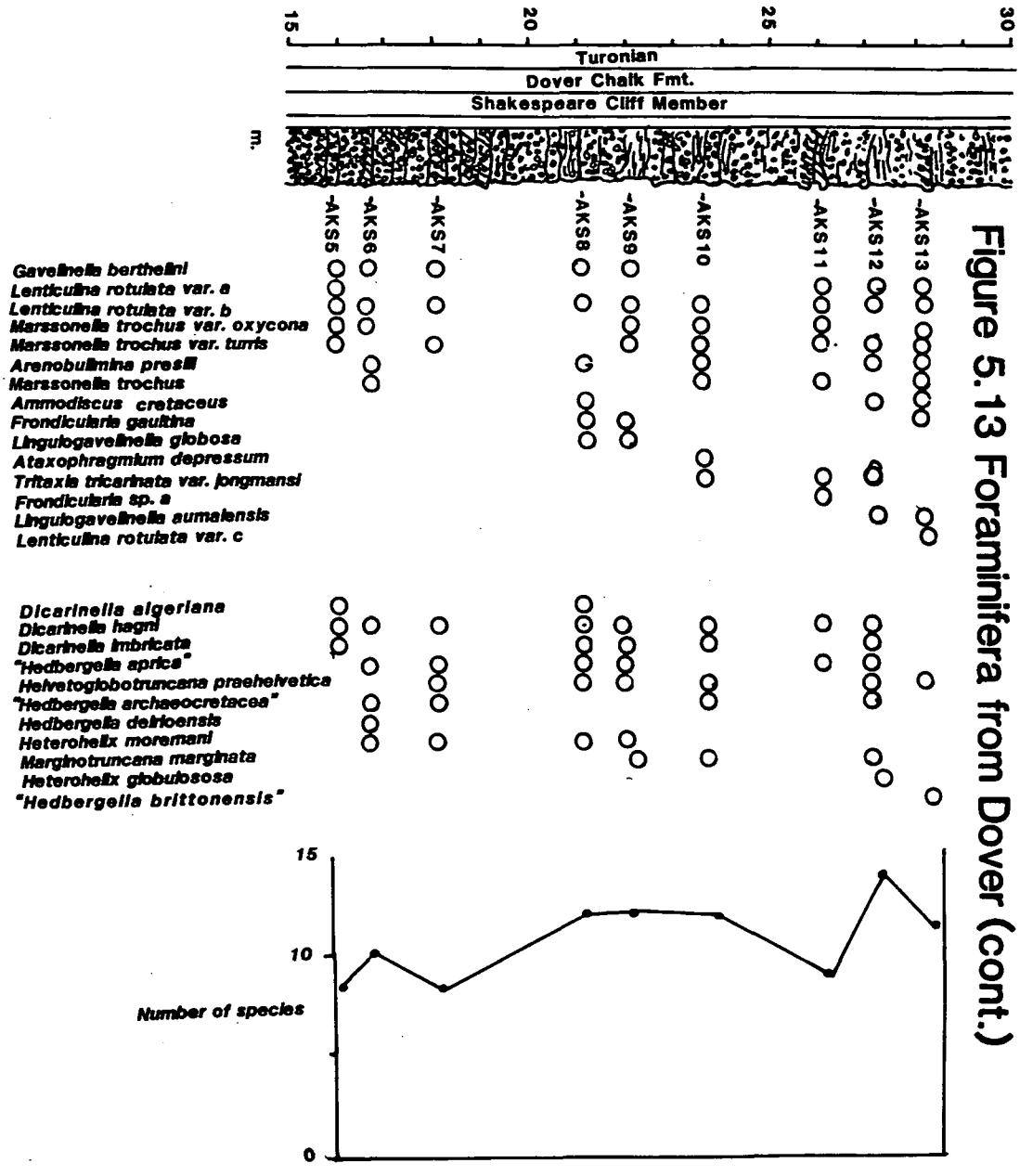

Figure 5.13 Foraminifera from Dover (cont.)

In addition, a small number of prominent marls are present.

The Plenus Marl Formation at Dover is the thinnest, at 2.5m, of the four onshore basinal sections studied (see 5.8(i), 5.9(i), 5.10(i)). The sub-Plenus erosion surface is well developed with the dark grey clay-rich marls infilling a suite of burrows (Thalassinoides, Chondrites and Planolites) within the underlying chalk marl. Beds 1-4, at 1.85m, are well represented, whilst beds 5, 6 and 8 are reduced.

The overlying Dover Chalk Formation shows a marked change in facies from the clay-rich marl of the Plenus Marls to highly nodular intraclast-rich chalks with well indurated hardgrounds in the basal 1.2m. This latter, the Melbourn Rock facies, is particularly well represented at Dover and contains abundant limonite-stained chalk pebble intraclasts and coarse calcarenite shell debris, particularly comminuted inoceramid and echinoderm tests. Further up the sequence the nodularity of chalks decreases and a few prominent marls are present.

5.11(ii). $\delta^{13}C$ isotope curve.

The carbon stable isotope signature (Figure 5.14) shows a marked excursion in $\delta^{13}C$ value through the Plenus Marl Formation and the Melbourn Rock facies of the Dover Chalk Formation. It shows a $\delta^{13}C$ enrichment from the background level of 2.5-3 ‰ (PDB) to a maximum of 4.6 ‰ (PDB) in bed 8 of the Plenus Marl Formation. The enrichment shows a

Figure 5.14 Isotope curves from Dover (Carson, pers. com.)

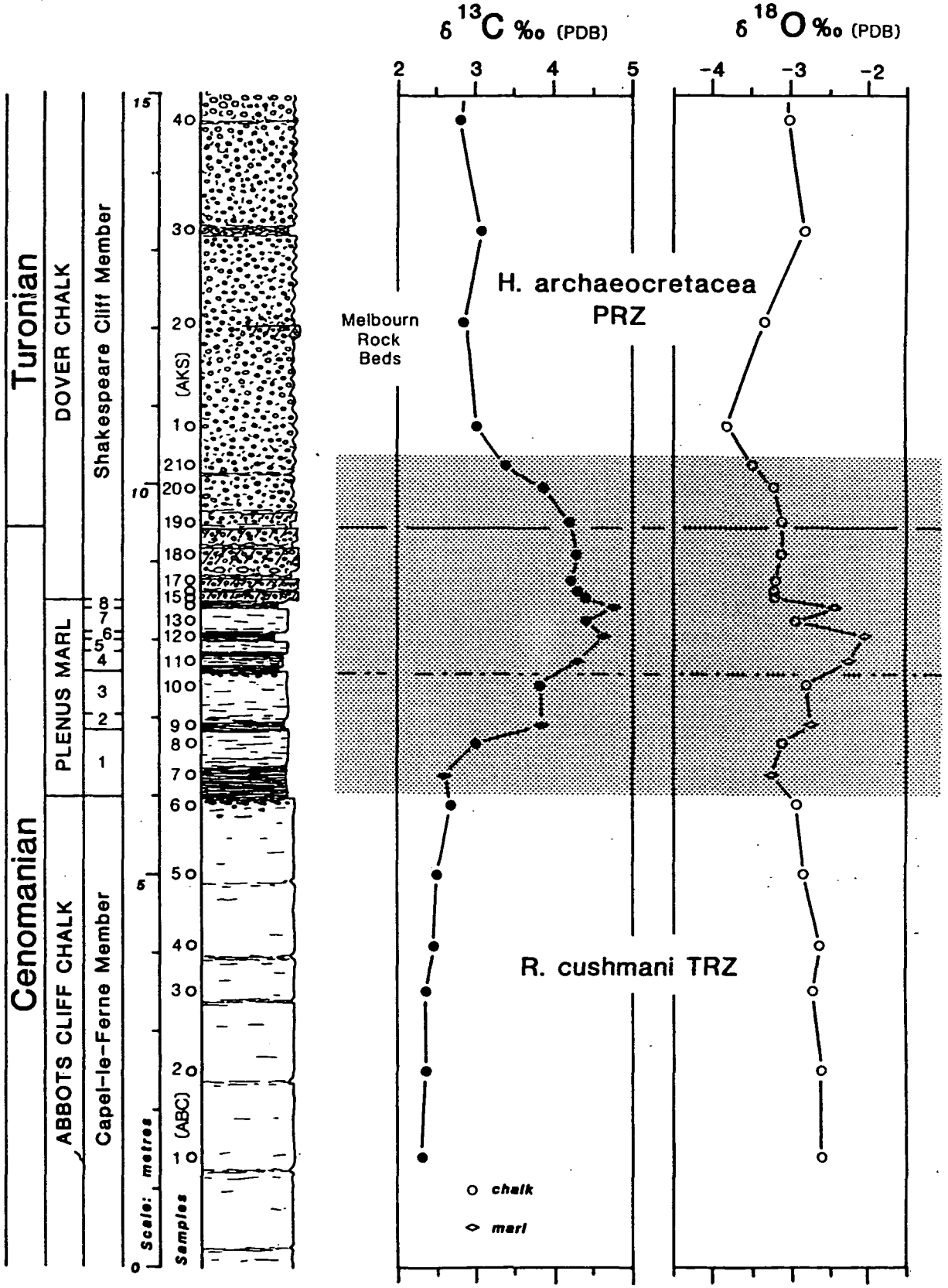

Figure 5.14 Isotope curves from Dover (cont.)

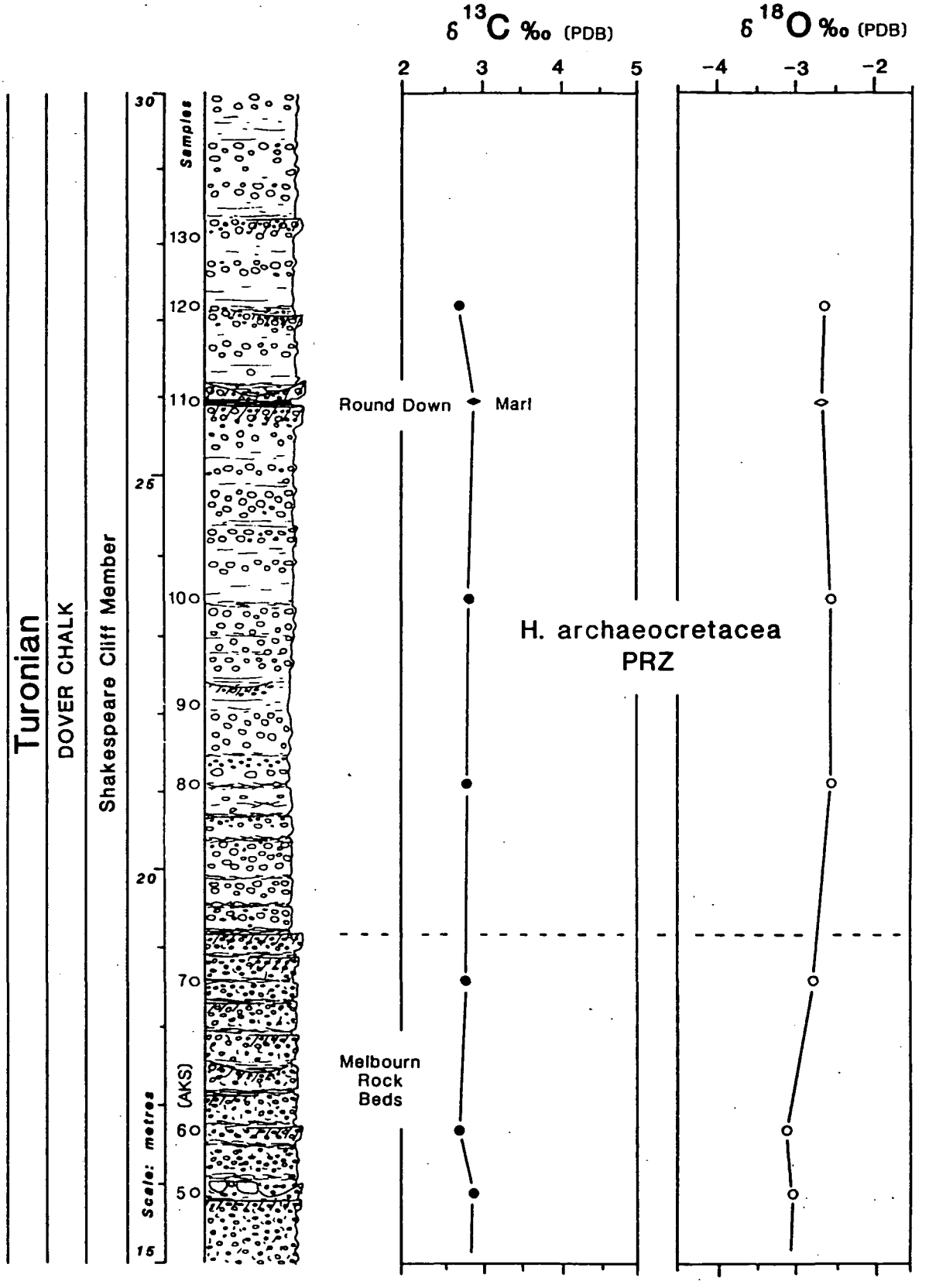

more rapid ascent through the Plenus Marls than descent through the first 2m of the Melbourn Rock facies (Carson, pers. comm.).

5.11(iii). Macropalaeontological biostratigraphy.

The presence of a Sciponoceras fauna in the basal hardgrounds of the Melbourn Rock at Dover suggests that the hardgrounds lie within the uppermost Cenomanian Neocardioceras juddii zone (Wright and Kennedy, 1981). A Watinoceras fauna has been recorded from Merstham (op cit.) which indicates that the higher beds of the Melbourn Rock are within the Turonian W. coloradoense zone. In addition, Upper Cenomanian Inoceramus pictus Sowerby are common in the basal hardgrounds and Mytiloides appears immediately above them (Woodroof, 1981). Thus this inoceramid faunal change is used to define the base of the Turonian, at 2.3m above the top of bed 8, Plenus Marl Formation.

In addition, the Turonian nannofossil marker Quadrum gartneri appears (sample 20, Figure 8.4) just above this level (Cooper, pers. comm.).

5.11(iv)). Foraminiferal biostratigraphy

The presence of R. cushmani (samples 1-10), and R. greenhornensis (samples 1, 3, 7 and 8), place the lower part of the sequence up to bed 3 (Plenus Marls) within the upper

part of the R. cushmani i.z.. "H". archaeocretacea appears in the basal part of the Dover Chalk Formation (samples 21-25, 26, 27, 30, 31, 33), and places up to sample 35 within the "H". archaeocretacea i.z.. The presence of H. helvetica (samples 35, 36, 38-40) places these samples within the H. helvetica i.z..

5.11(v). Foraminiferal assemblage.

The number of the foraminiferal population recovered varies considerably across the interval (Figure 5.15), which is a result of the interaction of benthonic diversity, planktonic diversity and preservation.

Within the Abbots Cliff Chalk Formation (samples 1-6), the population varies between 310 specimens (maximum) and 55 (minimum) per sample. The planktonic diversity remains constant but the benthonic diversity largely mirrors the population numbers, with a marked drop in sample 4. The planktonic : benthonic ratio increases in the base of the sequence (samples 1-3), recovers and decreases (samples 4 and 5), to recover at the top of the unit (sample 6). Within the planktonic population the rotaliporid component forms much less than 50% of the total population. It decreases at the base of the sequence (samples 1, 2), decreases (sample 5) and recovers (sample 6). The praeglobotruncanid/dicarinellid

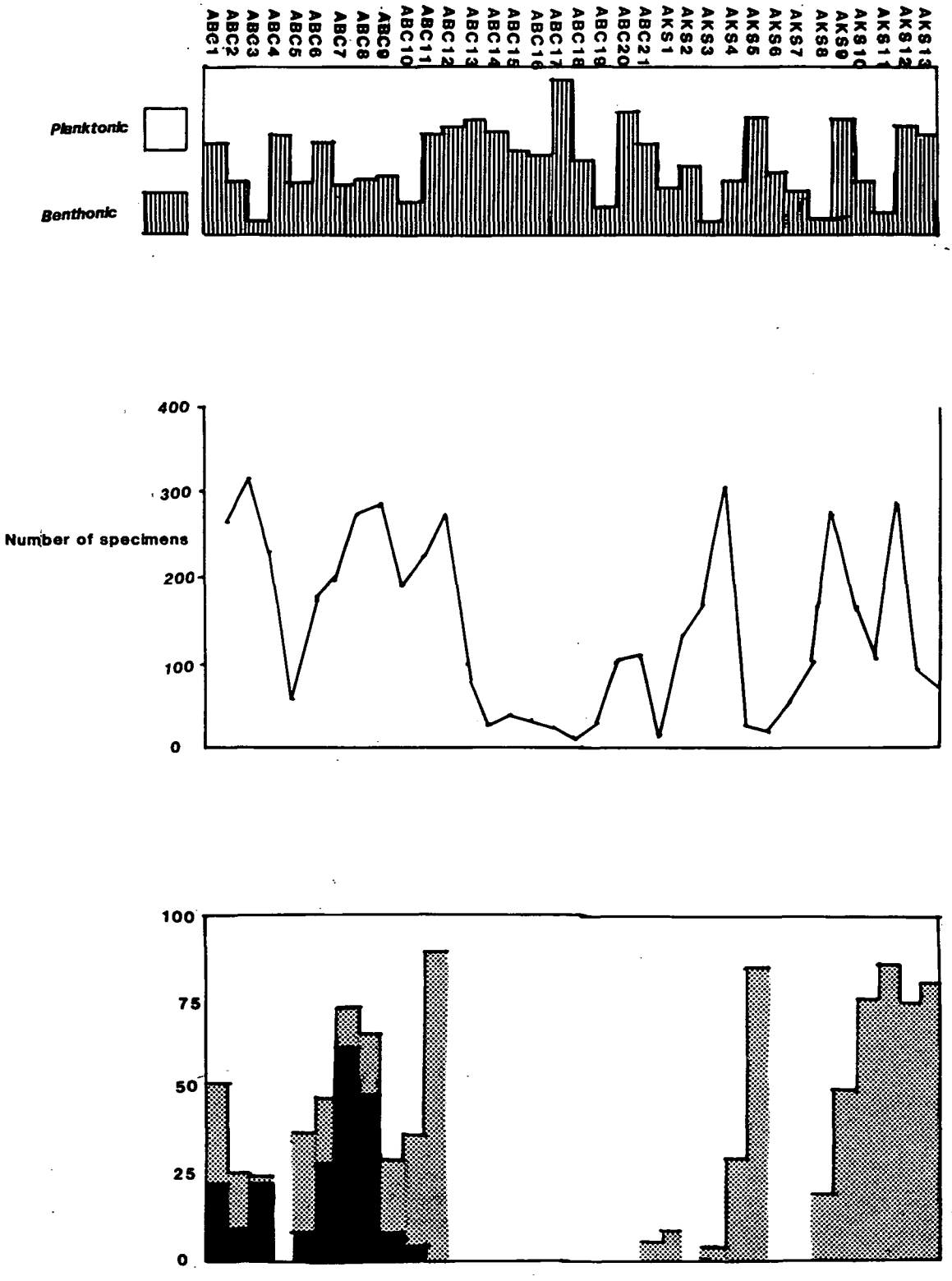

Figure 5.15 Foraminiferal details from Dover

component remains constant and major changes occur in the hedbergellid population.

The Plenus Marl Formation, in contrast shows major changes in diversity, population numbers and the relative numbers of planktonic and benthonic specimens. Bed 1 shows an increase in the number of specimens (~250). The benthonic diversity declines through the bed. The planktonic diversity continues on the same level as from the Abbots Cliff Chalk Formation. The planktonic : benthonic ratio is high with around 75% planktonics. Within the planktonic population the rotaliporid component continues the increase started in the top of the Abbots Cliff Chalk Formation, rising to over 60% of the total. At the top of bed 1 T. macfadyeni, G. baltica, A. advena, A. depressum, P. plana, R. greenhornensis, G. cenomana and G. intermedia all disappear.

Through beds 2-3 the benthonic diversity shows a steady decline, as does the total number of specimens, from 190 to 40 with a slight increase in bed 4 (sample 11). The planktonic : benthonic ratio shows a sharp decrease and remains steady at around 75% of the total population. Within the planktonic population the rotaliporid population declines sharply, with R. cushmani disappearing in the middle of bed 3 (sample 10). Unlike the Abbots Cliff Chalk Formation, the praeglobotruncanid/dicarinellid component becomes the dominant portion of the planktonic population. The benthonic population

becomes dominated by an assemblage of L. rotulata var. , G. berthelini, L. globosa and T. chapmani. The specimens from beds 4 to 8 show pitted tests indicative of dissolution, the intensity of which is most marked in the tests of the planktonic species.

The decline in the total number of specimens continues into the Dover Chalk Formation as does the benthonic diversity. The assemblage is dominated by benthonic taxa with a moderate planktonic : benthonic ratio. The number of planktonic specimens recovered was generally very low and in many cases there were not sufficient specimens to warrant a detailed breakdown of the planktonic population. All the specimens exhibit pitted tests indicative of dissolution.

5.12. BritOil 48/22-1. (Enclosure 1, Figure 5.16).

5.12(i). Lithostratigraphy.

The succession comprises some 66m of limestone of which approximately 62m is part of the Hildra Formation. The position of the Plenus Marl Formation is problematic and the gamma ray deflection is poor, probably occuring at around 126m downhole (Copestake, pers. comm.).

5.12(ii). δ 13C isotope curve.

There is no carbon isotope curve available for BritOil

Figure 5.16 Foraminifera from BritOil 48/22-1

48/22-1.

5.12(iii). Macropalaeontological biostratigraphy.

No macrofossils have been recorded from BritOil 48/22-1 (Copestake, pers. comm.).

5.12(iv). Foraminiferal biostratigraphy.

The first appearance downhole of R. cushmani occurs in sample 19 and thus the top of the R. cushmani i.z. is at 124m downhole.

5.12(v). Foraminiferal assemblage.

Only the sequence from the base of the R. cushmani i.z. has been studied in detail (samples 14-22). The number of specimens shows a steady decline from 180 (maximum) to 50 (minimum) per sample. The planktonic : benthonic ratio is low until sample 19 when the planktonics become dominant, forming at least 80% of the total population thereafter. Within the planktonic population the rotaliporid component is low, always less than 10%. R. cushmani disappears in sample 19. After sample 19 the praeglobotruncanid/ dicarinellid component becomes the dominant part of the planktonic population.

5.13. Carbon isotope curve and stratigraphy.

Carbon isotope curves have been used for correlation

of Cretaceous sediments by Scholle and Arthur (1980), Jenkyns (1985), Hilbrecht and Hoefs (1986) and Schlanger et al. (1987).

The carbon isotope curve at Beer Stone Adit (figure 5.5), shows a marked excursion, at the limonitic hardground within the Pinnacles Member, in the δ 13C value from 2 0/00 (PDB) to just over 4 0/00 (PDB). The larger value from the chalk matrix, lower values provided by intraclasts contained within the hardground (Carson, pers. comm.).

The carbon isotope curve from Dover (Figure 5.14), shows an excursion through the Plenus Marl Formation from a background level of 2.5-3.0 0/00 (PDB) to a maximum of 4.6 0/00 (PDB) in bed 8 of that unit (Carson, pers. comm.). Thus the limonitic hardground at Beer is equivalent to at least the Plenus Marl Formation.

G. intermedia disappears at the top of bed 1 (Plenus Marls) and R. cushmani disappears in the base of bed 4. Their recovery from the top of the limonitic hardground at Beer, (sample 6), suggests intense reworking of material in the Beer Stone Adit sequence, which is also bourne out by the ammonites on the top of the Haven Cliff Hardground (5.5(iii)).

5.14. Rotaliporid population and eustasy.

The rotaliporids possess the "deep water" features (Hart, 1980a; Caron, 1983a; Hart, 1985; Hart and Ball, 1986) of

low trochospire, well-developed keels and supplementary apertures. Their distribution in the boreal realm is restricted (Carter and Hart, 1977). The rotaliporid population in the sections studied varies in its relative dominance within the planktonic population, the distribution of species and the size of the individuals within each population.

5.14(i). Relative dominance of rotaliporid population.

Within the total planktonic population the rotaliporid component varies. In Goban Spur, the rotaliporids consistantly form more than 60% of the total planktonic population. In contrast, in the basinal sections of the Anglo-Paris Basin, the rotaliporid component is variable and gradually decreases in its presence eastwards (through White Nothe, Isle of Wight, Eastbourne, Dover). In all these sections the rotaliporid component rises in bed 1 of the Plenus Marl Formation (Figure 5.17).

5.14(ii). Distribution of rotaliporid species.

R. deecki was only recorded from Goban Spur where it forms a very small part (3%) of the total planktonic population. R. greenhornensis is more prevalent, forming 15% of the total planktonic population at Goban Spur but it is more sporadically distributed in the Anglo-Paris Basin sections. R. cushmani is found in all sections until its

Figure 5.17 Planktonic population from selected sites

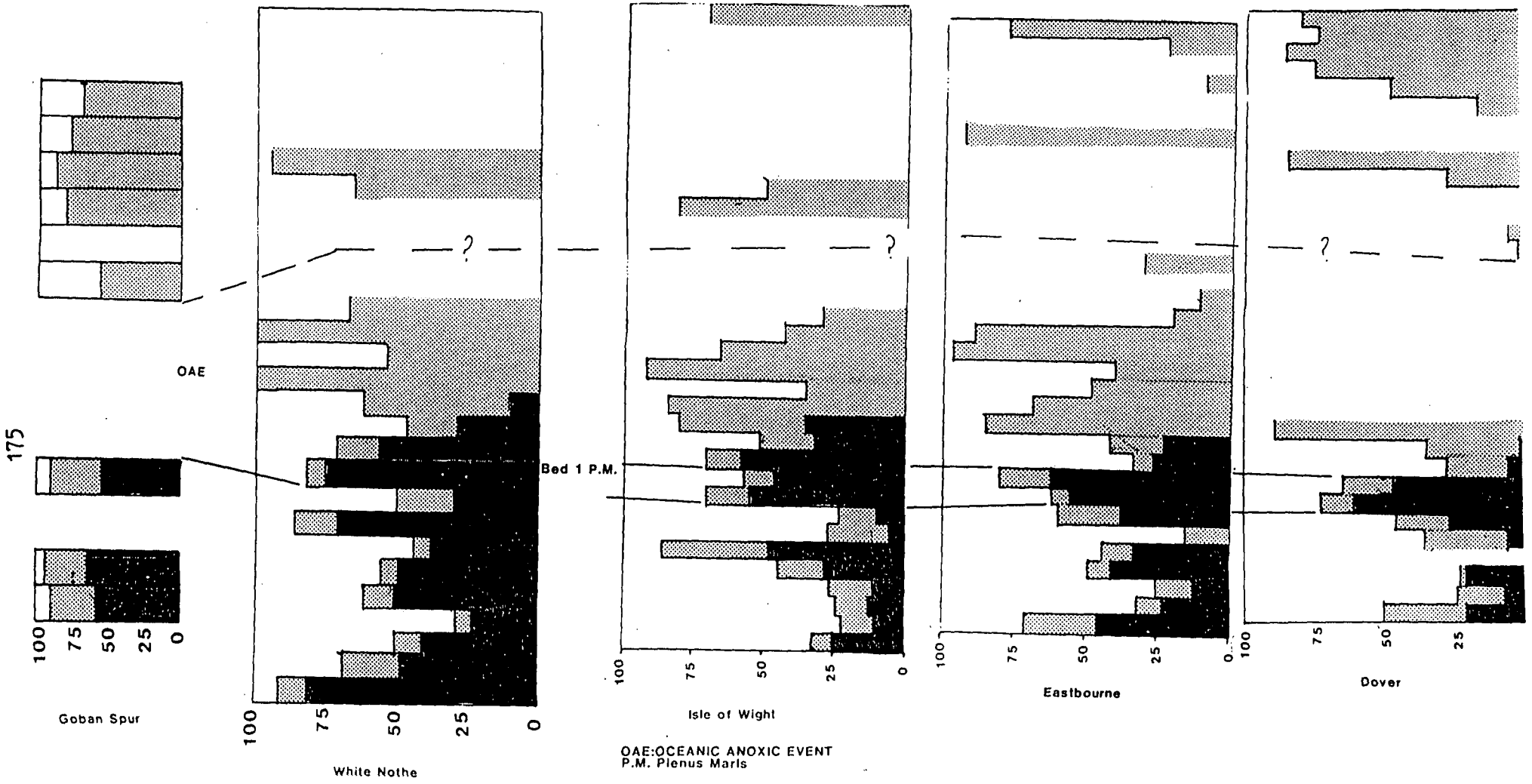

disappearance at the top of bed 3, Plenus Marl Formation (Figures 5.1, 5.17).

5.14(iii). Size of the R. cushmani specimens.

During ontogeny, extant planktonic foraminifera add chambers and progressively sink in the water column until the test is vacated during gametogenesis (Bé et al., 1966; Bé and Anderson, 1976; Spindler et al., 1979; Bé, 1980; Bé et al., 1983). Thus the relative proportions of neanic to gerontic individuals of deeper water forms is a measure of depth. The greater the number of gerontics, the deeper the water.

Text figure 5.1
Measured characteristics of X-rayed *Rotalipora cushmani* (Morrow)

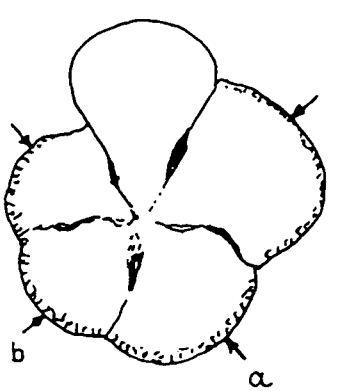

For each sample the individuals of the R. cushmani population were measured (see section 2.6 for method). The parameters taken (Text Figure 5.1) were the maximum distance across the test from the penultimate chamber of the last whorl (b) and the maximum distance across the test from the first chamber of the last whorl (a). The last chamber was not measured because in some specimens it was slightly inclined

Figure 5.18 X-ray of *R. cushmani* from Goban Spur

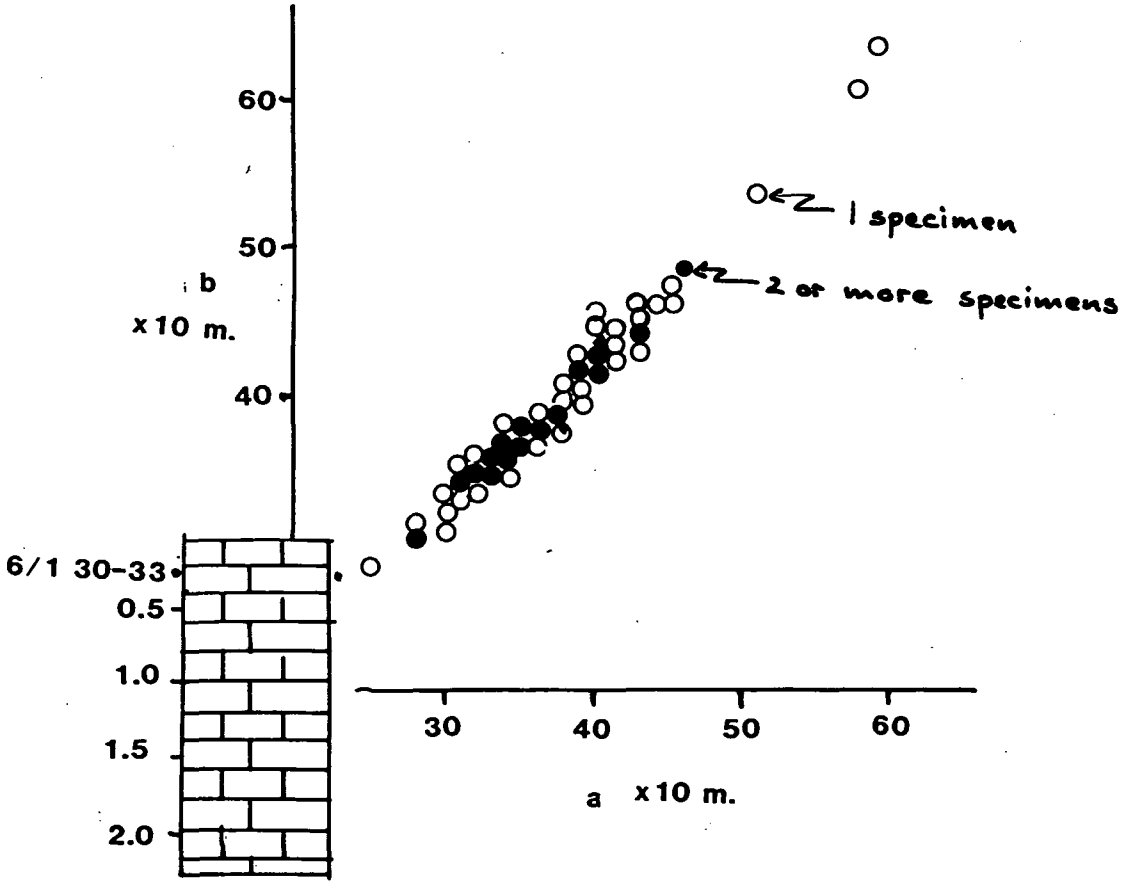

Figure 5.19 X-ray of *R. cushmani* from from White Nothe

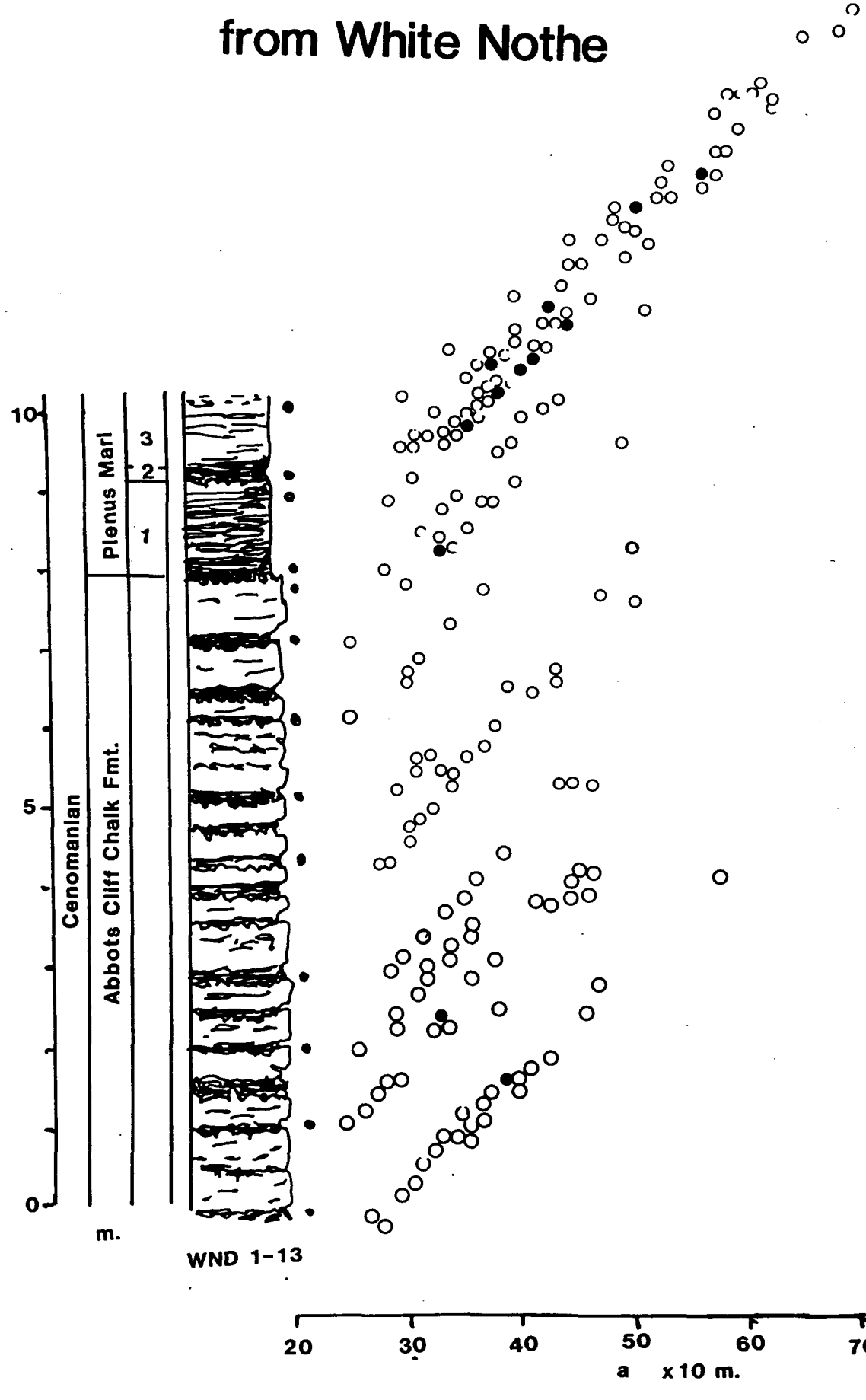

Figure 5.20 X-ray of *R. cushmani* from Isle of Wight

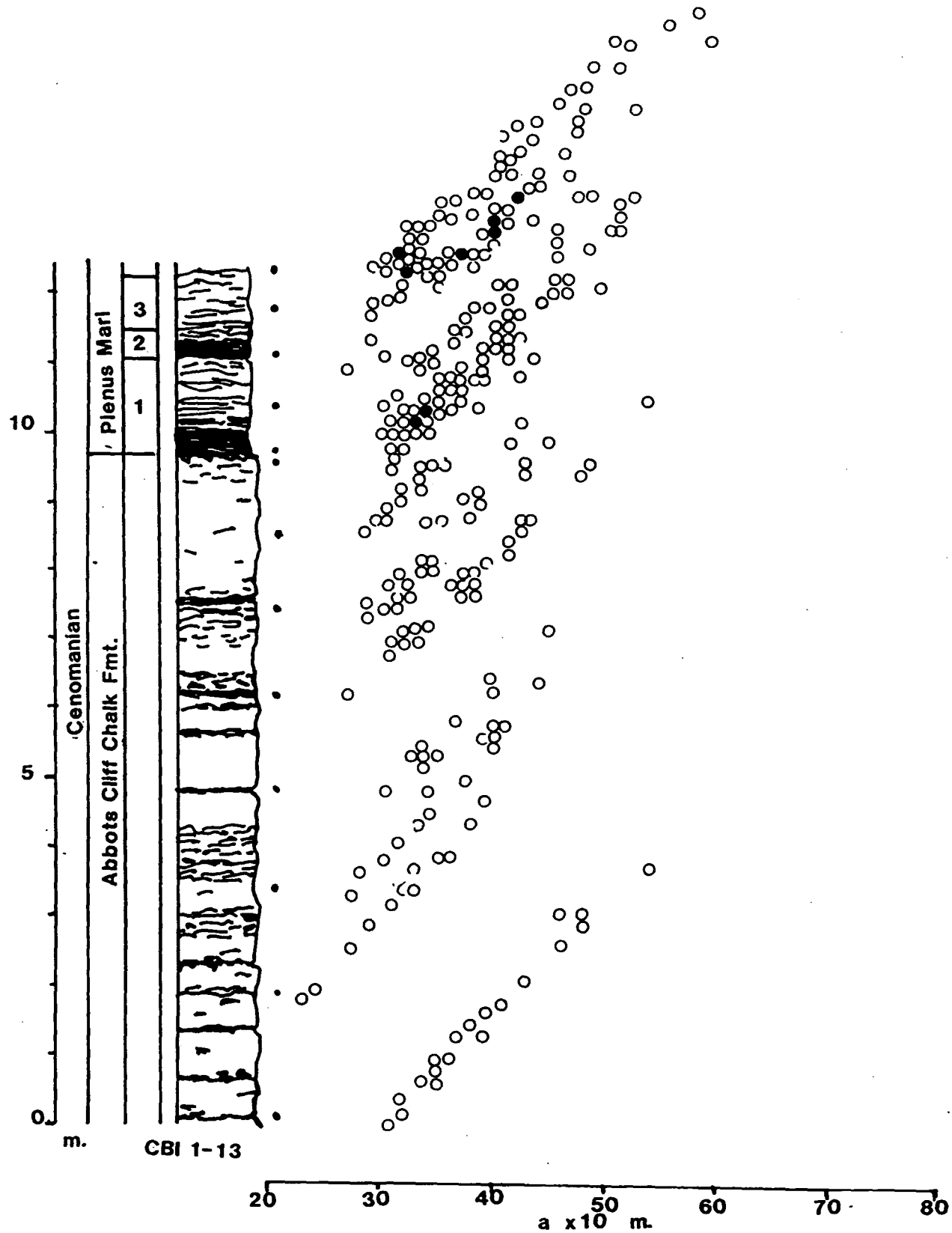

Figure 5.21 X-ray of *R. cushmani* from Eastbourne

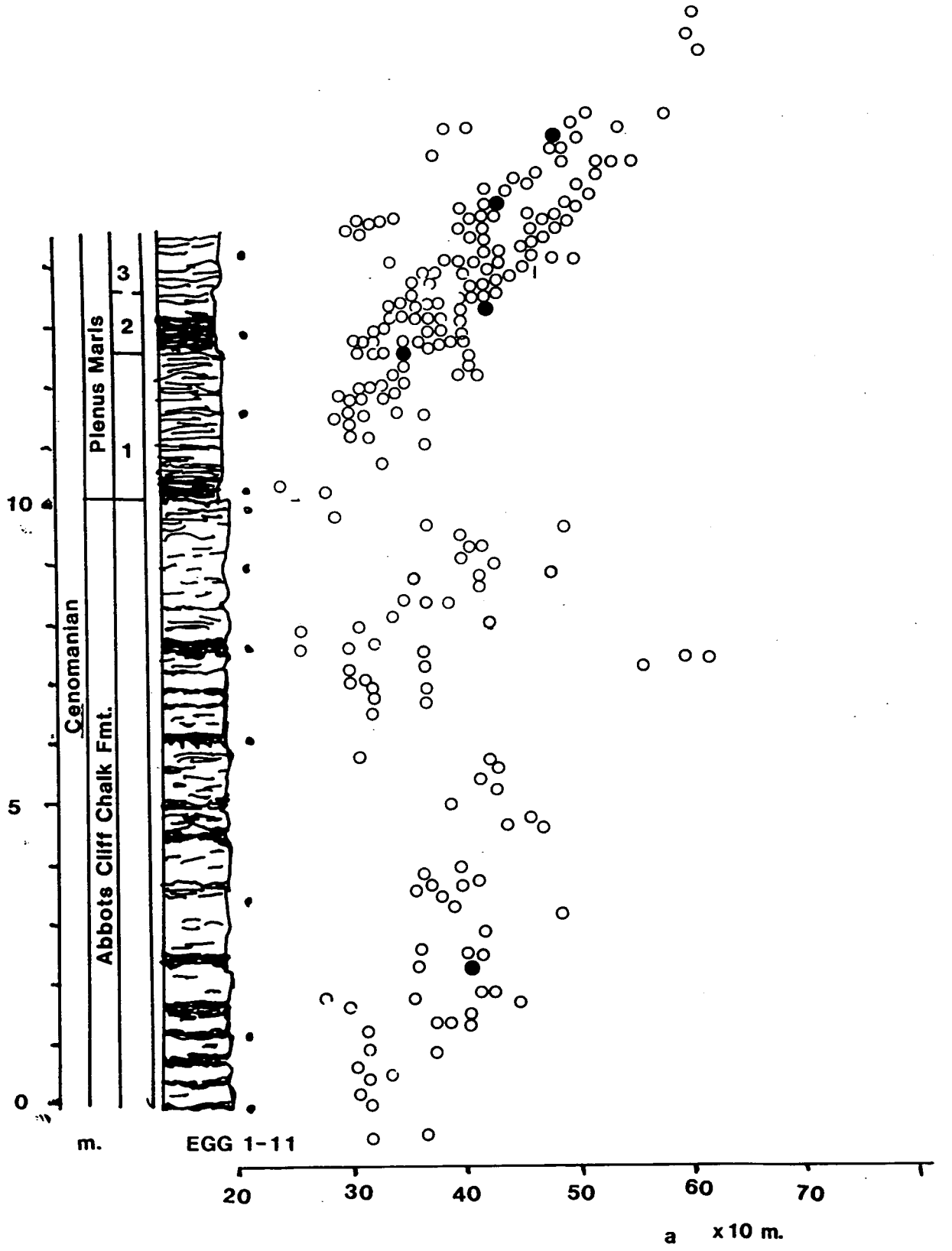

Figure 5.22 X-ray of *R. cushmani* from Dover

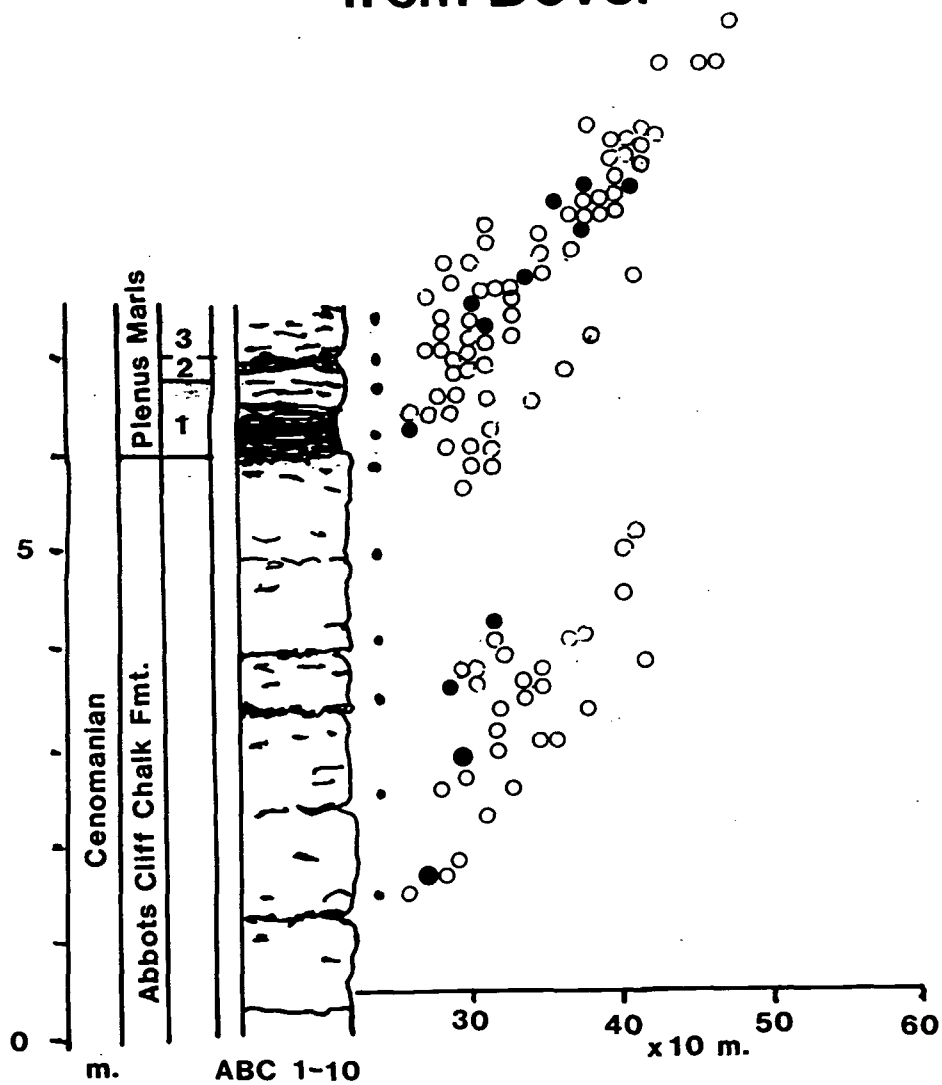

umbilically and thus such a measurement would have produced a spuriously short width.

Goban Spur:

The R. cushmani population at Goban Spur shows a population with test sizes of up to 60-65x10^{-5}m (figure 5.18).

White Nothe:

Within the Abbots Cliff Chalk Formation (samples 1-9), the maximum test size is variable but just achieves a value greater than 50-53x10^{-5} m. In bed 1 of the Plenus Marl Formation (sample 10 and 11), the maximum test size increases dramatically but decreases through beds 2 and 3 (Figure 5.19).

Isle of Wight:

Within the Abbots Cliff Chalk Formation the maximum test size is variable and is rarely above 50-53x10^{-5}m. In bed 1 of the Plenus Marl Formation the maximum test size increases to 59-63x10^{-5}m and remains high in bed 2 but decreases very slightly into the top of bed 3 (Figure 5.20).

Eastbourne:

Within the Abbots Cliff Chalk Formation the maximum test size is variable but slightly more than in White Nothe, Isle of Wight and Dover. In bed 1 of the Plenus Marl Formation there is a significant increase in test size reaching a maximum of 60-63x10^{-5}m. This high value is maintained through bed 2 but declines markedly in bed 3 (Figure 5.21).

Dover:

Within the Abbots Cliff Chalk Formation the maximum test size is variable but does not achieve a value greater than $40\text{-}42\text{x}10^{-5}$ m. In bed 1 of the Plenus Marl Formation there is a modest increase to $40\text{-}42\text{x}10^{-5}$ m which is maintained through bed 2 but declines sharply in bed 3 (Figure 5.22).

The four sections produce a composite picture with three main features:

(i) the water depth decreases from west to east.

(ii) the lower part of the Plenus Marl Formation, particularly bed 1, is a deep water facies.

(iii) the rate of change in water depth appears rapid marked by the sharp change in maximum test size.

A late Cenomanian transgression has been recognized on the Falklands Plateau (Sliter, 1976), in Poland (Marcinowski, 1974), in northwest Europe (Hancock and Kaufmann, 1979), on the Russian Platform (Naidin, 1983) and globally (Cooper, 1977; Matsumato, 1980; Morner, 1981; Vail et al., 1977; Haq et al., 1987).

An increased sample resolution ffrom the Abbots Cliff Chalk Formation would permit a more detailed appraisal of any water depth changes. This approach would also permit the differentiation of phases within a planktonic foraminiferal biozone and also whether sea level changes are gradual (sensu

Hancock and Kaufmann, 1979), or sharp (sensu Vail et al., 1977).

5.15. Benthonic foraminifera: bathymetric considerations.

The limited distribution of certain genera across the shelf and onto the continental shelf of extant benthonic foraminifers has long been recognized (Bandy and Annal, 1957; Valentine and Mallory, 1965; Bandy and Chierici, 1966; Frerichs, 1970), and the Cretaceous bathymetric distribution of benthonic foraminifers (Sliter and Baker, 1972) of southern California show several features with increasing depth: increase in agglutinated foraminifera, lowering diversity and abundance.

Goban Spur, in contrast to the other sections, yielded a high rotaliporid component compared to the rest of the planktonic population including R. cushmani, R. greenhornensis and R. deecki, indicative of a deeper water assemblage (5.14).

The associated benthonic assemblage only forms 3% of the total population (5.3(v); Hart, 1987b), also indicative of a deeper water assemblage. The presence of any well-preserved calcareous forms infers that the assemblage has not been affected by the lysocline. It also shows several other differences from the other sections:

(i) a restricted diversity of T. macfadyeni, L. rotulata var. a, G. reussi, G. intermedia, A. advena, N. sp.a, E.

brevis, M. trochus, M. trochus var. oxycona, Pseudobolivina sp.a, Lagena sp.a, Gyroidina sp.a and Lenticulina sp.a. The last four species being restricted to Goban Spur.

(ii) all the forms show a low size variability.

Thus these features of low benthonic diversity and size variability, dominance of rotaliporids and high planktonic : benthonic ratio suggest a deep bathyal water assemblage.

Chapter 6: The late Cenomanian Anoxic Event and the associated foraminiferal changes: Dover, a case study.

6.1. Introduction.

The late Cenomanian sea level rise (see 5.14), brought a high-stand on the continental shelf coupled with an expansion in the oxygen minimum zone (Jenkyns, 1980; Hart, 1985; Schlanger et al., 1987; Arthur et al., 1987): this adversely affected both the planktonic and benthonic foraminifera. The rise in the oxygen minimum layer may be positioned using the carbon isotope curve (Schlanger et al., 1987; Arthur et al., 1987). The details of this change may best be discerned by looking at the most expanded section against the carbon isotope curve, for example Dover.

At Dover, (see 5.11 (ii)), the δ 13C enrichment occurs gradually through the Plenus Marl Formation, reaching its peak in bed 8, then slowly declining to its background level at 2.5m from the base of the Dover Chalk Formation (Figure 5.14).

The changes in the foraminiferal population characterized by lowering of diversity, extinction and dwarfism. The changes in the planktonic and benthonic populations are not coeval and are thus reviewed separately.

6.2. The late Cenomanian Anoxic Event and the benthonic taxa.

The benthonic assemblage shows a steady decrease in diversity (Figure 5.13) up the Plenus Marl Formation, together with

a change in species composition:

(i) at the top of bed 1, G. baltica, G. intermedia, G. cenomanica, A. advena, P. plana, T. pyramidata, T. macfadyeni, P. mariae become extinct.

(ii) through beds 2-8 the assemblage comprises M. trochus, M. trochus var. turris, M. trochus var. oxycona, E. mariae, E. brevis, L. rotulata var. a, L. rotulata var.b, G. reussi, G. berthelini, L. globosa, Nodosaria sp.a, A. cretaceus, Marssonella sp.a, T. chapmani and T. tricarinata.

Within the marssonellid population the dominant morphotype is M. trochus var. turris which is characterized by an equal rate of growth in width and height of new chambers, giving the test straight sides in side view. Also associated with this is the aberrant M. sp.a which is only found from beds 2-8 and the two basal hardgrounds of the Shakespeare Cliff Member.

Within the eggerellinid population E. brevis becomes dominant over E. mariae. The former is characterized by a squat test as opposed to the more elongate test of the latter. Thus, the smaller chamber growth indicative of E. brevis may represent a stunted form of E. mariae.

The only representative of the genus Tritaxia recorded from this interval is T. tricarinata which is subtriangular with triserial growth. This form is smaller than the tritaxid population from below of T. pyramidata and T. macfadyeni and thus may represent a dwarf ecophenotype of these forms.

The textularids first appear in bed 2 in this study with T. chapmani, the population of which shows a reduction in size through beds 2-8, though only one specimen shows a smaller height than it should for the number of chambers (Figure 4.1). Though dwarfism is not conclusive, the population does display a reduction in the number of specimens recovered and their size through beds 2-8.

Within the nodosarids, the assemblage is dominated by L. rotulata var.a and L. rotulata var.b, the former only being present to the top of bed 3. Though the number of specimens recovered decreased towards the top of bed 8, the specimen size remained consistant. Although N. sp.a was evident in bed 2, it was not recorded from the other beds.

The gavelinellid population shows a marked change with the dominance of the G. reussi - G. berthelini plexus. These characteristic forms with a flattened umbilical surface and a variably developed boss on the spiral surface are notably smaller than the G. baltica, G. intermedia, G. cenomanica population they replace. Coupled with G. berthelini, L. globosa becomes prevalent, though the spcimens of this species are slightly smaller in the last three beds of the Plenus Marl Formation.

(iii) through the Shakespeare Cliff Member (Dover Chalk Formation), the benthonic diversity remains low but does show a small recovery towards the top of the sequence. A. preslii, T. tricarinata var. jongmansi, L. aumalensis and L. rotulata var.c augment the benthonic assemblage well above the horizon where the

$\delta^{13}C$ level returns to its background value. Thus although the oxygen depleted waters have receded, the benthonic assemblage shows a poor recovery.

Oxygen deficient benthonic foraminiferal assemblages have been recognized in the Devonian (Gutschick and Wuellner, 1983); in the Nigerian (Nyong and Ramanathan, 1985), the Brazilian (Mello *et al.* in press), and the English (Hart and Bigg, 1981) Cretaceous; in the Miocene and Pliocene of the Mediterranean (Katz and Thunell, 1984); in the Recent sediments of the southeastern Pacific Ocean (Ingle *et al.*, 1980), and from Jurassic to Holocene levels (Bernhard, 1986).

Nyong and Ramanathan (1985), recorded a late Cenomanian anoxic benthonic assemblage of *Gavelinella* sp., *Gabonita* sp., and *Ammobaculites subcretacea* from the Calabar Flank, S.E. Nigeria. This shows some similarity with a limited fauna dominated by gavelinellids. The specimens were not illustrated or described so no detailed comparison of the gavelinellid populations is possible.

The late Cenomanian anoxic (Arthur *et al.*, 1987) benthonic assemblage (Hart and Bigg, 1981) from across the "Black Band" in Lincolnshire, (Engand), was very poor. Although the sequence is not as complete as Dover, the assemblage shows many similarities. *G. cenomanica* and *G. intermedia* disappear below the anoxic event, whilst *L. globosa* and *G. tourainensis* (= *G. reussi* - *G. berthelini* plexus) occur across it. The "Black Band" itself (the peak of the

δ13 C enrichment (Arthur et al., 1987)), only yielded A. cretaceus (Hart and Bigg, 1981), although Glomospira sp., T. chapmani and Haplophragmoides sp. have also been recorded (Martinez-Rodriguez and Crump, 1987; Brasier, pers. comm.)

A Cenomanian anoxic benthonic assemblage from the Mancos Shelf (New Mexico) yielded Gavelinella dakotensis, Neobulimina cadadensis, Dentalina basisplanata, Citharina kochii and Lenticulina sp. (Bernhard, 1986). The tests were small to medium sized with little ornamentation on the nodosarids. This assemblage is similar to the one recorded at Dover with small Lenticulina spp. and G. dakotensis. G. dakotensis is very similar to G. reussi with a flattened test and a small boss on the spiral side.

From the Sergipe Basin, Brazilian margin, a late Cenomanian anoxic benthonic community comprised of Lingulogavelinella thalmanniformis, G. berthelini, Dentalina sp. and Gabonella spp. has been recorded (Mello et al., in press). The Gabonella spp. and L. thalmanniformis exhibit dwarfism but the nodosarids show little size reduction and ornamentation (Koutsoukos, pers. comm.). This assemblage is very similar to the one recorded at Dover with smooth Lenticulina spp., G. berthelini and elongate nodosarids.

Thus the late Cenomanian anoxic benthonic community may be characterized by forms of the G. reussi - G. berthelini lineage, smooth Lenticulina spp. and Nodosaria spp. or Dentalina spp. with the addition of regional forms such as L. globosa and Textularia chapmani (Europe) and L. thalmanniformis and Gabonella spp. (South

Atlantic).

G. reussi is present in the pre-OAE fauna and proliferates rapidly into the form G. berthelini after the extinction of G. baltica, G. cenomanica and G. intermedia. Thus the G. reussi - G. berthelini plexus is probably tolerant of low levels of dissolved oxygen as is Lenticulina rotulata var.b which is also present in the pre-OAE fauna. In contrast, Textularia chapmani is only present during the anoxic event and may represent a specialist form tolerant of low levels of dissolved oxygen.

There is a general relationship between feeding habits and test morphology (Jones and Charnonk, 1985) in extant benthonic foraminifera. In addition, their microhabitats have been recognized (Frankel, 1974; Severin, 1983; Kitazato, 1984; Corliss, 1985; Jones, 1986) within the sediment profile and this has been applied to fossil communities (Severin, 1983; Jones and Charnock, 1985). The assemblage from Dover may be characterized:

EPIFAUNAL: Ammodiscus, Trochammina, Gyroidinoides, Gavelinella, Lingulogavelinella, Ramulina, Lenticulina.

INFAUNAL: Textularia, Eggerellina, Tritaxia, Ataxophragmium, Vaginulina, Dentalina, Plectina, Pseudospiroplectinata, Marssonella, Arenobulimina.

6.3. The late Cenomanian Anoxic Event and the planktonic taxa.

The planktonic foraminifera show a gradual increase in diversity, reaching a peak at the top of bed 1, Plenus Marl Formation. There follows a steady decline through the succeeding beds of the Formation, reaching its nadir in the base of the Shakespeare Cliff Member: this clearly mirrors the δ13C curve.

The peak in diversity at the top of bed 1 is coincident with the increasing water depth, (see 5.14). The rotaliporid component decreases with the rising oxygen minimum zone, finally disappearing at the top of bed 3, with R. greenhornensis disappearing before R. cushmani (Hart, 1985; Figure 5.13), at a δ13C value of 3.5 - 4.0 ‰ (PDB) which is below the maximum value of 4.0 - 4.5 ‰ (PDB) reached in bed 8. In the Muhlberg section (West Germany), Rotalipora cushmani disappears at a δ13C value of 3.8 ‰ (PDB) (Hilbrecht and Hoefs, 1986). After the loss of the rotaliporids, the dicarinellids assume dominance but the number of specimens recovered becomes very low in bed 6 which remains the case through into the first 2m of the Shakespeare Cliff Member. The planktonic diversity slowly increases to reach its pre-OAE value.

There is no statistical difference between the empty tests of extant planktonic foraminifera in the basal anoxic waters of the Gulf of Mexico and the population in the overlying surface waters, although there may be some incipient dissolution of the spinose forms (Penrose and Kennet, 1979). Thus as the assemblage at Dover contains a hedbergellid population across the anoxic event, which are the thinnest walled planktonics, the assemblage is not

significantly altered by dissolution.

The evolutionary relationships are covered in Chapter 7.

Thus the sequence of foraminiferal changes may be shown (Figure 6.1) at punctuated intervals with the expansion in the oxygen minimum zone:

Bed 1: Plenus Marls (Figure 6.1 A). Rise in sea level, rich benthonic community and planktonic assemblage, O_2 minimum zone not affecting the shelf.

Bed 2: Plenus Marls (Figure 6.1 B). Benthonic community impoverished but planktonic community stable (with slight loss of rotaliporids). O_2 minimum zone upon the shelf but only affecting the basal waters.

Bed 4: Plenus Marls (Figure 6.1 C). Poor benthonic community and loss of rotaliporids. O minimum zone moved onto the shelf and part of the way up into the water column.

Bed 8: Plenus Marls (Figure 6.1 D). O_2 deficiency tolerant benthonic taxa established and very low planktonic count. O minimum zone expanded to its fullest extent up the water column.

Figure 6.1

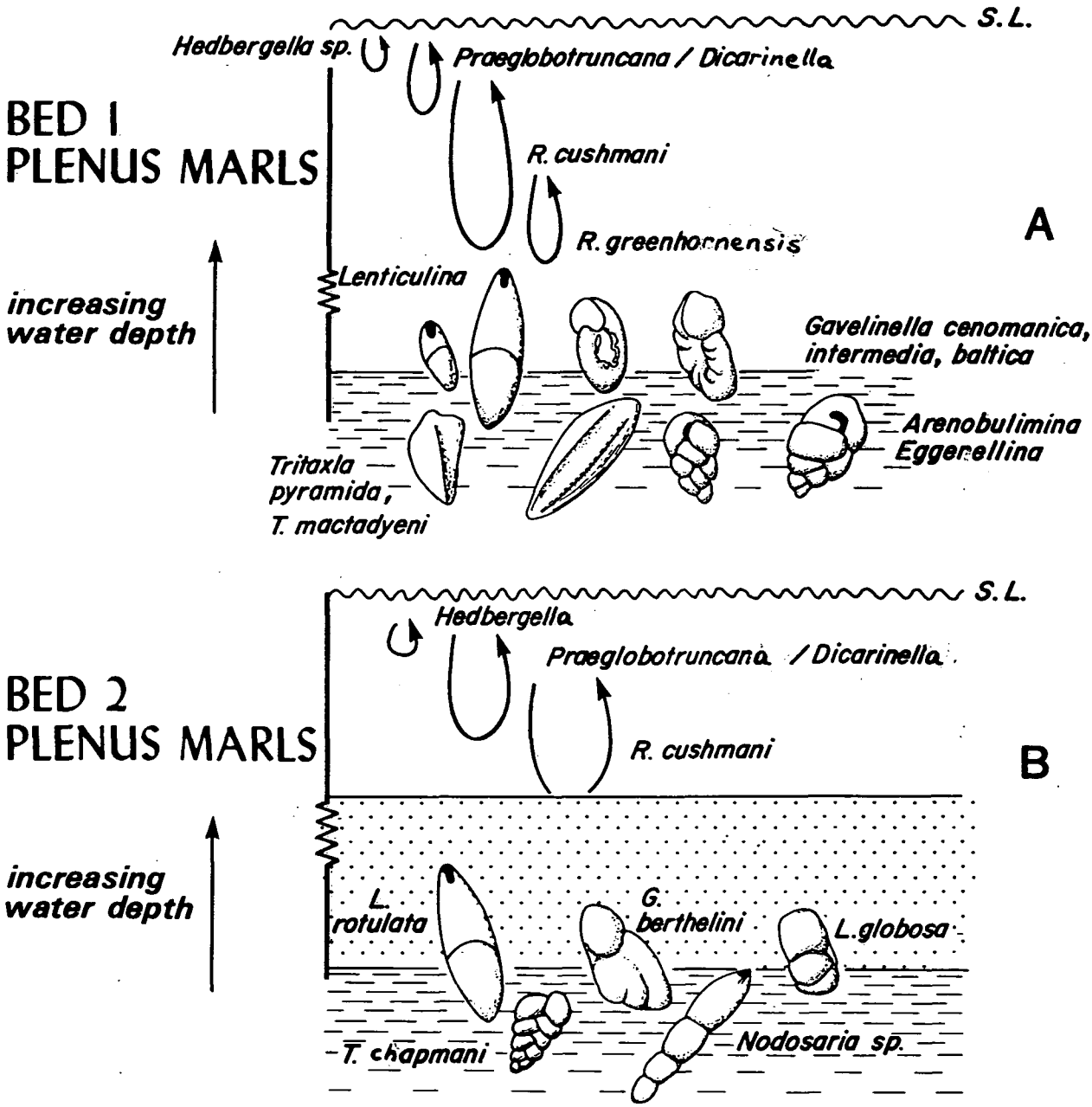

Late Cenomanian Anoxic Event and the benthonic and Planktonic foraminifera

Figure 6.1

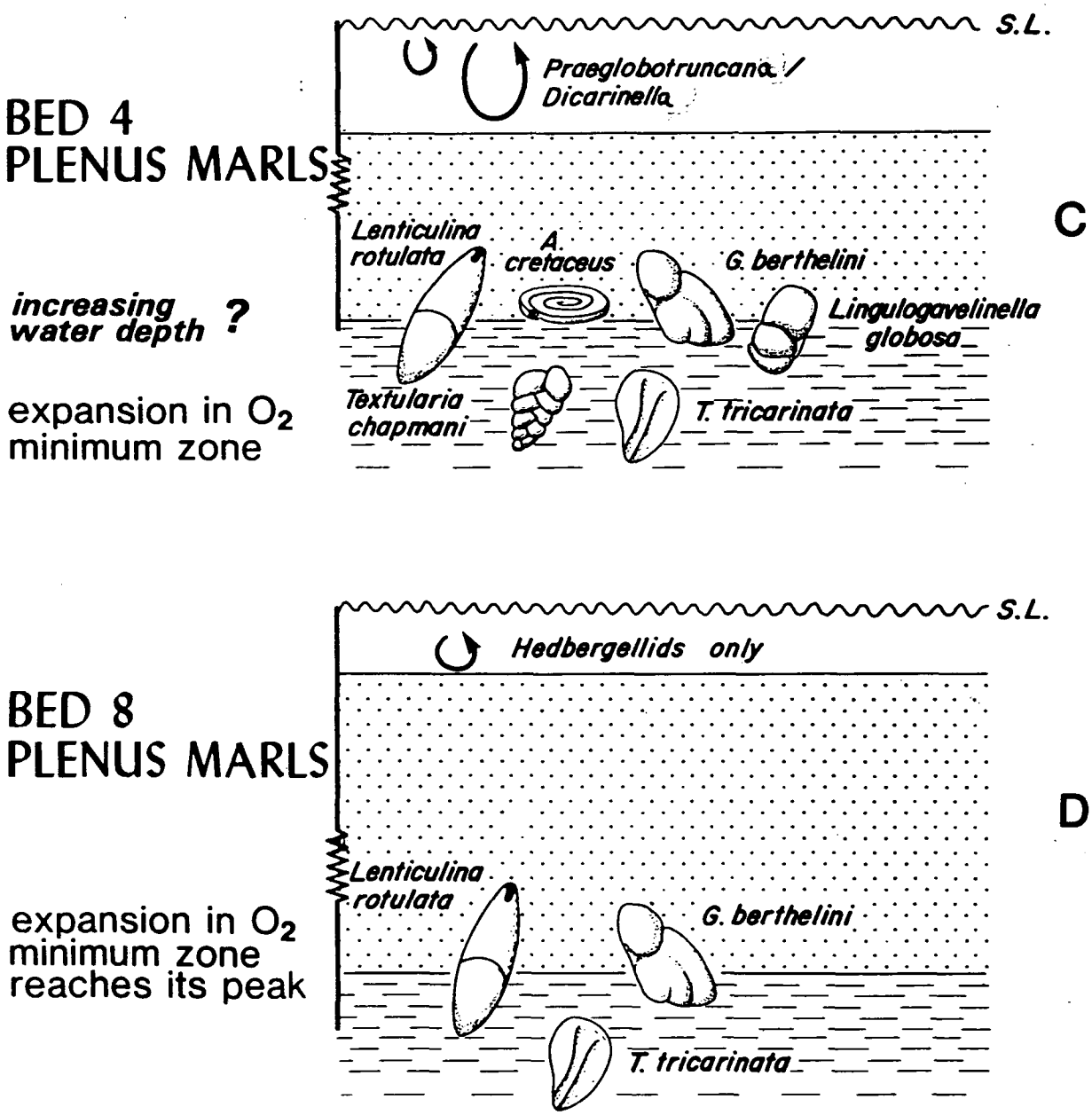

Late Cenomanian Anoxic Event and the benthonic and Planktonic foraminifera

Chapter 7: The late Cenomanian Anoxic Event and the evolution of the planktonic foraminifera.

The distribution of mid Cretaceous foraminifera in northwest Europe has been noted (Hart and Bailey, 1979), and the effect of oceanic anoxic events on foraminiferal evolution (Hart, 1980a; Caron, 1983a; Caron and Homewood, 1983; Hart, 1985; Hart and Ball, 1986; Arthur et al., 1987).

The rise in the oxygen minimum zone caused the extinction of the rotaliporids and initially the decimation of the planktonic population, with very low planktonic numbers recorded. The post OAE saw the re-establishment of the surviving taxa and a period of explosive evolution of forms adapted to capitalise on the deeper water niche vacated by the rotaliporids. The pre-late Cenomanian OAE foraminiferal population had developed through the Albian and most of the Cenomanian to produce well differentiated tripartite groups based upon test architecture of Hedbergella spp., Praeglobotruncana spp. (and some "early dicarinellids") and Rotalipora spp. (Figure 7.1). These three different morphotypes were adaptations to a progressively deeper water niche for gametogenesis (Hart, 1980a; Caron and Homewood, 1983), in the gerontic portion of their lifecycle (Figure 7.1). A consequence of a deeper water position for gametogenesis was a decrease in the frequency of gametogenesis. Thus the rotaliporids were the most susceptible to a rise in the oxygen minimum zone.

Figure 7.1

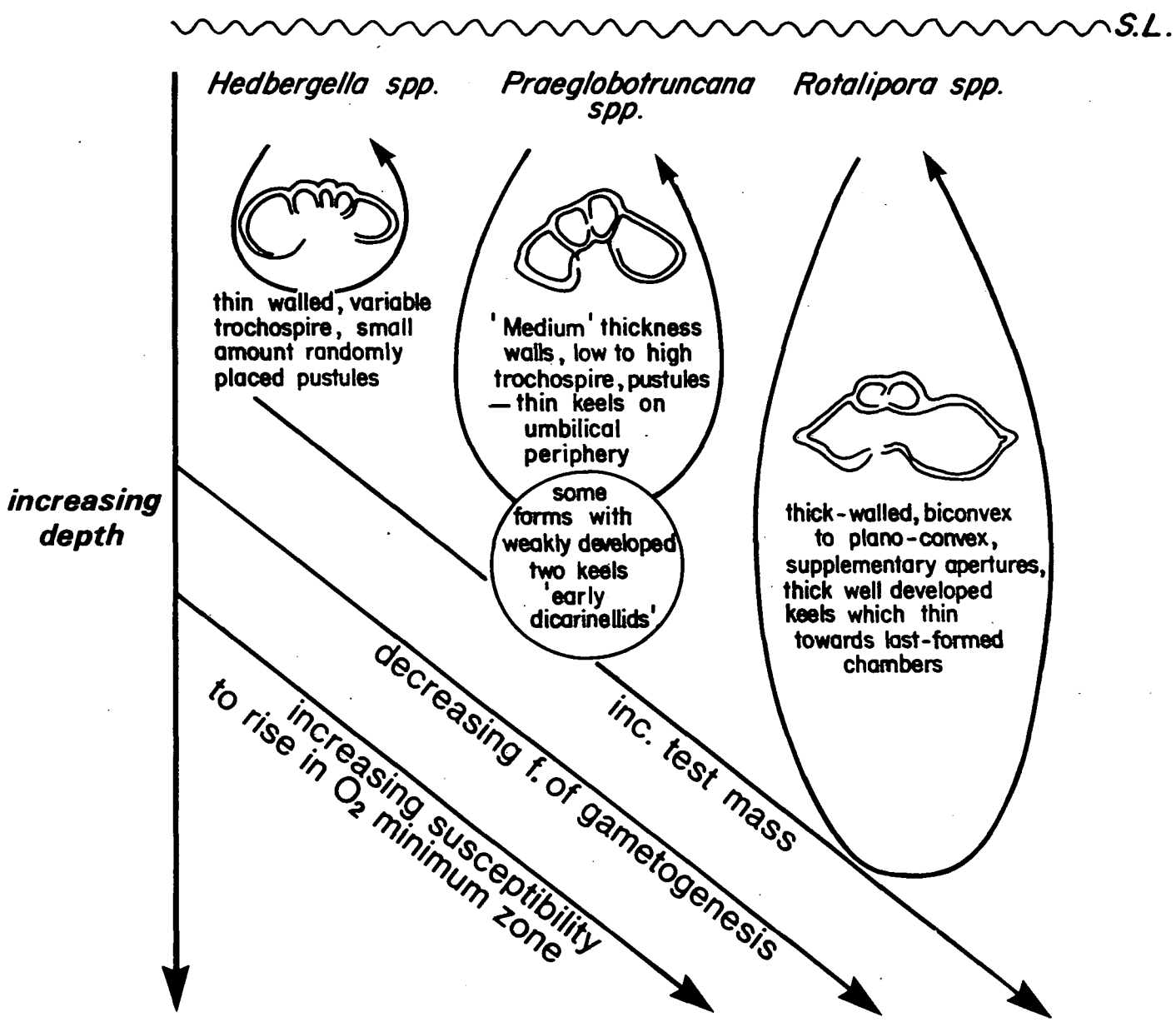

Pre late Cenomanian OAE foraminiferal populations and their ontology. ammended from Caron & Homewood (1983)

The extinction of the rotaliporids followed the pathway R. deeki(?), then R. greenhornensis, then R. cushmani (Hart, 1985: see 6.3), R. deeki and R. greenhornensis being restricted to deeper water assemblages than R. cushmani. The pre-OAE globotruncanid population contains forms with two faintly developed keels (especially on the initial chambers of the last whorl) with a lower trochospire. On the demise of the rotaliporids, these forms rapidly increase in both numbers and keel definition, thus obtaining a more pronounced dicarinellid aspect. This population includes D. algeriana, D. hagni and D. imbricata, although the keels of the latter are only slightly offset around the whorl and are very close to the keel configuration of D. hagni. In addition, the differentiation of P. stephani and D. algeriana is problematical as in many cases the keels are poorly separated, if at all. Within the hedbergellid population there is a slight proliferation of forms with H. planispira, H. aprica and H. brittonensis increasing their numbers. Both praeglobotruncanids/dicarinellids and hedbergellids exhibit a sharp drop in numbers coupled with the continued gradual rise in the δ 13C level (and rising oxygen minimum zone). With the waning of the δ 13C level there are four important developments:

(i) the appearance of "H". archaeocretacea. H. archaeocretacea is derived from the H. aprica group and is a rapid development: many of the specimens show poorly developed peripheral pustules and umbilical structures (Figure 7.2).

(ii) the appearance of H. praehelvetica. Some specimens within the H. delrioensis group during the anoxic event show very low trochospires, these develop with the waning of the anoxic event into the wider umbilical, trochospired form of H. praehelvetica. However, their absolute numbers are low (Figure 7.2).

(iii) further differentiation of the dicarinellids. Within the dicarinellid population the species-specific features become more acute. The D. algeriana stock show well separated and stepped keels. D. imbricata and D. hagni groups show a moderate increase in the size of the specimens, lower trochospires and an increase in the angle of the keels of the former (Figure 7.2).

(iv) the heterohelicid population. The pre-OAE heterohelicid population is dominated by the H. moremani group; with the waning of the oxygen minimum zone the more expanded chambered forms of the H. globulosa group appear derived from the former. In addition, nearly all the heterohelicid population is now striate, with variably developed thin costae on the tests. In some cases, these are concentrated on the first formed chambers of the test (Figure 7.2).

The proposed phylogenic relationships of mid-Cretaceous planktonic foraminifera have variously placed emphasis on such features as apertural position, height of the trochospire and the presence/absence of keel(s). Bandy (1961),

Figure 7.2

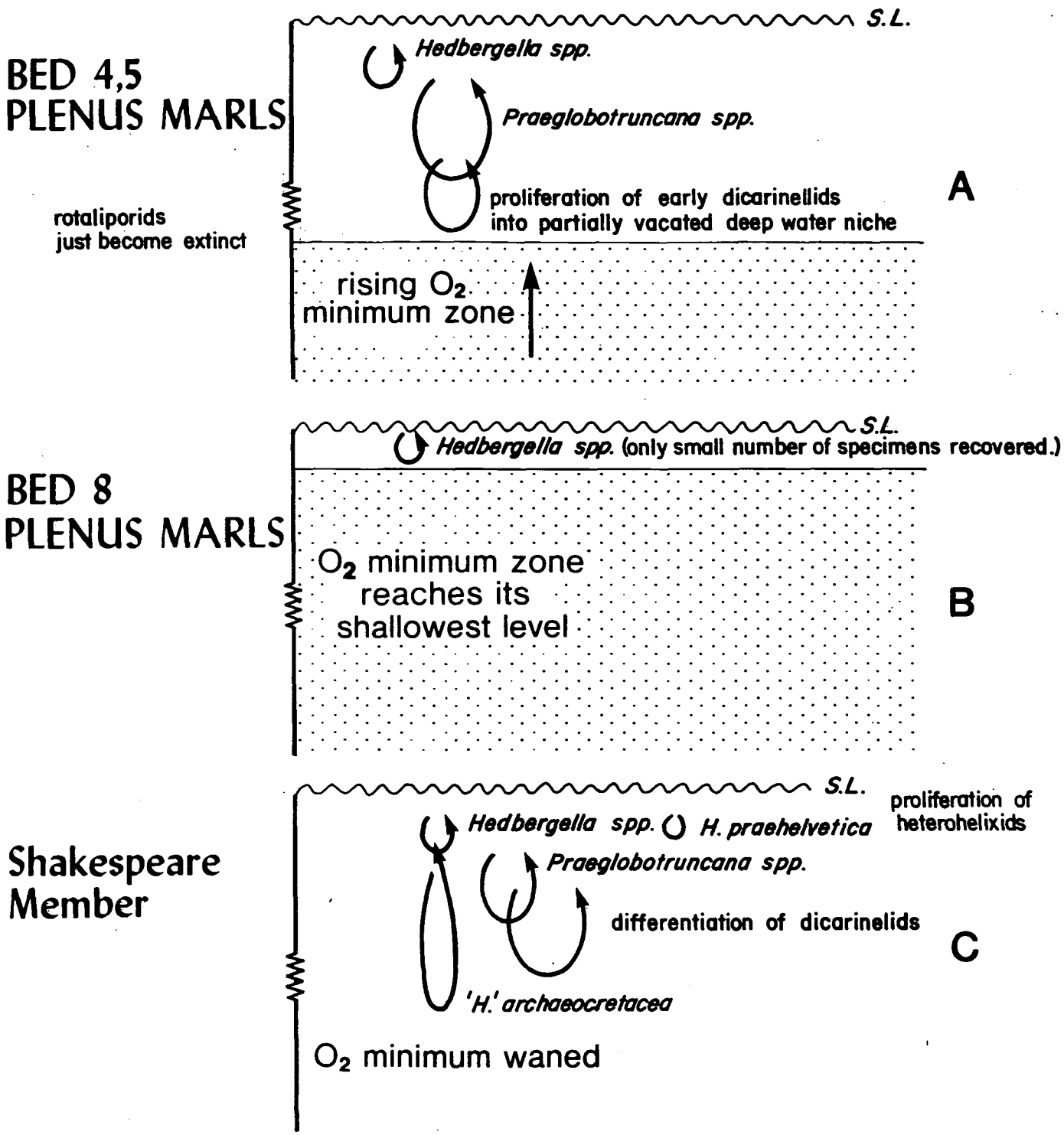

Schematic representation of evolutionary 'micro events' within the planktonic foraminiferal population during the late Cenomanian OAE

placed much emphasis on the presence of keels and suggested that the rotaliporid group gave rise to the globotruncanids in the late Cenomanian and that H. helvetica was derived from P. delrioensis. In contrast, Neagu (1969), derived the globotruncanids from the praeglobotruncanids in the middle to late Turonian. Wonders (1980), agrees with this but states that only D. algeriana crossed the Cenomanian - Turonian boundary and that the hedbergellids gave rise to the whiteinellids. Similarly, Banner (1981), proposed that the praeglobotruncanids gave rise to the dicarinellids in the early Turonian. This, largely, was proposed by Caron (1983b), with the praeglobotruncanids being the ancestral stock of the dicarinellids and the whiteinellids deriving from the hedbergellids. In addition, she proposed that the helvetoglobotruncanids were an early Turonian offshoot of the hedbergellid stock.

This study proposes that the dicarinellids were derived from the praeglobotruncanids, in broad agreement with Neagu (1969), Wonders (1980), Banner (1981) and Caron (1983b), but that it occurred twice in the late Cenomanian.

The presence of the more specialist deep water rotaliporids prior to the OAE restrained the development of the praeglobotruncanid population. The formers' demise, with the rising oxygen minimum zone, facilitated rapid dicarinellid proliferation, both prior to the shallowest position of the zone and on its waning. Equally, the rapid appearance of "H". archaeocretacea was a deep water strategy. Its initial

success past the moving praeglobotruncanid / dicarinellid population may be due to the increased frequency of gamatogenesis of the surface-dwelling hedbergellids.

A common test morphology (Text-Figure 7.1) of low trochospire, peripheral test thickening (lines of pustules, 1-2 keels), and wide differentiated (supplementary apertures and infraliminal accessory apertures) umbilical regions is shown by Rotalipora spp., H. archaeocretacea and Dicarinella spp. This movement towards a keeled disc shape has several reprecussions for the test:

(i) increase in test mass.

(ii) increase in surface area:volume ratio.

(iii) movement in the centre of gravity.

The physical analysis of empty tests of extant species shows that the co-efficient of resistance (Ø) increases as the test approximates more towards a disc (McNown and Malaika, 1950; Lipps, 1979). (The larger planktonic foraminifera are inappropriate for the application of Stokes Law, (Lipps, 1979)). The strategic secretion of calcite around the periphery in the form of keels shows several important features:

(i) it is remarkably consistant within a stable population (Rotalipora spp.).

(ii) thicker, more substantial keel(s) on the initial chambers of the last whorl weakening progressively around the periphery.

The keels may possibly be the remains of concentrated spine bases which would result in an extended disc shape but with a much lower increase in overall test mass (Text Figure

7.1a). In addition, the thicker spines on the initial chambers of the last whorl would tend to maintain a regular overall outline in spiral view (Text Figure 7.1b).

Text figure 7.1(a)

Increase in test diametre with addition of spines

7.1(b) Smoothing of test outline in spiral view

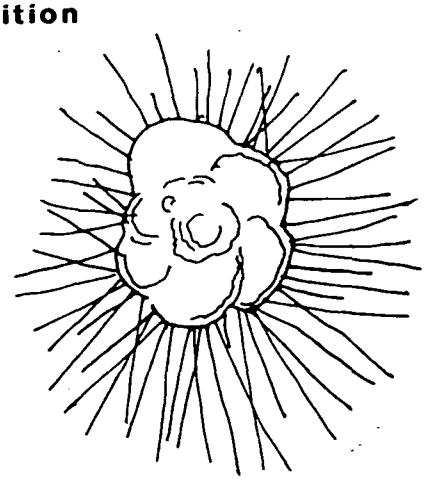

This configuration would greatly increase the co-efficient of resistance (Ø), but only if the test were orientated perpendicular to the direction of motion of the test. There is no evidence of the orientation of the tests of extant foraminifera in the water column (Hemleben, pers. comm.). Whatever the physical interactions of the test and the sea water, the role of the ectoplasm has yet to be assessed properly. The increase in the surface area:volume ratio may cause transport problems of nutrients through the ectoplasm and endoplasm but the opening of the chambers to the umbilicus results in the minimal distance between the individual chambers and the ectoplasm, the so-called MinLOC (sensu Brasier, 1982, 1986). The development of supplementary apertures and infralaminal accessory apertures facilitates this. The latter

may be a protective adaptation for the wide open umbilicus.

Chapter 8: Other faunal groups and the late Cenomanian Anoxic Event.

8.1. Introduction.

Some of the macrofaunal changes across the Cenomanian - Turonian boundary in England have been documented (Jefferies, 1963; Kennedy and Wright, 1981; Woodroof, 1981). Some microfaunal changes have been investigated (ostracods: Kaye, 1964; Weaver, 1981, 1982; dinoflagellates: Clarke and Verdier, 1967; nannoplankton: Crux, 1980, 1982) but several detailed studies are as yet unpublished (ostracods: Horne, pers. comm; dinoflagellates: Tocher, pers. comm.; nannoplankton: Cooper, pers. comm.).

8.2. Macrofaunal changes.

The macrofaunal assemblages found through the Plenus Marl Formation (Figure 8.1), as exemplified by Merstham, show several important features (Jefferies, 1963). The benthonic community exhibits a marked faunal change at the top of bed 1 and subsequent reduction in diversity through the successive beds (2-8), with a particularly low faunal count from the top of bed 3. In addition, there is no aragonitic macrofauna recorded from beds 4 to 8 (Jefferies, 1963), and the ammonite record is very poor (kennedy and Wright, 1981). This implies some dissolution of the fauna, also evident in the foraminifera tests (see 5.8(v), 5.9(v), 5.10 (v), 5.11(v)), and ostracod valves (see 8.3(i)). Although the degree of dissolution is not very intense: the presumably most susceptible thin walled

Figure 8.1 Macrofossil changes through the Plenus Marl Formation (after Jefferies 1963)

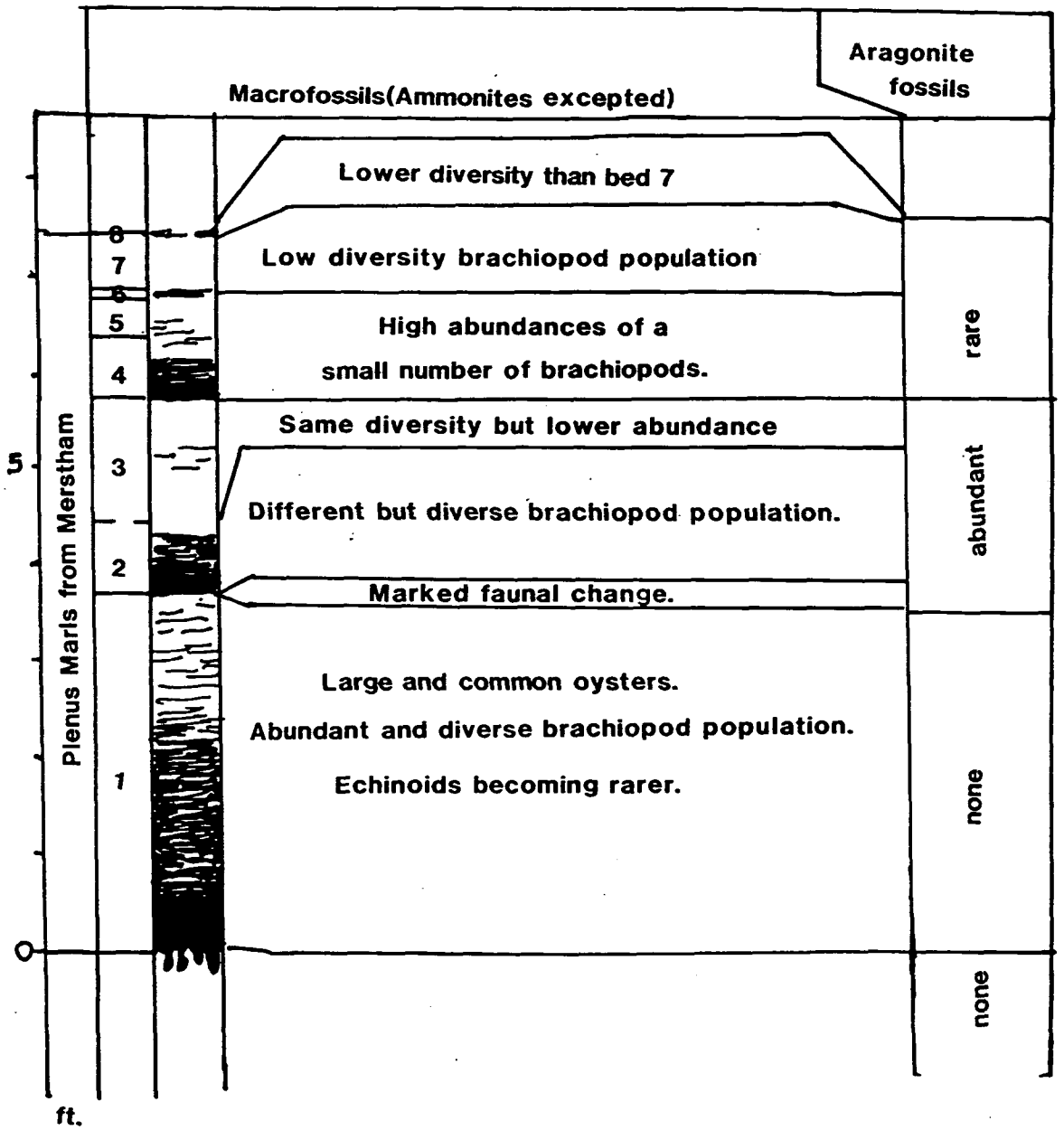

planktonic foraminifera are still preserved. The early Turonian benthonic fauna is characterized by only a small number of morphotypes, relatively small individual size and is dominated by suspension feeders such as Orbirhynchia and inoceramids (Woodroof, 1981).

8.3. Microfaunal changes.

(i) ostracods:

The ostracods from the Cenomanian of England have been described by Weaver (1981, 1982). The ostracod assemblage through the Cenomanian - Turonian succession at Dover is dominated by platycopids with the rest of the fauna comprised of podocopids (Figure 8.2)(Horne, pers. comm.). The former exhibit a drop in absolute numbers after bed 1 but not an appreciable drop in diversity. Their absolute numbers continue to decline through the successive beds (2-8) and only begin to recover about 1.5m above bed 8 of the Plenus Marl Formation (Horne, pers. comm.). In contrast, the podocopids show a dramatic decline in diversity through beds 1-8 of the Plenus Marl Formation, particularly at the tops of beds 1 and 4 (Figure 8.5, 8.6). These extinctions resulted in only three podocopids surviving into the overlying Dover Chalk Formation. The post-OAE ostracod population remains poor both in abundance and diversity well into the Dover Chalk Formation (Horne, pers. comm.). The durability of the platycopid population through the OAE in contrast to the podocopids may be due to their ontogenetic strategy of retaining neanics within the carapace for three instars prior to release into the

Figure 8.2 Ostracods from Dover

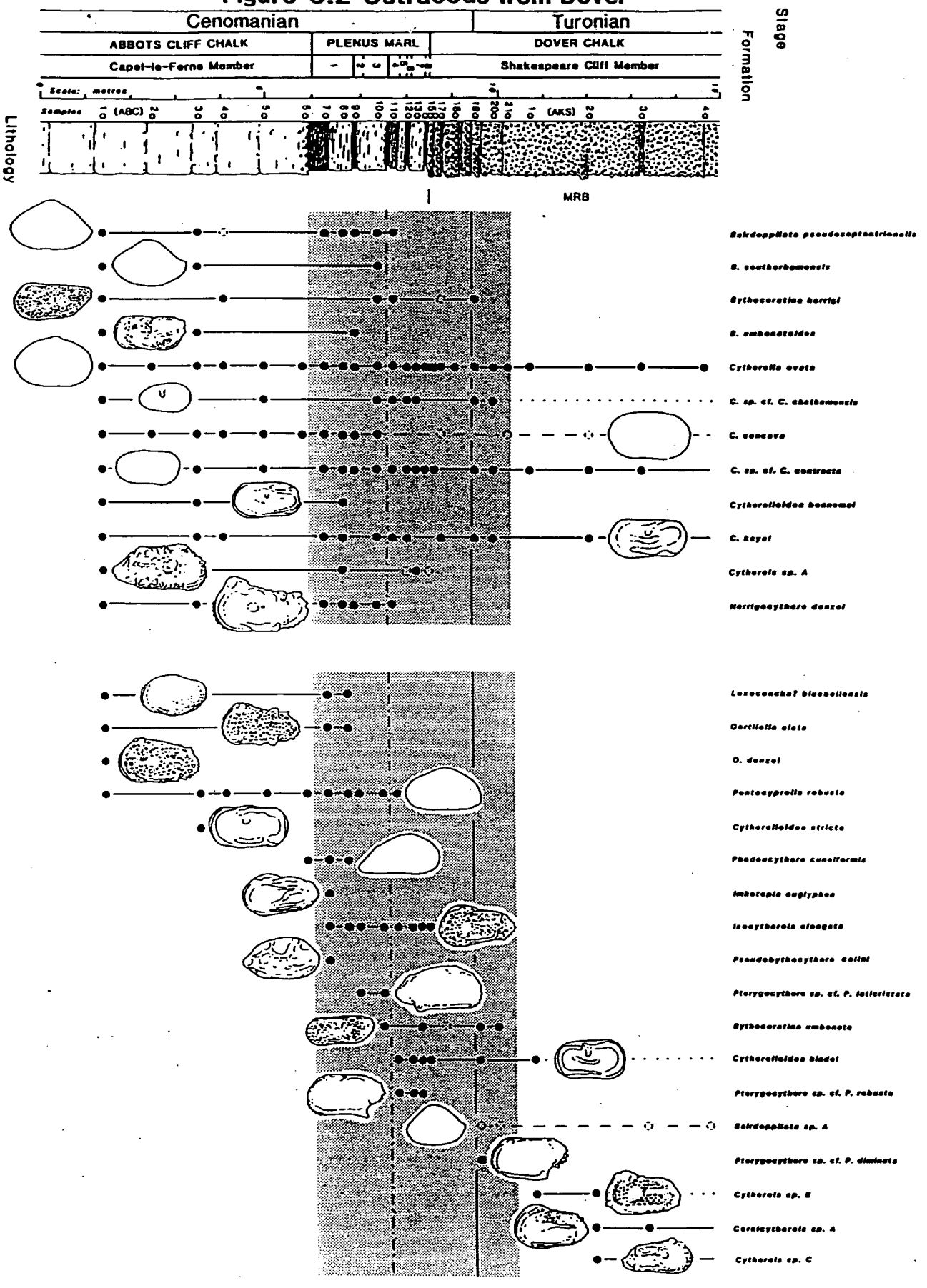

(after Jarvis *et al.* in press)

Figure 8.2 Ostracods from Dover(cont.)

(after Jarvis *et al.* inpress)

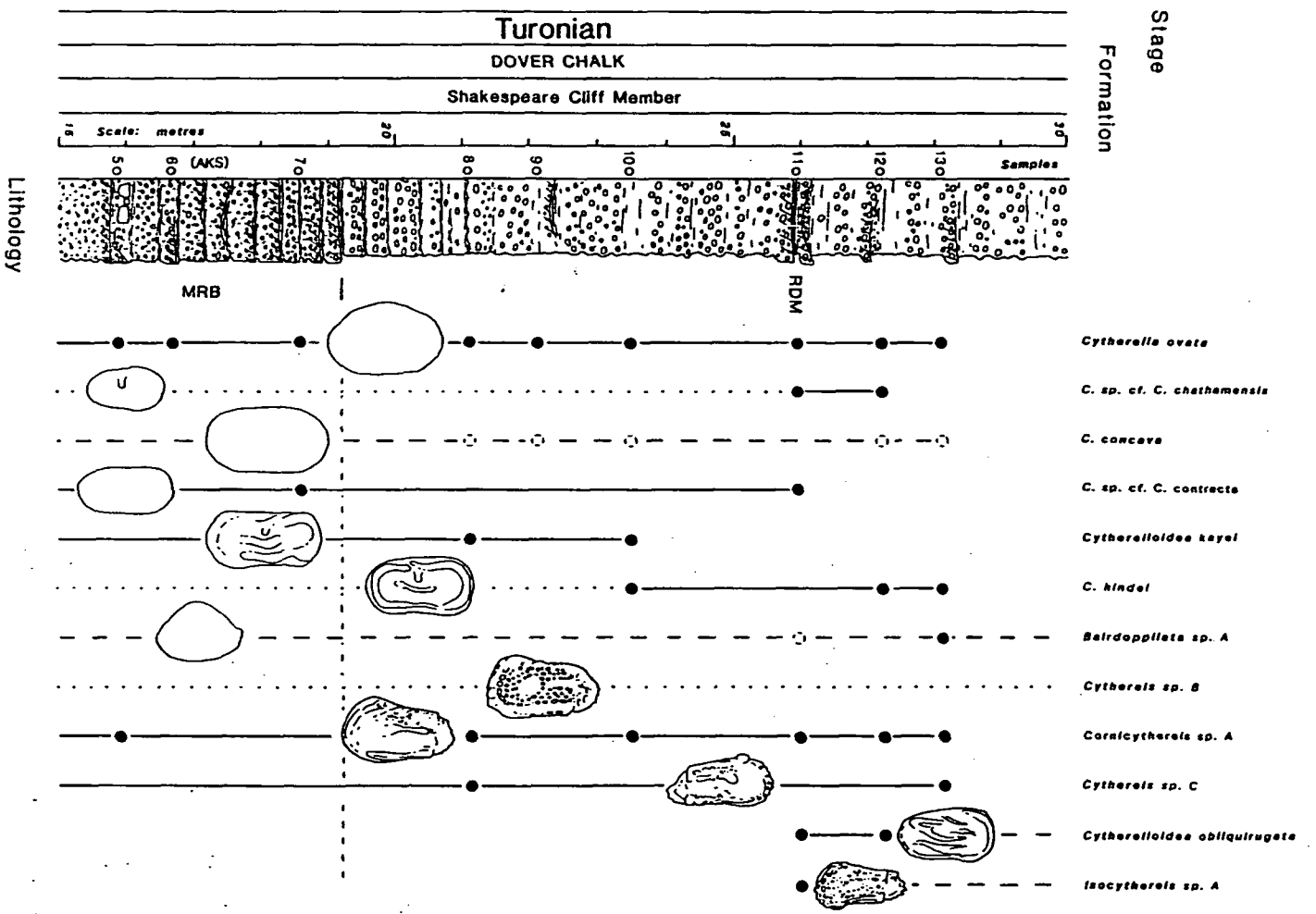

Figure 8.3 Dinoflagellates from Dover

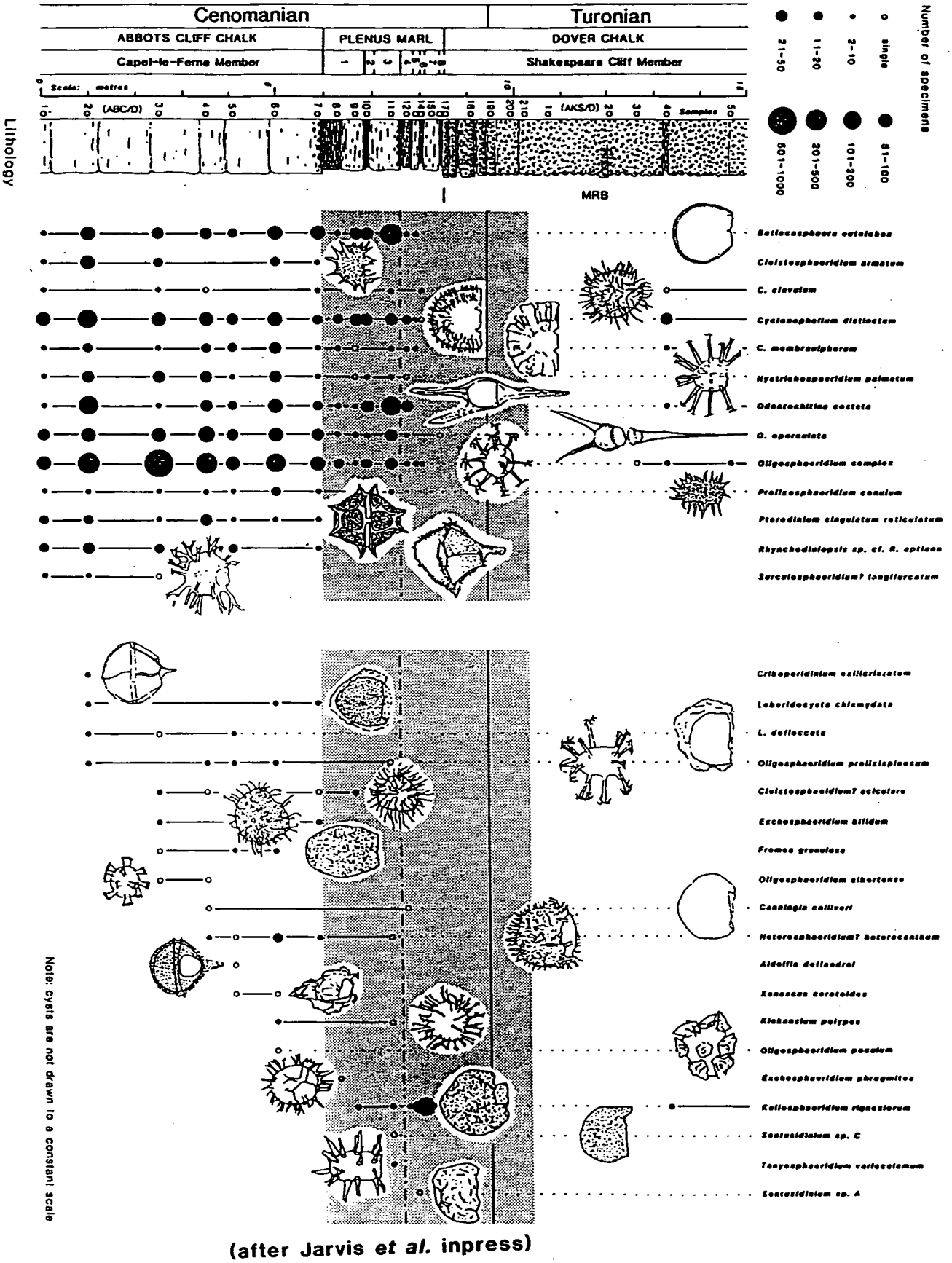

(after Jarvis *et al.* inpress)

Figure 8.3 Dinoflagellates from Dover(cont.)

(after Jarvis *et al.* in press)

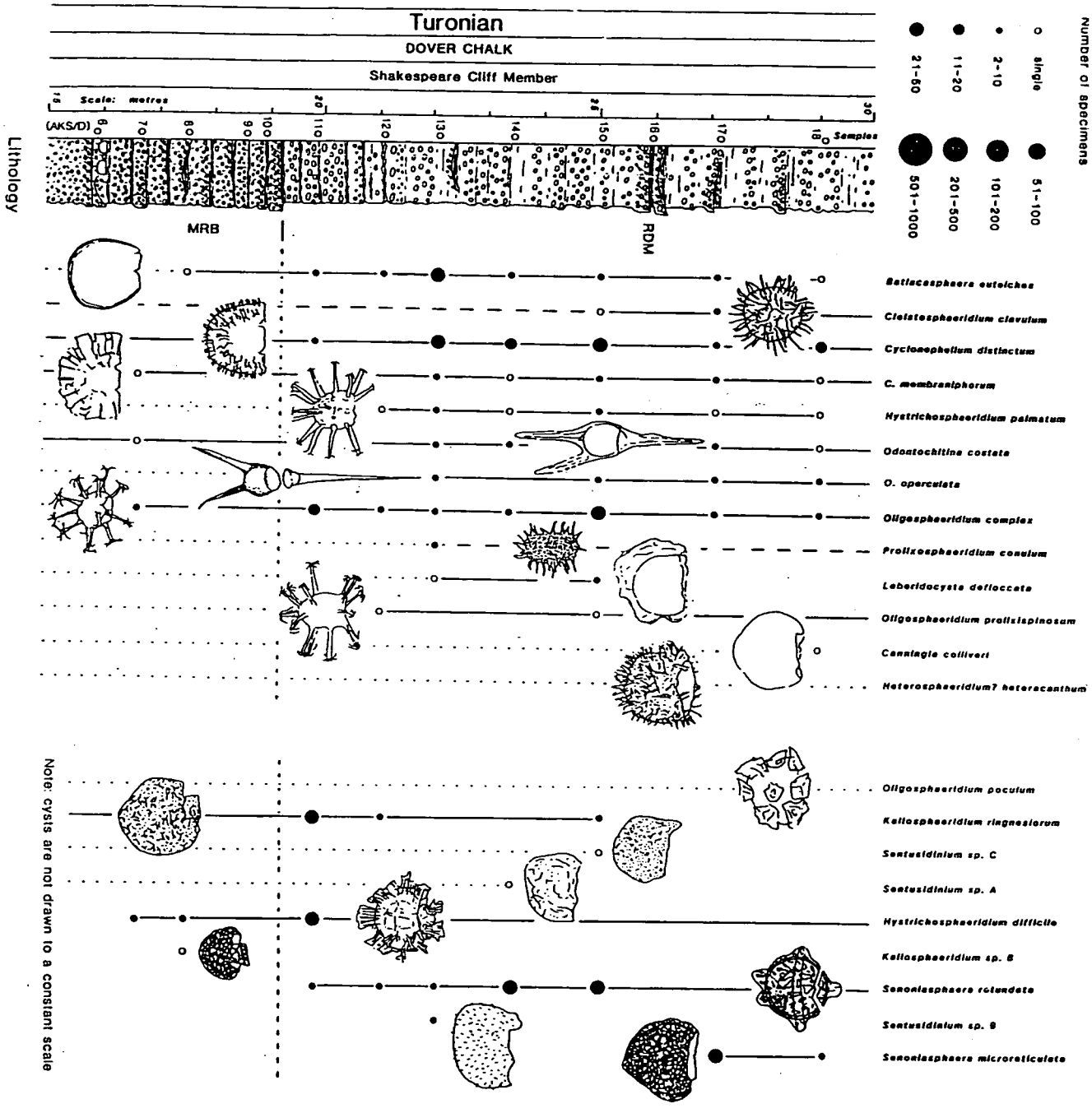

environment. A high proportion of Cytherella specimens in bed 4 and the higher parts of the Plenus Marl show dissolution effects, with valves displaying rough, etched surfaces in contrast to their normal smooth appearance.

(ii) dinoflagellates:

The dinoflagellate cysts across the Cenomanian - Turonian boundary have been investigated from the Isle of Wight (Clarke and Verdier, 1967). The dinoflagellate cyst assemblage from the late Cenomanian - Turonian succession at Dover (figure 8.3), exhibits a drop in diversity just below the sub Plenus erosion surface, recovering to its initial level in bed 3 of the Plenus Marl Formation (Tocher, pers. comm.)(Figure 8.5, 8.6). After bed 3, the diversity declines rapidly to zero at the top of bed 8. The dinoflagellate cysts reappear 3.5m above bed 8 and slowly recover in diversity to reach the pre-OAE level in the late Turonian (op cit.). The absence of cysts in the Melbourn Rock facies is probably not a preservational phenomenon but a true reflection of the devastation of the dinoflagellate encysting population (Tocher, pers. comm.), because their decline begins within the Plenus Marl Formation.

(iii) nannoplankton;

The nannoplankton population across the late Cenomanian - Turonian boundary succession at Dover shows a marked decline in beds 7 and 8 of the Plenus Marl Formation, with some extinctions at these levels (Figures 8.4, 8.5, 8.6). The diversity continues to decline to its lowest level in the

Figure 8.4 Nannoplankton from Dover

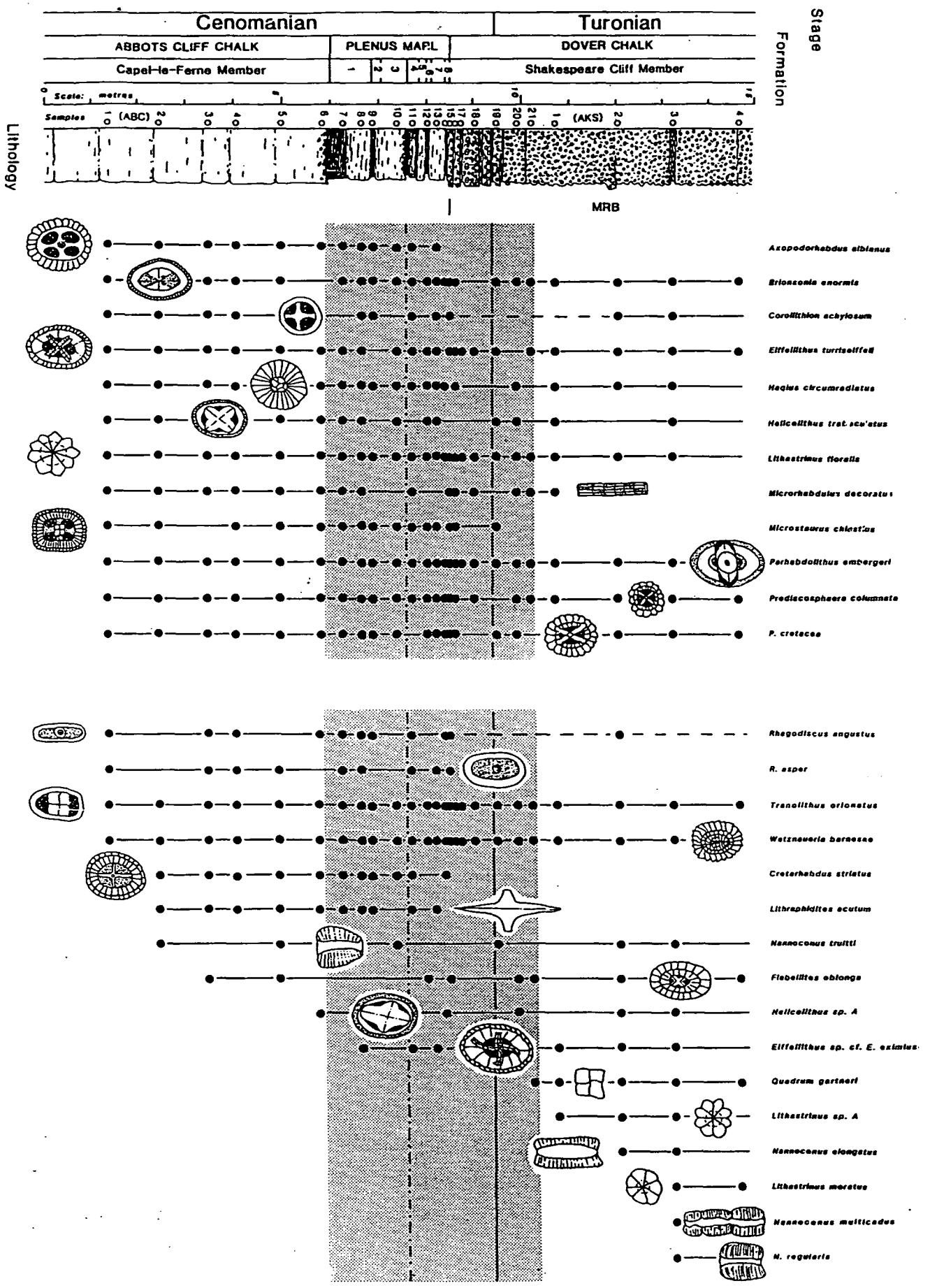

(after Jarvis *et al.* in press)

Figure 8.4 Nannoplankton from Dover(cont.)

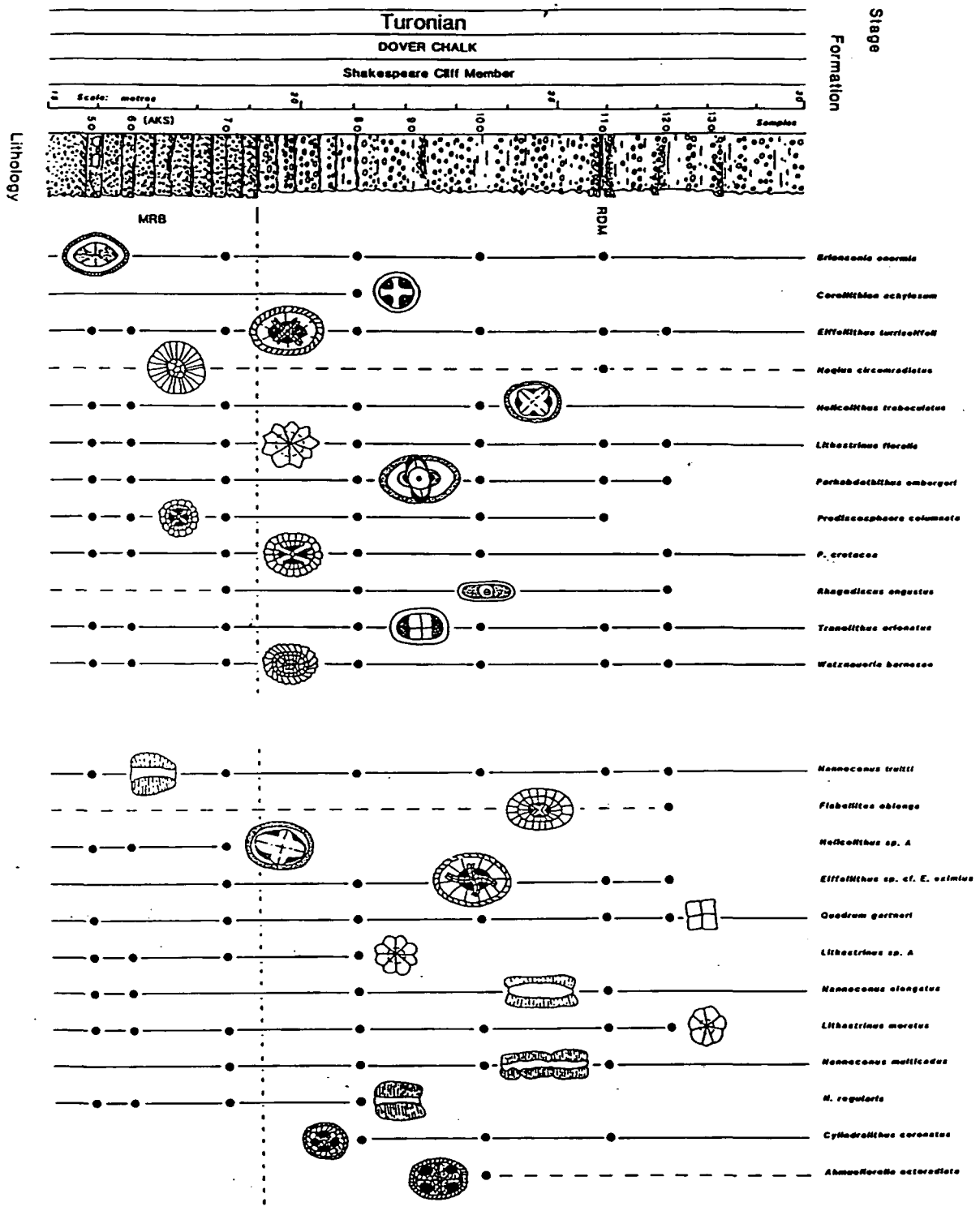

(after Jarvis *et al.* in press)

Figure 8.5 Diversities from Dover

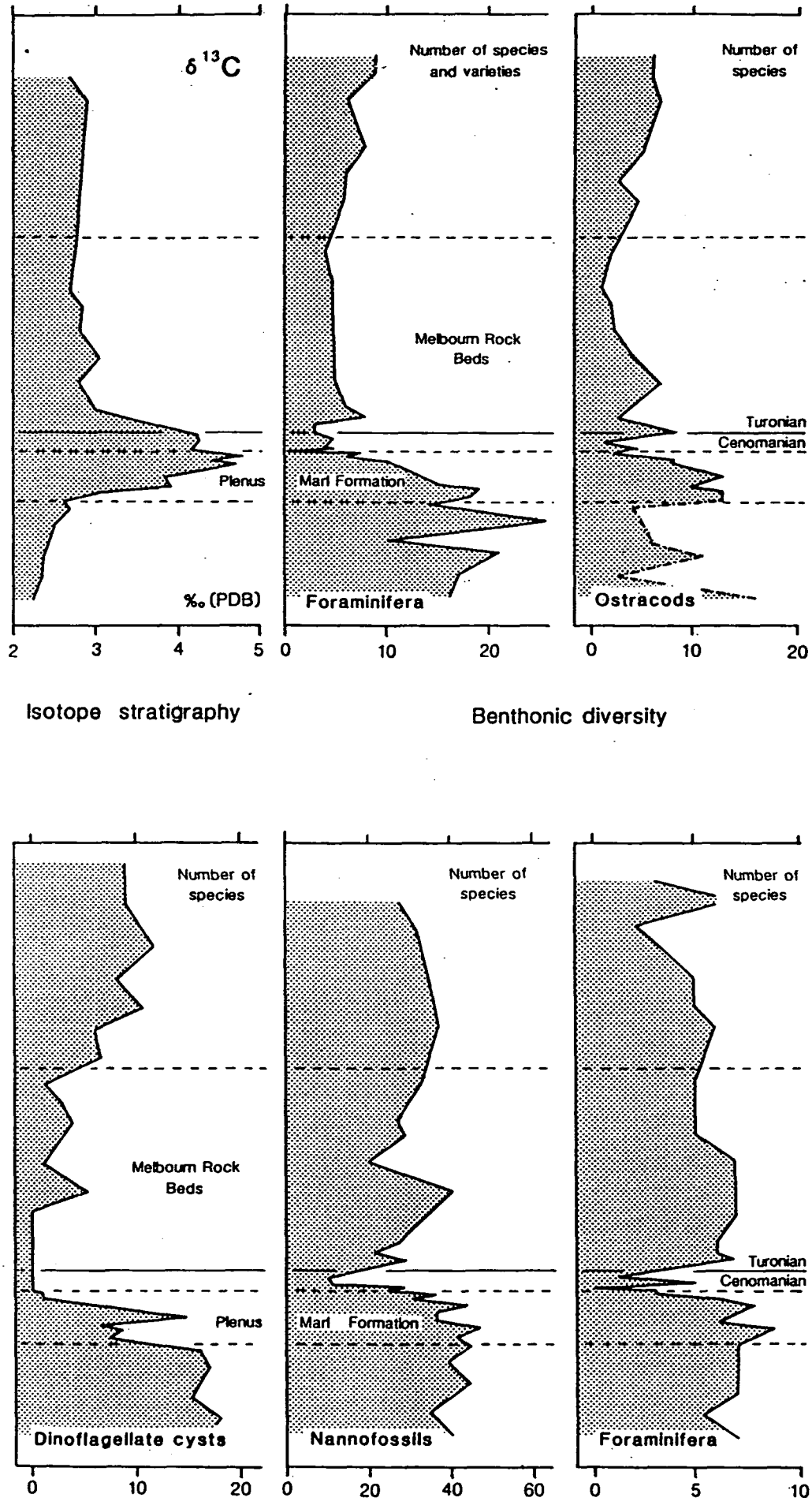

(after Jarvis *et al.* in press)

Figure 8.6 Abundances from Dover

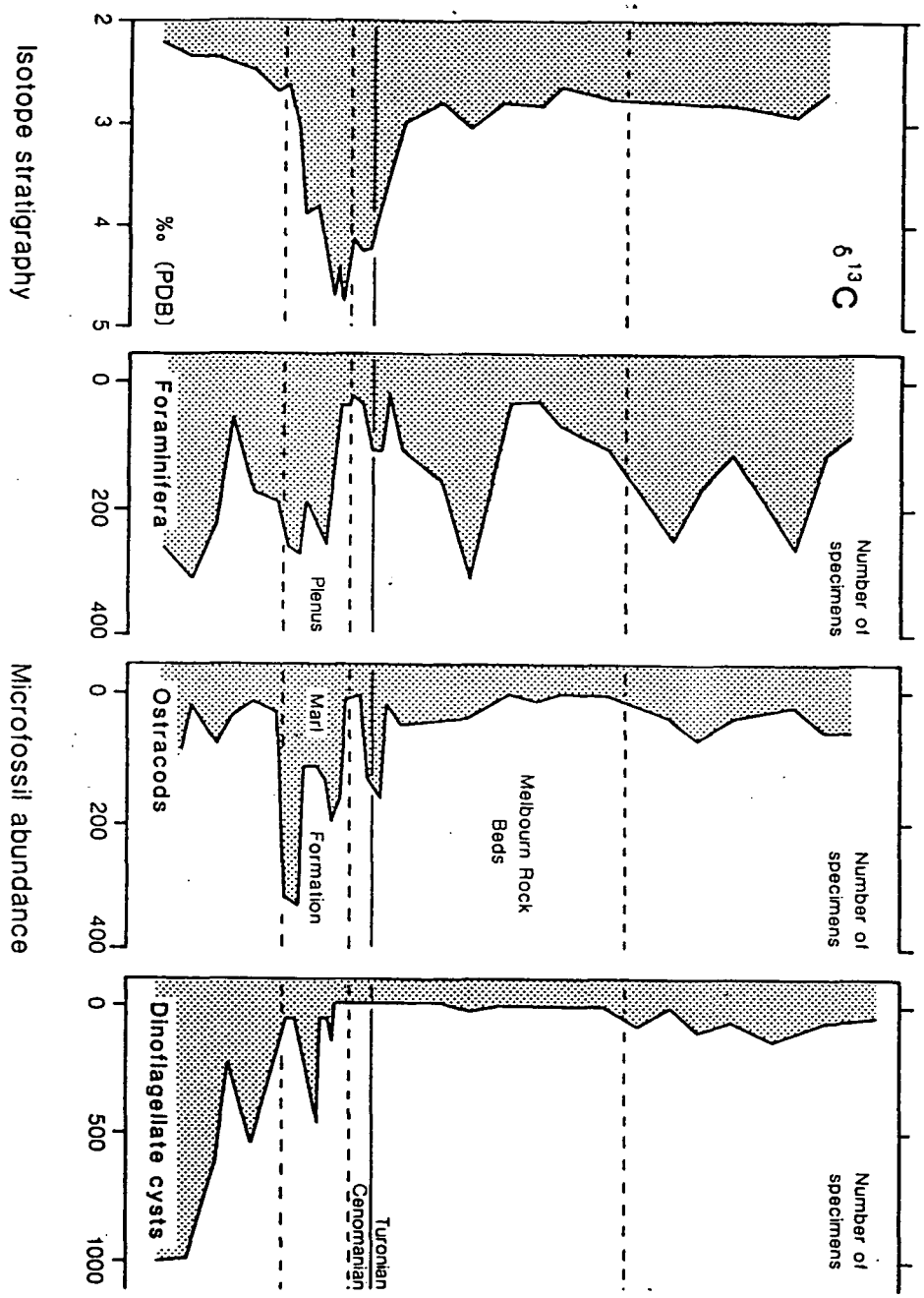

(after Jarvis *et al.* in press)

second incipient hardground of the Melbourne Rock facies (Dover Chalk Formation). The nannoplankton diversity rapidly increases after the waning of the OAE with the proliferation of several new species (Cooper, pers. comm.).

8.4. Overview.

The pattern of macrofaunal and microfaunal changes may be summarized sequentially as:

(i) Just below the sub-Plenus erosion surface-
loss of small number of dinoflagellate species.

(ii) bed 1, Plenus Marls-
high diversity of benthonic foraminifera, ostracods, benthonic macrofauna.

(iii) top bed 1-
extinction of some benthonic foraminifera, ostracods (podocopids), decline in macrofaunal diversity.

(iv) beds 2-3 -
poor benthonic macrofauna
continued decline in benthonic foraminifera.

(v) top bed 3-
extinction of rotaliporids
initial decline in dinofalgellate cyst diversity.

(vi) bed 4-
rapid decline in dinoflagellate cyst diversity
continued decline in benthonic foraminifera and low ostracod diversity.

(vii) beds 5-8 -

planktonic and benthonic foraminifera,
ostracods and dinoflagellates reach lowest diversities
nannoplankton diversity begins decline
macrofauna poor.

(viii) top bed 8-
$\delta^{13}C$ value reaches its peak
very low dinoflagellate numbers and diversity
planktonic and benthonic foraminifera diversities
low
ostracod diversity very low, limited benthonic
macrofauna

(ix) within first metre of Melbourn Rock facies-
dinoflagellates absent
nannoplankton diversity at its lowest
benthonic and planktonic foraminifera,
ostracod and benthonic macrofaunal diversities very low.
$\delta^{13}C$ value begins to wane.

(x) subsequent 20m of Dover Chalk Formation-
$\delta^{13}C$ value quickly returns to background level
benthonic macrofauna and foraminifera,
ostracod diversities recover but to lower than
pre-OAE values
planktonic foraminiferal diversity recovers
dinoflagellates reappear but with lower than
pre-OAE diversity and abundance.

Thus it is evident that the rising oxygen minimum zone adversely affected the benthos prior to the deeper

water planktonics (rotaliporids) and then subsequently the shallow water planktonics (praeglobotruncanids, hedbergellids, dinoflagellates and nannoplankton).

Chapter 9: Implications of the study.

9.1. Biostratigraphical implications.

The use of deep water planktonic foraminifera for biostratigraphy limits their use in onshore sections (e.g. Rotalipora spp, "H". archaeocretacea). In addition, the OAE means there is a gap between the extinction of the rotaliporids and the development of "H". archaeocretacea and this results in an unrefined biostratigraphic interval. The identification of biostratigraphically useful planktonic foraminifera in thin section from burrows within hardgrounds of attenuated sequences, such as Shapwick Grange Quarry (Chapter 5.6 (iv)), permits the dating of infilling events during the formation of these omission surfaces. Thus the detailed sampling of the burrow phases may allow the more accurate dating of the down-moved, though subsequently eroded, overlying sediment. The measurement of the size of tests within the rotaliporid population permits the analysis of eustatic changes across the Anglo-Paris Basin (Chapter 5.14 (iii)). Thus the detailed sampling of the sequences within the R. cushmani i.z. and the measurement of the specimens would provide data on the most subtle eustatic movements. These changes could be utilised to delimit the R. cushmani i.z..

9.2. The late Cenomanian "Event" and Mass Extinctions.

Major faunal turnovers (mass extinctions) have recieved

much attention, notably the Cretaceous - Tertiary "event". A periodicity in extinction of 26 m.y has been recognized (Fischer and Arthur, 1977; Raup and Sepkoski, 1984; Raup, 1985; Sepkoski and Raup, 1986; Raup, 1987), with the late Cenomanian comprising one of these important "events". The idea of a meteor impact for the terminal Cretaceous faunal turnover (Alvarez et al., 1980), has led to the assertion of an extraterrestrial cause for the others (Raup, 1986), and the "Nemesis" death star to account for the regularity.

This detailed late Cenomanian faunal study indicates that the extinction of marine biota depended on their relative niche with respect to the rise in the oxygen minimum zone. The very sequential nature of the extinctions, from benthonics (foraminifera, ostracods, macro-organisms) to deep water planktonics (rotaliporids), to shallow water planktonics (dinoflagellates then nannoplankton), argues heavily against the impact theory induced by the proximity of "Nemesis".

The details of other Cretaceous faunal turnovers are not completely integrated but some conclusions may be drawn. In the Aptian, deep water planktonic foraminifera were not present but there were extinctions within the benthonic foraminiferal population (Hart et al., 1981), and the hedbergellids pass into the Albian. At the K-T boundary the benthonic foraminifera undergo extinctions and only the thin-walled "hedbergellid" population cross the boundary (Hart, 1981). In addition, the K-T boundary shows a marked drop in species diversity within the dinoflagellate cyst assemblage (Hansen, 1977), with only

the cosmopolitan forms passing across the boundary (Tocher, pers. comm). Thus the similarities in the three events are apparent but the relative position of the faunal changes for each group need to be established.

9.3. Interpretation of the planktonic : benthonic ratios.

The ratio of planktonic : benthonic foraminifera may be utilised to make estimates of depths of deposition of sedimentary rocks (Grimsdale and Morkhoven, 1955). These have been used in the Cretaceous to map eustacy (Barr, 1961; Diver, 1968; Flexer and Starinsky, 1970; Hart and Carter, 1975; Bailey, 1978; Hart, 1980). Whilst P:B ratios are important and useful under stable marine conditions, the very poor post-OAE benthonic fauna (in all groups - macro-organisms, foraminifera and ostracods - Chapter 8.3(i) and 8.4), means that they must be used with caution during, at least, the early Turonian, to avoid spuriously deep water depth values.

9.4. Investigation of orbital forcing.

The recognition of orbital forcing as a mechanism for the formation of sedimentary\palaeontological cycles has developed over the last hundred years (Croll, 1875; Berger et al., 1984). Cretaceous rhythms have recieved much attention (Barron et al., 1985; Arthur et al., 1986; Herbert and Fischer, 1986). For the optimal biotic changes the Cenomanian strata are more suitible for study since the OAE radically reduced the

benthonic diversity (foraminifera, ostracods, macro-organisms) found in most of the Turonian strata.

9.5. The pattern of onshore to offshore in the evolution of shelf communities.

Community trophic analysis of late Cretaceous shelf faunas indicates that major ecological innovations appeared in nearshore environments and then expanded outward across the shelf at the expense of older community types (Jablonski et al., 1983), due to the differential extinction rates of onshore as opposed to offshore clades, or from differential origination rates of new ecological associations or evolutionary novelties in nearshore environments (op cit.). The rising oxygen minimum zone would account for the extinctions of the specialist offshore species with the surviving nearshore forms evolving into the vacated niches on the waning of the oxygen minimum zone.

References:

Alvarez, L.W., Alvarez, W., Asaro, F. and Michel, H.V. (1980). Extraterrestrial cause for the Cretaceous - Tertiary extinction. Science (Wash.), 208, 1095-1108.

Arnold, A.J. (1982). Techniques for biometric analysis of foraminifera. Third North American Palaeontological Convention Procs., 1 , 13-15

Arthur, M.A., Bottjer, D.J., Fischer, A.G., Hattin, D.E., Kauffmann, E.G., Scholle, P.A. (1986). Rhythmic bedding in Upper Cretaceous pelagic carbonate sequences: varying sedimentary response to climatic forcing. Geology, 14 , 153-156.

Arthur, M.A., Schlanger, S.O. and Jenkyns, H.C. (1987) The Cenomanian - Turonian Oceanic Anoxic Event, II: Palaeoceanographic controls on organic matter production and preservation. In: Brooks, J. and Fleet, A. (Eds.) (1987) . Spec. Pub. Geol. Soc. Lond., Marine Petroleum Source Rocks.

Bailey, H.W. (1978). A foraminiferal biostratigraphy of the lower Senonian of southern England. Unpubl. Ph.D thesis CNAA Plymouth Polytechnic.

Ball, K.C. (1985) A foraminiferal biostratigraphy of the Upper Cretaceous of the southern North Sea Basin (U.K Sector). Unpubl. Ph.D thesis CNAA Plymouth Polytechnic.

Bandy, O.L. (1967). Cretaceous planktonic foraminiferal zonation. Micropaleontology, 13 , (1) , 1-31.

Bandy, O.L. and Annal, R.E. (1957). Distribution of Recent foraminifera off the west coast of Central America. Am. Assoc. Pet. Geol. Bull., 41 , 2037-2053 figs.1-3.

Bandy, O.L. and Chierici, M.A. (1966). Depth temperature evaluation of selected California and Mediterranean bathyal foraminifera. Marine Geology, 4 , 259-271 figs. 1-10.

Banner, F.T (1982). A classification and introduction to the Globerinacea. In: Banner, F.T. and Lord, A.R. (Eds.) (1982). Aspects of Micropalaeontology, George Allen and Unwin, London.

Barnard, T. and Banner, F.T. (1953). Arenaceous foraminifera from the Upper Cretaceous of England. Quart. Jour. Geol. Soc. Lond., 109 , 173-216.

Barnard, T. and Banner, F.T. (1980). The Ataxophragmiidae of England: Part 1, Albian - Cenomanian Arenobulimina and Crenaveneuilina. Revista Espanola de Micropaleontoligia, 7 , 383-430.

Barr, F.T. (1961) Upper Cretaceous planktonic foraminifera from the Isle of Wight, England. Palaeontology, 4 , (4) , 522-580.

Barron, E.J., Arthur, M.A. and Kauffmann, E.G. (1985). Cretaceous rhythmic bedding sequences: a plausible link between orbital variations and climate. E.P.S.L.

Bé, A.W.H. (1980). Gametogenic calcification in a spinose planktonic foraminifer, Globigerinoides sacculifer, (Brady). Marine Micropalaeontology, 5 , 283-310.

Bé, A.W.H. and Anderson, O.R. (1976) Gametogenesis in planktonic foraminifera. Science, 192 , 890-892.

Bé, A.W.H., Anderson, O.R., Faber, W.W. and Caron, D.A. (1983). Sequence of morphological and cytoplasmic changes during gametogenesis in the planktonic foraminifer Globigerinoides sacculifer (Brady). Micropaleontology, 29 , (3) , 310-325.

Bé, A.W.H., Jongebloed, W.L. and McIntyre, A. (1969). X-ray microscopy of Recent planktonic foraminifera. Jour. Paleont., 43 , (6) , 1384-1397.

Bé, A.W.H., McIntyre, A. and Breger, D.L. (1966) The shell structure of a planktonic foraminifera Globorotalia menardii. Ecologae Geol. Helv., 59 , (2) , 885-927.

Bein, A. and Reiss, Z. (1976). Cretaceous Pithonella from Israel. Micropaleontology, 22 , (1) , 83-91.

Berger, A.L., Imbrie, J., Hays, G., Kukla,G. and Saltzman, B. (Eds.) (1984). Milankovitch and climate: understanding the response to orbital forcing. Reidel Publ. Co., 532 + 434 pp.

Bernhard, J.M. (1986) Characteristic assemblages and morphologies of benthic foraminifera from anoxic organic-rich deposits: Jurassic through Holocene. Jour. Foram. Research, 16 , (3) , 207-215.

Berthelin, M. (1880). Memoire sur les foraminifères fossiles de l'étage Albien de Montcley (Doubs.). Mém. Soc. Geol. France, (3) , 1 (5), 1-84.

Birkelund, T., Hancock, J.M., Hart, M.B., Rawson, P.F., Remane, J., Robaszynski, F., Schmidt,F., Surlyk,F. (1984). Cretaceous stage boundaries - Proposals. Bull. Geol. Soc. Denmark, 33 , 3-20.

Bolli, H.M. (1945). Zur stratigraphie der Oberenkriede in der höheren helverischen Decken. Ecologae Geol. Helv., 37 , (2) , 217-328.

Brasier, M.D. (1982). Architecture and evolution of the foraminiferid test - a theoretical approach. In: Banner, F.T. and Lord, A.R. (Eds) Aspects of Micropalaeontology, 1-39 , George Allen and Unwin, London.

Brasier, M.D. (1986). Form, function and evolution in benthic and planktonic foraminiferid test architecture. In: Leadbeater, B.S.C. and Riding, R. (Eds) Biomineralization in Lower Plants and Animals. 251-268 . The Systematics Association Spec. Vol., 30

Brotzen, F. (1942). Die foraminiferengatung Gavellinella nov. gen. und die systematik der Rotaliformes. Sveriges Geologiska Undersokning Arsbok, 36 , (8) , 1-60.

Butt, A.A. (1966). Foraminifera of the type Turonian. Micropaleontology, 12 , (2) , 168-182.

Caron, M. (1966). Globotruncanidae du Cretace superieur du syndual de la Gruyere (Préalpes Medranes, Suisse). Revue de Micropaleonologie, 9 , (2) , 68-93.

Caron, M. (1983a). La spéciation chez les Foraminiferes planctiques: une réponse adaptée aux constraintes de l'environment. Zitteliana, 10 , 671-676.

Caron, M. (1983b). Taxonomie et phylogenie de la famille des Globotruncanidae. Zitteliana, 10 , 677-681.

Caron, M. (1985). Cretaceous planktic foraminifera. In: Bolli, H.M., Saunders, J.B., Perch-Nielsen, K. (Eds.). Plankton Stratigraphy. 17-86. Cambridge Univ. Press.

Caron, M. and Homewood, P. (1983). Evolution of early planktic foraminifers. Marine Micropalaeontology, 7 , 453-462.

Carsey, D.O. (1926). Foraminifers of the Cretaceous of Central Texas. Texas University Bulletin, 2612 , 1-56.

Carter, D.J. and Hart, M.B. (1977). Aspects of mid-Cretaceous stratigraphical micropalaeontology. Bull. Br. Mus. Nat. Hist. (Geol.), 29 , 1-135.

Chapman, F. (1891-8). The Foraminifera of the Gault of Folkestone. Jl. R. Microsc. Soc., parts i-x.

Cifelli, R. (1969). Radiation of Cenozoic planktonic foraminifera. Systematic Zoology, 18 , 154-168.

Clarke, R.E.A. and Verdier, J.P. (1967). An investigation of the microplankton assemblages from the Chalk of the Isle of Wight, England. Verhandelingen der koninkluke nederlandse akademie van wetenschappen, Afd. Natuurkunde. (E erste reeks, Deel), 14 , (3) , 1-96.

Cooper, M.R., (1977). Eustacy during the Cretaceous: its implications and importance. Palaeoclim., Palaeogeog. and Palaeoecol., 22 , 1-60.

Corliss, B.H. (1985). Micro-habitats of benthic foraminifera within deep sea sediments. Nature, 314 , 435-438.

Croll, J. (1875). Climate and time in their geological relations, a theory of secular change of the Earths climate. Daldy, Ibister Co. London, xvi , 517pp.

Crux, J.A. (1980). A biostratigraphical study of Upper Cretaceous calcareous nannofossils from south-east England and north France. Unpubl. Ph.D thesis, Univ. of Lond., 1-299.

Crux, J.A. (1982). Upper Cretaceous (Cenomanian to Campanian) calcareous nannofossils. In: Lord, A.K. (Ed.). A stratigraphical index of calcareous nannofossils. 81-13. Publ. Ellis Horwood.

Cushman, J.A. (1926). Eouvigerina, a new genus from the Cretaceous. Contr. Cushman Lab. Foram. Res., 2 , (1) , 3-6.

Cushman, J.A. (1936). New genera and species of the Families Verneuilinidae and Valvulinidae and of the subfamily Virgulininae. Spec. Publ. Cushman Lab. Foram. Res., 6 , 1-71.

Cushman, J.A. (1937). A monograph of the Family Verneuilinidae. Spec. Publ. Cushman Lab. Foram, Res., 7 1-157.

Cushman, J.A. (1938). Cretaceous species of Gumbelina and related genera. Contr. Cushman Lab. Foram. Res., 14 2-28.

Cushman, J.A. (1946). Upper Cretaceous foraminifera of the Gulf Coastal region of the United States and adjacent areas. Prof. Pap. U.S. Geol. Surv., 206 , 1-241.

Cushman, J.A. and Parker, L.F. (1934). Notes on some of the earlier species originally described as Bulimina. Contr. Cushman Lab. Foram. Res., 10.

Dam, A. ten (1946). Arenaceous foraminifera and Lagenidae from the Neocomian (Lower Cretaceous) of the Netherlands. Jour. Paleont., 20 , (6) , 570-577.

Dam, A. ten (1950). Les foraminifères de l'Albien des Pays-Bas. Soc. Geol. France Mem., 29 , 1-66.

Deegan, C.E. and Scull, B.J. (1977). A standard lithostratigraphic nomenclature for the Central and Northern North Sea. Rep. Inst. Geol. Sci. London, 77\25 36pp.

Diver, W.D. (1968). The foraminiferal Planktonic\Benthonic ratios across the Lower\Middle Chalk boundary in the Redhill area, Surrey. Unpubl. M.Sc. thesis, Univ. of London.

Ehrenberg, C.G. (1840). Die Bildung der europaischen, libyschen und arabischen Kreidefelsen und des Kreidemergels aus Mikroskopischen organismen. K. Preuss. Akad. Wiss. Berlin, Abh., 91pp.

Fischer, A.G. and Arthur, M.A. (1977). Secular variations in the Pelagic Realm. S.E.P.M. Spec. Publ. No. 25, 19-50.

Fleury, J.J. (1980). Les zones de Gavrovo-Tripolitza et du Pinde-Olonos (Grece Continentale et Péloponnese du Nord). Evolution d'une plate-forme et d'un bassin dans leur cadre alpin. Societe Geologique du Nord, 4 , 1-648.

Flexer, A. and Starinsky,A. (1970). Correlation between phosphate content and the foraminiferal plankton\benthos ratios in Chalks (late Cretaceous, Northern Israel), Palaeoenvironmental significance. Sedimentology, 14 , 245-258.

Franke, A. (1925). Die foraminiferen der pommerschen Kreide. Abh. aus dem geol.-pal. Inst. der Univ. Griefswald, 1-96.

Franke, A. (1928). Die Foraminiferen der Oberen Kreide Nord - und Mitteldeutschlands. Abh. preuss geol. Landesanst, 111 , 1-207.

Frankel, L. (1970). A technique for investigating micro-organism associations. Jour. Paleont., 44 ,(3), 375-577.

Frerichs, W.E. (1970). Distribution and ecology of benthonic foraminifera in the sediments of the Andaman Sea. Cushman Found. Foram. Res. Contr., 21 , 123-147.

Frerichs, W.E. (1971). Evolution of planktonic foraminifera and palaeotemperatures. Jour. Paleont., 45 , (6) , 963-968.

Fuchs, W. (1967). Die Foraminiferenfauna und Nannoflora eines Bohrkernes aus dem hoheren Mittel-Alb. der Teitbohrung DELFT 2, (NAM), Neiderlande. Jb. Geol. Bundesanst., 110 , (2) , 245-341.

Gandolfi, R. (1942). (Canton Ticino) Riv. Ital. Palaeo. Stratigr., 48 , (4) , 1-160.

Gawar-Biedowa, E. (1969). The Genus Arenobulimina Cushman from the Upper Albian and Cenomanian of the Polish lowlands. Roc. Pol. Tow. Geol., 34 , 1-3.

Glaessner, M.F. (1937). Planktonforaminifera aus der Kreide und dem Eozan und Ihre Stratigraphische Bedeutung. Etyudy Micropalaeo. Moscow, 1 , (1) , 27-52.

Gorbenko, V.F. (1957). Pseudospiroplectinata, Novyy rod Foraminifer iz Verkhnemelovykh otlozhenly severo-zapadnogo Donbassa. Akad. Nauk SSSR, Doklady, 117 (5) , 879-880.

Graciansky, P.C. de, Poag, C.W. et al., (1985). Init. Repts. DSDP, 80 : Washington (U.S. Govt. Printing Office).

Grimsdale, T.F. and Morkhoven, F.P.C. von, (1955). The ratio between pelagic and benthonic foraminifera as a means of estimating depths of deposition of sedimentary rocks. World Petroleum Cong., 4th Proc., Sect. 1\D, 473-491.

Gutschick, R.C. and Wuellner, D. (1983). An unusual benthic agglutinated foraminifer from late Devonian Anoxic Basinal Black Shales of Ohio. Jour. Paleont., 57 , (2) , 308-320.

Hamblin, R.J.O. and Wood, C.J. (1976). The Cretaceous (Albian - Cenomanian) stratigraphy of the Haldon Hills, South Devon, England. Newsletters in Stratigraphy, 4 , 135-149.

Hancock, J.M. (1976). The petrology of the Chalk. Proc. Geol. Ass., 86 , 499-535.

Hancock, J.M. (1983). Cretaceous. In: Petroleum Geology of the North Sea. JAPEC

Hancock, J.M. (1984). Cretaceous. In: Glennie, K.W. (Ed.) Introduction to the Petroleum Geology of the North Sea. 133-150 , Blackwell, London.

Hancock, J.M. and Kauffmann, E.G. (1979). The great transgressions of the Late Cretaceous. Jour. Geol. Soc. Lond., 136 , 175-186.

Hansen, J.M. (1977). Dinoflagellate stratigraphy and echinoid distribution in Upper Maastrichtian and Danian deposits from Denmark. Bull. Geol. Soc. Denmark., 26 , 1-26.

Haq, B.U., Hardenbol, J. and Vail, P.R. (1987). Chronology of fluctuating sea levels since the Triassic. Science, 235 , 1156-1167.

Hart, M.B. (1970). The distribution of the Foraminiferida in the Albian and Cenomanian of S.W. England. Unpubl. Ph.D. thesis, Imperial College, London.

Hart, M.B. (1980a). A water depth model for the evolution of the planktonic Foraminiferida. Nature, 286 (5770), 252-254.

Hart, M.B. (1980b). The recognition of Mid Cretaceous sea level changes by means of foraminifera. Cret. Res., 1 , 000-000.

Hart, M.B. (1981). Cretaceous. In: Jenkins, D.G. and Murray, J.W. (Eds.) Stratigraphical Atlas of Fossil Foraminifera., 149-227. Ellis Horwood.

Hart, M.B. (1982a). The marine rocks of the Mesozoic. In: Durrance, E.M. and Laming, D.J.C. (Eds.). The Geology of Devon, Univ. of Exeter, Exeter, 179-203.

Hart, M.B. (1982b). Turonian foraminiferal biostratigraphy of southern England. Mémoires du Muséum Nationale D'Histoire Naturelle, 46 , 203-207.

Hart, M.B. (1983) Planktonic foraminifera from the Cenomanian of the Wilmington Quarries, (S.E Devon). Proc. Ussher Soc., 5 , 406-410.

Hart, M.B. (1985). Oceanic Anoxic Event 2 on-shore and off-shore S.W. England. Proc. Ussher Soc., 6 , 183-190.

Hart, M.B. (1987a). Foraminifera of carbonate environments. In: Hart, M.B. (Ed.). Micropalaeontology of carbonate environments., British Micropalaeontological Soc. Series, Ellis Horwood. Chichester.

Hart, M.B. (1987b). Cretaceous foraminifers from Deep Sea Drilling Project site 612, North-West Atlantic Ocean. In: Poag, C.W. and Watts, A.B. et al. Init. Repts. DSDP, 95 , Washington (U.S. Govt. Printing Office).

Hart, M.B. and Bailey, H.W. (1979). The distribution of planktonic foraminiferida in the Mid-Cretaceous of N.W. Europe. Aspekte der Kreide Europas., IUGS Series A, 6 , 527-542.

Hart, M.B. and Ball, K.C. (1986). Late Cretaceous Anoxic Events, sea level changes and the evolution of the planktonic foraminifera. In: Summerhayes, C.P. and Shackleton, N.J. (Eds.). North Atlantic Palaeoceanography., Geol. Soc. Spec. Publ., 21 , 67-78.

Hart, M.B. and Bigg, P.J. (1981). Anoxic events in the late Cretaceous chalk seas of N.W. Europe. In: Neale, J.W. and Brasier, M.D. (Eds). Microfossils from Recent and Fossil Shelf Seas. British Micropalaeontological Soc. Series, 177-186.

Hart, M.B. and Carter, D.J. (1975). Some observations on the Cretaceous foraminiferida of south-east England. Jour. Foram. Res., 5 , (2) , 114-126.

Hart, M.B. and Weaver, P.P.E. (1977). Turonian microbiostratigraphy of Beer, S.E. Devon. Proc. Ussher Soc., 4 , 86-93.

Hart, M.B., Weaver, P.P.E. and Harris, C.S. (1979). Microfaunal investigation of Shapwick Grange Quarry, East Devon. Proc. Ussher Soc., 4 , 312-316.

Hedley, R.H. (1957). Microradiography applied to the study of foraminifera. Micropaleontology, 3 , (1) , 19-28.

Herbert, T.D. and Fischer, A.G. (1986). Milankovitch climatic origin of mid-Cretaceous black shale rhythms in central Italy. Nature, 321 , 739-743.

Hilbrecht, H. and Hoefs, J. (1986). Geochemical and Palaeontological studies on the δ13 C anomaly in Boreal and North Tethyan Cenomanian - Turonian sediments in Germany and adjacent areas. Palaeogeog., Palaeoclim., Palaeoecol., 53 , 169-189.

Ingle, J.C., Keller, G. and Kolpack, R.L. (1980). Benthic foraminiferal biofacies, sediment and water masses of the southern Peru - Chile Trench area, south-eastern Pacific Ocean. Micropaleontology, 26 , (2) , 113-150.

Jablonski, D., Sepkoski, J.J., Bottjer, D.J. and Sheehan, P.M. (1983). Onshore and offshore patterns in the evolution of Phanerozoic Shelf communities. Science, 222 , 1123-1125.

Jarvis, I., Carson, G.A., Cooper, K., Hart, M.B., Leary, P.N., Tocher, B.A., Horne, D. and Rosenfeld, A. (1988) Chalk microfossil assemblages and the Cenomanian - Turonian (late Cretaceous) Oceanic Anoxic Event: new data from Dover, England. Cret. Res. in press.

Jarvis, I., Carson, G., Hart, M.B., Leary, P.N. and Tocher, B.A. (198). The Cenomanian - Turonian (Late Cretaceous) anoxic event in S.W. England: evidence from Hooken Cliffs near Beer, S.E. Devon. Newsletters in Stratigraphy, in press.

Jarvis, I., Leary, P.N. and Tocher, B.A. Mid Cretaceous (Albian - Turonian) stratigraphy of Shapwick Grange Quarry, S.E. Devon, England. Mesozoic Research, (in press).

Jarvis, I. and Tocher, B.A. (1983). The Cenomanian - Turonian boundary in S.E. Devon, England. In: Birkelund, T., Bromley, R.G. et al (Eds). Cretaceous Stage Boundaries Symposium, Copenhagen, Abstr., 94-97.

Jarvis, I. and Tocher, B.A. (1987). Field meeting: The Cretaceous of S.E. Devon. 14th-16th March, 1986. Proc. Geol. Ass., 98 , (1) , 51-66.

Jarvis, I. and Woodroof, P.B. (1984). Stratigraphy of the Cenomanian and basal Turonian (Upper Cretaceous) between Branscombe and Seaton, S.E. Devon, England. Proc. Geol. Ass., 95 , (3) , 193-215.

Jeffries, R.P.S. (1962). The palaeoecology of the Actinocamax plenus subzone (Lowest Turonian) in the Anglo-Paris Basin. Palaeontology, 4 , 609-647.

Jeffries, R.P.S. (1963) The stratigraphy of the Actinicamax plenus Subzone (Turonian) in the Anglo-Paris Basin. Proc. Geol. Ass., 74 , (1) , 1-43.

Jenkyns, H.C. (1980). Cretaceous anoxic events: from continents to oceans. Jour. Geol. Soc. Lond., 137 , 171-188.

Jenkyns, H.C. (1985). The early Toarcian and Cenomanian - Turonian anoxic events in Europe: comparisons and contrasts. Geol. Rdsch., 74 , 505-518.

Jones, R.W. (1986). Distribution of morphogroups of Recent agglutinated foraminifera in the Rockall Trough - a synopsis. Proc. R. Soc. Edinburgh, 88B , 55-58.

Jones, R.W. and Charnock, M.A. (1985). Morphogroups of agglutinating foraminifera: their life positions and feeding habits and potential applicability in (Palaeo)ecological studies. Revue de Palaeobiologie, 4 , (2) , 311-320.

Jukes-Browne, A.J. and Hill, W. (1903). The Cretaceous rocks of Britain. II. The Lower and Middle Chalk of England. Mem. Geol. Survey , U.K.

Jukes-Browne, A.J. and Hill, W. (1904). The Cretaceous Rocks of Britain. III. The Upper Chalk of England. Mem. Geol. Survey, U.K..

Katz, M.E. and Thunell, R.C. (1984). Benthic foraminiferal biofacies associated with middle Miocene to early Pliocene oxygen deficient conditions in the eastern Mediterranean. Jour. Foram. Res., 14 , (3) , 187-202.

Kauffman, E.G., Hattin, D.E. and Powell, J.D. (1977). Stratigraphic, palaeontologic and palaeoenvironmental analysis of the Upper Cretaceous rocks of Cimmaron County, northwestern Oklahoma. Geol. Soc. Amer. Mem., 149 , 1-150.

Kaufmann, (1865). In: Heer, O. Die Urwelt der Schweiz: F. Schulthess, 1-622.

Kaye, P. (1964). Revision of British marine Cretaceous Ostracoda with notes on additional forms. Bull. Brit. Mus. (Nat. Hist.) Geol., 10 , (2) , 35-79.

Keller, B.M. (1935). Microfauna from the Dneiper - Donetz basin (Chalk). Byull Moskov Obshch Ispyaley Prirody Otdel Geol., 13 , 522-558.

Kennedy, W.J. (1969). The correlation of the Lower Chalk of south-east England. Proc. Geol. Ass., 81 , 613-677.

Kennedy, W.J., Wright, C.W. and Hancock,J.M. (1982). Ammonite zonation and correlation of the uppermost Cenomanian and Turonian of southern England and the type areas of Sarthe and Touraine in France. In: Colloque sur le Turonien, Mémoires du Museum National d'Histoire Naturelle de Paris, Serie C, 49 , 175-181.

Khan, M.H. (1950). On some new foraminifera from the Lower Gault of Southern England. Jour. R. Micr. Soc., Ser. 3 , 70 , (3) , 268-279.

Kitazato, H. (1984). Microhabitats of benthic Foraminifera and their application to fossil assemblages. Benthos '83: Second International Syposium on Benthic Foraminifera, Pau, April 1983. 339-344.

Klaus, J. (1960). Etude biométrique et statistique de qeulques espèces de Globotrunceanidés. Ecol. Geol. Helv., 53 , 285-308.

Lalicker, C.G. (1935). New Cretaceous Textularidae. Contr. Cushman Lab. Foram. Res., 11 , (1) , No. 152, 1-13.

Lipps, J.E. (1979). Ecology and palaeoecology of planktic foraminifera. In: Lipps, J.E., Berger, W.H., Buzas, M.A., Douglas, R.G., Ross, C.A.. (Eds). SEPM Short Course No. 6, Houston, Texas.

Loeblich, A.R. JR. and Tappan, H. (1961). Cretaceous planktonic foraminifera: part 1 -Cenomanian. Micropaleontology, 7 , (3) , 257-304.

Loeblich, A.R. and Tappan, H. (1964). Treatise on invertebrate palaeontology. Part C, Protista 2, (Parts 1 and 2).

Lorenz, T. (1902). Geologische studien im Grenzgebiete zwischen helvenischer und ostalpiner facies 11.Der sudliche Rhaetikon. Naturt. Oes. Freiburg, Ber., 12 , 34-95.

Lozo, F.E. (1944). Biostratigraphic relations of some North Texas Trinity and Fredericksburg (Comanchean) foraminifera. Amer. Midland Naturalist, 31 , 513-584.

Marcinowski, R. (1974). The transgressive Cretaceous (Upper Albian through Turonian) deposits of the Polish Jura chain. Acta Geologica Polonica, 24 , (1) , 1-217.

Marie, P. (1941). Foraminifères de la Craie: les foraminiferes de la craie à Belemnitella mucronata du Bassin de Paris. Mus. National Hist. Nat. Mém. Paris, 12, 1-296.

Martinez - Rodriguez J.I. and Crump, M.G. (1987). Foraminifera of the Black Band, South Ferriby Quarry, South Humberside. Internal Rep. Univ. of Hull.

Matsumato, T. (1980). Inter-regional correlation of transgressions and regressions in the Cretaceous Period. Cret. Res., 1 , 359-373.

McNown, J.S. and Malaika, J. (1950). Effects of particle shape on settling velocity at low Reynolds numbers. Trans. Amer. Geophys. Union, 31 , 74-82.

Mello, M.R., Koutsoukos, E.A.M., Hart, M.B., Brassel,S.C. and Maxwell, J.R. Late Cretaceous Anoxic Events in the Brazilian continental margin. AAPG Symposium: Geochemistry in Exploration, Denver, Colorado, in press.

Mornod, L. (1950). Les Globorotalides du Crétacé superieur du Montsalvens (Prealpes friborgeoizes). Ecologae Geol. Helv., 42 , (2) , 573-596.

Mörner, N.A. (1981). Revolution in Cretaceous sea level analysis. Geology, 9 , 344-346.

Morrow, A.L. (1934). Foraminifera and ostracoda from the Upper Cretaceous of Kansas. Jour. Paleont., 8 , (2) , 186-205.

Mortimore, R.N. (1986). Stratigraphy of the Upper Cretaceous White Chalk of Sussex. Proc. Geol. Ass., 91 , (2) , 97-139.

Naidin, D.P. (1983). Late Cretaceous transgressions and regressions on the Russian Platform. Zitteliana, 10 , 107-114.

Neagu, T. (1969). Cenomanian planktonic foraminifera in the southern part of the Eastern Carpathians. Rocznik Polskiego Towarzystwa Geologicznego Annales de la société Géologique de Pologne, XXXIX.

Nyong, E.E. and Ramanathan, R.M. (1985). A record of oxygen-deficient palaeoenvironments in the Cretaceous of the Calabar Flank, S.E. Nigeria. Jour. African Earth Sci., 3 , (4) , 455-460.

d'Orbigny, A. (1840). Mémoire sur les foraminiferes de la craie blanche du bassin de Paris. Soc. Géol. France, Mem., 4 , (1).

Owen, M. (1970). Turonian foraminifera of Southern England. Unpubl. Ph.D. thesis, Univ. of London.

Penrose, N.L. and Kennet, J.P.(1979). Anoxic and aerobic basins in the Northern Gulf of Mexico: comparison of microfossil preservation. Abstr. Confr. Publ. Geol. Soc. Amer. 92nd Annual Meeting, 493pp.

Perner, J. (1892). Foraminifery ce skeho Cenomanu. Ceska Akad. Cisare Frantiska Josefa, Pal. Bohemiae, Praha, 2 , (1) , 1-48.

Pessagno, E.A. Jr. (1967). Upper Cretaceous planktonic foraminifera from the Western Gulf coastal plain. Palaeontographica Americana, 37 , parts 1 and 2.

Phillips, W. (1818). A selection of facts from the best authorities arranged so as to form an outline of the geology of England and Wales. London.

Phillips, W. (1821). Remarks on the Chalk cliffs in the neighbourhood of Dover, and on the Blue Marls covering the Green Sand, near Folkestone. Appendix: Containing some account of the Chalk Cliffs etc. on the coast of France opposite to Dover. Trans. Geol. Soc. Lond., 5 , 16-51.

Plummer, H.J. (1931). Some Cretaceous foraminifera in Texas. The Univ. of Texas Bull. Contributions to Geology, 3101 , 109-238.

Postuma, J.A. (1971). Manual of Planktonic Foraminifera. Elsevier Publ. Co., Amsterdam, London, 1-420.

Price, R.J. (1977). The evolutionary interpretation of the Foraminiferida Arenobulimina, Gavellinella and Hedbergella in the Albian of North West Europe. Palaeontology, 20 , (3) , 503-527.

Raup, D.M. (1985). Rise and fall of periodicity. Nature, 317 , 304-305.

Raup, D.M. (1986). The Nemesis affair - A story of the death of dinosaurs and the ways of science. Norton W.W., 220pp.

Raup, D.M. (1981). Mass extinction: A commentary. Palaeontology, 30 , (1) , 1-13.

Raup, D.M. and Sepkoski, J.J. Jr. (1984). Periodicity of extinctions in the geologic record. Proc. Nat. Acad. Sci. (U.S.A.), 81 ,801-805.

Reichel, M. (1950). Observations sur les Globotruncana du gisement de la Breggia (Tessin). Eclog. Geol. Helv., 42 , (2) , 596-617.

Renz, O. (1936). Stratigraphische und mikropaleontologische Unetrsuchungen. Ecol. Geol. Helv., 29 , (1) , 1-149.

Reuss, A.E. (1844). Geognostische Skizzen aus Bohmen. C.W. Medau (Prag.), 2 , 304pp.

Reuss, A.E. (1845). Die Versteinerungen der bohmischen Kreideformation. Part 1, 1-58.

Reuss, A.E. (1851). Die foraminiferen und Entomostraceen des Kreidemergels von Lemberg. Abh. Haidinger's Naturwissenschaftlich, Part 2 , 1-148.

Reuss, A.E. (1860). Die foraminiferen der Westphalischen Kreideformation. Sber. Akad. Wiss., Math.- nat. Kl., 40 141-238.

Reuss, A.E. (1862). Entwurf eniner systematischen zusammenstellung der foraminiferen. Sber. Akad. Wiss., Wien, Math.- nat. Kl., 44 , 355-396.

Reuss, A.E. (1863). Die foraminiferen des norddeutschen Hils und Gault. Sber. Akad. Wiss., Wien, Math.- nat. Kl., 44 , 5-100.

Robaszynski, F. and Caron, M. (1979). Atlas de foraminifères planctoniques du Crétacé moyen (Mer Boréale et Tethys). Cahiers de Micropaléontologie, Editions du centre national de la recherche scientifique, Parts 1 and 2.

Robinson, N.D. (1986). Lithostratigraphy of the Chalk Group of the North Downs, southeast England. Proc. Geol. Ass., 97 , (2) , 141-170.

Roemer, F.A. (1842). Neue Kreideforaminiferen. Neues Jb. Min. geogn. Geol. Petref.-Kunde, Stuttgart, 273-373.

Scheibnerova, V. (1962). Stratigrafia strednej a vrchnej kreidy tetydnej oblast na zaklade Globotrunknid. Geologicky Sbornik, Bretislava, 13, (2) 197-226.

Schijfsma, E. (1946). The foraminifera from the Hervien (Campanian) of the Southern Limburg. Med. Geol. Stiching, ser. C., (7), Maarlem.

Schijfsma, E. (1950). La position stratigraphique de Globotruncana helvetica Bolli en Tunisie. Micropaleontology, 1 , (4) , 321-334.

Schlanger, S.O., Arthur, M.A., Jenkyns, H.C. and Scholle, P.A. (1987). The Cenomanian - Turonian Oceanic Event, 1. Stratigraphy and distribution of organic-rich beds and the marine 13 C excursion. In: Brooks, J. and Fleet, A. (Eds). Marine Petroleum Source Rocks. Spec. Publ. Geol. Soc. Lond.

Scholle, P.A. and Arthur, M.A. (1980). Carbon Isotope fluctuations in Cretaceous pelagic limestones: potential stratigraphic and exploration tool. A.A.P.G. Bull., 64 , (1) , 67-87.

Sepkoski, J.J. and Raup, D.M. (1986). Periodicity in marine extinction events. In: Elliot, D. (Ed.). Dynamics of extinction, 3-36 , John Wiley and Sons, N.Y..

Severin, K.P. (1983). Test morphology in benthic foraminifera as a discriminator of biofacies. Marine Micropaleontology, 8 , (1) , 65-76.

Sigal, J. (1952). Apercu stratigraphique sur la Micropaleontologie du Crétacé. 19th Congr. Internat., Monogr. Reg., Alger., ser.1 , (26), 1-47.

Sliter, W.V. (1976). Cretaceous foraminifers from the southwestern Atlantic Ocean, Leg 36, Deep Sea Drilling Project. In: Barker, P.F., Dalziels, I.W.D. et al. Init. Rep. DSDP, 36 , Washington (U.S. Govt. Printing Office).

Sliter, W.V. and Baker, R.A. (1972). Cretaceous bathymetric distribution of benthic foraminifers. Jour. Foram. Res., 2 , (4) , 167-183.

Smit, J. (1982). Extinction and evolution of planktonic foraminifera after a major impact. Geol. Soc. Amer. Spec. Paper 190.

Spindler, M., Hemleben, C., Bayer, U., Bé, A.W.H. and Anderson, O.R. (1979). Lunar periodicity of reproduction in the planktonic foraminifer Hastigerina pelagica. Mar. Ecol. Prog. Ser., 61-64.

Tappan, H. (1940). Foraminifera from the Grayson Formation of Northern Texas. Jour. Palaeont., 14 , (2) , 93-126.

Todd, R., Low, D. and Mello, J.F. (1965). Smaller foraminifers. In: Kummel, B. and Raup, O. Handbook of Palaeontological Techniques, W.H. Freeman and Co., San Francisco.

Trujillo, E.F. (1960). Upper Cretaceous foraminifera from Near Redding, Shasta County, California. Jour. Palaeo., 34 , (2) , 290-346.

Vail, P.R., Mitchum, R.M. and Thompson III, S. (1977). Seismic stratigraphy and global changes of sea level, Part 3: relative changes of sea level from coastal onlap. In: Payton, C.E. (Ed). Seismic stratigraphy - application to hydrocarbon exploration, AAPG Mem. 26, 63-81.

Valentine, J.W. and Mallory, B. (1965). Recurrent groups of bounded species in mixed death assemblages. Jour. Geol., 73 , 683-701.

Waples, D.W. (1985). A reappraisal of anoxia and richness of organic material, with emphasis on the Cretaceous North Atlantic. In: Graciansky, P.C.,de, Poag, C.W. et al. Init. Rep. DSDP, 80 , Washington (U.S. Printing Office).

Weaver, P.P.E. (1981). Ostracoda in the British Cenomanian. In: Neale, J.W. and Brasier, M.D. (Eds). Microfossils from Recent shelf seas, 156-162, Ellis Horwood Ltd. Chichester.

Weaver, P.P.E. (1982). Ostracoda from the British Lower Chalk and Plenus Marls. Monogr. Palaeontogr. Soc. London, 135 , (562) , 127.

Williams-Mitchell E. (1948). The zonal value of foraminifera in the Chalk of England. Proc. Geol. Ass., 59 , 91-112.

Williamson, M.A. (1979). Cretaceous foraminifera from the Celtic Sea (B.P. Borehole 93\2-1). Unpubl. MSc. thesis, Univ. of Wales, Aberystwyth.

Wonders, A.A.H. (1980). Middle and late Cretaceous planktonic foraminifera of the Western Mediterranean area. Utrecht Micropalaeontological Bull., 24 , 5-156.

Woodroof, P.B. (1981). Faunal and stratigraphic studies in the Turonian of the Anglo-Paris Basin. Unpubl. Ph.D. thesis. Univ. of Oxford.

Wright, C.W. and Kennedy, W.J. (1981). The Ammonoidea of the Plenus Marls and the Middle Chalk. Palaeontogr. Soc. London, 148pp.

Wright, C.W. and Kennedy, W.J. (1984). The Ammonoidea of the Lower Chalk Part 1. Monogr. Palaeontogr. Soc. London, 137 , 1-126.

Plate 1.

1. Ammodiscus cretaceus (Reuss)
lateral view, S6Q18, x200

2. Ammodiscus cretaceus (Reuss)
lateral view, ABC5, x100

3. Ammodiscus cretaceus (Reuss)
lateral view, ABC5, x150

4. Ammodiscus cretaceus (Reuss)
lateral view, ABC14, x100

5. Ammodiscus cretaceus (Reuss)
lateral view, ABC14, x150

6. Ammodiscus cretaceus (Reuss)
lateral view, ABC19, x150

7. Ammodiscus cretaceus (Reuss)
lateral view, ABC11, x100

8. Ammobaculites sp.a
lateral view, CB1 2, x35

9. Haplophragmium aequale (Reuss)
whole specimen, lateral view, CB1 5, x35

10. Haplophragmium aequale (Reuss)
initial coil of test, lateral view, CB1 5, x100

11. Haplophragmium aequale (Reuss)
terminal chamber of test, apertural view, CB1 5, x100

12. Haplophragmium aequale (Reuss)
terminal chamber of test, apertural view, CB1 5, x100

13. Subbdelloidina sp.a
lateral view, CB1, x150

14. Textularia chapmani (Lalicker)
side view, ABC9, x75

15. Textularia chapmani (Lalicker)
apertural view, ABC9, x150

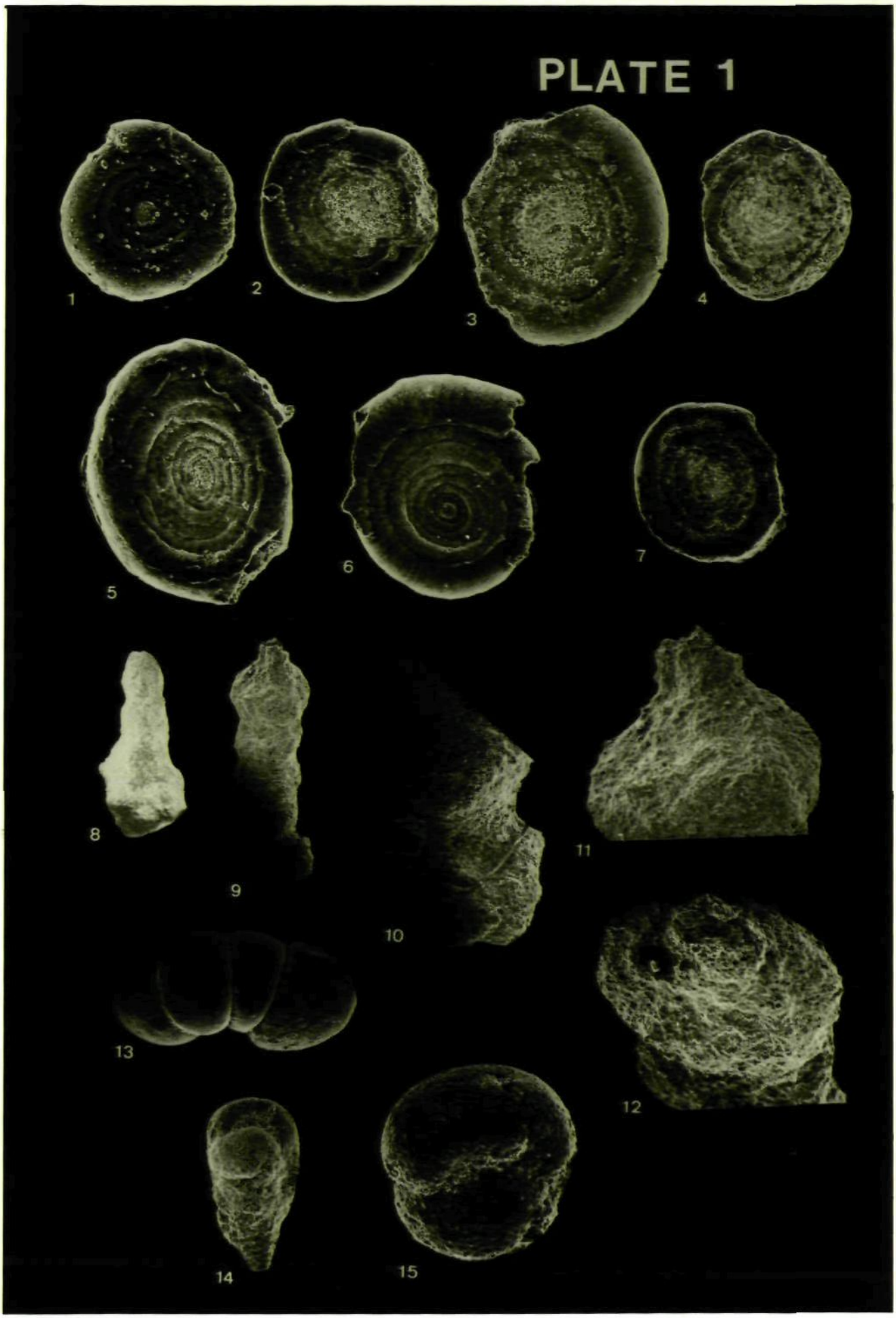
PLATE 1
1
2
3
4
5
6
7
8
9
10
11
12
13
14
15

Plate 2.

1. Textularia chapmani (Lalicker)
lateral view, ABC9, x100

2. Textularia chapmani (Lalicker)
apertural view, ABC9, x200

3. Textularia chapmani (Lalicker)
lateral view, ABC9, x150

4. Textularia chapmani (Lalicker)
lateral view, ABC9, x150

5. Textularia chapmani (Lalicker)
apertural view, ABC9, x200

6. Textularia chapmani (Lalicker)
apertural view, ABC9, x150

7. Textularia chapmani (Lalicker)
lateral view, ABC9, x100

8. Textularia chapmani (Lalicker)
close-up of aperture, ABC9, x350

9. Textularia chapmani (Lalicker)
lateral view, ABC9, x100

10. Textularia chapmani (Lalicker)
apertural view, ABC9, x200

11. Textularia chapmani (Lalicker)
apertural view, ABC10, x200

12. Textularia chapmani (Lalicker)
lateral view, ABC10, x200

13. Textularia chapmani (Lalicker)
apertural view, ABC11, x150

14. Textularia chapmani (Lalicker)
lateral view, ABC11, x100

PLATE 2

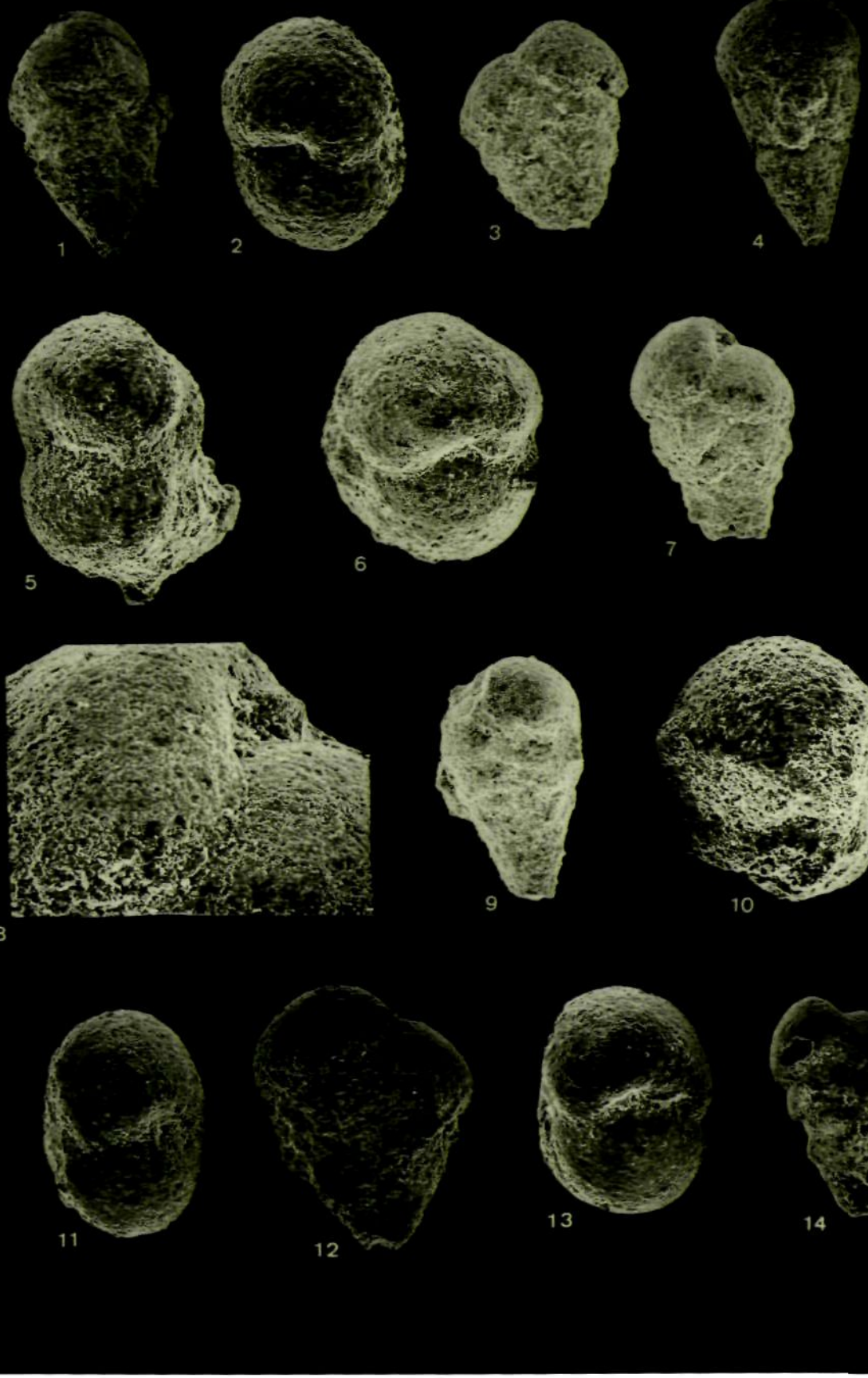

Plate 3.

1. Textularia chapmani (Lalicker)
apertural view, ABC11, x200

2. Textularia chapmani (Lalicker)
lateral view, ABC11, x200

3. Textularia chapmani (Lalicker)
apertural view, ABC11, x150

4. Textularia chapmani (Lalicker)
lateral view, ABC11, x150

5. Textularia chapmani (Lalicker)
lateral view, ABC13, x200

6. Textularia chapmani (Lalicker)
apertural view, ABC13, x200

7. Textularia chapmani (Lalicker)
lateral view, ABC14, x100

8. Textularia chapmani (Lalicker)
apertural view, ABC14, x150

9. Pseudobolivina sp.a
lateral view, Goban Spur 5\2 13-17, x100

10. Pseudobolivina sp.a
apertural view, Goban Spur 5\2 13-17, x150

11. Trochammina depressa (Lozo)
lateral view, B.P 93\2-1, 1116, x200

12. Pseudospiroplectinata plana (Gorbenko)
lateral view, ABC7, x75

13. Pseudospiroplectinata plana (Gorbenko)
lateral view, ABC7, x75

14. Pseudospiroplectinata plana (Gorbenko)
lateral view, ABC7, x75

15. Pseudospiroplectinata plana (Gorbenko)
close-up of initial coil, ABC7, x75

Plate 3 cont'd:

16. Pseudospiroplectinata plana (Gorbenko)
lateral view, incomplete specimen, ABC8, x100

17. Pseudospiroplectinata plana (Gorbenko)
close-up of aperture, ABC8, x350

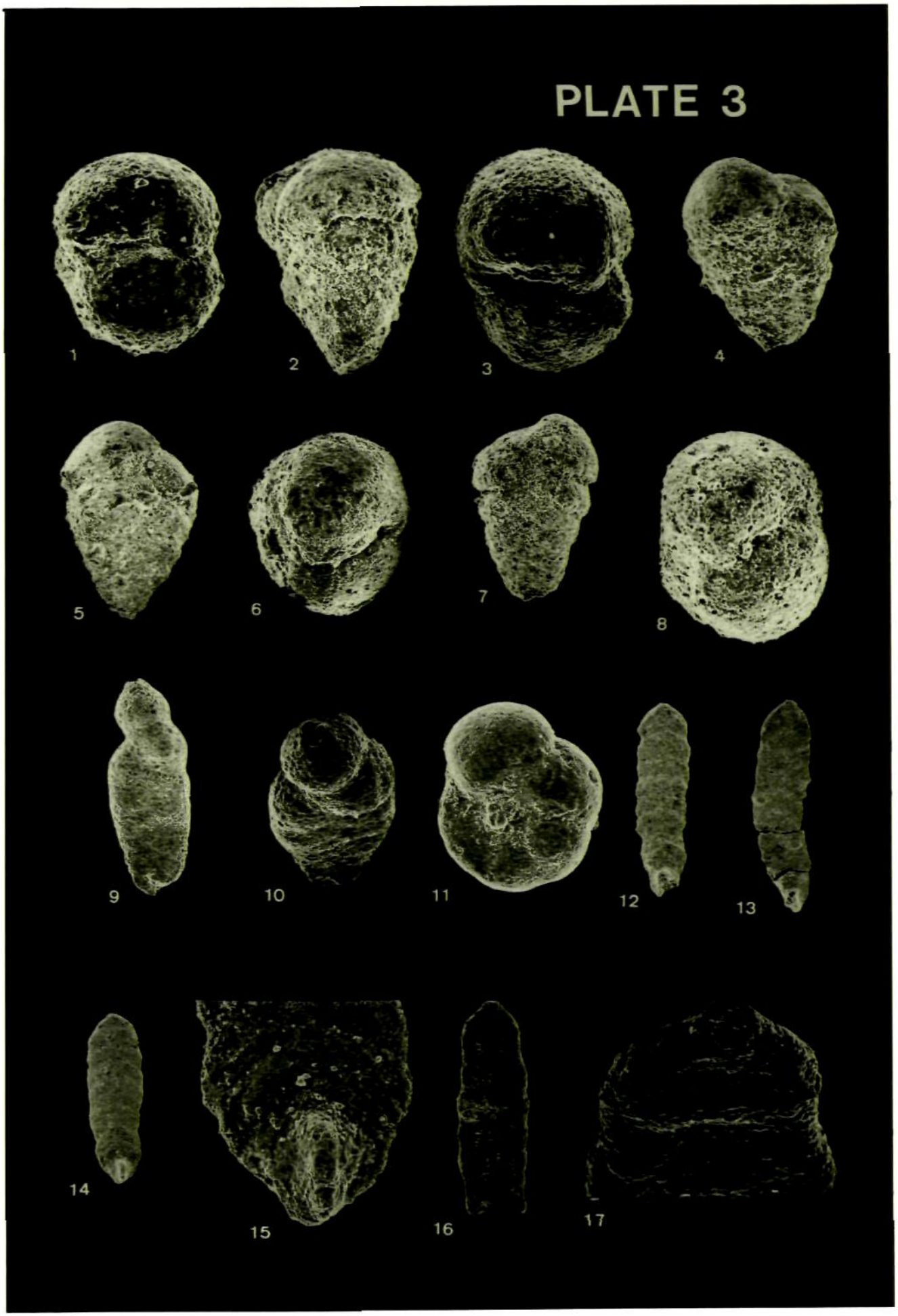
PLATE 3
1
2
3
4
5
6
7
8
9
10
11
12
13
14
15
16
17

Plate 4.

1. Tritaxia macfadyeni (Cushman)
lateral view, Goban Spur 6\1 30-33, x100

2. Tritaxia macfadyeni (Cushman)
lateral view, Goban Spur 6\1 30-33, x150

3. Tritaxia macfadyeni (Cushman)
oblique apertural view, Goban Spur 6\1 30-33, x200

4. Tritaxia macfadyeni (Cushman)
lateral view, Goban Spur 6\1 30-33, x150

5. Tritaxia macfadyeni (Cushman)
lateral view, Goban Spur 6\1 101-105, x150

6. Tritaxia macfadyeni (Cushman)
oblique apertural view, Goban Spur 6\1 101-105, x350

7. Tritaxia macfadyeni (Cushman)
lateral view, Goban Spur 6\1 101-105, x150

8. Tritaxia macfadyeni (Cushman)
close-up of test wall, Goban Spur 6\1 101-105, x500

9. Tritaxia macfadyeni (Cushman)
lateral view, Goban Spur 6\1 101-105, x150

10. Tritaxia macfadyeni (Cushman)
oblique apertural view, Goban Spur 6\1 101-105, x200

11. Tritaxia macfadyeni (Cushman)
close-up of aperture, Goban Spur 6\1 101-105, x750

12. Tritaxia macfadyeni (Cushman)
lateral view, ABC7, x50

13. Tritaxia macfadyeni (Cushman)
lateral view, ABC7, x50

14. Tritaxia pyramidata (Reuss)
lateral view, ABC6, x150

15. Tritaxia pyramidata (Reuss)
lateral view, ABC6, x50

Plate 4 cont'd

16. Tritaxia pyramidata (Reuss)
oblique apertural view, ABC6, x75

PLATE 4

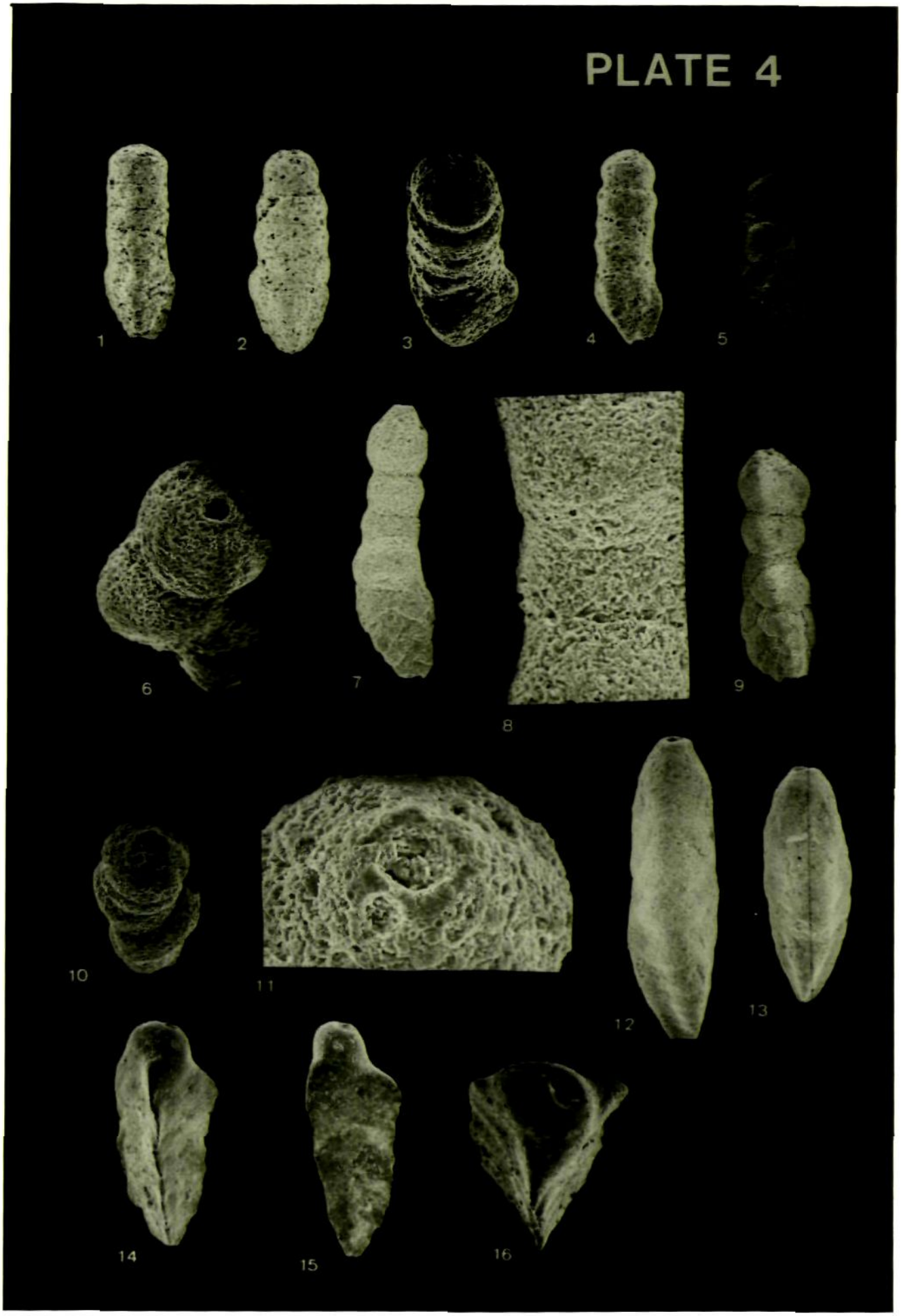

Plate 5.

1. Tritaxia tricarinata (Reuss) Reuss
lateral view, ABC5, x150

2. Tritaxia tricarinata (Reuss) Reuss
lateral view, ABC5, x150

3. Tritaxia tricarinata (Reuss) Reuss
lateral view, ABC6, x150

4. Tritaxia tricarinata (Reuss) Reuss
lateral view, ABC7, x150

5. Tritaxia tricarinata (Reuss) Reuss
lateral view, ABC20, x200

6. Tritaxia tricarinata (Reuss) Reuss
lateral view, ABC21, x150

7. Tritaxia tricarinata (Reuss) Reuss
close-up of test wall, ABC21, x350

8. Tritaxia tricarinata var. jongmansi
lateral view, AKS12, x75

9. Tritaxia tricarinata var. jongmansi
lateral view, AKS9, x75

10. Tritaxia tricarinata var. jongmansi
lateral view, AKSc, x75

11. Tritaxia tricarinata var. jongmansi
lateral view, AKSc, x100

12. Tritaxia tricarinata var. jongmansi (incomplete specimen)
lateral view, AKS H, x75

13. Tritaxia tricarinata var. jongmansi
lateral view, AKS H, x75

14. Tritaxia tricarinata var. jongmansi
lateral view, AKS11, x75

Plate 5 cont'd

15. *Tritaxia tricarinata* var. *jongmansi*
lateral view, AKS9, x75

PLATE 5

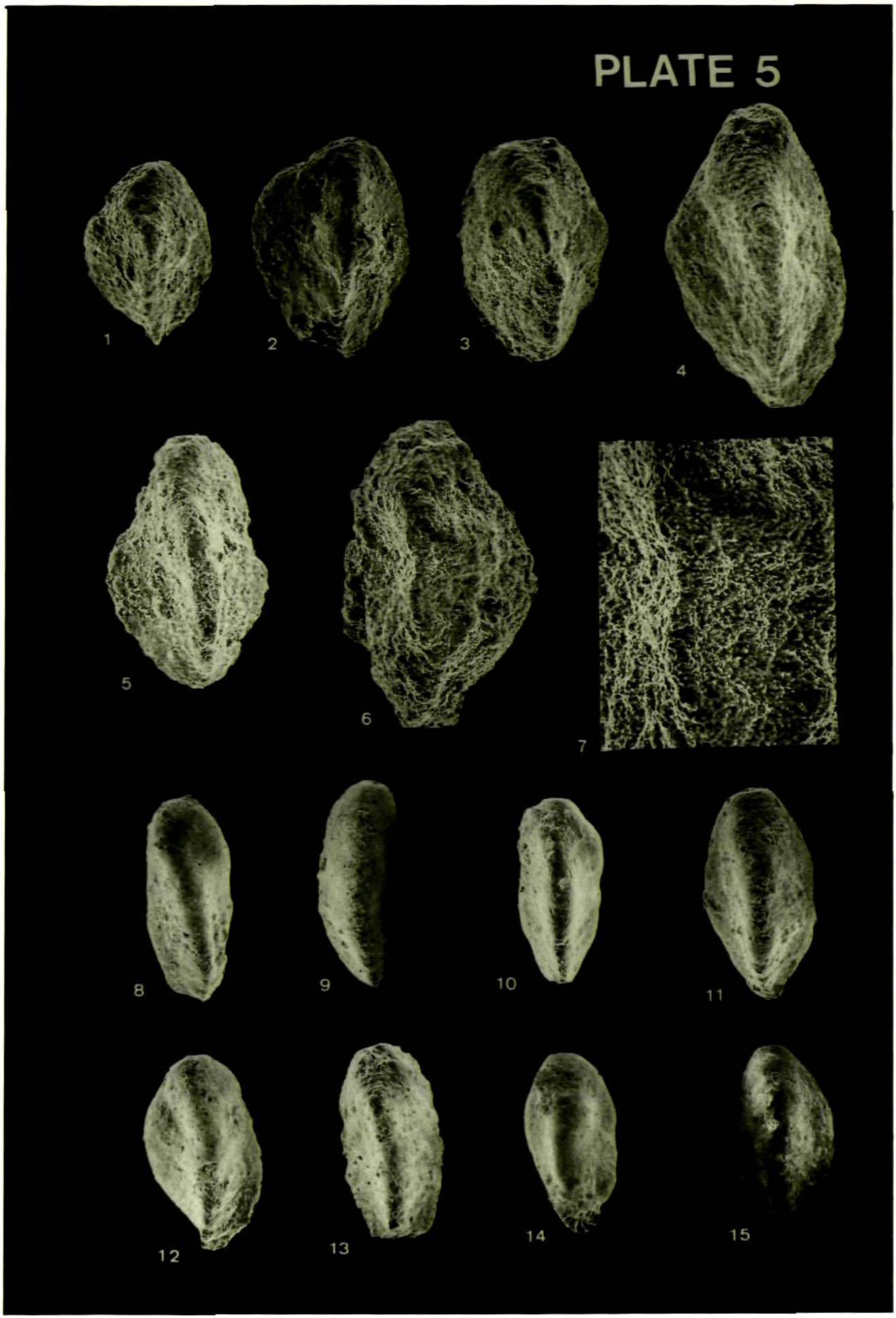

Plate 6.

1. Arenobulimina bulletta (Barnard and Banner)
lateral view, ABC1, x100

2. Arenobulimina bulletta (Barnard and Banner)
lateral view, ABC1, x100

3. Arenobulimina bulletta (Barnard and Banner)
oblique apertural view, ABC1, x100

4. Arenobulimina bulletta (Barnard and Banner)
close-up of aperture, ABC1, x200

5. Arenobulimina advena (Cushman)
lateral view, ABC7, x100

6. Arenobulimina advena (Cushman)
apertural view, ABC7, x100

7. Arenobulimina advena (Cushman)
lateral view, ABC7, x75

8. Arenobulimina advena (Cushman)
lateral view, ABC8, x100

9. Arenobulimina preslii (Reuss)
lateral view, AKS7, x200

10. Arenobulimina preslii (Reuss)
lateral view, AKS1, x200

11. Arenobulimina sp.a
lateral view, ABC5, x200

12. Arenobulimina sp.a
apertural view, ABC5, x150

13. Dorothia gradata (Berthelin)
lateral view, ABC1, x150

14. Dorothia gradata (Berthelin)
oblique apertural view, ABC1, x150

PLATE 6

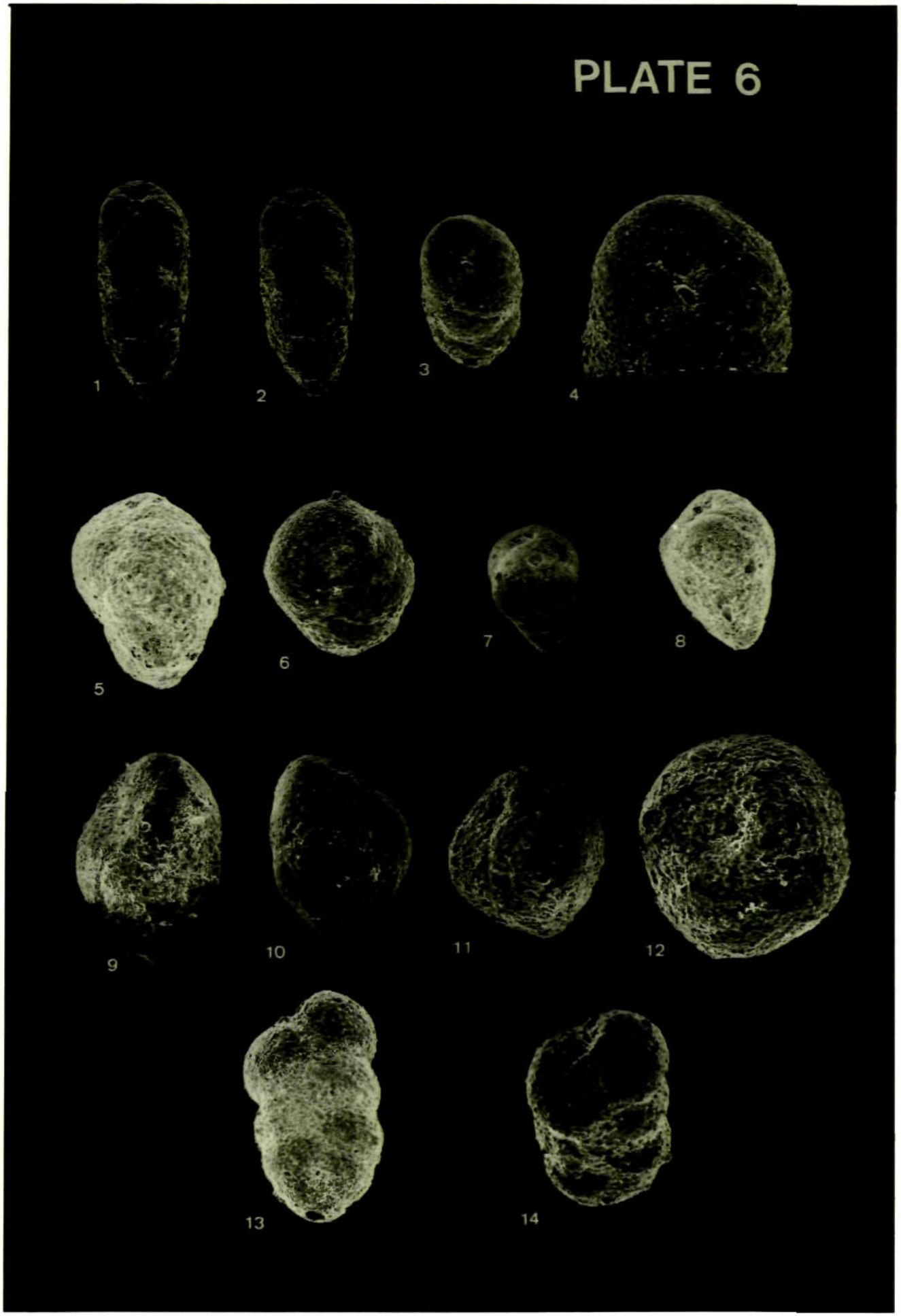

Plate 7.

1. Marssonella sp.a
apertural view, ABC9, x200

2. Marssonella sp.a
lateral view, ABC9, x100

3. Marssonella sp.a
lateral view, ABC9, x100

4. Marssonella sp.a
apertural view, ABC10, x200

5. Marssonella sp.a
lateral view, ABC9, x100

6. Marssonella sp.a
apertural view, ABC9, x200

7. Marssonella sp.a
lateral view, ABC10, x150

8. Marssonella sp.a
close-up of test wall, ABC10, x500

9. Marssonella trochus d'Orbigny
lateral view, ABC9, x150

10. Marssonella trochus d'Orbigny
close-up of test wall, ABC9, x500

11. Marssonella trochus d'Orbigny
lateral view, ABC9, x100

12. Marssonella trochus d'Orbigny
lateral view, ABC9, x150

13. Marssonella trochus d'Orbigny
lateral view, ABC10, x150

14. Marssonella trochus d'Orbigny
lateral view, ABC12, x200

15. Marssonella trochus d'Orbigny
lateral view, ABC16, x200

Plate 7 cont'd

16. Marssonella trochus d'Orbigny
lateral view, ABC20, x200

PLATE 7

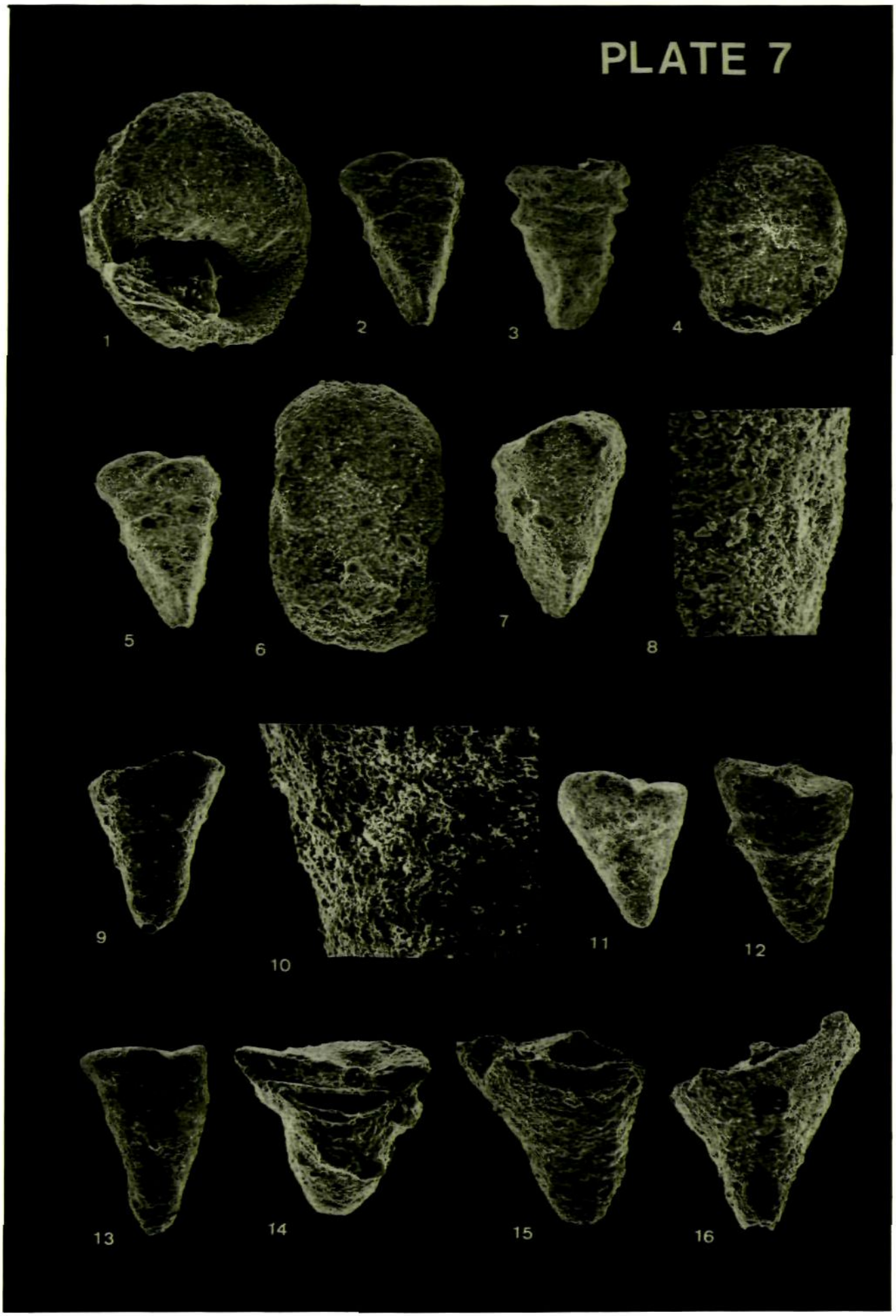

Plate 8.

1. Marssonella trochus d'Orbigny
CBl 14

2. Marssonella trochus d'Orbigny
WND 21

3. Marssonella trochus var. turris
WND 1

4. Marssonella trochus var. turris
WND 15

5. Marssonella trochus var. turris
WND 25

6. Marssonella trochus var. turris
WND 25

7. Marssonella trochus var. oxycona
CBl 21

8. Marssonella trochus var. oxycona
CBl 28

9. Marssonella trochus var. oxycona
WND 23

PLATE 8

Plate 9.

1. Marssonella trochus var. turris
lateral view, ABC10, x150

2. Marssonella trochus var. turris
lateral view, ABC10, x200

3. Marssonella trochus var. turris
lateral view, ABC11, x100

4. Marssonella trochus var. turris
lateral view, ABC14, x150

5. Marssonella trochus var. turris
lateral view, ABC14, x100

6. Marssonella trochus var. turris
lateral view, ABC14, x150

7. Marssonella trochus var. turris
lateral view, ABC16, x150

8. Marssonella trochus var. turris
lateral view, ABC20, x200

9. Marssonella trochus var. turris
lateral view, ABC20, x150

10. Marssonella trochus var. turris
lateral view, ABC21, x200

11. Marssonella trochus var. oxycona
lateral view, ABC3, x200

12. Marssonella trochus var. oxycona
lateral view, ABC2, x100

13. Marssonella trochus var. oxycona
lateral view, ABC2, x200

14. Marssonella trochus var. oxycona
lateral view, ABC12, x200

15. Marssonella trochus var. oxycona
lateral view, ABC20, x200

Plate 9 cont'd

16. *Marssonella trochus* var. *oxycona*
lateral view, AKS12, x150

PLATE 9

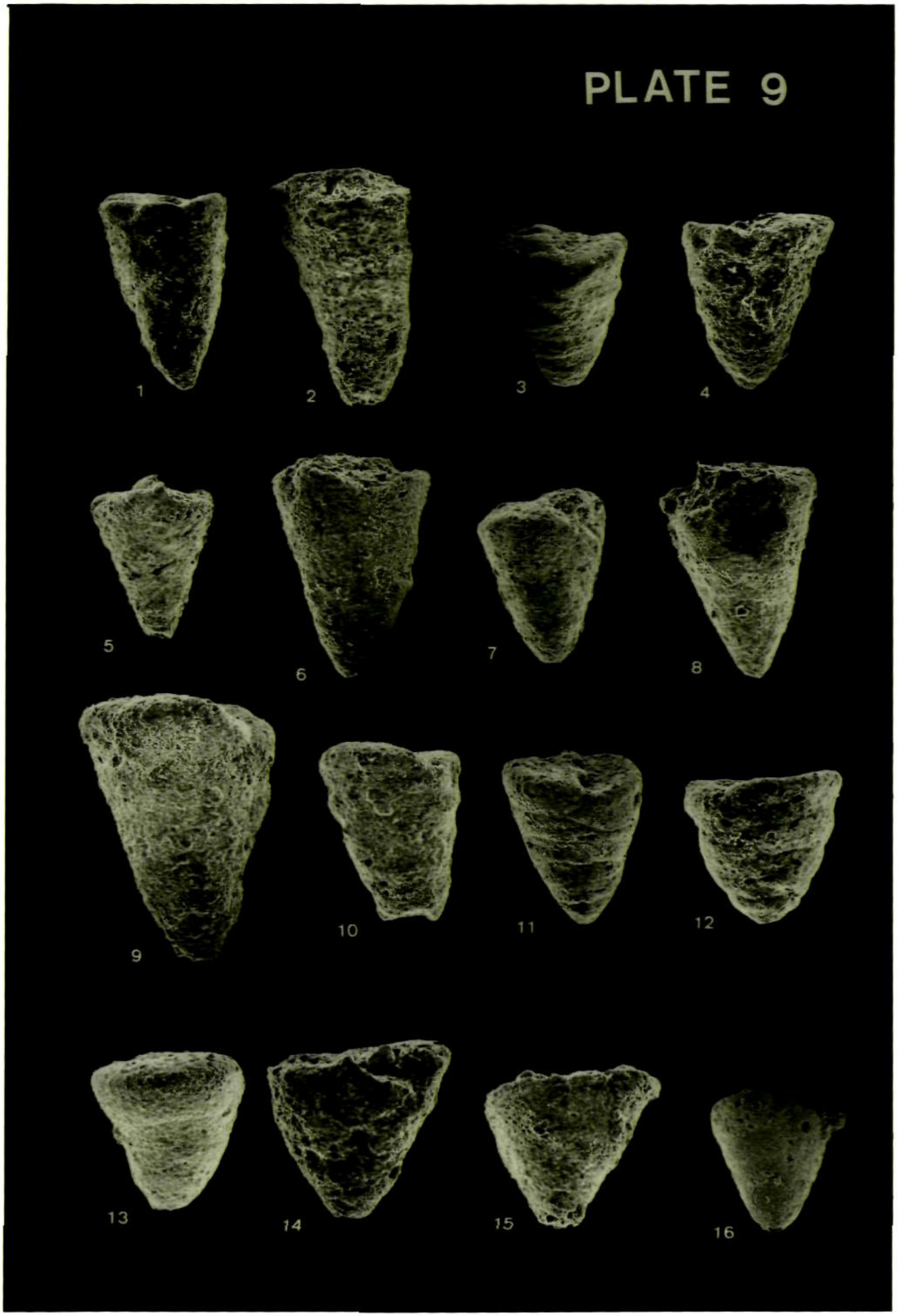

Plate 10.

1. Eggerellina brevis (d'Orbigny)
apertural view, ABC1, x200

2. Eggerellina brevis (d'Orbigny)
lateral view, ABC2, x150

3. Eggerellina brevis (d'Orbigny)
apertural view, ABC1, x100

4. Eggerellina brevis (d'Orbigny)
lateral view, ABC1, x150

5. Eggerellina brevis (d'Orbigny)
apertural view, ABC1, x200

6. Eggerellina brevis (d'Orbigny)
apertural view, ABC9, x150

7. Eggerellina mariae ten Dam
lateral view, ABC1, x150

8. Eggerellina mariae ten Dam
apertural view, ABC1, x200

9. Eggerellina mariae ten Dam
close-up of aperture, ABC1, x500

11. Eggerellina murchisoniana (d'Orbigny)
lateral view, ABC1, x200

12. Eggerellina murchisoniana (d'Orbigny)
apertural view, ABC1, x200

PLATE 10

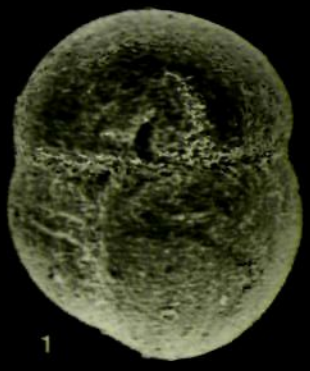
1


2

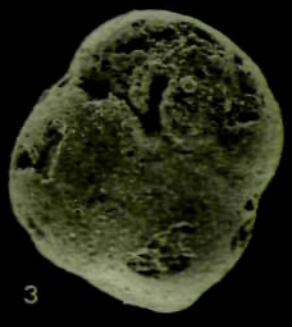
3

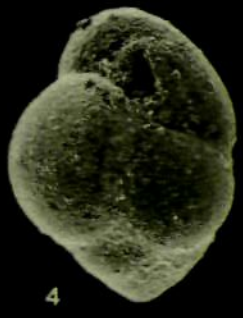
4

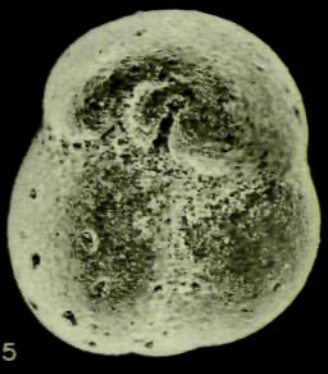
5

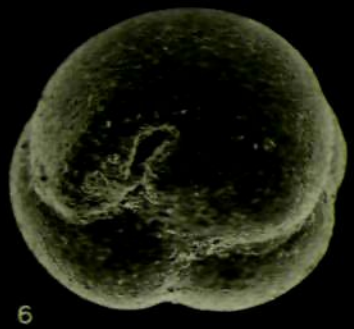
6

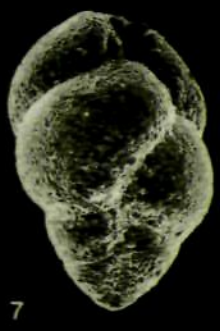
7

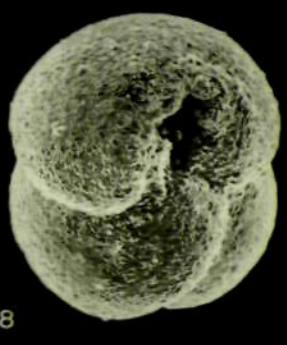
8

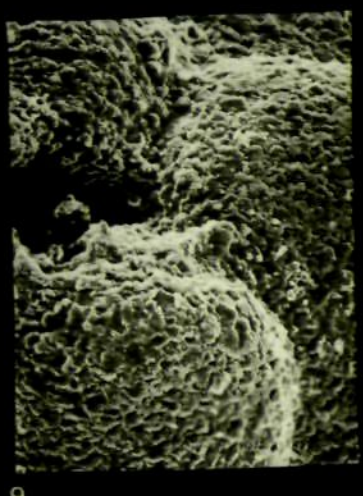
9

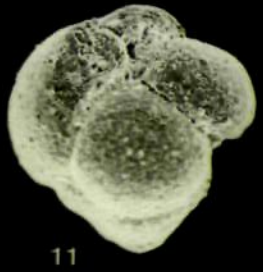
11

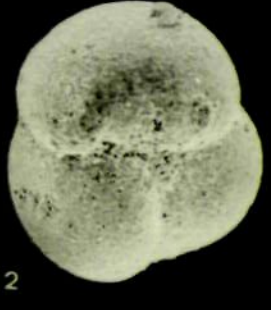
12

Plate 11.

1. Plectina mariae (Franke)
lateral view, ABC1, x150

2. Plectina mariae (Franke)
lateral view, ABC1, x100

3. Plectina mariae (Franke)
lateral view, ABC1, x150

4. Plectina mariae (Franke)
lateral view, ABC1, x150

5. Plectina mariae (Franke)
oblique apertural view, ABC1, x200

6. Plectina mariae (Franke)
oblique apertural view, ABC1, x200

7. Plectina mariae (Franke)
oblique apertural view, ABC1, x150

8. Plectina mariae (Franke)
oblique apertural view, ABC1, x200

9. Plectina mariae (Franke)
close-up of initial portion of test, ABC1, x350

10. Plectina mariae (Franke)
lateral view, ABC2, x150

11. Plectina mariae (Franke)
close-up of test wall, ABC2, x350

12. Plectina mariae (Franke)
lateral view, ABC2, x200

13. Plectina cenomana Carter and Hart
lateral view, ABC5, x150

14. Plectina cenomana Carter and Hart
oblique apertural view, ABC5, x200

PLATE 11

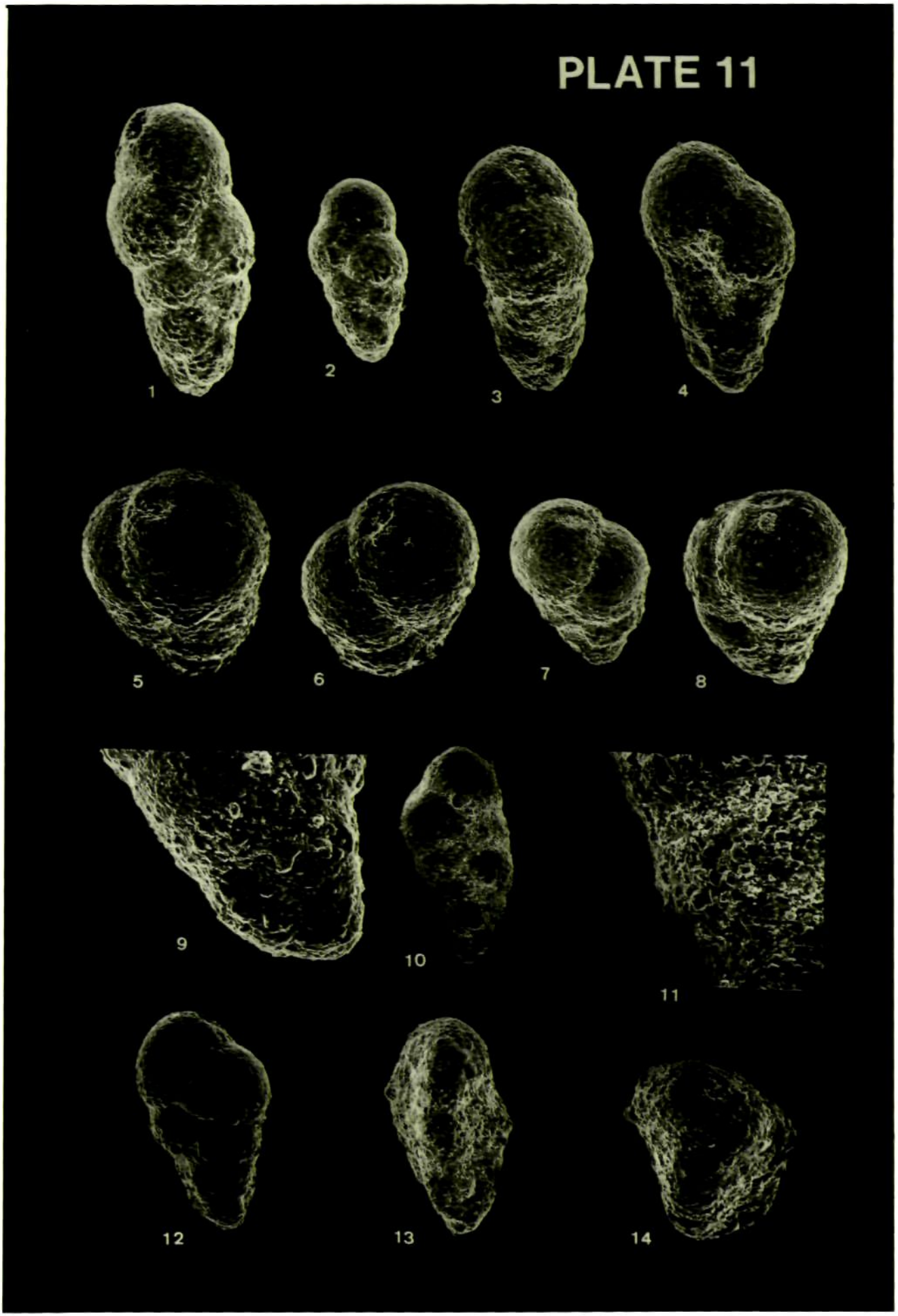

Plate 12.

1. Ataxophragmium depressum (Perner)
lateral view, ABC3, x200

2. Ataxophragmium depressum (Perner)
apertural view, ABC3, x200

3. Ataxophragmium depressum (Perner)
oblique apertural view, ABC6, x150

4. Ataxophragmium depressum (Perner)
lateral view, ABC5, x150

5. Ataxophragmium depressum (Perner)
lateral view, ABC7, x150

6. Ataxophragmium depressum (Perner)
oblique apertural view, ABC7, x150

7. Ataxophragmium depressum (Perner)
lateral view, ABC7, x150

8. Ataxophragmium depressum (Perner)
lateral view, ABC7, x150

9. Ataxophragmium depressum (Perner)
lateral view, ABC8, x150

10. Ataxophragmium depressum (Perner)
lateral view, ABC8, x150

11. Ataxophragmium depressum (Perner)
apertural view, ABC8, x150

PLATE 12

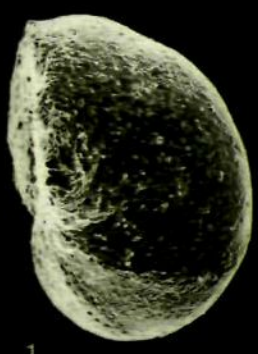
1

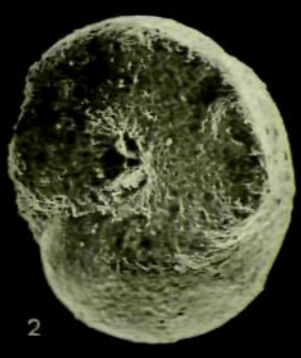
2

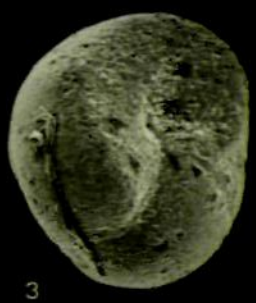
3

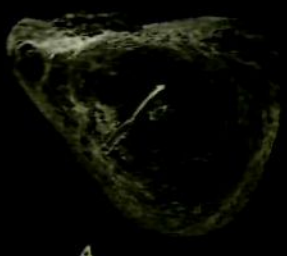
4

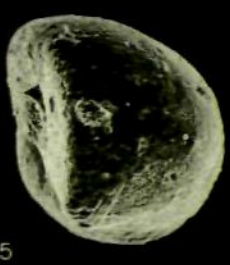
5

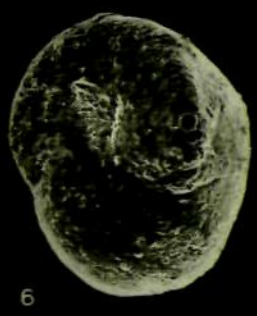
6

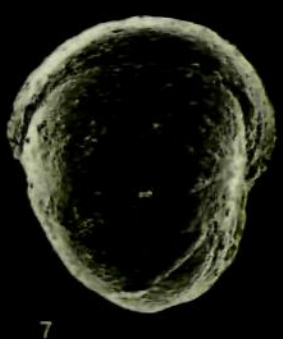
7

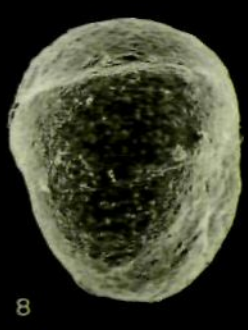
8

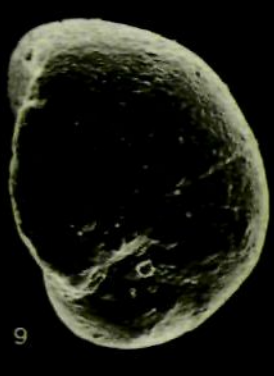
9

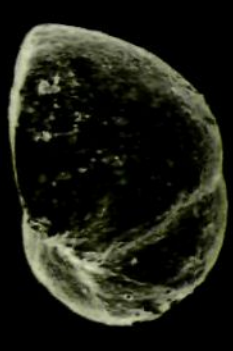
10

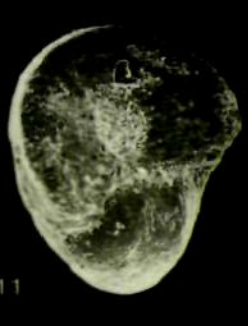
11

Plate 13.

1. Pseudotextulariella cretosa Cushman
   BSA1

2. Pseudotextulariella cretosa Cushman
   apertural view, BritOil 48\22-1 490', x100

3. Pseudotextulariella cretosa Cushman
   lateral view, BritOil 48\22-1 490', x150

4. Quinqueloculina antiqua Franke
   lateral view, B.P 93\2-1 1108', x200

5. Quinqueloculina antiqua Franke
   lateral view, B.P 93\2-1 1090', x200

6. Nodosaria sp.a
   apertural view, ABC3, x350

7. Nodosaria sp.a
   lateral view, ABC3, x50

8. Nodosaria sp.a
   apertural view, ABC4, x500

9. Nodosaria sp.a
   lateral view, ABC4, x75

10. Nodosaria sp.a
    apertural view, ABC4, x350

11. Nodosaria sp.a
    lateral view, ABC4, x75

12. Nodosaria sp.a
    lateral view, ABC8, x100

13. Nodosaria sp.a
    apertural view, ABC8, x350

14. Nodosaria sp.a
    lateral view, ABC11, x75

15. Nodosaria sp.a
    apertural view, ABC11, x350

PLATE 13

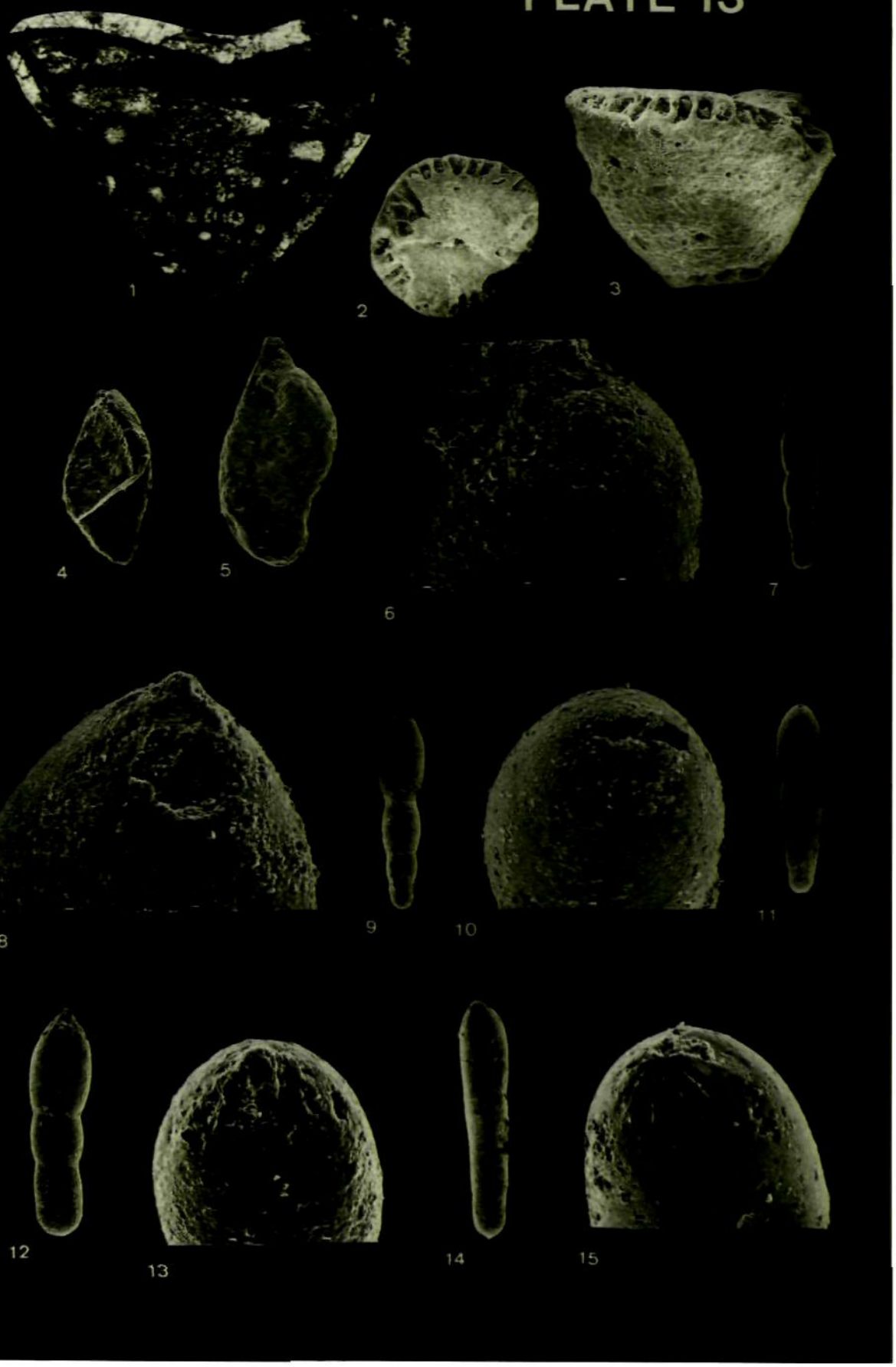

Plate 14.

1. Astacolus sp.a
   lateral view, ABC5, x100

2. Astacolus sp.a
   oblique apertural view, ABC5, x350

3. Dentalina sp.a
   lateral view, ABC5, x50

4. Dentalina sp.a
   oblique apertural view, ABC5, x350

5. Dentalina sp.a
   oblique apertural view, ABC8, x500

6. Dentalina sp.a
   lateral view, ABC8, x75

7. Dentalina sp.b
   lateral view, ABC7, x75

8. Dentalina sp.b
   lateral view, ABC7, x75

9. Dentalina sp.b
   oblique apertural view, ABC7, x350

10. Dentalina sp.b
    lateral view, ABC8, x75

11. Dentalina sp.b
    oblique apertural view, ABC8, x350

12. Dentalina sp.b
    lateral view, ABC8, x75

13. Dentalina sp.b
    oblique apertural view, ABC8, x750

14. Dentalina sp.b
    oblique apertural view, ABC8, x350

15. Dentalina sp.b
    lateral view, ABC8, x75

Plate 14 cont'd

16. Dentalina sp.c
oblique apertural view, ABC9, x350

17. Dentalina sp.c
lateral view, ABC9, x75

18. Dentalina sp.c
close-up of test wall, ABC9, x750

PLATE 14

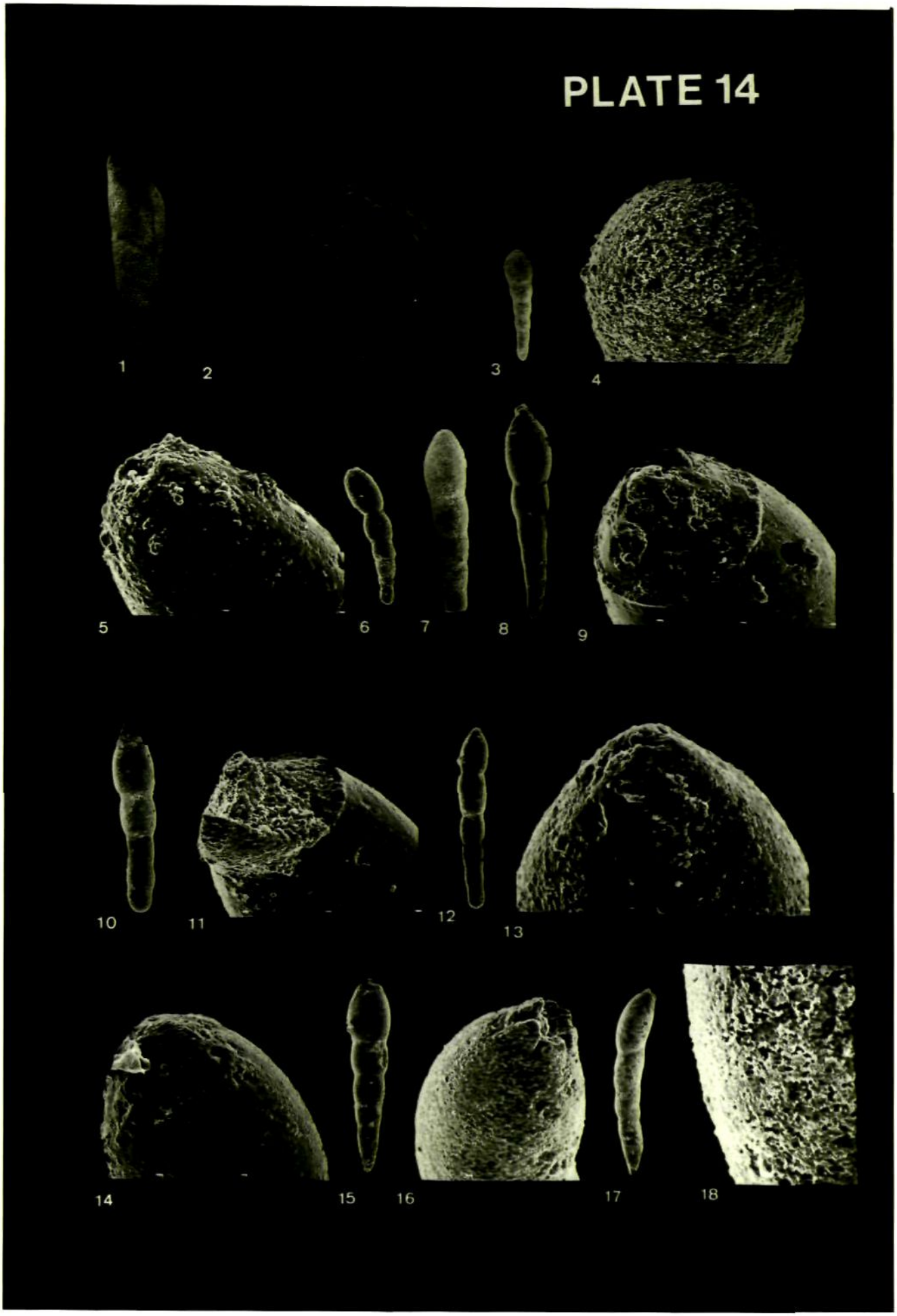

Plate 15.

1. Frondicularia cordai Reuss
lateral view, ABC5, x35

2. Frondicularia gaultina Reuss
lateral view, ABC3, x35

3. Frondicularia sp.a
lateral view, CB1 36, x35

4. Frondicularia sp.a
lateral view, S6Q18, x100

5. Lagena sp.a
lateral view, Goban Spur 5\1 30-33, x150

6. Lagena sp.a
apertural view, Goban Spur 5\1 30-33, x150

7. Lenticulina ovalis (Reuss)
lateral view, AKS6, x100

8. Lenticulina ovalis (Reuss)
apertural face, AKS6, x100

9. Lenticulina ovalis (Reuss)
lateral view, AKS6, x100

10. Lenticulina rotulata var.a (Lamarck)
lateral view, ABC1, x50

11. Lenticulina rotulata var.a (Lamarck)
apertural face, ABC1, x75

12. Lenticulina rotulata var.a (Lamarck)
close-up of aperture, ABC1, x350

PLATE 15

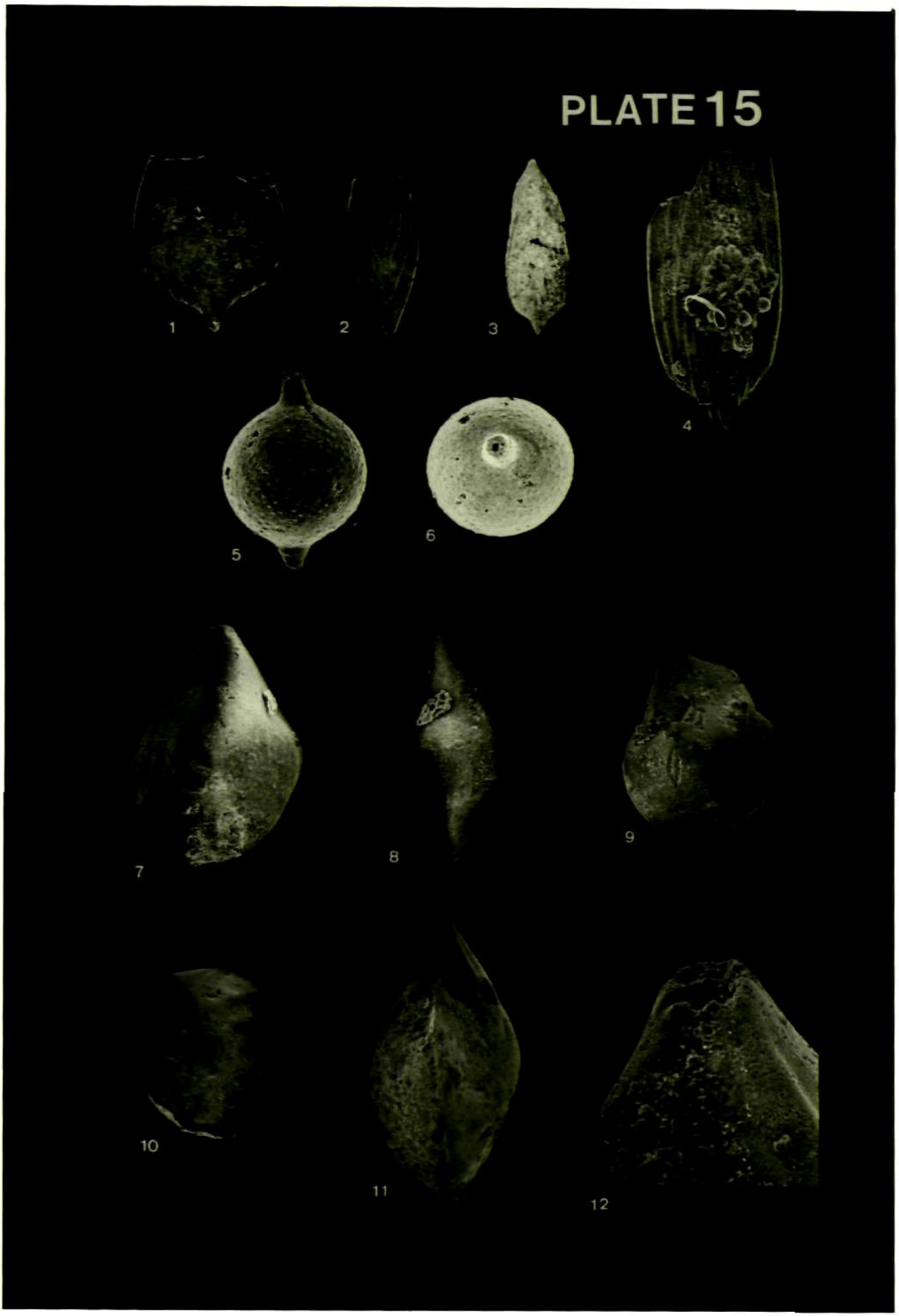

Plate 16.

1. Lenticulina rotulata var.a (Lamarck)
lateral view, ABC2, x150

2. Lenticulina rotulata var.a (Lamarck)
apertural face, ABC2, x150

3. Lenticulina rotulata var.a (Lamarck)
lateral view, ABC3, x100

4. Lenticulina rotulata var.a (Lamarck)
apertural face, ABC3, x100

5. Lenticulina rotulata var.a (Lamarck)
lateral view, AKS3, x100

6. Lenticulina rotulata var.a (Lamarck)
apertural face, AKS3, x100

7. Lenticulina rotulata var.b (Lamarck)
lateral view, ABC1, x100

8. Lenticulina rotulata var.b (Lamarck)
apertural face, ABC1, x100

9. Lenticulina rotulata var.b (Lamarck)
lateral view, ABC1, x150

10. Lenticulina rotulata var.b (Lamarck)
apertural face, ABC1, x150

11. Lenticulina rotulata var.b (Lamarck)
lateral view, ABC1, x150

12. Lenticulina rotulata var.b (Lamarck)
apertural face, ABC2, x100

PLATE 16

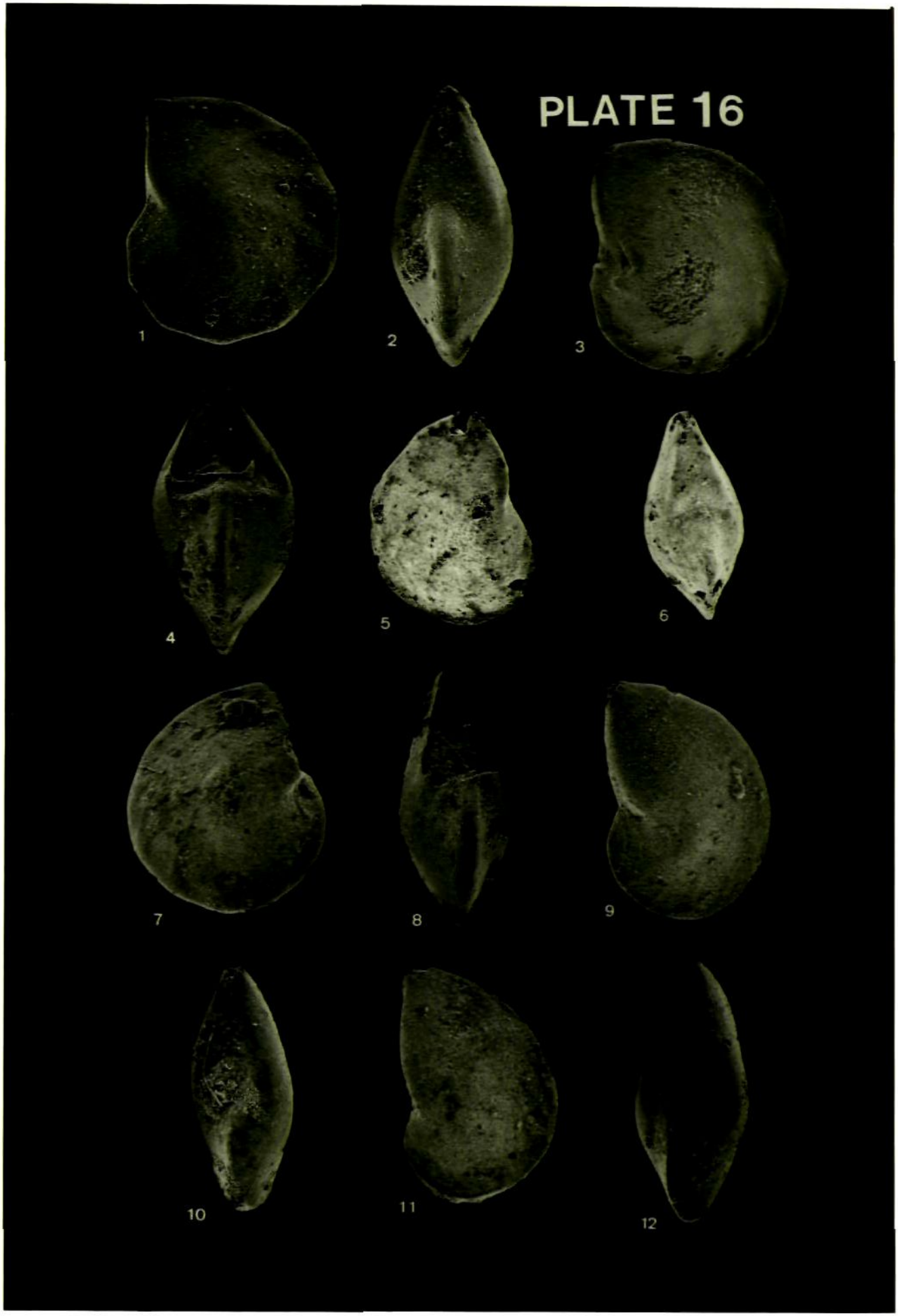

Plate 17.

1. Lenticulina rotulata var.b (Lamarck)
apertural face, ABC3, x100

2. Lenticulina rotulata var.b (Lamarck)
lateral view, ABC3, x100

3. Lenticulina rotulata var.b (Lamarck)
apertural face, B.P 93\2-1 1120', x200

4. Lenticulina rotulata var.b (Lamarck)
lateral view, B.P 93\2-1 1120', x200

5. Lenticulina rotulata var.b (Lamarck)
lateral view, AKS1, x200

6. Lenticulina rotulata var.b (Lamarck)
apertural face, AKS1, x200

7. Lenticulina rotulata var.b (Lamarck)
lateral view, AKS2, x150

8. Lenticulina rotulata var.b (Lamarck)
apertural face, AKS2, x150

9. Lenticulina rotulata var.b (Lamarck)
apertural face, AKS2, x150

10. Leenticulina rotulata var.b (Lamarck)
lateral view, AKS2, x200

11. Lenticulina rotulata var.b (Lamarck)
apertural face, AKS7, x150

12. Lenticulina rotulata var.b (Lamarck)
lateral view, AKS7, x150

13. Lenticulina rotulata var.c (Lamarck)
lateral view, B.P 93\2-1 1120', x100

14. Lenticulina rotulata var.c (Lamarck)
apertural face, B.P 93\2-1 1120', x100

PLATE 17

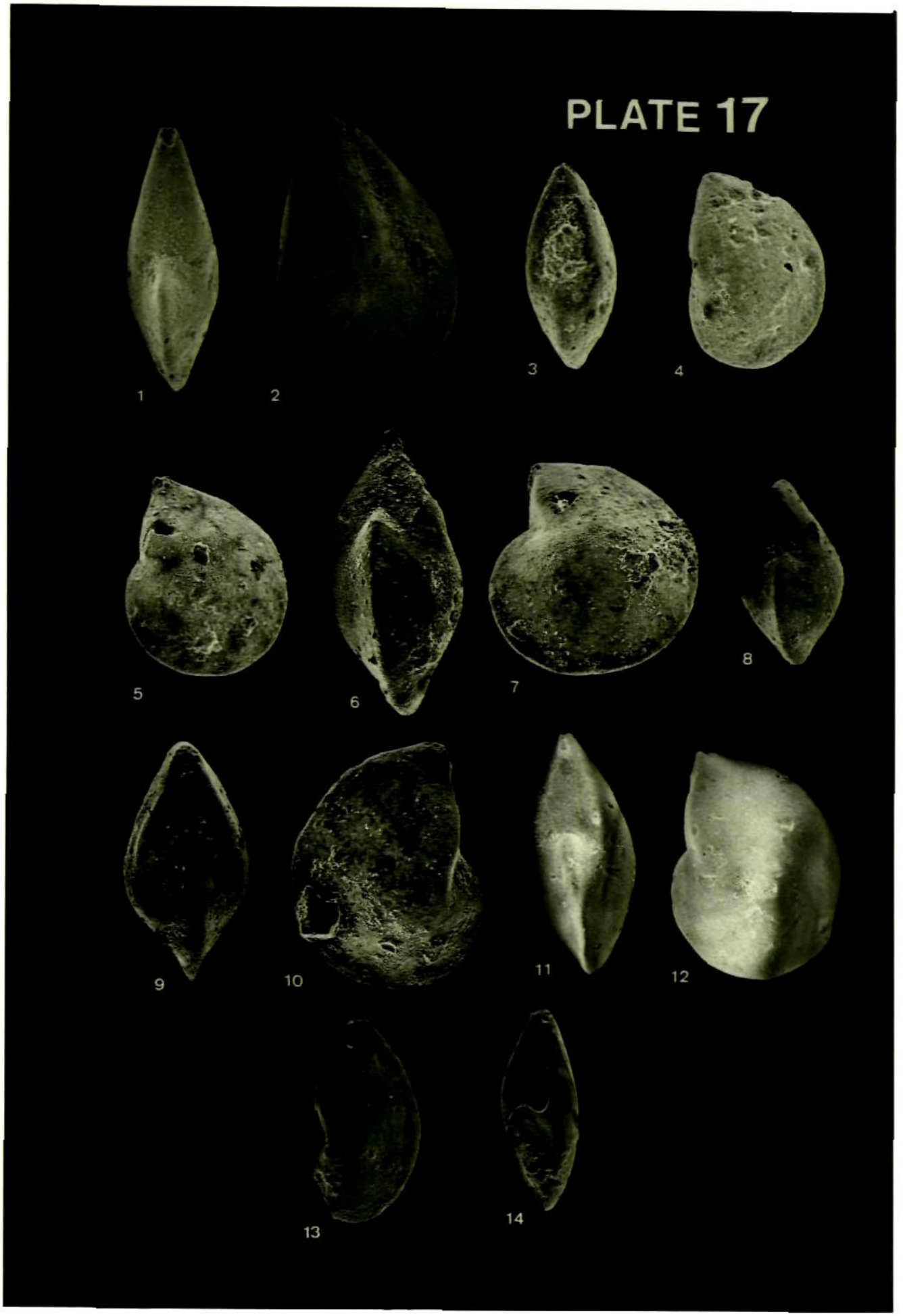

Plate 18.

1. Lenticulina sp.a
lateral view, Goban Spur 5\2 13-17, x200

2. Lenticulina sp.a
close-up of apertural face, Goban Spur 5\2 13-17, x750

3. Lenticulina sp.a
apertural face, Goban Spur 5\2 13-17, x200

4. Marginulina sp.a
lateral view, B.P 93\2-1 1090', x150

5. Marginulina sp.a
oblique apertural view, B.P 93\2-1 1090', x500

6. Marginulinopsis acuticostata (Reuss)
lateral view, BritOil 48\22-1 490', x200

7. Marginulinopsis acuticostata (Reuss)
apertural view, BritOil 48\22-1 490', x350

8. Marginulinopsis acuticostata (Reuss)
lateral view, BritOil 48\22-1 490', x200

9. Neoflabellina sp.a
lateral view, ABC10, x75

10. Neoflabellina sp.b
lateral view, B.P 93\2-1 1090', x200

11. Neoflabellina sp.b
oblique apertural view, B.P 93\2-1 1090', x350

12. Neoflabellina sp.b
close-up of aperture, B.P 93\2-1 1090', x750

13. Pandaglandulina sp.a
lateral view, ABC4, x100

14. Pandaglandulina sp.a
apertural view, ABC4, x350

15. Pandaglandulina sp.a
lateral view, ABC4, x100

16. Pandaglandulina sp.a
apertural view, ABC4, x350

PLATE 18

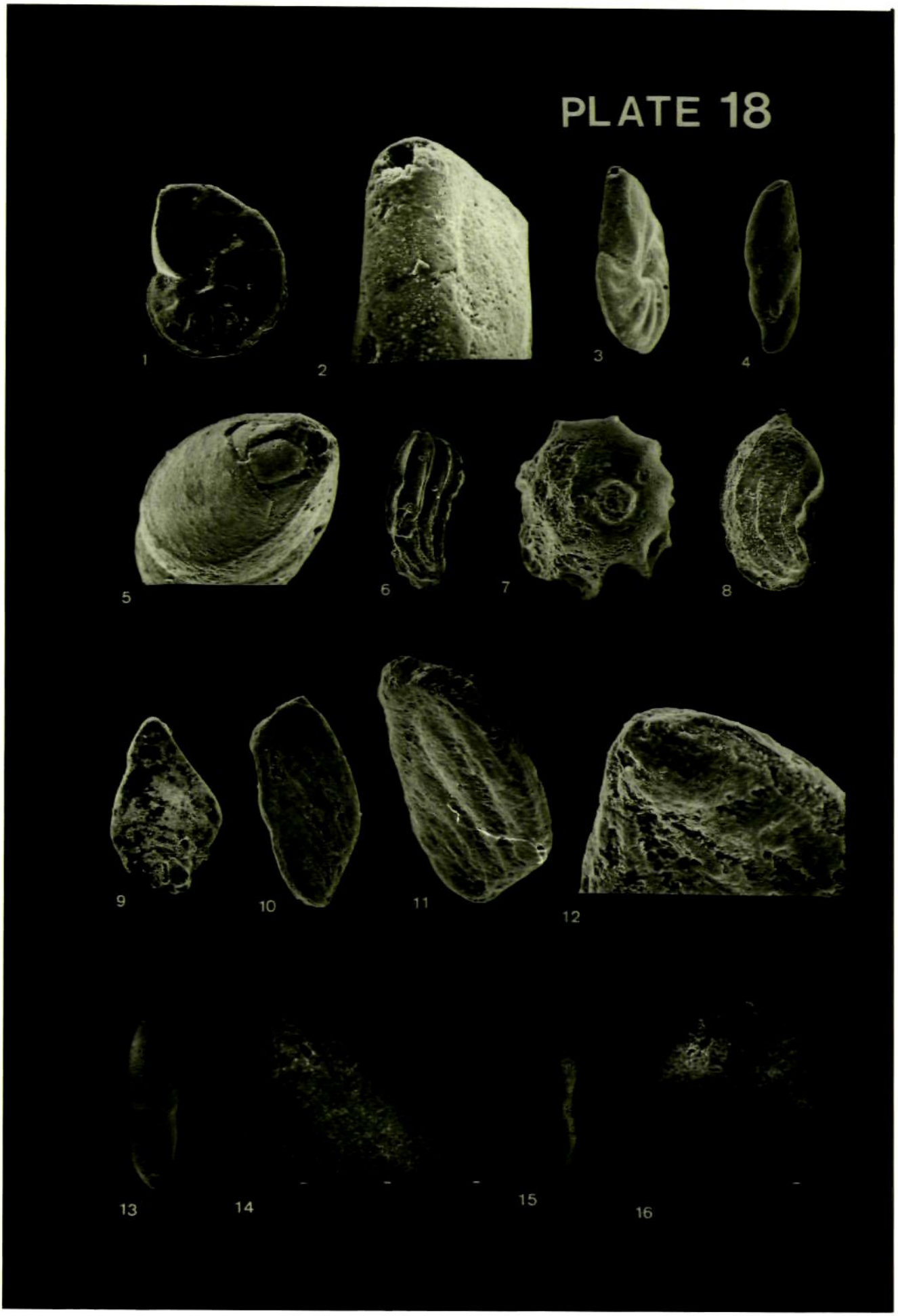

Plate 19.

1. Planularia? sp.a

   lateral view, ABC10, x100

2. Vaginulina costulata Roemer form a
   lateral view, ABC7, x50

3. Vaginulina costulata Roemer form a
   lateral view, of aperture, ABC7, x200

4. Vaginulina costulata Roemer form a
   lateral view of initial portion of test, ABC7, x200

5. Vaginulina costulata Roemer form b
   lateral view, ABC8, x50

6. Vaginulina costulata Roooemer form b
   lateral view, ABC9, x50

7. Vaginulina costulata Roemer form b
   lateral view, ABC9, x50

8. Vaginulina costulata Roemer form c
   lateral view, ABC7, x75

9. Vaginulina costulata Roemer form c
   close-up lateral view of aperture, ABC7, x150

10. Vaginulina costulata Roemer form c
    close-up lateral view of aperture, ABC9, x75

11. Vaginulina costulata Roemer form d
    oblique lateral view, ABC8, x50

12. Eoguttulina? sp.a
    lateral view, CB1 1, x150

13. Ramulina aculeata (d'Orbigny) form a
    lateral view, ABC1, x100

14. Ramulina aculeata (d'Orbigny) form a
    lateral view, ABC3, x150

15. Ramulina aculeata (d'Orbigny) form a
    close-up of test wall, ABC3, x350

Plate 19 cont'd.

16. Ramulina aculeata (d'Orbigny) form a lateral view, ABC8, x200

17. Ramulina aculeata (d'Orbigny) form b lateral view, ABC1, x150

18. Ramulina aculeata (d'Orbigny) form b oblique apertural view, ABC1, x200

PLATE 19

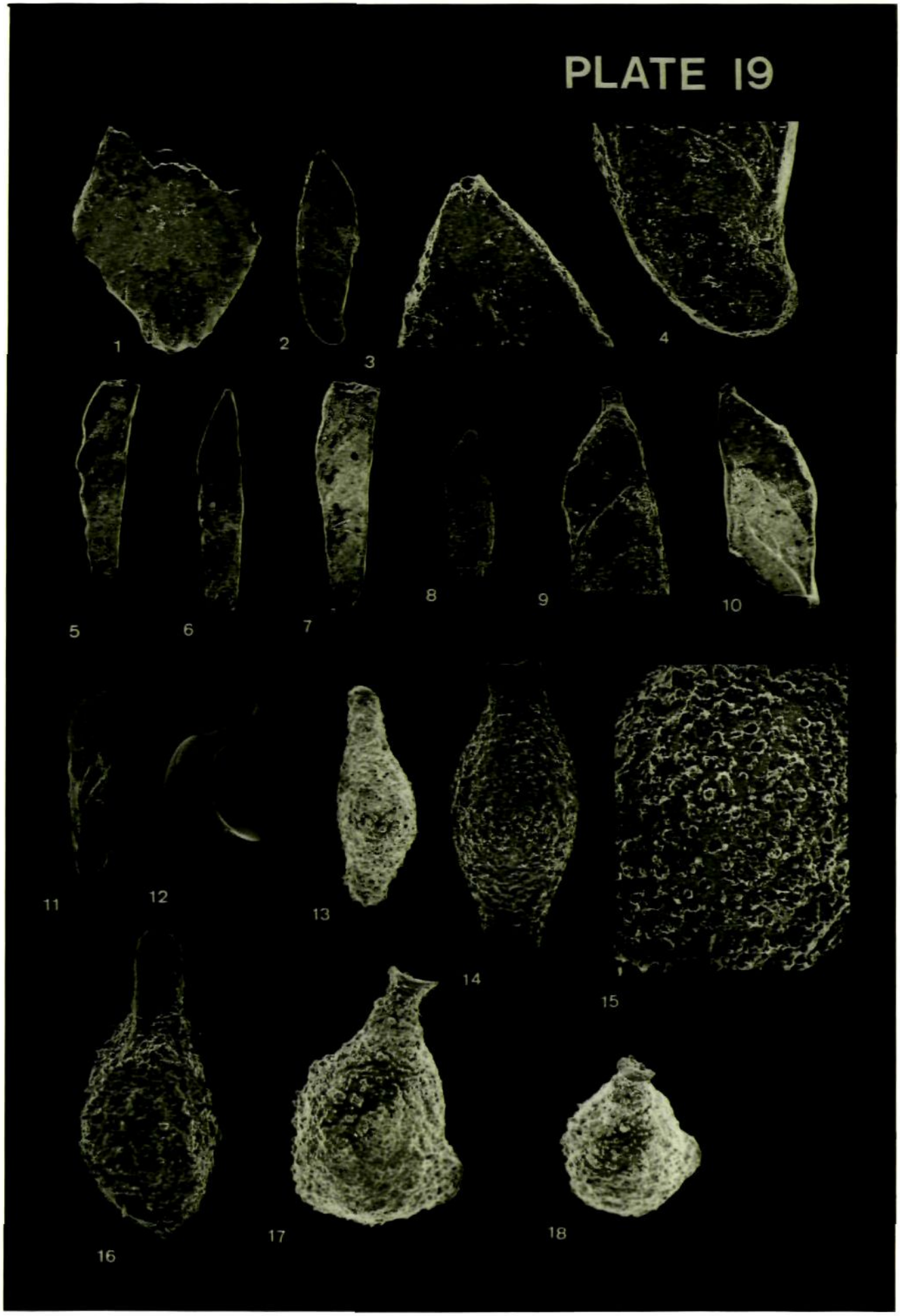

Plate 20.

1. Ramulina aculeata (d'Orbigny) form c
   lateral view, ABC3, x100

2. Ramulina aculeata (d'Orbigny) form d
   lateral view, ABC5, x150

3. Ramulina aculeata (d'Orbigny) form d
   lateral view, ABC5, x150

4. Ramulina aculeata (d'Orbigny) form e
   lateral view, ABC9, x75

5. Ramulina aculeata (d'Orbigny) form f
   lateral view, AKS11, x150

6. Ramulina aculeata (d'Orbigny) form f
   lateral view, AKS11, x200

7. Tristix excavatum (Reuss)
   lateral view, CB1 4, x50

8. Tristix excavatum (Reuss)
   apertural view, CB1 4, x100

9. Oolina sp.a
   lateral view, ABC3, x200

10. Oolina sp.a
    oblique apertural view, ABC3, x200

11. Oolina sp.a
    lateral view, ABC3, x200

12. Oolina sp.a
    oblique apertural view, ABC3, x200

13. Praebulimina sp.a
    lateral view, B.P 93\2-1 1035', x500

14. Praebulimina sp.a
    initial portion of test, B.P 93\2-1 1035', x500

Plate 20 cont'd

15. Praebulimina sp.a
lateral view, B.P 93\2-1 1035', x500

16. Praebulimina sp.a
oblique apertural view, B.P 93\2-1 1035', x500

PLATE 20

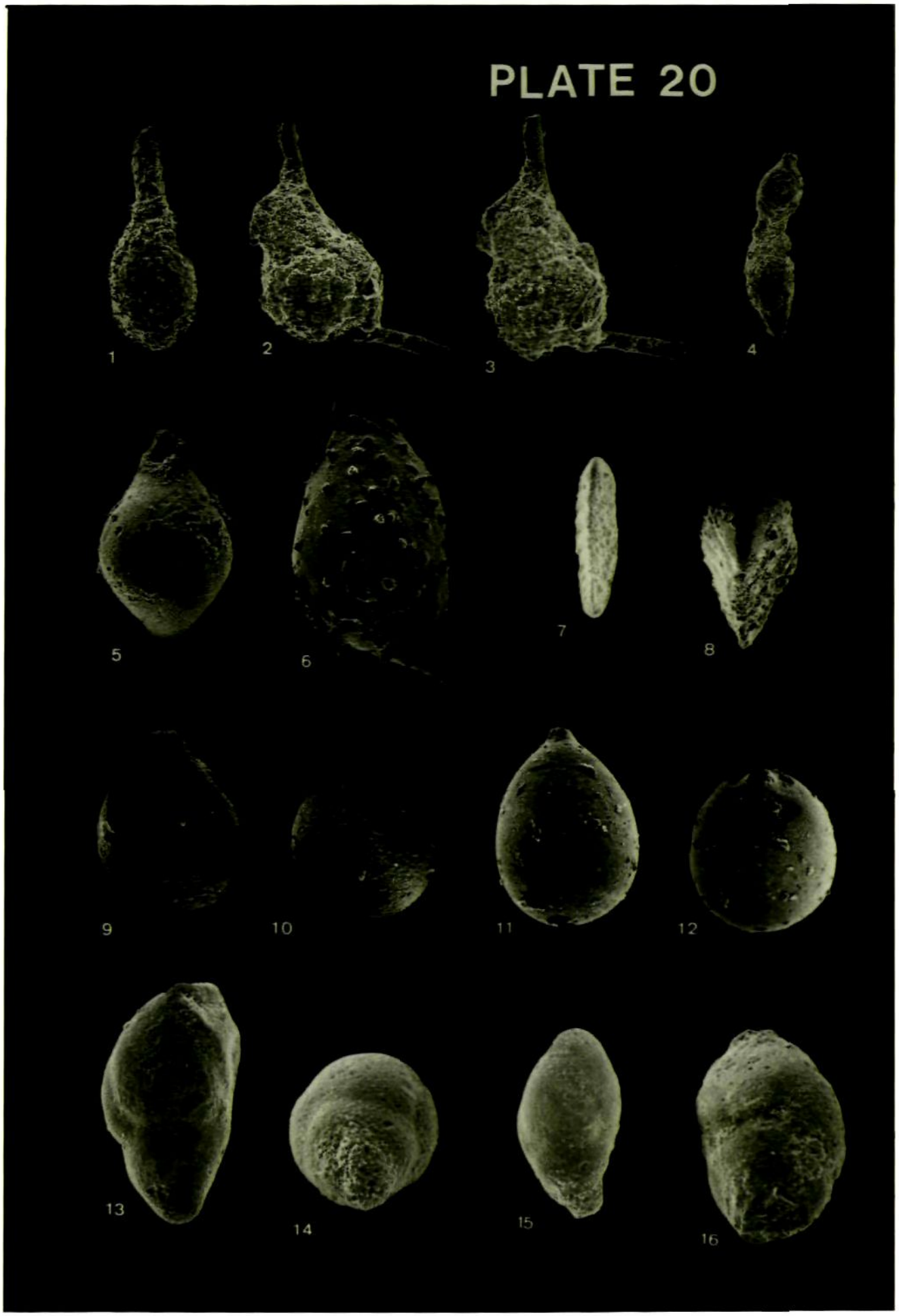

Plate 21.

1. Guembelitria cenomana (Keller)
lateral view, Goban Spur 6\1 124-126, x750

2. Guembelitria cenomana (Keller)
lateral view, Goban Spur 6\1 124-126, x750

3. Guembelitria cenomana (Keller)
last portion of test, Goban Spur 6\1 124-126, x1000

4. Guembelitria cenomana (Keller)
lateral view, ABC1, x750

5. Guembelitria cenomana (Keller)
lateral view, ABC1, x750

6. Guembelitria cenomana (Keller)
last portion of test, ABC4, x750

7. Guembelitria cenomana (Keller)
lateral view, ABC4, x500

8. Guembelitria cenomana (Keller)
lateral view, ABC1, x500

9. Guembelitria cenomana (Keller)
lateral view, ABC1, x500

10. Guembelitria cenomana (Keller)
lateral view, AKS2, x750

11. Guembelitriella sp.a
lateral view, ABC1, x500

PLATE 21

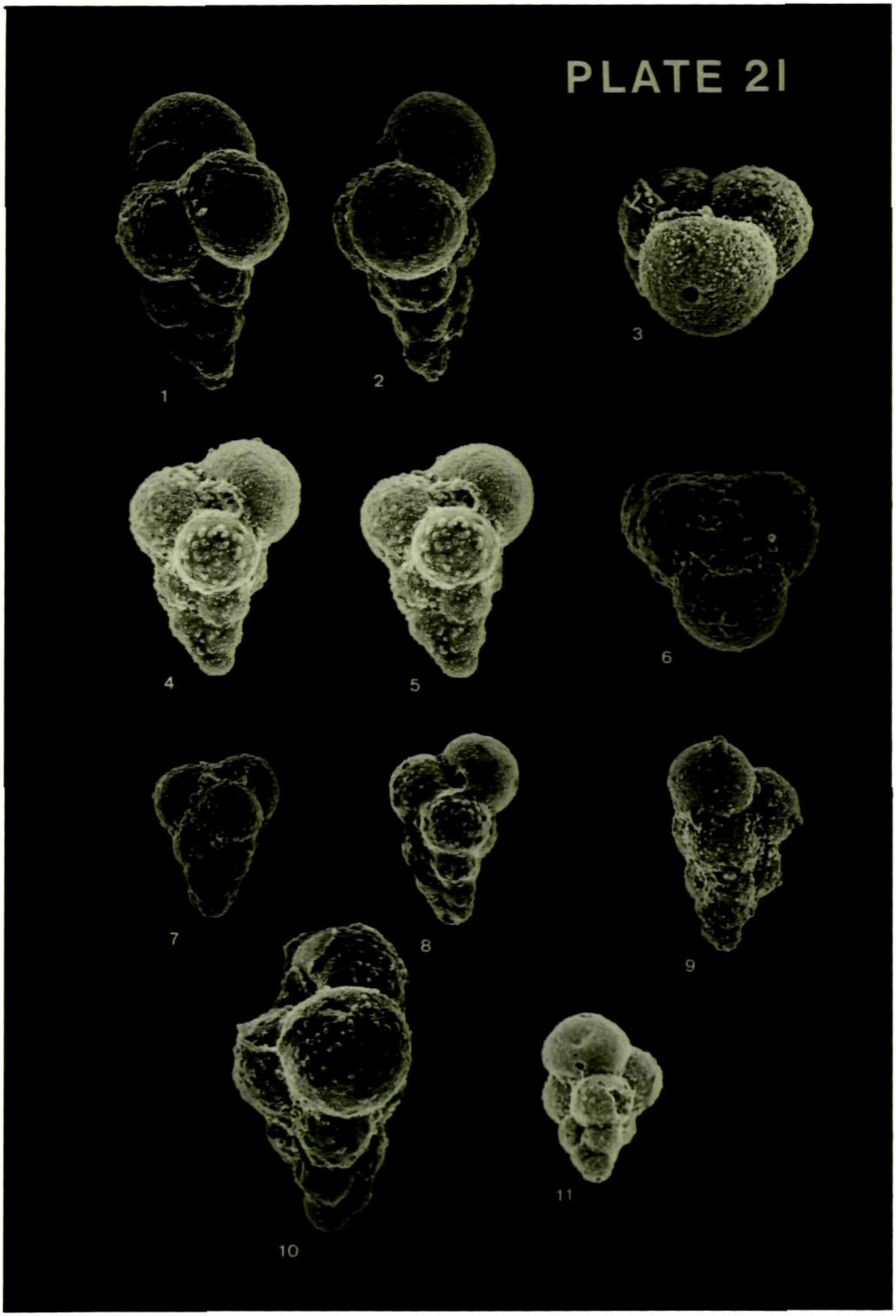

Plate 22.

1. Heterohelix moremani (Cushman)
lateral view, Goban Spur 6\1 124-126, x500

2. Heterohelix moremani (Cushman)
lateral view, Goban Spur 6\1 124-126, x750

3. Heterohelix moremani (Cushman)
lateral view, Goban Spur 6\1 124-126, x500

4. Heterohelix moremani (Cushman)
oblique apertural view, Goban Spur 6\1 124-126, x500

5. Heterohelix moremani (Cushman)
close-up of initial portion of test, Goban Spur 6\1 124-126, x1500

6. Heterohelix moremani (Cushman)
lateral view, ABC1, x350

7. Heterohelix moremani (Cushman)
lateral view, ABC1, x500

8. Heterohelix moremani (Cushman)
lateral view, ABC1, x350

9. Heterohelix moremani (Cushman)
lateral view, ABC4, x750

10. Heterohelix moremani (Cushman)
lateral view, ABC4, x500

11. Heterohelix moremani (Cushman)
lateral view, ABC20, x500

12. Heterohelix moremani (Cushman)
lateral view, ABC21, x750

13. Heterohelix moremani (Cushman)
lateral view, AKS1, x500

14. Heterohelix globulosa (Ehrenburg)
lateral view, ABC20, x750

15. Heterohelix globulosa (Ehrenburg)
lateral view, AKS8, x350

Plate 22 cont'd

16. Heterohelix globulosa (Ehrenburg)
close-up of ornament, AKS8, x1000

PLATE 22

Plate 23.

1. Globigerinelloides bentonensis (Morrow)
umbilical view, ABC4, x500

2. Globigerinelloides bentonensis (Morrow)
spiral view, ABC4, x500

3. Globigerinelloides bentonensis (Morrow)
umbilical view, Goban Spur 6\1 70-72, x500

4. Globigerinelloides bentonensis (Morrow)
apertural view, Goban Spur 6\1 70-72, x500

5. Globigerinelloides bentonensis (Morrow)
spiral view, Goban Spur 6\1 70-72, x500

6. "Hedbergella" aprica (Loeblich and Tappan)
umbilical view, SGQ11, x200

7. "Hedbergella" aprica (Loeblich and Tappan)
spiral view, SGQ11, x200

8. "Hedbergella" aprica (Loeblich and Tappan)
EGG23

9. "Hedbergella" archaeocretacea (Loeblich and Tappan)
umbilical view, SGQ15, x200

10. "Hedbergella" archaeocretacea (Loeblich and Tappan)
apertural view, SGQ15, x200

11. "Hedbergella" archaeocretacea (Loeblich and Tappan)
spiral view, SGQ15, x200

12. "Hedbergella" archaeocretacea (Loeblich and Tappan)
CB1 26

13. "Hedbergella" brittonensis (Loeblich and Tappan)
SGQ15

14. "Hedbergella" brittonensis (Loeblich and Tappan)
WND 15

PLATE 23

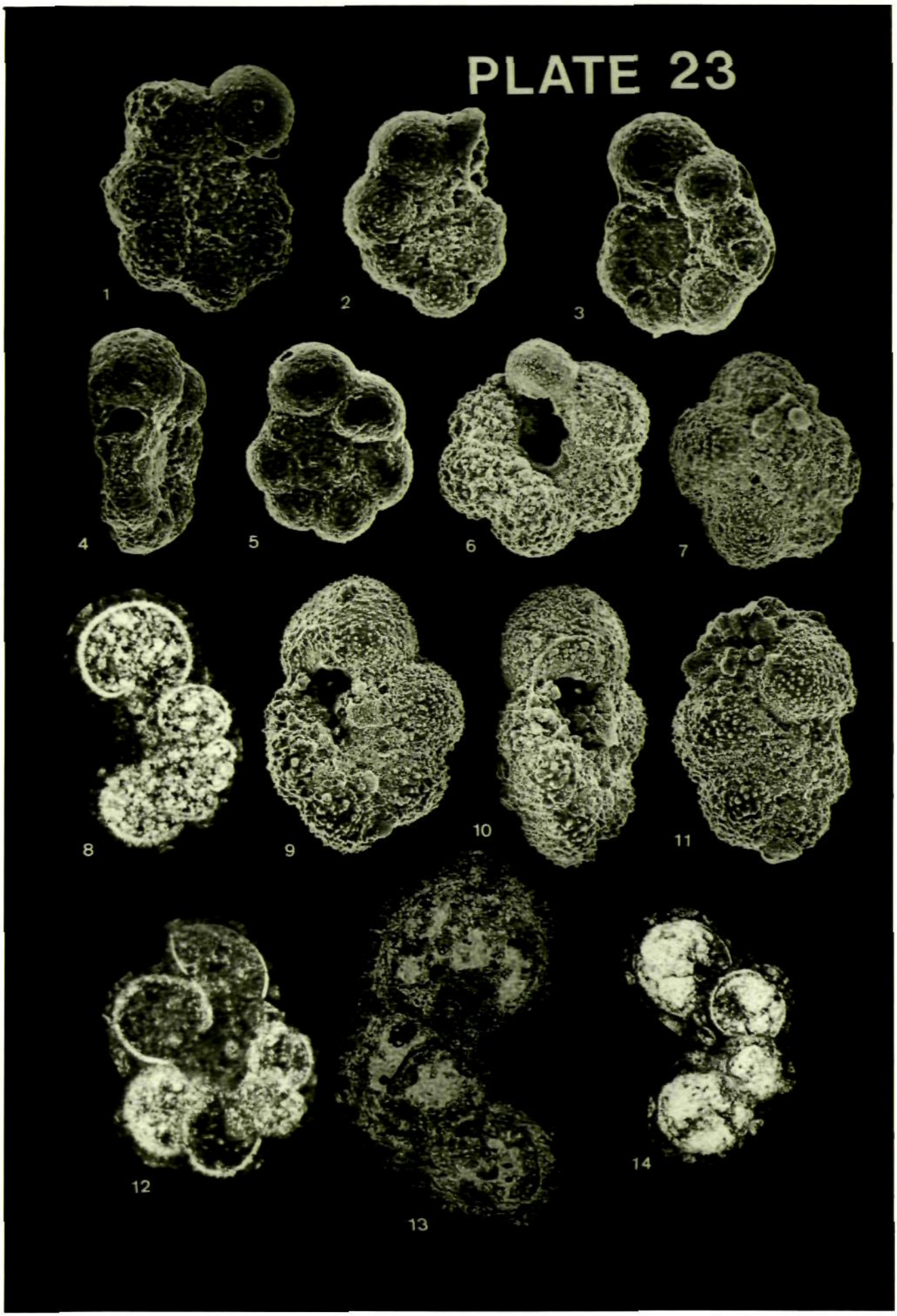

Plate 24.

1. Hedbergella delrioensis (Carsey)
apertural view, Goban Spur 5\1 7-10A, x200

2. Hedbergella delrioensis (Carsey)
close-up of aperture, Goban Spur 5\1 7-10A, x500

3. Hedbergella delrioensis (Carsey)
umbilical view, Goban Spur 5\1 7-10A, x200

4. Hedbergella delrioensis (Carsey)
spiral view, Goban Spur 5\1 7-10A, x150

5. Hedbergella delrioensis (Carsey)
oblique peripheral view, Goban Spur 5\1 7-10A, x200

6. Hedbergella delrioensis (Carsey)
umbilical view, Goban Spur 5\1 7-10A, x200

7. Hedbergella delrioensis (Carsey)
close-up of umbilical area, Goban Spur 5\1 7-10A, x500

8. Hedbergella delrioensis (Carsey)
spiral view, Goban Spur 5\1 7-10A, x200

9. Hedbergella delrioensis (Carsey)
peripheral view, ABC1, x200

10. Hedbergella delrioensis (Carsey)
close-up of periphery, ABC1, x350

11. Hedbergella delrioensis (Carsey)
SGQ6

12. Hedbergella planispira (Tappan)
oblique spiral view, B.P 93\2-1 1035', x200

13. Hedbergella planispira (Tappan)
spiral view, B.P 93\2-1 1035', x200

14. Hedbergella planispira (Tappan)
umbilical view, B.P 93\2-1 1035', x200

PLATE 24

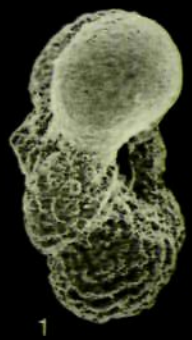
1

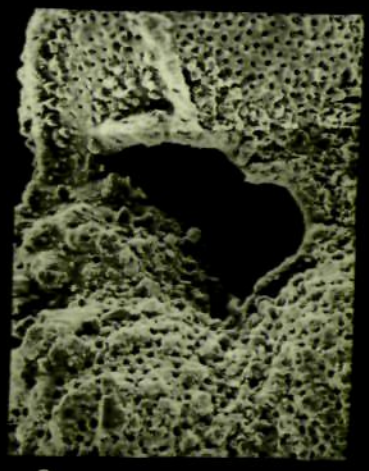
2


3

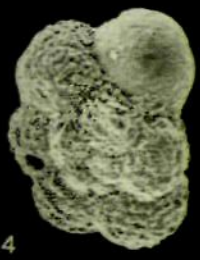
4

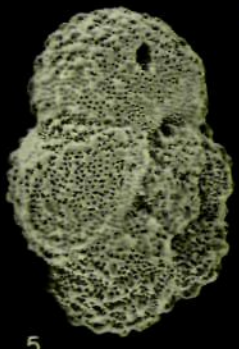
5

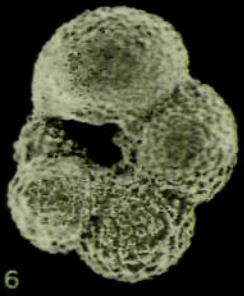
6

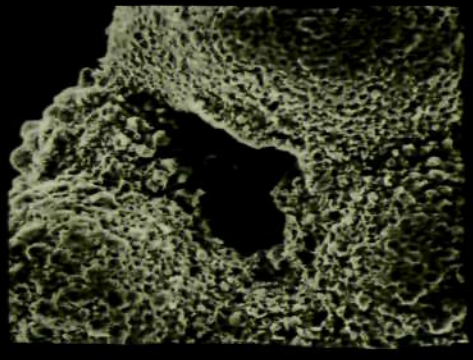
7

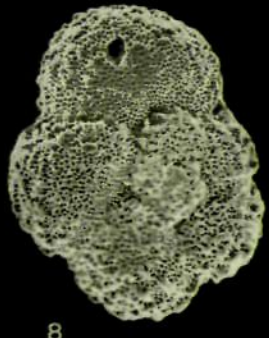
8

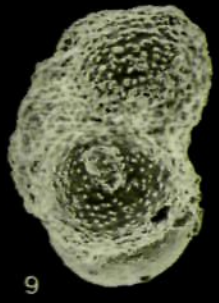
9

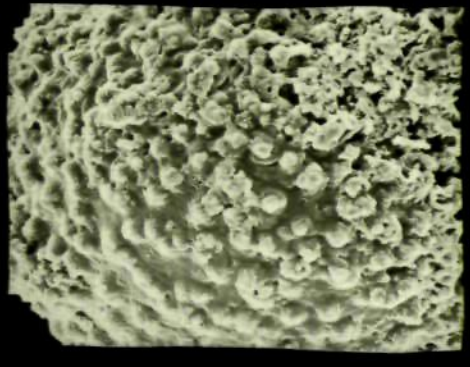
10

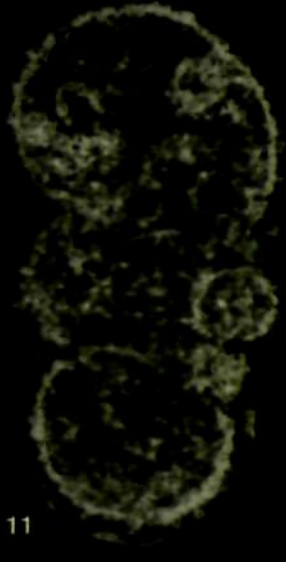
11

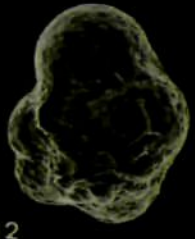
12

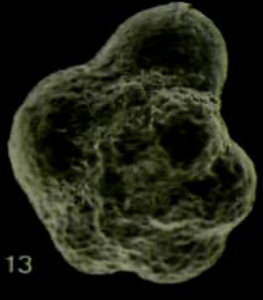
13

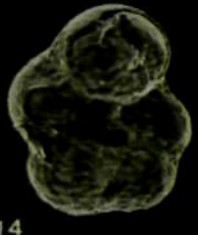
14

Plate 25.

1. Hedbergella simplex (Morrow)
BSA 10

2. Hedbergella washitensis (Casey)
SGQ6

3. Helvetoglobotruncana praehelvetica (Trujillio)
spiral view, B.P 93\2-1 1030', x200

4. Helvetoglobotruncana praehelvetica (Trujillio)
oblique apertural view, B.P 93\2-1 1030', x350

5. Helvetoglobotruncana praehelvetica (Trujillio)
close-up of periphery, B.P 93\2-1 1030', x750

6. Helvetoglobotruncana praehelvetica (Trujillio)
BSA 11

7. Helvetoglobotruncana praehelvetica (Trujillio)
CB1 17

8. Helvetoglobotruncana praehelvetica (Trujillio)
CB1 31

9. Helvetoglobotruncana praehelvetica (Trujillio)
CB1 26

10. Helvetoglobotruncana praehelvetica (Trujillio)
EGG 25

11. Helvetoglobotruncana helvetica (Bolli)
AKS11

12. Helvetoglobotruncana helvetica (Bolli)
spiral view, B.P 93\2-1 1090', x200

Plate 25 cont'd.

13. Helvetoglobotruncana helvetica (Bolli)
peripheral view, B.P 93\2-1 1090', x200

14. Helvetoglobotruncana helvetica (Bolli)
oblique peripheral view, B.P 93\2-1 1090', x350

PLATE 25


1

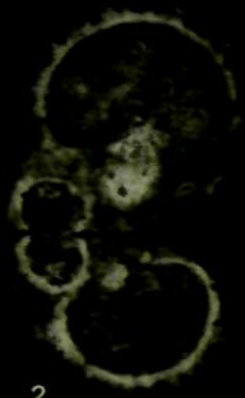
2

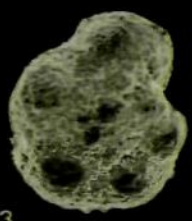
3

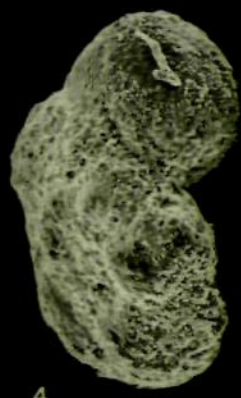
4

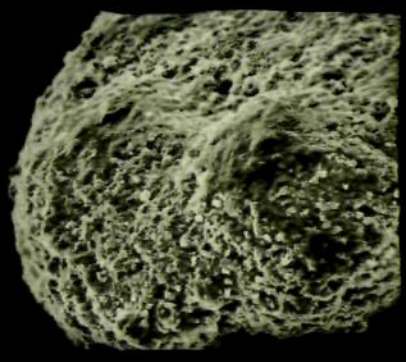
5


6

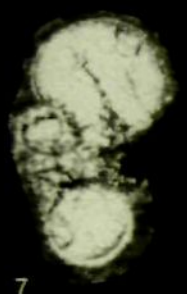
7

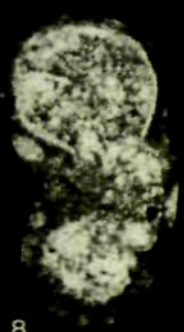
8


9


10


11

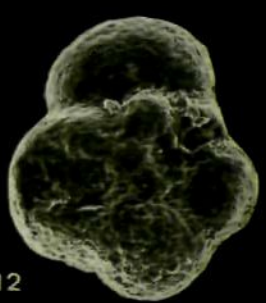
12

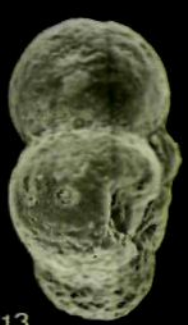
13

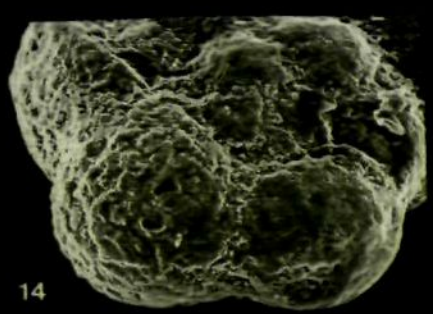
14

Plate 26.

1. Praeglobotruncana delrioensis (Plummer)
SGQ7

2. Praeglobotruncana gibba Klaus
SGQ7 Little Beach Member

3. Praeglobotruncana gibba Klaus
apertural view, Goban Spur 6\1 30-33, x150

4. Praeglobotruncana stephani (Gandolfi)
SGQ7 Pinnacles Member

5. Praeglobotruncana stephani (Gandolfi)
spiral view, Goban Spur 6\1 30-33, x200

6. Praeglobotruncana stephani (Gandolfi)
apertural view, Goban Spur 6\1 30-33, x200

7. Praeglobotruncana stephani (Gandolfi)
umbilical view, Goban Spur 6\1 30-33, x200

8. Praeglobotruncana stephani (Gandolfi)
spiral view, Goban Spur 6\1 30-33, x150

9. Praeglobotruncana stephani (Gandolfi)
peripheral view, Goban Spur 6\1 30-33, x200

10. Praeglobotruncana stephani (Gandolfi)
spiral view, Goban Spur 6\1 30-33, x200

PLATE 26

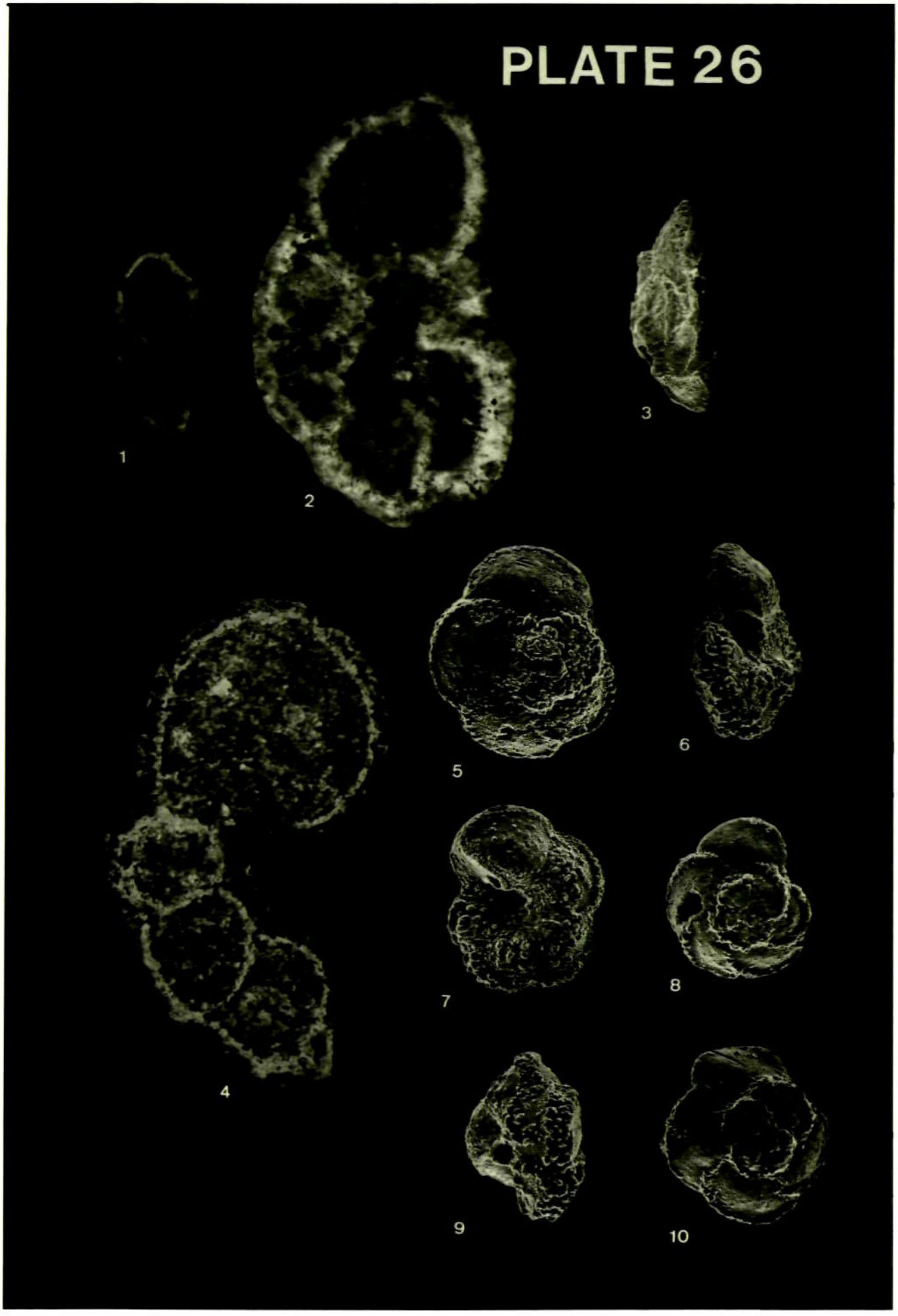

Plate 27.

1. Dicarinella algeriana (Caron)
umbilical view, Goban Spur 5\1 76-78, x150

2. Dicarinella algeriana (Caron)
apertural view, Goban Spur 5\1 76-78, x200

3. Dicarinella algeriana (Caron)
spiral view, Goban Spur 5\1 76-78, x110

4. Dicarinella hagni (Scheibnerova)
spiral view, Goban Spur 5\1 76-78, x150

5. Dicarinella hagni (Scheibnerova)
apertural view, Goban Spur 5\1 76-78, x100

6. Dicarinella hagni (Scheibnerova)
close-up of keels, Goban Spur 5\1 76-78, x350

7. Dicarinella hagni (Scheibnerova)
apertural view, Goban Spur 5\1 76-78, x200

8. Dicarinella hagni (Scheibnerova)
spiral view, Goban Spur 5\1 76-78, x150

9. Dicarinella hagni (Scheibnerova)
CB1 34

10. Dicarinella hagni (Scheibnerova)
WND28

11. Dicarinella imbricata (Mornod)
peripheral view, Goban Spur 5\1 76-78, x200

12. Dicarinella imbricata (Mornod)
spiral view, Goban Spur 5\1 76-78, x200

PLATE 27

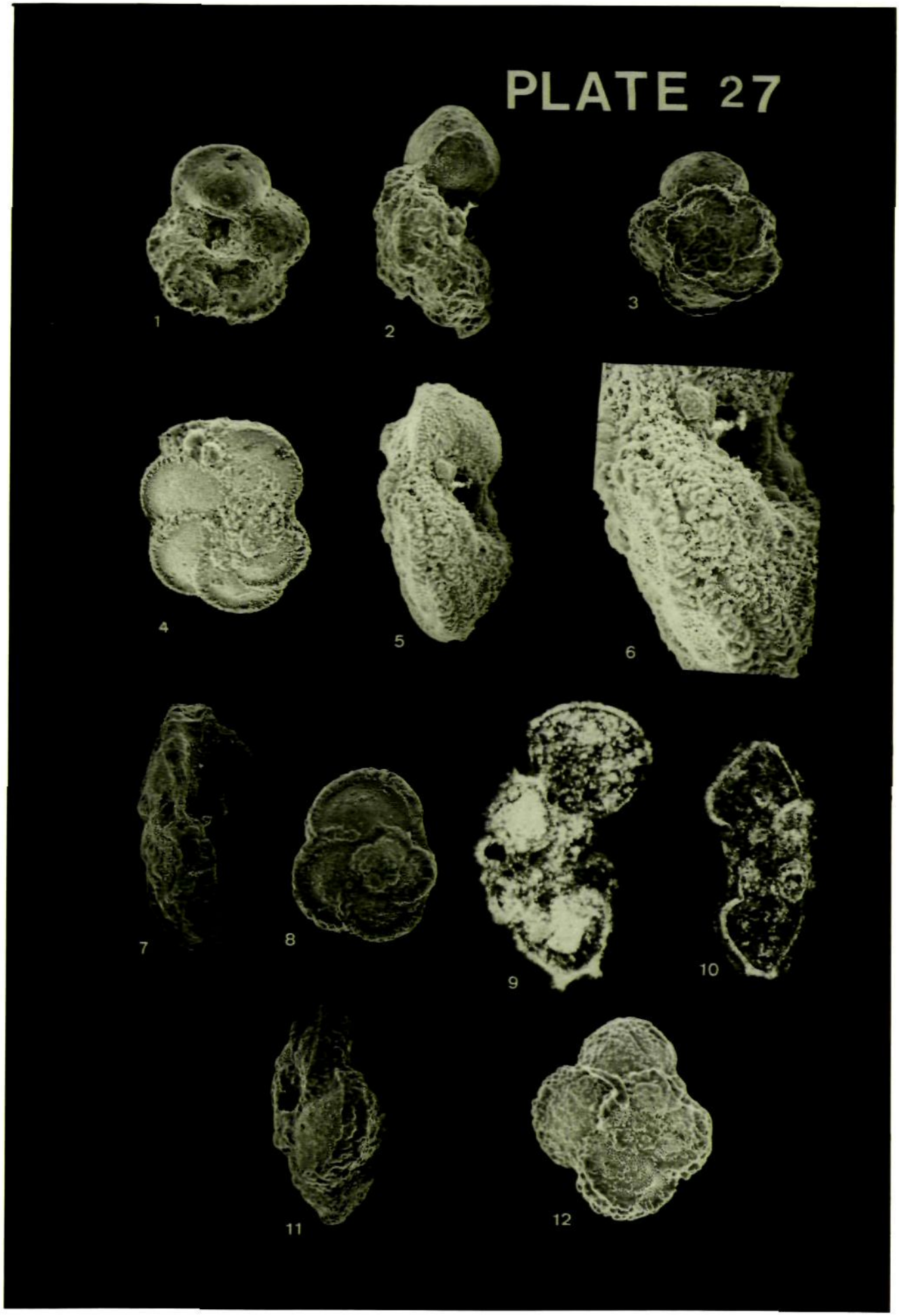

Plate 28.

1. Marginotruncana marginata (Reuss)
umbilical view, AKS10, x150

2. Marginotruncana marginata (Reuss)
apertural view, AKS10, x200

3. Marginotruncana marginata (Reuss)
spiral view, AKS10, x200

4. Marginotruncana marginata (Reuss)
spiral view, AKS10, x150

5. Marginotruncana sp. cf. M. sigali (Reichel)
spiral view, AKS12, x100

6. Marginotruncana sp. cf. M. sigali (Reichel)
apertural view, AKS12, x150

7. Marginotruncana sp. cf. M. sigali (Reichel)
spiral view, AKS12, x100

8. Marginotruncana sp. cf. M. sigali (Reichel)
peripheral view, AKS12, x150

9. Rotalipora appenninica (Reuz)
SGQ7

10. Rotalipora cushmani (Morrow)
umbilical view, Goban Spur 6\1 30-33, x150

11. Rotalipora cushmani (Morrow)
apertural view, Goban Spur 6\1 30-33, x150

12. Rotalipora cushmani (Morrow)
spiral view, Goban Spur 6\1 30-33, x150

13. Rotalipora cushmani (Morrow)
spiral view, Goban Spur 6\1 30-33, x150

14. Rotalipora cushmani (Morrow)
umbilical view, Goban Spur 6\1 30-33, x150

PLATE 28

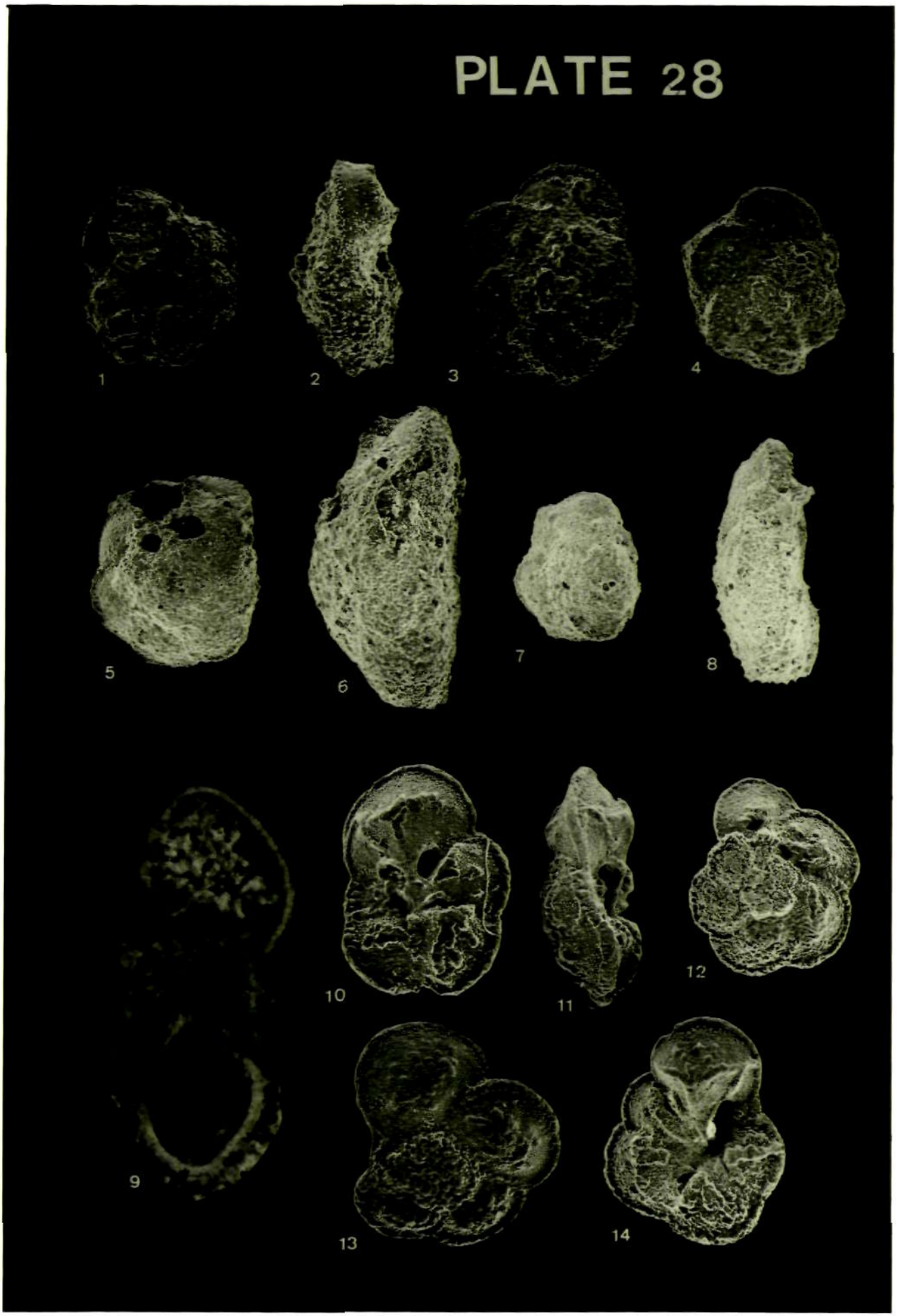

Plate 29.

1. Rotalipora cushmani (Morrow)
BSA 6

2. Rotalipora cushmani (Morrow)
CB1 10

3. Rotalipora cushmani (Morrow)
WND 11

4. Rotalipora deecki (Franke)
umbilical view, Goban Spur 6\1 30-33, x100

5. Rotalipora deecki (Franke)
apertural view, Goban Spur 6\1 30-33, x200

6. Rotalipora deecki (Franke)
spiral view, Goban Spur 6\1 30-33, x150

7. Rotalipora greenhornensis (Morrow)
Umbilical view, Goban Spur 6\1 30-33, x150

8. Rotalipora greenhornensis (Morrow)
apertural view, Goban Spur 6\1 30-33, x150

9. Rotalipora greenhornensis (Morrow)
spiral view, Goban Spur 6\1 30-33, x150

10. Rotalipora sp. cf. reicheli Mornod
S6Q.5

11. Pleurostomella subnodosa (Reuss)
lateral view, Goban Spur 5\2 13-17, x150

12. Pleurostomella subnodosa (Reuss)
close-up of aperture, Goban Spur 5\2 13-17, x150

13. Pleurostomella subnodosa (Reuss)
lateral view, Goban Spur 5\2 13-17, x100

14. Pleurostomella subnodosa (Reuss)
close-up of aperture, Goban Spur 5\2 13-17, x500

Plate 29 cont'd

15. Gyroidina sp.a
apertural view, Goban Spur 6\1 30-33, x350

16. Gyroidina sp.a
lateral view, Goban Spur 6\1 30-33, x350

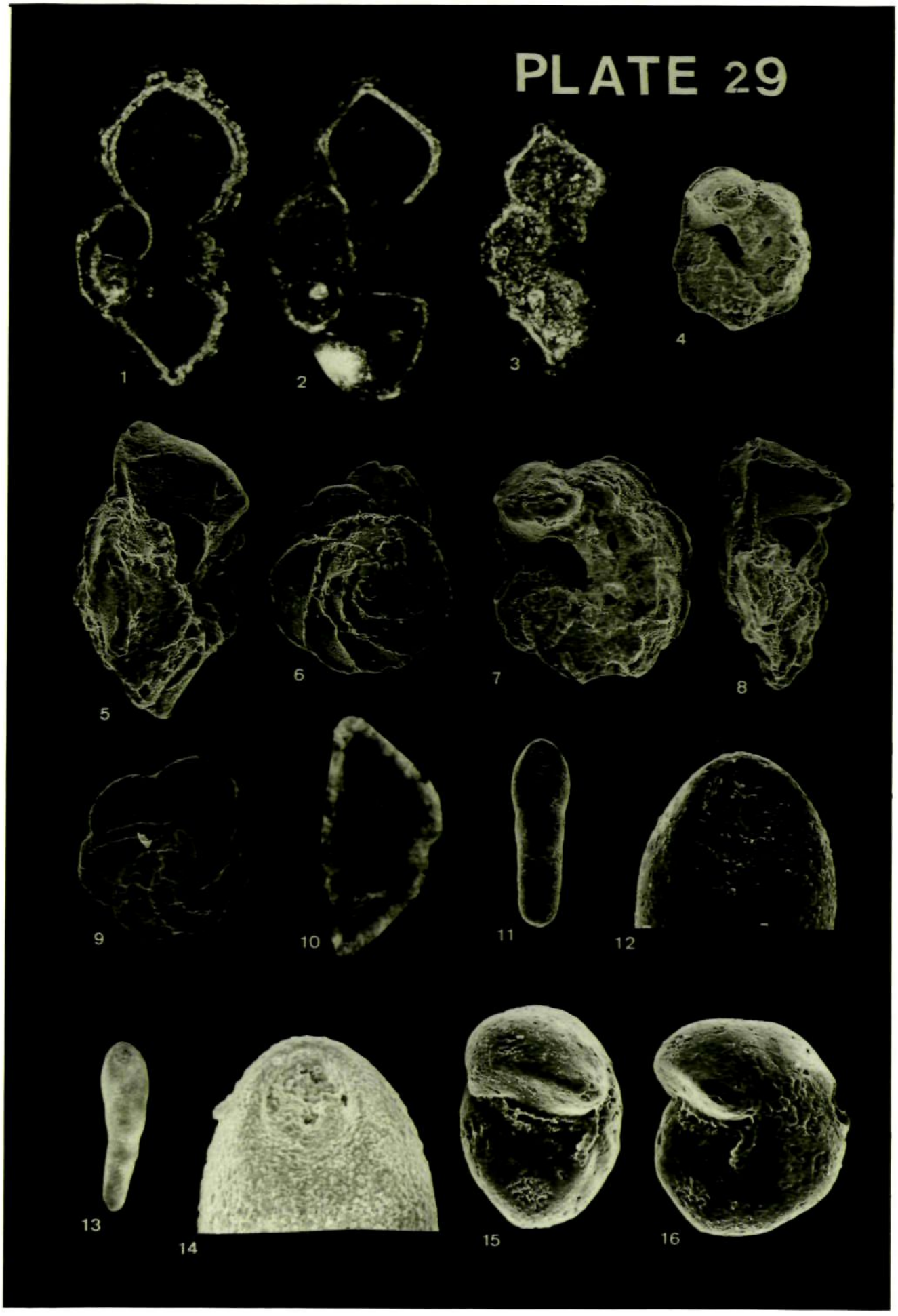
PLATE 29
1
2
3
4
5
6
7
8
9
10
11
12
13
14
15
16

Plate 30.

1. Gyroidinoides parva (Kahn)
lateral view, ABC2, x200

2. Gavelinella baltica Brotzen
oblique apertural view, ABC2, x150

3. Gavelinella baltica Brotzen
lateral view, ABC1, x100

4. Gavelinella baltica Brotzen
lateral view, ABC2, x100

5. Gavelinella baltica Brotzen
oblique apertural view, ABC2, x100

6. Gavelinella baltica Brotzen
close-up of test wall, ABC2, x500

7. Gavelinella baltica Brotzen
lateral view, ABC2, x150

8. Gavelinella berthelini (Keller)
apertural view, ABC12, x200

9. Gavelinella berthelini (Keller)
umbilical view, ABC12, x200

10. Gavelinella berthelini (Keller)
oblique apertural view, ABC13, x200

11. Gavelinella berthelini (Keller)
lateral view, ABC14, x200

12. Gavelinella cenomanica (Brotzen)
lateral view, ABC1, x150

13. Gavelinella cenomanica (Brotzen)
oblique apertural view, ABC4, x150

14. Gavelinella cenomanica (Brotzen)
lateral view, ABC4, x100

Plate 30 cont'.

15. Gavelinella cenomanica (Brotzen)
close-up of umbilical thickening, ABC4, x200

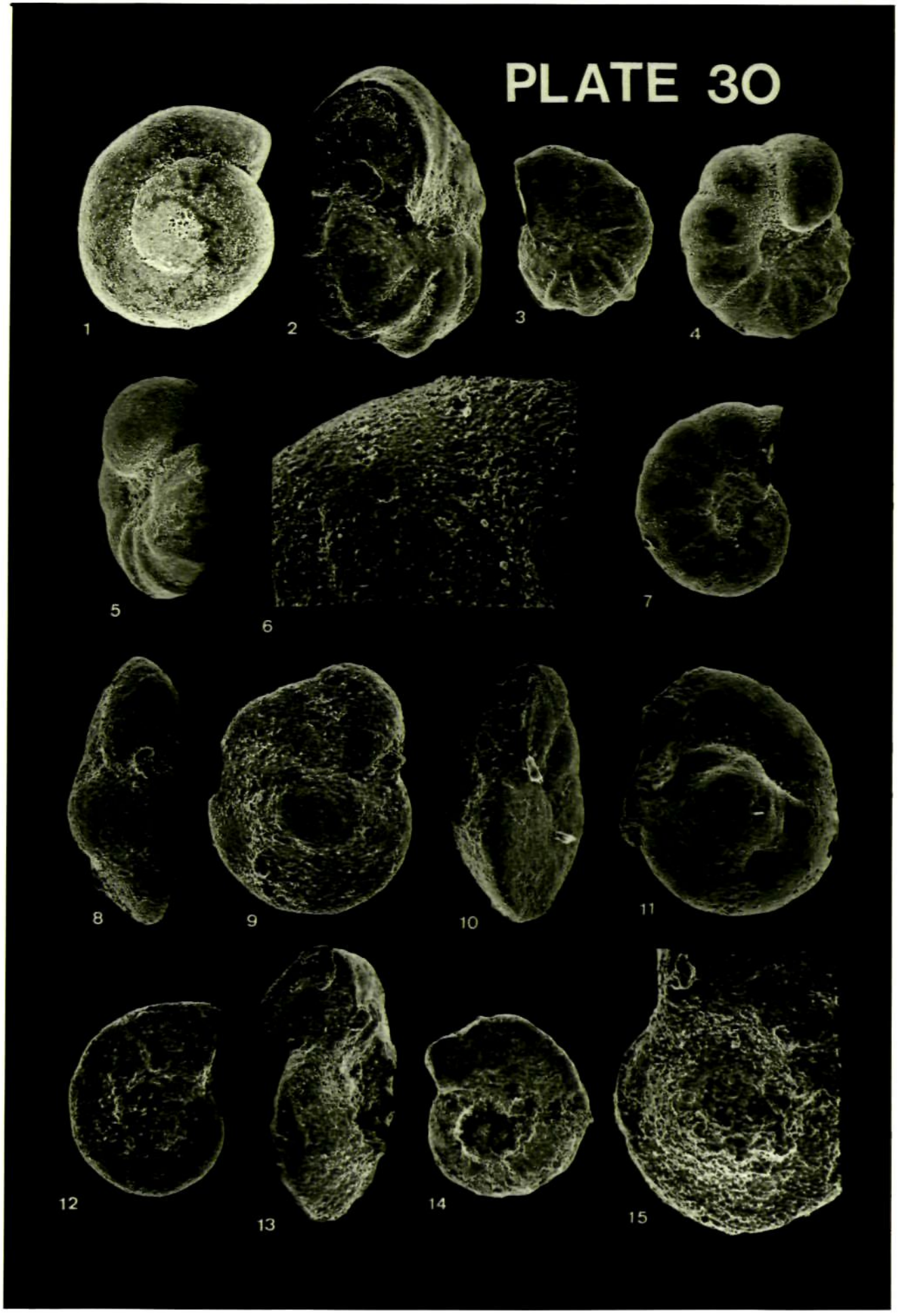
PLATE 30
1
2
3
4
5
6
7
8
9
10
11
12
13
14
15

Plate 31.

1. Gavelinella intermedia (Berthelin)
lateral view, B.P 93\2-1 1050', x200

2. Gavelinella intermedia (Berthelin)
apertural view, B.P 93\2-1 1050', x200

3. Gavelinella intermedia (Bethelin)
apertural view, B.P 93\2-1 1050', x350

4. Gavelinella reussi (Kahn)
lateral view, ABC4, x200

5. Gavelinella reussi (Kahn)
apertural view, ABC4, x200

6. Gavelinella reussi (Kahn)
lateral view, ABC4, x200

7. Lingulogavelinella globosa (Brotzen)
apertural view, SGQ8, x200

8. Lingulogavelinella globosa (Brotzen)
lateral view, SGQ8, x150

9. Lingulogavelinella globosa (Brotzen)
lateral view, SGQ8, x200

10. Lingulogavelinella aumalensis (Sigal)
oblique apertural view, AKS15, x200

11. Lingulogavelinella aumalensis (Sigal)
lateral view, AKS15, x200

12. Pithonella ovalis (Kauffmann)
AKS8, x750

13. Pithonella ovalis (Kauffmann)
AKS7, x750

14. Calcareous (?) sphere
B.P 93\2-1 1090', x350

Plate 31 cont'd.

15. Calcareous (?) sphere
B.P 93\2-1 1090', x1000

16. Cemented calcareous (?) spines
ABC9, x100

PLATE 31